Durham E-Theses

Unconventional Offshore Petroleum-extracting oil from active source rocks of the Kimmeridge Clay Formation of the North Sea

RAJI, MUNIRA

How to cite:

RAJI, MUNIRA (2018) *Unconventional Offshore Petroleum-extracting oil from active source rocks of the Kimmeridge Clay Formation of the North Sea*, Durham theses, Durham University. Available at Durham E-Theses Online: http://etheses.dur.ac.uk/12476/

Use policy

The full-text may be used and/or reproduced, and given to third parties in any format or medium, without prior permission or charge, for personal research or study, educational, or not-for-profit purposes provided that:

- a full bibliographic reference is made to the original source
- a link is made to the metadata record in Durham E-Theses
- the full-text is not changed in any way

The full-text must not be sold in any format or medium without the formal permission of the copyright holders.

Please consult the full Durham E-Theses policy for further details.

Academic Support Office, Durham University, University Office, Old Elvet, Durham DH1 3HP
e-mail: e-theses.admin@dur.ac.uk Tel: +44 0191 334 6107
http://etheses.dur.ac.uk

University of Durham

Doctoral Thesis

Unconventional Offshore Petroleum-extracting oil from active source rocks of the Kimmeridge Clay Formation of the North Sea

Munira Raji

Thesis submitted in accordance with the regulations for the degree of Doctor of Philosophy in the University of Durham, Department of Earth Sciences.

September, 2017

How to cite:

Munira, Raji (2017) Unconventional Offshore Petroleum-extracting oil from active source rocks of the Kimmeridge Clay Formation of the North Sea. Department of Earth Science, Durham University, United Kingdom.

Abstract

The organic-rich Upper Jurassic Kimmeridge Clay Formation is the major source rock for conventional oil and gas in the North Sea with a maximum thickness of 1,100 m. TOC values range from 2 wt.%-10 wt.% and predominantly Type II (bacterially-degraded algal, and a mix of Type I (mainly algal) kerogens. The δ13Corg values for the investigated samples range from -29.73 ‰ to -26. 88 ‰, these values are characteristic of marine organic matter with terrestrial input. Sixteen billion barrels of commercial reserves have been discovered in conventional reservoirs in the UK Viking Graben area with 29 billion barrels discovered in the Norwegian sector of the North Sea. However, this principal UK conventional hydrocarbon province is reaching the maturity phase of field exploration, leading to a growing interest for unconventional hydrocarbons in the UK and some part of Europe.

The purpose of this study is to evaluate the unconventional hydrocarbon potential of the Kimmeridge shale to identity sweet-spot areas using multidisciplinary analogues from successful unconventional resource plays in North American. Conventional and unconventional source rock analyses show that the Kimmeridge Clay Formation contains a significant amount of un-expelled residual oil both within the source rock and in the interbedded sandstone in the South Viking Graben area. As a consequence, this source rock and juxtaposed non-source lithofacies (sand interbeds) can form a hybrid shale resource system. Due to its high organic richness and favourable sweet-spot reservoir properties such as lithology, thickness, kerogen type, level of thermal maturity and hydrocarbon generative potential, the Kimmeridge Clay Formation could be the first offshore unconventional resource in the future.

TOC, Rock-Eval S_1, $T_{max,}$ mineralogical content and the formation of organic, interparticle and intraparticle porosities at peak oil maturity are all factors that have influenced the retention and drainage of the observed oil. The examination/analysis of their interrelationships provides a useful framework and signature for future prediction of sweet spot areas for viable unconventional resources.

Contents

List of figures

Chapter 1:

Chapter 2:

Chapter 3:

Chapter 4:

Chapter 7:

List of Tables

Chapter 1:

List of Abbreviations

TOC: Total Organic Carbon

S_0: Free gas (C_1-C_5)

S_1: Free oil

S_2 : Generated oil

S_3: CO_2 from organic oxygen

OI: Oxygen Indices

PI: Production Indices

HI: Hydrogen Indices

GI: Generation Indices

Aroms: Aromatic

Sats: Saturates

HCl: Hydrochloric Acid

HF: Hydroflouric Acid

SEM: Scanning Electron Microscopy

T_{max} : Tempeature of Maximum S_2 yield

KCF: Kimmeridge Clay Formation

OM: Organic Matter

AOM: Amorphous Organic Matter

TCD: Thermal Conductivity Detector

FID: Flame Ionization Detector

NDIR: non-dispersive infrared detection cell.

API gravity: American Petroleum Institute gravity

SEM: Scanning Electron Microscopy

FIB: Focused Ion Beam

QEMscan: Quantitative Evaluation of Minerals by scanning electron microscopy

Declaration and Copyright Statement

The work in this thesis is based on research carried out at the Department of Earth Sciences, Durham University, United Kingdom. No part of this thesis has been submitted elsewhere for any other degree, diploma or other qualification and it is all my own work unless referenced to the contrary in the text.

September, 2017

Copyright © by Munira Raji, 2017

"The copyright of this thesis rests with the author. No quotations from it should be published without the author's prior written consent and information derived from it should be acknowledged".

Preface and Acknowledgements

This study on "*Unconventional Offshore Petroleum-extracting oil from active source rocks of the Kimmeridge Clay Formation of the North Sea"* was carried out at the Department of Earth Sciences, Durham University, UK. The study was funded by Three Field Exploration/IGILTD, Trap Oil and part funding from Durham University Doctorate Scholarship Grant.

This project consists of the introductory chapter, five scientific paper and a discussion/conclusion chapter which cover the various aspect of unconventional potential of Kimmeridge Clay source rock in the South Viking Graben of the North Sea. Additional data and further information on the technique used for assessment are added as appendices at the end of each chapter.

The first part of this project was presented at the American Association of Petroleum Geologists (AAPG) conference on April 6-9 2014 in Houston, at the 'Brae Play' conference on 23rd-24th April in Aberdeen, and Mineralogical Society Meeting on 25th September 2014 in Durham. The second half of this study was presented at the British Sedimentological Research Group conference on 19th December 2014 in Nottingham, at the Unconventional Resource Technology Conference in 20th -22nd July 2015 in San Antonio. The final part of this project was presented at the Joint TSOP-AASP-ICCP (The Society for Organic Petrology, The Palynological Society, The International Committee for Coal and Organic Petrology) conference on 20th, September 2016 in Houston.

This study would not have been possible without the help, guidance and support from my institution supervisors, Dr. Darren R. Grocke and Professor Chris G. Greenwell, and my industry supervisor the late Dr. Chris Cornford. I owe my main supervisor, Dr Darren R. Grocke my deepest gratitude for being such an amazing and brilliant supervisor. Darren has been wonderful to me since the first day I joined his group, his support and appreciation for my enthusiasm in my research and presenting it at several local and international conferences has provided me with valuable life experiences both personally and career-wise. My sincere gratitude goes

to all my three supervisors whose valuable support, thoughtful comments, expertise was critical to the completion of this project.

I would like to express my gratitude to my co-author Professor Sue Rimmer of Southern Illinois University for her mentorship, encouragement and valuable technical support during and after my visiting fellowship at her Kerogen and Density Gradient Centrifugation Laboratories in Carbondale, Illinois, USA.

I would like to thank Integrated Geochemical Limited (IGILTD) for financial sponsorship and for the use of their p: IGI-3 software and database for the interpretation of the geochemistry data. Special thanks to the British Geological Survey, Keyworth for the provision of Kimmeridge source rock samples used for all the analyses carried out in this study. Many thanks to Newcastle University (Geology Department) for the use of their petrographic microscope for the completion of the petrographic study. I am grateful to Leon Bowen of the Physic department (Durham University) for his technical training and support with the Scanning Electron Microscope (SEM) Analysis. I am also grateful to the Engineering Department of Durham University for their help in analysing shale-sand interbed sample using Micro-CT. I am thankful for the valuable technical training and support from Bill Hugget at the Density Gradient Centrifugation Lab in Carbondale.

Personal thanks to my family and friends (Akinniyi Akinwumiju, Tonia Emaikwu-Odedina, Oluwatobi Olobayo-Sulaiman, Sarah Biejat, Patience Igah-Bosah, Loraine Pastoriza, Barbara Mutedzi, Amelia Ketzle and Rikan Kareem) for their continuous encouragement and support throughout my PhD. I would like to thank my husband, Dola Idowu for his inspiration and motivation. Thank you for dealing with all my moaning, worries, stress and planning during the final stage of my PhD. To my perfect little son, Alpha Faramade Preston Idowu, I say thank you for giving me more reasons to carry on.

Dedication

This work is dedicated to the lovely memory of Chris Cornford 1947-2017. Thank you for your mentorship and sponsorhip, and for teaching me the values of hard work.

Research Rationale

The past several years have seen record highs in the consumption of petroleum resources globally with oil accounting for 32.9 % of global energy consumption (BP Statistical Review of World Energy, June 2016; World Energy Resources, 2016). In 2016, the global oil consumption grew by 1.9 million barrels per day (BP Statistical Review of World Energy, June 2016). Population growth along with economic and social development is key driver for increased petroleum demand and changes in the petroleum industry over the past 20 years have been very significant to accommodate these global demands (World Energy Council, 2013).

The term "unconventional resources" refers to natural oil and gas found in low porosity fine-grained shale, hybrid shale (shale with interbedded sandstone) and tight sand formations (Meckel and Thomasson, 2008; Jarvie, 2012). Unconventional shale oil recovery accounts for 30% of the global recoverable oil reserves (BP Statistical Review of World Energy, June 2016). Over the past two decades, the development and improvement in drilling technologies has led to the growth of research and investments in unconventional resources (U.S. Department of Energy, 2013). Unconventional resources have become increasingly important in their contribution to the global energy base (Energy Information Administration. 2012), and are gradually becoming more common worldwide.

To date a number of North American onshore basins have been characterised in terms of their unconventional potential and production: exploration is spreading rapidly to onshore areas of Europe, South America, Asia and Africa (World Energy Resources, 2013). In the UK, the principal conventional hydrocarbon province, the North Sea, is reaching the maturity phase of field exploration (Oil & Gas UK Activity Survey, 2016), leading to a growing interest for unconventional hydrocarbon within the UK and other parts of Europe. The UK has relatively limited onshore unconventional resources, with the most prospective being the Carboniferous Bowland Shale (Armstrong et al., 1997; Andrews, 2013; DECC, 2013) and the Jurassic shale of the Wessex area (Greenhalgh, 2016). Onshore exploration in the UK has become highly political due to a number of factors including environmental concerns, planning

permission from local authorities, issues with mineral rights, land access and ownership, lack of adequate incentives for development and public protest (Pyhäranta, 2017). In contrast the unconventional potential of offshore basins has been practically ignored. Based on a review of public domain data and recent conferences, and publications, there appears to be no reported offshore unconventional exploration activity anywhere in the world.

The North Sea petroleum system comprises the UK and Norwegian Central, Witch Ground and Viking Grabens and is majorly sourced from the Upper Jurassic Kimmeridge Clay Formation (Draupne Formation in Norway). These areas are now considered to be in a mature phase of exploration (Østvedt et al., 2005; Oil and Gas UK, 2016). Recent re-evaluation of a large database of conventional source rock analyses and recent pyrolysis data show that the Kimmeridge Clay Formation of the UK contains large volumes of residual (i.e. un-expelled) oil buried below c. 3.2 km (Cornford et al., 2014). Petroleum expulsion efficiency is about 2-12 %, suggesting significant amounts of oil and gas remain within the source rock and in the migration paths of the basin (Cornford, 1994; Cornford et al., 2014). This Upper Jurassic oil-prone source rock has been overlooked as a significant potential source—for unconventional shale oil accumulation.

There is currently no reported unconventional exploration activity-offshore anywhere in the world (Scotland Means Business, 2014). It is likely that offshore unconventional resources have largely been ignored even in the United States, due to abundant onshore production and the perception that offshore drilling costs are likely to be considerably higher than onshore (British Geological Survey, 2013). This thesis addresses this through comparison of the attributes of both onshore and offshore shale play and the issues relating to their exploitation. The research in this thesis was undertaken to evaluate the potential of offshore unconventional resources in the South Viking Graben area of the North Sea and to provide a comparison in terms of geology, geochemistry, thermal history and mineralogical properties with those of known working onshore unconventional plays.

Some of the advantages of exploring for unconventional resources offshore UK include: larger basin centres; the continuous subsidence in the North Sea allows drilling directly into an actively generating world class oil-prone source rock; the availability of existing under-utilised drilling platforms and pipelines in the North Sea; drilling deviated wells from onshore; existing seismic surveys and well data to define extent and thickness; large database of geology, geochemistry and mineralogy from conventional drilling to define the structural and tectonic history, organic-richness, kerogen types, thermal maturation, burial history, mineralogical composition and geochemical properties; limited environmental constraints compared to onshore; unlimited water supply to use in hydraulic fracturing; and a lack of significant political issues.

The important question to be answered in this thesis is whether the remaining residual oil in the Upper Jurassic Kimmeridge Clay Formation in the South Viking Graben area can be potentially developed and explored for unconventional resources commercially.

Aim

This study attempts to evaluate future prospects of offshore unconventional liquid hydrocarbon with the aim to identify producible "sweet-spot" areas for optimum extraction of the remaining residual oil in the South Viking Graben area of the North Sea. A sweet-spot has been defined as an area with certain reservoir properties and attributes where well penetration will be most economical for optimum recovery (Pilcher, et al., 2012; Avanzini et al., 2016). These reservoirs properties and attributes include: source rock thickness and distribution, lithology, organic-richness, kerogen type, optimum maturity, composition of minerals, and type of porosity (Jarvie et al., 2007; Loucks et al., 2009; Modica and Lapierre, 2012; Sharma and Chopra, 2016; Hackley and Cardott, 2016). Producible sweet-spots in a source rock can only identified in an area where all or some of these reservoir properties are present (Jarvie, 2007). The source rock is required to have significant thickness and quality of organic matter, which has to undergo sufficient increased depth of burial, thermal

maturation to transform kerogen to generate hydrocarbon (Aplin and Macquaker, 2011; Jarvie, 2012).

Once the hydrocarbon is generated, the oil is expelled and ultimately migrates to accumulate in sandstone reservoirs, and the source rock still contains the portion of the oil that was not expelled. As a consequence such shales and juxtaposed non-source lithofacies can form the targets for the exploration for 'unconventional shale oil' (Jarvie, 2012). Characterisation of the varying source rock will help to enhance the ability to predict future prospectivity of the Upper Jurassic Kimmeridge Clay Formation across the North Sea.

Evaluation of these parameters can be identified by geochemical analyses of source rocks with the integration of different data such as mineralogy, petrographic, and porosity of borehole material. This thesis represents the first non-proprietary evaluation of offshore unconventional resources in the South Viking Graben area which focuses on the remaining potential of un-expelled oil in the Kimmeridge Clay Formation. It consists of five scientific journal style papers covering the various aspects in the identification of sweet-spots parameters in the South Viking Graben area. In order to achieve the principal aim of this study, the following objectives will be addressed.

Objectives

In view of the exploration history of the South Viking Graben area, this thesis attempts to:

i. Use prior knowledge to identify area (s) extent, thicknesses of the source rock.
ii. Define sedimentary facies based on lithology and the systematic variation in scale of sand-shale interbeds.
iii. Generate litho and organo-facies mapping and modelling of Viking Group in the South Viking Graben area.
iv. Apply onshore reservoir parameters and general criteria for successful shale oil and gas exploration to identify unconventional "sweet spot" in the South Viking Graben using North American analogues.

v. Investigate the effects and role of interbedded sandstones on shale reservoir properties in the retention and expulsion of liquid petroleum.

vi. Identify where the retained oil is located within these actively generating oil-prone source rocks at peak maturity.

vii. Quantify Total Organic Carbon (TOC) richness, free hydrocarbon (S_1), generated hydrocarbon (S_2) and Hydrogen Index (HI) and porosity for samples at various stages of kerogen maturation.

viii. Classify the nature, type and distribution of porosity in organic-rich mudstone dominated, sandstone dominated and mudstone-sandstone interface lithofacies.

ix. Investigate the effect of demineralisation on isolated Kimmeridge Clay kerogens and on the quality of organic matter, kerogen type, maceral composition, thermal maturation and the generative potential.

List of Papers

Paper 1: Raji, M., Gröcke, D. R., Greenwell, C. H., and Cornford, C., 2017. Source Rock facies Mapping and Modelling of the Viking Graben. To be submitted to Journal of Geological Sciences.

Paper 2: Raji, M., Gröcke, D. R., Greenwell, C. H., Gluyas, J. G. and Cornford, C., 2015.The Effect of Sand Interbedding on Shale Reservoir Properties. Journal of Marine and Petroleum Geology 67, 154-169. http://dx.doi.org/10.1016/j.marpetgeo.2015.04.015.

Paper 3: Raji, M., Gröcke, D. R., Greenwell, C. H., and Cornford, C., 2015. Pyrolysis, Porosity and Productivity in Unconventional Mudstone Reservoirs: 'Free' and 'Adsorbed' Oil. Proceedings of the Unconventional Resources Technology Conference held in San Antonio, Texas, USA, 20-22 July 2015.

Paper 4: Raji, M., Gröcke, D. R., Greenwell, C. H., and Cornford, C., 2017. The Nature of Organic Porosity in Mudstone-Sandstone Interbeds *To be submitted* to Journal of Marine and Petroleum Geology

Paper 5: Raji, M., Rimmer, M., S., Gröcke, D. R., Greenwell, C. H., and Cornford, C., 2017. The Effect of Demineralization on Isolated Kimmeridge Clay Kerogens, North Sea and Isolated Kerogens of Lower Lias Limestone-Shale Sequences *To be submitted to* Journal of Unconventional Resource Technology.

Chapter 1: Introduction

This chapter investigates the regional tectonic evolution and structural history of the North Sea and discusses its relation to the petroleum system of the South Viking Graben area. Overviews of unconventional resources, challenges, sweet-spot identification and a broad outline of key features of the US and other shale systems are discussed. A brief assessment of the Kimmeridge Clay Formation as a potential unconventional reservoir is also discussed. Synopsis of the various aspects investigated in each of the research papers given as Chapters 3-7 are also discussed at the end of this chapter.

1.1: Introduction to the North Sea Petroleum System

The North Sea is a globally well-known prolific hydrocarbon province that has been much explored and studied (Goff, 1983; Baird, 1986, Barnard and Bastow, 1991, Ziegler, 1992; Færseth, 1996; Cornford, 1998; Johnson and Fisher, 1998; Isaksen et al., 2002; Evans et al., 2003; Fraser et al., 2003; Kubala et al., 2003). The North Sea province comprises the Central and the Northern North Sea, and lies in the offshore areas of the United Kingdom, Denmark and Norway (Figure 1-1).

Over 4000 exploration and appraisal wells have been drilled on the UK Continental Shelf (UKCS) since the 1960s (Johnson et al., 2005), where about 8.3 billion m^3 (48 billion barrels) of oil equivalent and over 4200 billion m^3 (127 trillion cubic feet) of gas have been found (Cornford et al., 2014). An estimated 1 billion m^3 (about 6 billion barrels) of oil and 800 billion m^3 (about 20 trillion cubic feet) of gas are estimated as yet to be found in the North Sea area (Cornford et al., 2014; Scotland Means Business, 2014). However, it is believed that the principal UK conventional hydrocarbon province is now reaching the maturity phase of field exploration (Østvedt et al., 2005; Scotland Means Business, 2014), leading to a growing interest for unconventional hydrocarbons within the North Sea by operators and governments in the UK and some parts of Europe (Kimmeridge Energy, 2012; Andrews, 2013; Cornford et al., 2014).

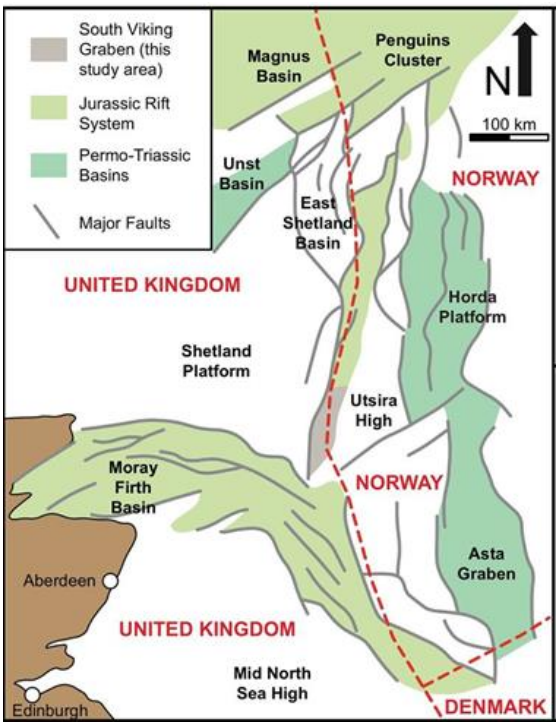

Figure 1-1: Structural elements of the North Sea showing the framework of the Viking Graben (modified from Dominguez, 2007).

Despite the burgeoning exploitation of onshore unconventional shale gas and shale oil in the United States (Jarvie et al., 2007; Jarvie, 2012), there is currently no reported offshore unconventional exploration activity in offshore anywhere in the world.

There is currently no need to look offshore for unconventional resources in the United States due to abundant onshore production (British Geological Survey, 2013). Nebula Resources was awarded three licences for the offshore Irish Sea in 2014 to begin exploration for unconventional shale gas but no information on such activity has been issued from this company since 2015 (Scotland Means Business, 2014). In 2013, Trapoil Ltd and Extract Petroleum obtained a Promote Licences P.1938 on the 27th Licence Round for a 100% working interest in the blocks in the South Viking Graben, North Viking Graben and in the East Shetland Basin to drill the first exploratory unconventional offshore wells in areas of organic-rich mature Upper Jurassic Kimmeridge Clay and Heather Formations (Trap Oil Ltd Relinquishment Report, 2014). These licences were relinquished in 2014 due to the cost of maintaining such licences and limited realisation opportunities in the current oil price environment (Trap Oil Ltd Relinquishment Report, 2014). Though the price of oil remains depressed, there is still interest in these unconventional offshore systems for potential

future exploitation. However, before addressing the future prospects for North Sea unconventional offshore systems, it is of interest to understand the background geological evolution of this important petroleum system.

1.2: Tectonic Evolution and Geological History of the North Sea

The North Sea has experienced a complex structural and tectonic history (Ziegler, 1990; Faerseth, 1996; Coward et.al., 2003; Johnson et.al., 2005). The occurrence of two major extensional and compressional tectonic events influenced the structural and tectonic evolution of the North Sea. These major Caledonian and Variscan events are associated with the break-up of Pangea are discussed in Section 1.2.1 and 1.2.2 below.

1.2.1: The Caledonian Phase of the North Sea Evolution

The Caledonian phase encompasses the Ordovician, Silurian and Early Devonian in north-west Europe, resulting from the collision between Laurentia, Baltica and Avalonia landmass between 510 Ma and 390 Ma (Coward et al., 2003; Johnson et al., 2005). Following the formation of the Gondwana super continent in the Early Palaeozoic, Laurentia, Baltica and Avalonia continents rifted to the north leading to the opening of the Iapetus Ocean (Johnson et al., 2005). The northern and southern Iapetus Ocean separated Laurentia from Baltica and Avalonia, and the Tornquist Sea lies between Avalonia and Baltica (Figure 1-2) forming the third arm of the triple convergence zone (Ziegler, 1989, 1990, 1992; Faerseth, 1996; Coward et al., 2003; Johnson et al., 2005). Baltica collided with Laurentia following the closure of the Iapetus Ocean and major uplift and orogenic events occurred (Husmo et al., 2003). As Laurentia and Baltica converged towards the south, the Avalonia drifted to the North. In the Ordovician (about 450 Ma), Baltica and the Avalonia plates collided. Due to the collision of the two continental plates subduction of the south eastern part of the Iapetus Ocean and the Tornquist Sea under the Eastern Avalonia occurred. The Tornquist suture zone along northern Iapetus was formed and acted as an extensional plate margin in the Late Proterozoic to Early Palaeozoic time. Finally, the Laurentia plate collided with the western part of Avalonia resulting in major uplifts and the Acadian Orogeny (Ziegler, 1975, 1990; Faerseth, 1996; Coward et al., 2003).

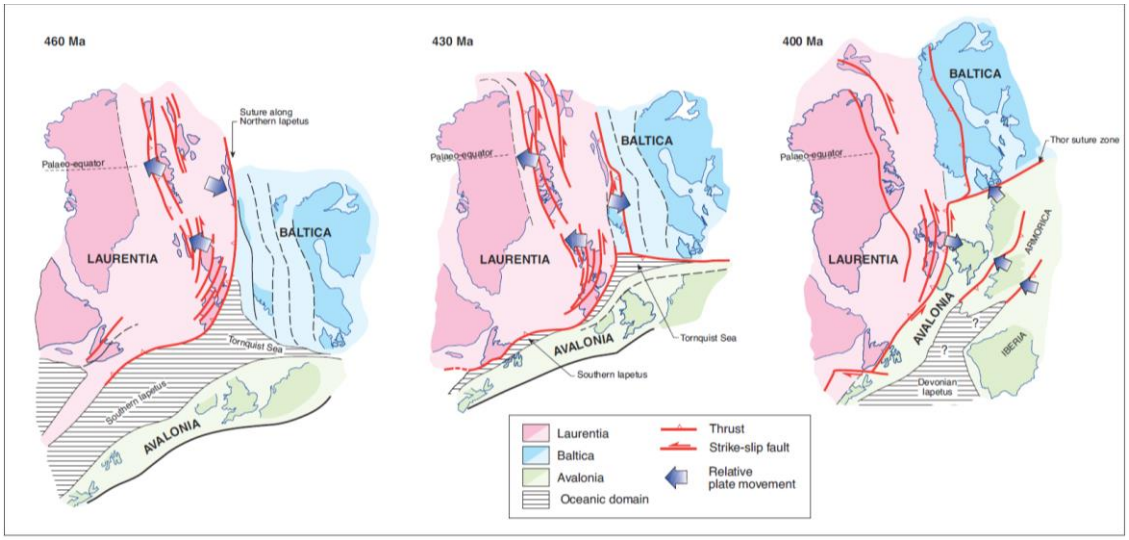

Figure 1-2: Evolution of the Caledonides in the North Atlantic (taken from Coward et al., 2003)

The Caledonian mountain chain from north to south is situated in the North Sea area. Structurally, the Caledonian basement of the North Sea consists of northeast-southwest Caledonide and east-west Variscan structures in the Palaeozoic (Ziegler, 1990; Faerseth, 1996; Cornford and Brook, 1989). The east-west structural compression is bounded by a T-junction in the south, where the London-Brabant massif developed as a structural high throughout the Late Palaeozoic (Ziegler, 1990; Errat et al., 1999; Jones et al., 2003; Davies et al., 1999). The collapse of the North Atlantic Caledonian fold-belt formed the Orcadian Old Red Sandstone Basin followed by reactivation of the previous Caledonian fault systems at the end of the Caledonian phase (Faerseth, 1996; Coward et al., 2003; Johnson et al., 2005.

1.2.2: The Variscan Phase of the North Sea Evolution

The Variscan (Hercynian) phase occurred between 380 Ma to 250 Ma in the Late Devonian to Late Permian period. This orogenic phase was produced by the suture of the Gondwana and Laurussia during the formation of the super continent Pangea (Ziegler, 1989, 1992). In the Late Devonian, Gondwana collided with Laurussia in the north; the small archipelago of Armorica collided with the south of Laurussia, marking the beginning of the Variscan phase forming mountains east of the pre-existing Caledonians. The North Sea area was subjected to a tropical climate and the area of the North Sea moved to the north, where the Caledonian mountains had been

severely eroded. During the Carboniferous, a low-lying flat coastal plain, which forms an unconformity in the North Sea area, developed (Ziegler, 1989, 1990; Klemperer and White, 1989).

The Variscan mountain range was uplifted, thrusted and eroded into the newly formed basins. In the Carboniferous, cyclicity, subsidence and transgression occurred in the North Sea area resulting in the deposition of mudstones and deltaic sediments. Several forests sprang up on the coastal plains, followed by continuous formation of peats which formed the Westphalian coal source rock interbedded with fluvial and marine sediments. Continuous Variscan compression of the Appalachian Mountains occurred throughout the Carboniferous, forming basins in the northern North Sea and grabens systems in the southern North Sea (Coward et al., 2003). The Viking Graben area acted as the locus for transport for the eroded Caledonian mountain belt, where thick deltaic sediments formed in northern England and the North Sea (Glennie and Underhill, 1998; Coward et al., 2003).

The Northern Permian and Southern Permian extensional basins also developed towards the end of the Variscan phase. Widespread volcanic activities also occurred in the Late Carboniferous to Early Permian resulting in the formation of tuffs, sills, dykes and basaltic lavas in the northern North Sea (Ziegler, 1975). Aeolian and fluvial deposits of the Rotliegend Group and Zechstein salt were deposited in a topographic fault-bounded Northern Permian Basin (Klemperer and White, 1990; Hodgson et al., 1992; Smith et al., 1993; Helgeson, 1999).

1.3: The South Viking Graben area of the North Sea

The South Viking Graben is an asymmetric graben located within the United Kingdom (UK) and Norwegian sectors of the northern North Sea, and is bounded by the East Shetland Platform to the west and the Utsira High to the east (Figure 1- 1). Formation of the Viking Graben was initiated during the Permo-Triassic from two major phases of extension followed by a of period regional subsidence (Glennie, 1986; Erratt et al., 2010) with compressional tectonics and uplift (Ziegler, 1990, 1992). The Permo-Triassic rifting episode was followed by a period of post-rift cooling in the Early-Middle Jurassic. However, the Jurassic extensional phase was more prominent

in the Viking Graben area (Coward et.al 2003). During the Middle Jurassic; a domal uplift in the central area of the North Sea Basins arguably initiated the development of the Central and Viking grabens (Glennie, 1986; Ziegler, 1990, 1992). In the Late Jurassic-Early Cretaceous, block faulting and tilting created the grabens, together with some strike-slip movements offsetting the graben margin faults. These offset zones played a key role in focussing coarse clastics into the deep water of the grabens, which formed the submarine fans of the Brae Member (Stow, 1983; Turner et al., 1987).

Separation of the Viking Graben into northern and southern sectors occurred during structural development in the Jurassic (Richards et al., 1993). In the Middle Jurassic (Callovian to Oxfordian), structural extension produced continuous rapid subsidence in these grabens. These processes combined to produce a relatively isolated deep water basin which became relatively sediment starved in the Upper Jurassic. The distal connection of the Boreal seaway and the absence of water circulation led to the development of deep restricted (and thus anoxic) basins where organic-rich Kimmeridge Clay sediments accumulated (Cooper and Barnard, 1984; Cornford and Brookes, 1989; Gautier, 2005).

Rapid subsidence and burial favoured the maturation of the accumulated source rocks with oil generation beginning in the Cretaceous and attaining peak generation during the Tertiary (Cornford, 1998; Justwan et al., 2005). During the Upper Jurassic to Early Cretaceous (Kimmeridgian to Ryazanian), the active western graben margin fault shed coarse clastics to form the Brae Formation conglomerates and sands, deposited into the deep water trough of the south Viking Graben (Partington et al., 1993). The pebbly to fine sandstones of the Brae Formation are interpreted as proximal deep water slope apron fans derived from the East Shetland Platform and Fladen Ground Spur (Underhill, 1998; Justwan et al., 2005; Stow, 1983). The organic-rich mudstone and interbedded fan sands, together with distal and inter-fan areas, form the basis of a potential sweet spot (area of high production, *vide infra*) for a hybrid unconventional petroleum system.

A hybrid shale resource is a system within which 'hot shale' and organic-lean sandstone and siltstone intervals are intimately interbedded (Jarvie, 2007).Though deep water persisted, bottom water oxygenation returned in the Early Cretaceous as the graben became a connection between the Boreal and Tethys oceans (Cornford and Brookes, 1989). By the Late Cretaceous, rifting in the North Sea region essentially ceased, with regional thermal subsidence most prominent near the axis of the abandoned rift resulting in basin depocenters for syn- and post-rift sediments (Cornford and Brookes, 1989; Cornford, 1984; Ziegler, 1990; Cooper et al., 1995; Faerseth, 1996; Gautier, 2005; Johnson et al., 2005; Erratt et al., 2010). Major source rocks and reservoirs were formed during the pre-rift, syn-rift and post-rift phases of basin evolution in the Jurassic and early Cretaceous period (Johnson et.al. 2005). The Early Tertiary uplift caused significant erosion and subsequent deposition of clastic sediments in the Oligocene to Miocene, and glacial sediments in the Pleistocene (Ziegler, 1990; Rundberg and Eidvin, 2005). The main focus of this PhD thesis throughout is the evaluation of the Upper Jurassic Kimmeridge Clay Formation source rock as a potential offshore unconventional shale resource in the South Viking Graben area of the North Sea.

1.4: Kimmeridge Clay (Draupne) Formations

Source rocks is defined as sedimentary rock such as organic-rich shale, mudstone, siltstone and limestone that have generated or have the potential to generate oil and gas in sufficient commercial quantities (Tissot and Welte, 1984). The major source rock for the North Sea oil and gas is termed the Kimmeridge Clay Formation in the UK and the Draupne Formation in Norway (Cornford and Brooks, 1983; Goff, 1983). These dark, olive-grey calcareous to non-calcareous mudstones in the South Viking Graben area range in age from Volgian to Ryazanian (Cornford and Brooks, 1983). While the Kimmeridge Clay mudstone is the major source rock for oil, the underlying Heather Formation also has potential for gas and oil in the North Sea area (Cornford, 1998; Justwan et al., 2005).

The Kimmeridge Clay Formation sediments were deposited in a restricted marine embayment of the Boreal seaway in the north, which resulted from crustal stretching

and formation of the three main North Sea grabens (Cornford and Brookes, 1989; Cooper et al., 1995; Erratt et al., 2010). Sediment accumulation followed the widespread subsidence that occurred during the Late Jurassic to Early Cretaceous rifting episodes. Concomitant global sea-level rise led to the Late Jurassic marine transgression event, which resulted in the deposition of the organic-lean mudstone sediments of the Oxfordian Heather Formation under oxic bottom water conditions. With the closing of the Boral-Tethyan connection (Figure 1-2), high sedimentation rates, elevated organic matter productivity (probably controlled by nutrient supply) and increased water depths all led the development of stratified anoxic bottom waters (Cornford et al., 1983). As such, with greatly improved organic matter preservation, this resulted in the deposition of the thick, organic-rich Kimmeridge Clay Formation (Cornford and Brookes, 1989; Tyson, 1996, 1995, 2004).

During the Upper Jurassic, conglomerates and sands were periodically transported as submarine fans by gravity flow across the uplifted graben edge of the Shetland Platform and into the main graben (Partington et al., 1993). These sands were fed into the basin via graben-edge'notches' formed over ramps/transfer zones (transform fault lineations) which breached the uplifted footwall. These coarse clastics sediments, called the 'Brae Member' were deposited into the anoxic basin of the main South Viking Graben, where they are found interbedded with the mudstones of the Kimmeridge Clay Formation (Leythaeuser et al., 1984, 1987; Turner et al., 1987). This sediment association where the Kimmeridge Clay Formation and organic-lean sandstone and siltstone intervals are intimately interbedded is termed a 'hybrid' shale system and forms the target for this PhD study.

In order to evaluate and assess the unconventional potential for the remaining un-expelled oil in the Kimmeridge Clay Formation source rock, an understanding of the tectonic control, source rock deposition, burial, maturation, generation of hydrocarbons, and the migration and remigration of those hydrocarbons is of utmost importance. An overview of conventional and unconventional resources and adapted criteria for a successful unconventional shale play is given in Section 1.5 and 1.6 in this chapter. This evaluation and assessment involves using several analytical

procedures to investigate the Kimmeridge Clay Formation source rock, and these methods are discussed in detail in Chapter 2. The results of these analytical procedures, as applied to the Kimmeridge Clay Formation, are further discussed in detail in Chapters 3, 4, 5, 6 and 7 and summarised in Chapter 8.

1.5: Conventional and Unconventional Oil and Gas Resources

Conventional oil and gas resources differ from unconventional resources based on the reservoir properties of the rock formation, structural mechanism responsible for trapping the hydrocarbon and drilling techniques. Definition of conventional resources with an overview of unconventional resources and comparison between them are discussed in Section 1.5 below.

1.5.1: Conventional Resources

Conventional oil and gas is defined as hydrocarbons that have migrated from the source rocks into highly permeable (> 1 mD) reservoir rocks, sealed by cap rocks and are extracted by the conventional methods of drilling, pumping and compression techniques (Andrews, 2013; Holditch, 2013; Caineng et al., 2015). The oil and gas are usually found in high porous and permeable sandstone and carbonate reservoirs, and trapped in the reservoir by an impermeable cap rock, which when breached by drilling allows the flow of hydrocarbon into the well (Andrews, 2013; Holditch, 2013).

1.5.2: Unconventional Resources: An Overview

Unconventional oil and gas are defined as that oil and gas exploitable by directly drilling and fracturing of low permeability (< 0.1 mD) fine-grained rocks acting as both source and reservoir (Jarvie et al., 2007; Andrews, 2013; Abrams et al., 2014), with extensive basin centres targeted for unconventional exploration (Andrews, 2013). In both cases, the fine grained rocks (source rocks) should contain oil or/gas prone kerogen (Jarvie, 2014). Production of oil or gas from these unconventional resources is largely a function of the source rock maturity, thickness and generative potentials (Jarvie, 2011). For instance, studies from the US Barnett Shale have shown that unconventional exploitation of oil works best with oil-prone kerogen (Jarvie et al., 2007).

Until recently, organic rich shales and mudstones have been classified as petroleum source rocks, while highly porous (20-40 %) and permeable sandstones and carbonates have been classified as petroleum reservoirs. Shales are often less porous (4-7 % porosity) and saturated in hydrocarbons; however, due to insufficient permeability (< 1000 ηD) in most cases the rock must be fractured to allow exploration and exploitation of commercial amounts of hydrocarbon at a fast production rate (Jarvie et al., 2001; Yang and Aplin, 2010; Aplin and Macquaker, 2011; Loucks et al., 2012; Jarvie, 2012; Andrews, 2013; Holditch, 2013). Advances in drilling techniques and stimulation methods such as hydraulic fracturing and horizontal drilling has made possible the commercial exploration for natural oil and gas locked up in organic rich shale, such as the oil rich Kimmeridge Clay Formation studied here (Fan et al., 2010; Selley, 2011, 2012). This hydraulic fracturing process (Figure 1-3) involves initial perforating the drill casing with carefully controlled explosives and then injecting high pressured fluid (a mixture of water, chemicals and sand) down the well, where the pressure then creates fractures within the shale formation so oil or gas can flow into the well at the surface (Selley, 2005; Gale et al., 2007; Bowker, 2007; Selley, 2012; Gale et al., 2014). Generally, the shale reservoir should be brittle, so that it fractures easily, and silica rich shale is preferable for facile fracturing (Selley, 2005; Gale et al., 2014; Imber et al., 2014).

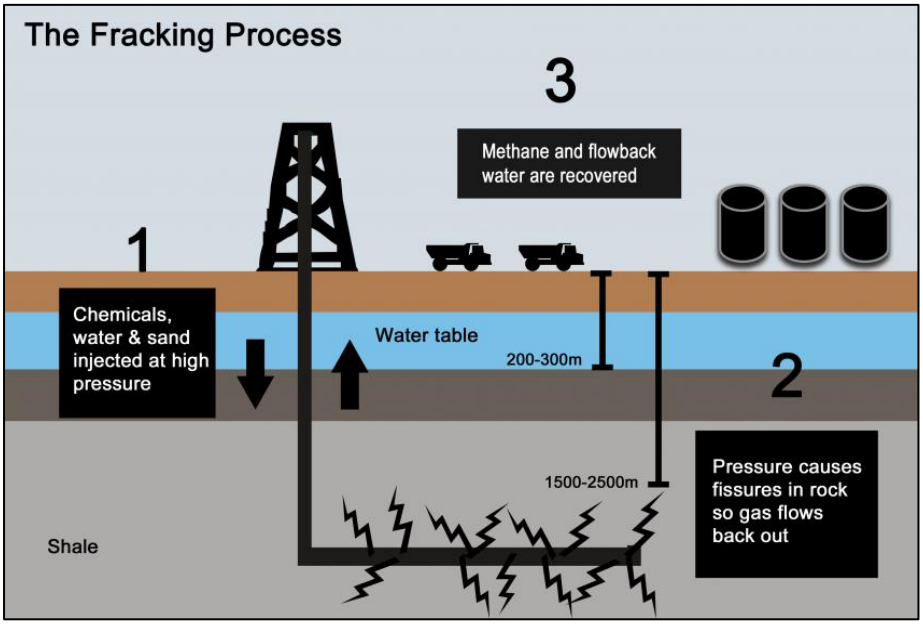

Figure 1-3: Hydraulic fracturing (fracking) stimulation process in unconventional resources (image from Energy and Climate Intelligence Unit Briefings, 2015).

Since 2008, there has been an emergent interest for evaluating shale oil and gas potential in Europe (Hartwig and Schulz, 2010 ; Galbraith, 2010; Weijermars, 2010; Gas Strategies, 2010; Kavalov et al., 2011), and in China (Shi et al., 2010 ;Luo et al., 2010; Caineng et al., 2010; Jiao et al., 2012). Risked technically recoverable resources for the whole of Europe were estimated at 883 tcf from an estimated gas-in-place of 4,895 tcf and 88.6 B bbl shale oil-in-place with a 24 % recovery factor (USEIA, 2013). China's shale exploration is still in its infancy with estimated technically recoverable shale oil reserves at around 32 billion barrels and 1,115 trillion cubic feet of shale gas (USEIA, 2013).

The most recent USEIA estimate of technically recoverable shale resources of the UK are at 26 trillion cubic feet of shale gas and 0.7 billion barrels of shale oil and condensate in the more organic-rich portions of the Carboniferous and Jurassic shale intervals (USEIA, 2015). However, shale gas drilling is presently limited in the UK with the only current activity being in the Upper Carboniferous shales of the Bowland Trough in Lancashire (DECC, 2010, 2011, 2013; Cuadrilla Resource, 2010, 2011; Andrews, 2013). The slow development of unconventional hydrocarbon resources in the UK followed a temporary setback in the preliminary exploration drilling for shale gas near to a fault zone in Blackpool in 2011, which triggered a series of minor earth tremors (Green et al., 2012; Rogers, 2013; Davies et al, 2013; Moreira de Camargo et al., 2014; USEAI, 2015; Smythe, 2016).

Challenges in unconventional resources differ from those encountered in a conventional resources play (Table 1-1). Each unconventional resource play is unique and varies from basin to basin. However, high capital expenditures are required for intensive exploration and to optimise the sweet-spot area to maximise return on any given drilling programme. Some other key challenges include: production rate, recovery rates, expected ultimate recovery (EUR) per well over time are critically linked to the economic feasibility of the shale reservoir (Chen et al., 2015). There are high costs due to horizontal drilling and multi-stage fracture stimulations, high production wells with sharp declines in production rates. Other environmental issues such as hydraulic frack fluid additives, water supply, soil stability also impact on the

cost of unconventional resource exploitation (Soeder and Kappel, 2009; Moreira de Camargo et al., 2014). Comparison between conventional and unconventional resources is highlighted in Tables 1-1 and 1-2.

Table 1-1: Comparison between conventional and unconventional resources

Conventional Reservoirs	Unconventional Reservoirs
Coarser- grained rocks	very fine-grained rocks
Hydrocarbon sourced from source rock (that is, shale and carbonate)	Self-source hydrocarbon from shale
Hydrocarbon migrates into sandstone and carbonate reservoirs	Hydrocarbon is generated in-situ in shale, interbedded sand-shale (hybrid), carbonate reservoirs (some short distanced migration)
Localised structural , stratigraphic or combination traps and seals	No trap, but seals
Porosity is important	Porosity not so important
Higher permeability > 0.1 md	Low permeability << 0.1 md
Significant production history	Limited production history

At this early stage of exploitation, there are no reliable indicators for identifying potential shale oil productivity in the UK. Reservoir parameters for successful shale oil and gas exploration vary per basin (Pitcher et al., 2012); however, general criteria for potential and resource estimates are largely based on the analogue information obtained from unconventional shale oil and gas production in the United States which vary considerably from basins to basins. The Upper Jurassic Haynesville Shale Formation of the southwestern US were formed under similar geological conditions (Kimmeridge Energy, 2012), and are therefore a good analogue for the Upper Jurassic Kimmeridge Clay Formation in the UK (Tables 1-3-1-5).

Table 1-2: Comparison between conventional and unconventional resources

Conventional Reservoirs	Unconventional Reservoirs
Late life-cycle development	Early life-cycle development
Few wells for economic production	Many multi-stage fracture stimulations for economic production
Base reserves on volumetrics	Base reserves on analogues
Assess entire prospect before drilling	Prospect driven by drilling
Well cost $4-8 MM	Well costs $6-10 MM
Well productivity profile easily establish	Longer period of testing (pilot projects)
Decline rates of production may be less than 20% per year	Steep decline rates up to 75 – 85% in the first 18 months of production

Table 1-3: Comparison of typical sweet-spot parameters for unconventional petroleum between Kimmeridge Clay Formation and successful shale plays in North America and Europe. ND denotes: no data.

Sweet-spot Parameters	Kimmeridge	Haynesville	Bakken	Eagle Ford	Barnett	Marcellus	Posidonia	Toarcian
Country/ state	UK	NW Louisiana and Eastern Texas	N. Dakota	Texas	Texas	NY-Penn	Germany	Northern Europe
Basin	North Sea	Sabine Uplift	Williston	Maverick	Fort Worth	Appalachian	Lower Saxony Basin	Paris
Stratigraphy	Upper Jurassic	Upper Jurassic	Devonian-Mississippian	Upper Cretaceous	Mississippian	Devonian	Lower Jurassic	Lower Jurassic
Age range (My)	152	~150	380-320	~99	360-320	400-360	183-175	183-175

Table 1-4: Comparison of typical sweet-spot parameters for unconventional petroleum between Kimmeridge Clay Formation and successful shale plays in North America and Europe. ND denotes: no data.

Sweet-spot Parameters	Kimmeridge	Haynesville	Bakken	Eagle Ford	Barnett	Marcellus	Posidonia	Toarcian
Primary Target	Kimmeridge Clay Formation (shale-sand interbeds)	Haynesville Formation	Middle Bakken	Carbonaceous Shale	Barnett Shale Formation	Marcellus Shale Formation	The Geverik Member	Banc de Roc
Depth range (ft.)	11,000-16,000	11,000-15,000	9,000-11,000	4,000-12,000	5,400-9,600	4,000-8,500	7,000-8,200	4,000-10,000
Thickness range(ft)	0-657	230-330	15-160	100-400	100-1500	50-200	164.04–229.65	328-985
Silica range (%)	25-40	30-35	20-70	30-50	75-95	80-100	20-55	26-58
Carbonate range (%)	60	14-21	5-10	20-35	7-25	0-30	35-60	30-60
Clay range (%)	20-50	20-44	35-45	10-15	12.5-37.5	30-60	43-50	20-30
Kerogen Type (I, II, III)	II	II	II/I	II	II	II/III	II/IIS	II
TOC range (wt. %)	2-5	2-6	3.5-40 (12 Avg)	4-6	0.9-12 .0 (5 Avg)	2-13 (4 Avg)	5-7	5-9
Maturity range (%Ro)	0.8	1.8-2.5	0.55-0.95	1.0-2.5	0.9-2.2 (1.6 Avg)	0.6-1.9	0.55–1.45	0.85

Table 1-4 (cont'd): Comparison of typical sweet-spot parameters for unconventional petroleum between Kimmeridge Clay Formation and successful shale plays in North America and Europe. ND denotes: no data

Sweet-spot Parameters	Kimmeridge	Haynesville	Bakken	Eagle Ford	Barnett	Marcellus	Posidonia	Toarcian
Maturity range (T_{max} °C)	430	410-464	427-470 (445 Avg)	422	432-491	400-450	430-470	435
Rock-Eval S_1 range (mgHC/grock)	1.2-5.51	nd	12	5	1.95	1.23	0.7-3.30	5

Table 1-5: Comparison of typical sweet-spot parameters for unconventional petroleum between Kimmeridge Clay Formation and successful shale plays in North America and Europe. ND denotes note data.

Sweet-spot Parameters	Kimmeridge	Haynesville	Bakken	Eagle Ford	Barnett	Marcellus	Posidonia	Toarcian
Rock-Eval S_2 (range mgHC/grock)	6.91-17.02	nd	35-180	nd	25.65	40.33	4.8-60.65	50-150
Rock-Eval HI range (mg/gTOC)	300-650	299-724	298-1,050 (430 Avg)	nd	45-434 (250 Avg)	50-507 (350 Avg)	375-630	600
Rock-Eval HI range (mg/gTOC)	300-650	299-724	298-1,050 (430 Avg)	nd	45-434 (250 Avg)	50-507 (350 Avg)	375-630	600
Porosity range (%)	15	8-12	8-12 (7 Avg)	2.5-13	4.0-9.6 (6 Avg)	4-12	6	12
Permeability range (mD or nD)	> 1 mD	10-650 nD	10-650 nD	400-1000 nD	200-300 nD (250 Avg)	0-70 nD	> 6 mD	> 5 mD
Pressure gradient range (psi/ft.)	0.45	0.7 - 0.9	0.50-0.80 (0.63 Avg)	0.45-0.7.	0.42-0.52. (0.47 Avg)	0.40-0.80.	0.50.	0.2-0.68
Water saturation range (%)	nd	25-30	30	20-35	25-35	2-35	30	nd
Oil Sulphur Content (%)	0.40	0.58	0.4	0.3	0.4	0.2	0.3	0.5
Oil API Gravity(°C)	38	15-20	40	40	40-59	38-60	38	38

Prediction and identification of sweet-spot areas is potentially the most important process in the evaluation of unconventional resources (Pilcher, et al., 2012; Pan et al., 2016). A sweet-spot is an area with certain reservoir properties and attributes where well penetration will be most economical for optimum recovery (Pilcher, et al., 2012). For locating "sweet-spot" in both unconventional oil and unconventional gas, the fine-grained rocks should be sufficiently thick (> 50 ft.) and contain mid (0.6 %Ro, 442 °C) to late mature (1.1 %Ro) organic matter (Smith et al., 2010; Charpentier and Cook, 2011; Gilman and Robinson 2011; Jarvie, 2012; Cornford, et al., 2014; Raji et al., 2015) with total organic carbon (TOC) values > 2 wt. % (Charpentier and Cook, 2011; Gilman and Robinson, 2011; Jarvie, 2012; Bent, 2012). Defining and predicting sweet-spot involves integration of important reservoir parameters such as lithology, area extent, depth, thicknesses, total organic carbon, maturity, mineralogy, porosity, permeability and adsorption capacity of a given source rock (Jarvie, 2012).

Some of these reservoir parameters for the Kimmeridge Clay Formation are listed in Table 1-3 to 1-5 with comparisons to some major successful North American and European shale reservoirs. The analytical techniques used in the investigation of these shale reservoir parameters by previous authors are briefly discussed in Section 1.6 and the adapted techniques used for this thesis are fully described in Chapter 2. A synopsis of this thesis and key results using these techniques is given in Section 1.8 of this chapter.

1.6: Previous work on Shale Reservoir Parameters for Identification of Sweet-spots

Shale reservoirs vary considerably from system to system in their characteristics, which results from a variety of geological, geochemical, mineralogical and petrophysical characteristics impacting upon the overall reservoir (Jarvie, 2012). Recent advances in the characterisation of unconventional reservoirs through evaluation of data from several shale plays clearly indicates that oil or gas content and total porosity is directly associated with the total organic carbon (TOC) content of the source rock (Ross and Bustin, 2009; Weniger et al., 2010; Bernard et al., 2011; Curtis et al., 2012; Cornford et al., 2014), and density of the organic matter changes as a

function of thermal maturity (Okiongbo et al., 2005; Romero-Sarmiento et al., 2013). High TOC values (> 2 %) are often associated with microporosity, which influences fracture development (Passey et al., 1990; Cornford, 1998). It has been previously reported that organic matter can develop micrometer to nanometer scales organic pore during thermal maturation (Bernard et al., 2011; Curtis et al., 2012; Loucks et al., 2012). Maturity of the source rock in terms of kerogen type (ideally marine Type I and Type II) and thermal maturation is also important for evaluating a source rock for its potential for oil or gas generation (Charpentier and Cook, 2011; Jarvie, 2012; Bergen et al., 2013).

Another important parameter is the mineral composition in shale reservoirs, as this varies widely across different shale plays, with current producing plays typically having < 35 % clay, reservoirs with > 30 % quartz or carbonate being more brittle in nature and subsequently responding more positively to hydraulic fracturing stimulation development (Passey et al., 1990; Cornford, 1998; Bustin and Bustin, 2010; Jarvie, 2007, 2012; Andrews, 2013). Typically, shale is conducive to holding natural and induced fractures under external forces such as natural and hydraulic fracturing (Bustin and Bustin, 2010; Ding et al., 2012; Jinzhou et al., 2014). An optimum combination of these reservoir parameters can lead to identification of sweet-spots and hence economically favourable productivity (Cornford et al., 2014; Pilcher, et al., 2012; Pan et al., 2016). The impact of each parameter is now explored in more detail.

1.6.1: Organic Matter Quantity

The concentration of organic matter in a source rock is usually reported as a weight percentage of organic carbon of the total rock, an estimation of original total organic carbon (TOC) based on present-day TOC has been described as one of the most important sweet-spot parameters (Jarvie, 2007; Romero-Sarmiento et al., 2013). The amount or organic matter and thus organic-richness of a source rock is measured using the TOC content (Espitalié et al., 1985a, 1985b; Espitalié and Bordenave, 1993). Examination of several shale reservoirs worldwide clearly indicates the shale reservoir must contain a potentially good-very good TOC of up ~2 % for a successful shale play (Jarvie, 2012; Ding et al., 2012; Andrews, 2013). The TOC, which is the

organic matter source for the generation of hydrocarbons also accounts for the development of porosity in organic matter (Jarvie, 2012; Romero-Sarmiento et al., 2013), which, together with abnormal high pressure, are the major factors that influence fracture development in shale reservoirs (Hill and Lombardi, 2002; Ding et al., 2012). The original mixture of organic matter in the petroleum system is called kerogen, which may be categorised into several types.

1.6.2: Kerogen Types

Kerogen is the insoluble part of this sedimentary organic matter, and hydrocarbon (oil and gas) is generated from the kerogen (Durand and Nicaise, 1980). Source rocks that are characterized by hydrogen-rich kerogen (high H/C ratio) produce oil (and possibly gas upon further maturation); whereas those with hydrogen-poor kerogen yield only gas (Horsfield and Douglas, 1980). The transformation process involved in the conversion of kerogen to hydrocarbon is accelerated by increased depth of burial, temperature, pressure, and duration of heating. The type of hydrocarbon, oil or gas, that a source rock generates, depends largely on the type of kerogen, chemical nature of the original organic matter, and maturation gas (Horsfield and Douglas, 1980).

Kerogens are classified into three major types: I, II and III (van Krevelen, 1950), and the typing is used in the evaluation of source rocks. Much of the recent work and classification of kerogens is due to the development of the combined thermal analysis methods encapsulated in the Rock-Eval® family of pyrolysis instruments (see fuller details in Chapter 2). The relationship between Rock-Eval® parameters such as Hydrogen Index (HI), Oxygen Index (OI), Total Organic Carbon (TOC), S_2 (Generated oil) and T_{max} have been used to identify the potential kerogen in a source rock (Espitalié et al., 1985a; Espitalié et al., 1985b; Gentzis et al., 1993; Cornford, 1998; Behar, 2001; Sykes and Snowdow, 2002; Sykes and Johansen, 2003; Dahl et al., 2004; Akinlua et al., 2005; King, 2015; Carvajal-Ortiz and Gentis, 2015; Raji et al., 2015) and are further explained in Chapter 2.

- Kerogen Type I is highly oil-prone, and is associated with marine or lacustrine source rocks. They are mainly derived from algal, with high HI values of >600 mg/g, and high H/C ratio.

- Kerogen Type II is oil and gas-prone, associated with marine source rocks, it is dominated by amorphous liptinitic such as exinite and sporinite derived from bacterially degraded algal kerogen, with moderate HI values between 350-600 mg/g and moderate H/C ratio.
- Kerogen Type III is gas-prone associated with terrestrial source rocks and dominated by vitrinite materials (see below) and is typically woody material. It has low values of HI of between 100-200 mg/g, with a lower H/C ratio.

Type II kerogen have the best characteristics for unconventional exploration compared to Type I and Type III; because they are oil prone and highly generative, though similar to Type I, but retain a high proportion of oil and gas in the source rock (Charpentier and Cook, 2011; Jarvie, 2012; Kimmeridge Energy, 2012; Andrews, 2013).

Other organic petrographic techniques such as optical characterisation, spore coloration microscopy, fluorescence and vitrinite reflectance have also been used to investigate kerogen type (Hutton, 1987; Gentzis et al., 1993; Johannes et al., 2006, 2007; Yalcin and Altunsoy, 2006; East et al., 2012; Bernard and Horsfield, 2014; Fishman et al., 2015; Furmann et al., 2015; Hackley et al., 2016). The origin and source of these organic matter can also be classified in terms of marine (aquatic) or continental (land) plant origins (Meyers, 1994; Galimov, 2006; Jarvis et al., 2011; Sun et al., 2016) using carbon and nitrogen (C/N) ratios (Meyers and Eadie, 1993; Meyers et.al., 1984a; Meyers and Benson, 1988; Meyers and Bernasconi, 2005) from carbon stable isotope analysis. The use and basis of these methods is further discussed in Chapter 2.

Within this present thesis, application of Rock-Eval pyrolysis, carbon isotope and organic petrographic analytical techniques were used for kerogen type identification throughout this research, and the results from these analyses are further discussed in Chapters 3, 4, 5 and 7.

1.6.3: Thermal Maturation

There are several techniques for assessing the maturity of a source rocks. The most commonly used maturity parameter is the Rock-Eval $T_{max;}$ temperature where maximum hydrocarbon generation has occurred from the kerogen and the hydrogen indices (HI), (Baird, 1986; Goff, 1983; Espitalié et al., 1985a; Cornford, 1998;

Charpentier and Cook 2011; McCarthy et al., 2011; Jarvie, 2012). Thermal maturity is used to understand how much heating a source rock has undergone, and its relationship to the extent of hydrocarbon. The thermal generation of oil and gas from kerogen occurs between 50 °C - 225 °C, at higher temperatures, the organic matter is over mature and potential oil and gas is generated (Andrews, 2013). Rock-Eval T_{max} values can give an indication of the maturity level of the source rocks, it classifies maturity as in the oil window using a T_{max} value range from < 432 °C (immature), 432 °C (early mature), 442 °C (mid-mature mature), 455 °C (late-mature) to > 465 °C (post-mature). The T_{max} values can also be converted into vitrinite reflectance (R_o) values using Jarvie's equation: $R_o = (T_{max} \times 0.018) - 7.16$ (Jarvie, 2001; Peters et al., 2005) for cross checking with complimentary historic vitrinite reflectance maturity indicators.

Vitrinite reflectance (%R_o) measurements are calculated from percentages of incident light reflected on polished vitrinite macerals under an incident plane polarised light microscopic. This can also be used as an indicator of maturity and kerogen types (Espitalié, 1986; Sweeney and Burnham, 1990; Hackley et al., 2013). Vitrinite occurs as dispersed organic matter as part of the kerogen in source rocks, it is derived from lignocellulosic higher plant tissue (Dow, 1977; Tissot and Welte, 1984). It can be used to identify source rock maturity area generation stages; where the onset of oil window maturity corresponds to 0.5 %R_o, and between 0.7-1.1 %R_o for mid-late oil window, gas generation > 1.1 % R_o, 1.3-2.2 %R_o for main gas window and > 2.2 %R_o for late gas window (Goff, 1983; Baird, 1986; Espitalié et al., 1985a; Cornford, 1998; Isaksen and Ledje, 2001; Justwan et.al., 2006; Jarvie, 2012). Investigation of thermal maturity of the Kimmeridge Clay Formation for this thesis was determined from results of Rock-Eval pyrolysis and optical microscopic techniques, as described in Chapter 2.

1.6.4: Mineralogy Composition

Mineralogical composition of the oil or gas bearing rocks is an important consideration in the evaluation of unconventional resources, and it varies widely across basins. High quartz (> 40 %) and moderate carbonate content (> 30 %) are thought to be key criteria for an excellent shale oil and gas play (Jarvie et al., 2007; Ding et al., 2012; Andrews, 2013). A low clay content and high quartz and carbonate

content in shale reservoirs increases the brittleness of the rock, and thus enhances artificial fracturing of the shales during production (Ding et al., 2012; Jarvie, 2012; Andrews, 2013). Current producing shale plays typically have > 50 % quartz, > 30 % carbonate and < 30 % clay (Table 1-3 to 1-5). The presence of swelling (those aluminosilicates that take up water and physically increase in volume) clay content, such as smectites, can however, reduce the porosity and permeability of the shale during drilling if the clays swell to fill pore, or fracture, space. Investigation of the mineral composition in the Kimmeridge Clay Formation for this thesis was carried out using X-ray-diffraction (XRD) and microscopic thin-section techniques (see Chapter 2).

1.6.5: Porosity

Porosity is the free space within fine grained rock that can store hydrocarbon, and permeability is the ability of the stored hydrocarbon fluid to pass through the rock (Loucks et al., 2012; Jarvie, 2012). Porosity is generally low (typically 4-7 %) in unconventional reservoirs owing to the fine grained nature of the minerals and high kerogen content (Jarvie, 2012). Pores may occur between minerals (inter-particle pores), within minerals (intra-particle pores) and within kerogen (organic porosity) in shale reservoirs (Loucks et al., 2012; Jarvie, 2012). Measuring the porosities of fine grained rocks can be problematic depending on the method of determination, grain size, mineralogy and burial depth (Swarbrick and Osborne, 1998; Hammes et al., 2016).

Numerous studies have been performed on laboratory measurements of porosity in shale using scanning electron microscopy (SEM) (Loucks et al., 2009, 2012; Bernard et al., 2012, 2013; Chalmers et al., 2012; Chalmers and Bustin, 2012; Hackley and Cardott, 2016; Swarbrick and Osborne, 1998; Hammes et al., 2016), broad ion milling (BIM)/focused ion beam (FIB) microscopy (Klaver et al., 2012; Newport, 2016; Hemes et al., 2015; Grathoff et al., 2016), with helium porosity and QEMScan electron microscopy (Cornford et al., 2014), by mercury injection porosimetry (Yang and Aplin, 2010), nitrogen and CO_2 injection (Ross and Bustin, 2009) and methane adsorption on the surface reactivity of the available solid organic carbon within

source rocks (Ross and Bustin, 2007, 2009; Weniger et al., 2010; Romero-Sarmiento et al., 2013; Rexter et al., 2014). These studies have yielded remarkable insights on the type and nature of porosity and pore networks within fine grained organic-rich shale in unconventional play assessment. In unconventional resources, the estimation of oil in place (OIP) are largely controlled by the distribution of the organic matter, kerogen type, thermal maturation, expulsion of hydrocarbon as well as retention processes from the formation of organic porosity and adsorption in the kerogen (Jarvie, 2012; Romero-Sarmiento et al., 2013).

For this thesis, focused ion beam-scanning electronic microscopy (FIB-SEM) was used to investigate the nature of the porosity in the Kimmeridge Clay Formation.

1.7: Assessment of Unconventional Reservoir Potential of the Kimmeridge Clay Formation

The study of the Upper Jurassic Kimmeridge Clay as an active source rock previously identified by Goff, 1983; Cornford and Brookes, 1989; Cooper et al., 1995; Erratt et al., 2010; Field, 1985; Isaksen and Ledje, 2001; Cornford and Brookes, 1989; Tyson, 1996, 1995, 2004; Tyson, 1996, 1995, 2004; Leythaeuser et al., 1984, 1987; Turner et al., 1987; Isaksen and Ledje, 2001; Erratt et al., 2010) shows that the organic matter quality and facies are highly variable across the North Sea. To date, > 50 billion barrels of oil equivalent (bn boe) have been produced from reservoirs for which the Kimmeridge Clay was the source rock using conventional drilling techniques with remaining reserves of around 24 billion boe, and a further 21 billion boe (recovery rates of 5%) or 42 billion boe (recovery rate of 10%) of estimated unconventional oil (Scotland Means Business, 2014). A TOC range of 2- 9 wt.% with an average of about 5.61 wt.% TOC have been recorded for the Kimmeridge Clay Formation, and due to its high organic matter content it could also be a good prospect for unconventional play in the future (Cornford et al., 2014).

The Upper Jurassic Kimmeridge Clay Formation was formed under similar structural and tectonic conditions to some of the North American shale plays (Table 1-3 to 1-5), and is stratigraphically equivalent to the Upper Jurassic Haynesville Formation, which was deposited in a shallow marine environment in the Late Jurassic (Winker

and Buffler, 1988; Nunn, 1990; Mancini and Puckett, 2005; Galloway, 2008; Mancini et al., 2005, 2008; Al-Haddad and Mancini, 2013). The Haynesville Formation was formed during Kimmeridgian to Tithonian (Nunn et al., 1984; Ewing, 2009), and the Kimmeridge Clay Formation range in age from Volgian to Ryazanian stages of the Late Jurassic (Goff, 1983; Cornford and Brookes, 1989; Cooper et al., 1995).

The Haynesville shale average layer thickness is about 60- 90 m, and these are characterised by mixed mudstone and siliciclastic lithologies (Nunn, 2012), similar to the thickness range of 70-200m in mudstone and interbedded sandstone of the Kimmeridge Clay Formation (Cornford et al., 2014).TOC values for the Haynesville range from 2-6 wt.%, and the mudstones contain abundant carbonate, clay and quartz, figures similar to TOC range of 2-9 wt.%, and predominantly quartz, carbonate, clay minerals for the Kimmeridge Clay Formation (Cornford et al., 2014). The Kimmeridge Clay is a classic Type II marine kerogen with some influence from terrestrial derived material, this is also similar to Type II kerogen for the Haynesville Formation (Mancini et al., 2006, 2008; Nunn, 2012) with 0.55 %Ro -1.3 %Ro thermal maturation (Nunn, 2012).

Regional source rock mapping together with maturation studies shows that the Kimmeridge Clay Formation is mature for oil generation (Cooper and Barnard, 1984; Cornford 1998; Goff, 1983; Cornford and Brookes, 1989; Cooper et al., 1995), with an original HI of up to 550 mg HC/g TOC (Cornford, 1994). Oil generation from this Type II Kimmeridge Clay source rock occurs between thermal maturity values 0.55-1.1 %Ro (Isaksen, 2004) and reached this maturity level in the Tertiary with the highest oil saturations occurring at a maturity of 0.8 % Ro (Cornford et al., 2014). Continuous subsidence since the Lower Cretaceous in the North Sea area suggests that oil is still actively being generated in the Kimmeridge Clay source rock (Cornford, 1994; Cornford et al., 2014).

At an early stage of maturation, the oil generated from kerogen in the mudstones will start to saturate any available porosity. With increasing maturation, the mudstone porosity will be filled and, subject to adequate permeability, localised expulsion will start to fill the open pore spaces of sandstones in close proximity. Pyrolysis, solvent

extraction and mass balance based on elemental analysis evidence demonstrate that oil expulsion efficiency is as high as 60 % at a given maturity level for thinly interbedded sand-shale (Cooles et al., 1986; Wilhelms et al., 1990; Cornford, 1994) and the mudstones will contain the retained oil prior to, during and after expulsion. The major influence on expulsion appears to be the thickness (> 50m) and organic-richness (> 2 % TOC) of the Kimmeridge source rocks (Cooles et al., 1986; Cornford, 1994; McAulliffe, 1980). This expulsion process results in some changes in the chemical composition through geo-chromatography fractionation leading to the expulsion of less polar molecules and asphaltenes and more saturates in the expelled oil (Leythaeuser et.al., 1984), leaving the retained 'residual' oil conversely enriched.

Geo-chromatographic fractionation of the expelled oil would likely occur as the oil undergoes expulsion and migration from the source rock into non-source rocks. In this process, the heavy oil (the higher molecular weight and more viscous, polar fraction dominated) with more polar hydrocarbon components is retained in the mudstones (adsorbed on the clay mineral surfaces), while the lighter oil is drained into the interbedded sandstones (Leythaeuser et.al., 1984). These organic-lean, but oil mature interbedded sandstones would be expected to have free oil (S_1) stored in their pores resulting in high productivities due to the short distances required for the migration of weakly adsorbed oil within the porous intervals (Leythaeuser et al., 1982, 1984, 1987). Migration of the generated oil from source rock have been attributed to buoyancy and pressure gradients; with oil and gas moving as two separate phases, and as the generated hydrocarbon migrates from the source rocks into lower temperature and pressure thinly interbedded mudstone-sands (Cornford et al., 1986; Cayley, 1987; Thomsen et al., 1990; Hunt, 1996)

Expulsion efficiency defined as the fraction of generated oil that has left the source rock (Cornford, 1998) are in the 2-12 % range (Cornford, 1994); meaning some amounts of oil remains within the mudstone, interbedded sandstone, and in the migration paths of the basin (Jarvie, 2012; Cornford et al., 2014). Expulsion efficiency changes with source rock maturity, and can be constructed from Rock-Eval data; where the decrease in Hydrogen Index reflects generation, the increase in Production

Index (PI) reflects retention, and the difference represents the amount of hydrocarbon expelled (Cornford, 1998). This low expulsion efficiency of the Kimmeridge Clay Formation is a good encouragement for future exploration of unconventional resources since it indicates that a significant amount of hydrocarbon remain to be discovered (Kimmeridge Energy, 2012; Cornford et al., 2014; Raji et al., 2015). Despite this potential, relatively few studies (Cornford et al., 2014; Kimmeridge Energy, 2014) are available on detailed investigations of the Kimmeridge Clay Formation as a potential for unconventional shale oil resources. This type of study is needed to solve the problems of energy demand in the UK, and this thesis is an attempt to address some of this need.

1.8: Syntheses of Research, Aim and Structures

In this section, the structure of the remainder of this thesis is summarised. For each Chapter, the aims and rationale for undertaking the work is detailed, followed by a brief description of the key findings.

Chapter 2: Geochemical Database Sample Collection and Analytical Methods

This chapter uses the available TOC and thermal maturity data available from IGI Ltd on p: IGI-3 database by applying the sweet-spot criteria adopted in Sections 1.5-1.6 in this chapter for selection of samples to be used for this study. The p: IGI-3 database assembled from over 7,000 core and cutting samples with total organic carbon (TOC), Rock-Eval and organic petrography data available in p: IGI-3 format were used for Chapters 3 and 5. The sample selection was initially based on the amount of organic matter using a cut-off range of > 2 % TOC and thermal maturation range of 0.5-0.8 $\%R_o$. Lithological criteria were based on visual observation of core materials from British Geological Survey (BGS) online offshore hydrocarbon wells material database. The selected core samples were then logged and collected at the British Geological Survey core stores in Nottingham and brought back to Durham for sample preparation prior to laboratory analyses. Independent TOC, Rock-Eval Pyrolysis, stable carbon isotope, XRD, thin-section petrography, FIB-SEM, organic petrography and kerogen isolation were performed at different laboratories on the selected samples. The results of these analyses discussed in detail in Chapters 4, 6 and 7 were

used to define unconventional shale oil potential of the Kimmeridge Clay Formation using the sweet-spots criteria adapted in Section 1.6-1.7 of this chapter in terms of their; thickness (> 20 m), the organic matter quality (> 2% TOC), kerogen type (classic Type II and I), thermal maturation (early-late oil window), mineralogical composition (predominantly quartz), porosity (organic, interparticle and intraparticle pores) and high oil saturation index (OSI).

Chapter 3: Source Rock, Distribution and Oil Potential

Initial literature reviews from previous author in Section 1.4 of this chapter shown that the Kimmeridge Clay Formation and the underlying Heather Formation collectively called the Viking Group is the major source rock for the North Sea hydrocarbon. As such, it is important to know the variation in thickness, facies and quality of the source rock across the study area. In this chapter, the thicknesses and distributions of these source rock horizons were systematically mapped from well top and base data based on grids from Millennium Atlas (Evans et al., 2013), with the near Base Cretaceous Unconformity (BCU) grid defined. The thicknesses were calculated from the mapped tops and bases, well formation data grids were created in Trinity software, where isopach and distribution maps were generated. This realistic approach was chosen since defining formation tops and bases from seismic data is beyond the scope of this study, and the well formation data were readily available online.

In order to unravel the variations in source rock facies and potential, geochemical database of over 7000 source rock cores and cutting samples from the BGS and Norwegian Petroleum Directorate (NPD) made available by IGI Ltd were used to characterise the source rocks into different organofacies. The geochemical data available include TOC and Rock-Eval, and organic petrographic data, the interpretation of these data was carried out using p: IGI-3 software. The TOC and Rock-Eval data was used to evaluate the organic-richness, which were ultimately used to define the oil and gas potentials of these source rocks. The average TOC values recorded for the Viking Group is up to 5 wt.% with a maximum of TOC of 11 wt.% indicating a fair to very good organic richness. In terms of maturity, burial

depth, Rock-Eval S_2 to S_1, HI and T_{max} data were used delineate the start of the oil window and as maturity indicator.

A combination of HI and T_{max} data was used to investigate the kerogen types, which were found to predominantly consist of Type II and Type III kerogens as end members, with the mixture of Type II/III kerogen dominating. Organic petrographic data shows the maceral is dominated by liptinite and vitrinite with some inertinite. A comparison of macerals abundance with Rock-Eval HI results on a sample by sample basis shows that there is a positive correlation between the Hydrogen Index (HI) of the source rocks and their maceral composition.

The work in this chapter has been prepared to be submitted to the Journal of Geological Sciences.

Chapter 4: the Effect of Sandstone in Unconventional Reservoir Properties

In Section 1.4, it was shown from previous studies that a significant part of the remaining and future potential of oil in this region is anticipated to be retained in the actively generating Kimmeridge Clay Formation source rocks buried below 3.4-4.3 km (Cornford et al., 2014). These organic-rich mudstone are intimately interbedded with coarse clastics sediments of the Brae Member termed a 'hybrid 'shale resource system. As such, this hybrid system may hold more volume of retained oil due to the increased storage capacity that may be present in the sand-silt interbeds.

The work in this chapter based on analyses of 18 mudstone-sandstone core samples from Well 16/17-14, 16/17-18, 16/18-2 and 16/17-19 was used to investigate in more detail the effect of sandstone interbeds on shale reservoir properties in terms of TOC, kerogen type, thermal maturation, free oil (S_1), generated oil (S_2) and hydrocarbon storage capacity. The 18 samples were selected based on the visual inspection of slabbed cores by estimating percentages of mudstone and sandstones at different intervals from four wells drilled between 1984 and 1991. Three gross facies were recognised across the study area; Kimmeridge Clay 'hot shale' (both Upper and Lower), an intermediate facies of interbedded sands and mudstones termed the tiger stripe facies, and massive sand and conglomerates of the Brae Formation.

The lithological differences between these source rocks are reflected by the wide ranges of TOC. The TOC is higher in the mudstone-dominated samples (6.3 wt.% average) than in the sandstone dominated samples (1.4 wt.% average). A clastic dilution model was proposed for the wide variation in TOC and maturity values. The kerogen type determined mainly from Rock-Eval analysis plots of Hydrogen Index (HI) versus T_{max} , HI versus Oxygen Index (OI), and TOC versus S_2 (remaining petroleum generation potential) indicate predominantly a classical Type II oil (and associated gas) prone kerogen in both the mudstones and sandstones. These source rocks are both derived from bacterially degraded algal organic matter, with the isotope and nitrogen composition reflecting the residue of different bacterial metabolic pathways (sulphate-reducing versus methane-generating bacteria). Rock-Eval T_{max} values of 432 °C (early mature) to 439 °C (mid-mature) equate to the 3-4 km interval placing the samples in a limited range of early oil window maturation.

The Oil Saturation Index (OSI= S_1/TOC) shows higher values for the sandstone-rich samples relative to the mudstones, and higher values for lower TOC samples at early-mature level of maturation. Migration of free oil (S_1) from the mudstone into the interbedded sandstone involves a short lateral distance through the sandstone pores from the source to storage in the interbeds which may result in high productivity. It is implied that the sand-rich samples have retained rather than drained oil because the abundance of sandy layers would be expected to define drainage.

The abundance and preservation of silicate minerals in the sand-rich samples suggest little diagenetic alteration which is likely to exert control on the brittleness with increased storage capacity due to larger matrix porosities of the sand-silt interbeds and lower adsorptive affinity in the interbedded sandstone. The unconventional reservoir potential of the Upper Jurassic source rocks in the area is therefore controlled by the lithology variation, clastic dilution, thicknesses, burial depth, organic-richness, maturity, amount of free S_1 oil, oil saturation, storage capacity and ability to capture portion of the expelled, as well as retained oil. Using the sweet-spot criteria in Section 1.6-1.7 of this chapter, this hybrid shale system can be modelled to produce liquid hydrocarbon like the North American analogues (e.g. Bakken, Barnett,

Eagle Ford, Haynesville and Marcellus shale plays). The work in this chapter has been published in the Journal of Marine and Petroleum Geology.

Raji, M., Gröcke, D. R., Greenwell, C. H., Gluyas, J. G. and Cornford, C., 2015. The Effect of Sand Interbedding on Shale Reservoir Properties. Journal of Marine and Petroleum Geology 67, 154-169.http://dx.doi.org/10.1016/j.marpetgeo.2015.04.015.

Chapter 5: Porosity and Productivity in the Kimmeridge Clay Formation

This chapter uses a large accessible public geochemical database of rock properties from the UK and Norwegian sectors of the South Viking Graben to investigate where the 'retained oil' is located at peak oil maturity. The majority of the assembled geochemical data in p: IGI-3 is from UK Quadrant 16 and Norwegian Quadrants 15, 16 and 17 from 65 wells that penetrated the Upper Jurassic-Early Cretaceous Kimmeridge "Hot Shale" and the underlying Brae Member of the Kimmeridge Clay Formation. These units comprising the Viking Group (discussed in detail in Chapter 3), where coarse clastic fan Brae sediments were injected mainly from the western boundary fault and deposited into the anoxic basins with the organic-rich Kimmeridge Clay hot shale (examined in Chapter 4). Geochemical data available includes TOC, Rock-Eval pyrolysis of 552 samples and 94 samples reporting a Saturate/Aromatic ratio, and 83 samples of carbon-normalised extract (CNE) value (mgExtract/g TOC). Helium porosity, light permeability and visual sand estimations analyses carried out on 34 samples from 6 of these wells by IGI Ltd were provided for this study.

In Chapter 4, it was recognised that free oil determined from Rock-Eval® S_1 (free hydrocarbon) yields is used to place limits on the drainage of oil from source mudstone to reservoir sand at the decimeter scale. The S_1 data in Chapter 4 indicate that the higher values of free hydrocarbon suggest that more oil is being retained in the mudstone, while higher S_1 values in the interbedded sands suggest the oil is being drained to saturate the larger pore spaces. It was then established that the Rock Eval obtained S_1 parameter is a key factor for investigating the retention and drainage of

retained un-expelled oil in the mudstones as well as expelled oil in the mudstone-sand interbeds, and leading to further investigation in Chapter 5.

The S_1 peak (kg free liquid per tonne of rock) data was used to determine the volume of oil that can be potentially produced by hydraulic fracking of these organic rich mudstones at peak oil maturity. In addition, solvent extracts also gives a measure of free oil, though solvent evaporation removes the light oil components (< C12 molecules) preferentially. Using the mass balance argument that indicates that the decrease in S_2 is an indication of 'oil generation', then S_1 would indicate 'oil retention' rather than production. This means an increase in S_1 is indicative of an increase in available storage of 'free oil S_1' and its decreases indicates loss of storage of 'free oil S_1' or decrease in adsorptive surface area.

Relationships between TOC and S_1 derived from cross-plots where the majority of > 2 wt.% TOC samples (89.5 %) show a strong positive correlation. The gradient indicated that the 'free oil S_1'is partitioned between the kerogen surface and micro-porosity, but given the size of the molecules the oil is more likely to be adsorbed onto the kerogen surface. Saturates and aromatic fractions yield (Sats+Aroms, kg/tonne) is consistently higher than the Rock-Eval S_1 yield, this shows a poor relationship. This means while thermal extraction from about T_{max} = 350 °C releases the 'free oil', the solvent extraction also removes adsorbed hydrocarbons and then possibly solvent swelling releases petroleum trapped in closed porosity. This means if storage is in mineral porosity both thermal and solvent extraction should give similar results but this is not the case.

Higher porosities were observed using logs and SEM (quantified using QEMscan mode) which cover the upper range of Helium porosities. The comparisons of S_1 volumes (1.8 vol. %) against mudstones porosities (1.62 vol.%), suggests that the open porosity is fully saturated with oil at peak maturity. The distributions of porosity and S_1 yields are similar, which means S_1 storage and hence porosity appear to be within the kerogen (intra-kerogen porosity) rather than between the grains (inter-granular mineral porosity). The work in this chapter leads to the recommendation that for an improved identification of 'sweet spot' targets for optimum liquid hydrocarbon

production, further mapping of both 'free' and 'adsorbed' oil and the nature of the different porosities at different maturation level is necessary.

The work in this chapter has been published in the Proceedings of the Unconventional Resources Technology Conference held in San Antonio, Texas, USA, 20-22 July 2015.

Raji, M., Gröcke, D. R., Greenwell, C. H., and Cornford, C., 2015. Pyrolysis, Porosity and Productivity in Unconventional Mudstone Reservoirs: 'Free' and 'Adsorbed' Oil. Proceedings of the Unconventional Resources Technology Conference held in San Antonio, Texas, USA, 20-22 July 2015.

Chapter 6: Nature and Type of Organic Porosity in the Kimmeridge Clay Formation

In Chapter 5, it was established that the free oil S_1 of the Kimmeridge Clay Formation appears to be mostly within the kerogen (intra-kerogen porosity) rather than between the grains (inter-granular mineral porosity) in the system. The resulting information obtained from this chapter suggested further investigation was required into the characterisation and nature of porosity of the Kimmeridge Clay Formation. In this work, further characterisation of porosity type at different level of maturity was achieved using high resolution focused ion beam milling and scanning electron microscopy (FIB-SEM) together with Energy Dispersive X-ray Spectroscopy (EDS) imaging techniques at various scales and resolutions. The main objective of this study is to systematically classify the texture, shape, sizes and distribution of the types of porosities of organic-rich Kimmeridge Clay Formation mudstones and sandstone interbeds at different levels of organic-richness and maturity.

In this study, 5 mudstone-sandstone core samples obtained from 3 wells from the British Geological Survey were imaged with a dual beam FIB-SEM. Three distinct types of porosity of varying shapes and sizes were observed across all samples; organic pores occurring within the organic matter, interparticle pores occurred between mineral grains, inter-crystalline pyrite and organic matter while intraparticle pores occurred within the mineral grains and the organic matter. The dominant porosities in the Kimmeridge appear to be interparticle and intraparticle pores

occurring mostly in the mineral grains, where the storage of the remaining un-expelled hydrocarbon is expected to be significant for unconventional shale reservoir. X-ray diffraction (XRD) and EDS results suggest these samples are dominated by quartz, clay, organic matter, mica and pyrite.

This work is currently being prepared to be submitted to Journal of Marine and Petroleum Geology

Chapter 7: Effect of Demineralisation on Kerogens

Kerogen is the insoluble part of sedimentary organic matter (OM) from which hydrocarbons are generated (Durand, 1980; Durand and Nicasie, 1980). Kimmeridge Clay source rocks that are characterized by hydrogen-rich kerogen produce oil (and possibly gas upon further maturation); whereas those with hydrogen-poor kerogen yield only gas (Horsfield and Douglas, 1980). The inorganic mineral of these source rocks consists mainly of quartz, clay, carbonates, pyrite and other trace elements. This chapter investigates the interaction between the kerogens and the inorganic mineral matrix during pyrolysis; in order to understand how mineral matter may affect the quality and quantity of organic matter, kerogen type, thermal maturation and generative potential of the Kimmeridge Clay Formation.

For this study, 27 core samples of organic rich Upper Jurassic mudstones from 10 wells within UK Quadrant 16 of the South Viking Graben were made available by the British Geological Survey. These samples covered a range of depths, maturities and lithologies and are compared to lower maturity sample sets from Lower Jurassic-Liassic outcrops from Dorset, Somerset and Glamorgan (South Wales). The first approach was the separation of organic kerogen from inorganic minerals by acid digestion using HCl and HF to obtain pure unaltered isolated kerogens. TOC, Rock-Eval, carbon stable isotope and organic petrographic analyses were undertaken on the whole rock and the isolated kerogens. Interpretation and comparisons between the whole-rock samples and isolated kerogen is investigated to understand how demineralisation affects kerogen quality.

In the North Sea samples, the TOC values in the whole rock samples is between 2.7-8.9 wt. % TOC, while the TOC values in the isolated kerogens (52-74 wt.%) are much higher. The isolated kerogens are expected to be higher than the whole rock samples; however, the range of TOC values in isolated kerogen suggests that not all mineral matrixes were removed during the demineralization process. Petrographic observations indicate that minerals such as quartz and clay (silicates), and carbonates had been removed, but that pyrite remained. The S_1 yield from isolated kerogen, plus non-reactive minerals (i.e., pyrite) left after the HCl/HF maceration (pyrite) ranges from 19 -105 mg HC/g kerogen isolate (average 40 mg HC/g kerogen isolate), whilst the whole rock (WR) S_1 values derived from the free oil in the kerogen plus minerals (carbonate, clay, silicates, pyrite) range from 1-10 mg HC/g rock (average: 3.7 mgHcmg HC/g rock). Given the difference in the range of S_1 values, it can be argued that the 'free oil S_1' is trapped in the porosity of the kerogen. This means any S_1 adsorbed on the mineral matrix is liberated during acid maceration, and attached to the kerogen upon sample drying.

In terms of maturity, the T_{max} values plotted against burial depth placed most of the samples within the oil window, and indicate no effect of demineralisation on oil window maturity. Vitrinite reflectance calculated from T_{max} values using the equation: Ro = (0.018 x* T_{max}) - 7.16) of Jarvie, 2007 were used as maturity parameter for the oil window. For the isolated kerogen and the whole rock, the calculated vitrinite reflectance data appears to fall within the early to mid- oil window with reflectance values ranging from 0.45-1.01 % Ro (with an average between 0.73 % Ro and 0.70 % Ro). HI values are slightly higher in the whole-rock samples, with values between 84-596 mg HC/g TOC and an average of 255 mg HC/g TOC, and for isolated kerogens, range from 103-424 mg HC/g TOC with an average of 235 mg HC/g TOC. However, the distribution of kerogen types is similar in both the isolated kerogen and whole rock indicating no effect of mineral removal on the determination of the kerogen types from HI values.

The work in this chapter has been prepared to be submitted to Journal of Unconventional Resource Technology.

Chapter 8: Summary, Conclusion and Recommendations for Future Work

A thorough integration of different data is important for the understanding of source rock properties. This final chapter summarises findings from the application and integration of geochemical, mineralogical, petrographic and porosity techniques in the assessment and evaluation of the Upper Jurassic Kimmeridge Clay Formation as a potential unconventional hydrocarbon resource. The key shale reservoir parameters for sweet-spots prediction and identification (such as lithology, mineralogy, area extent, depth, thicknesses, total organic carbon (TOC), maturity, porosity, and adsorption capacity of source rocks) identified in Chapter 1, based on analogues from successful shale plays in the United States and used throughout this research, are summarised in Chapter 8. A further research approach for maceral separation by density gradient centrifugation (DGC) is also discussed. This approach was adopted for this thesis but become unfeasible due to several failed attempts to completely remove minerals such as pyrite that are intimately attached onto the macerals. Finally, recommendations for future work for optimum exploration, production and economics that are predicted to work with a hybrid offshore unconventional system are made.

1.9: References

Abrams, M., Dieckmann, V., Curiale, J. and Clark, R., 2014. Hydrocarbon Charge Considerations in Liquid-Rich Unconventional Petroleum Systems. American Association of Petroleum Geologists Search and Discovery Article, (#80366).

Akinlua, A., Ajayi, T., Jarvie, D. and Adeleke, B., 2005. A Re-appraisal of the Application of Rock-Eval Pyrolysis to Source Rock Studies in the Niger Delta. Journal of Petroleum Geology, 28(1), pp.39-48.

Al Haddad, S. and Mancini, E., 2013. Reservoir characterization, modeling, and evaluation of Upper Jurassic Smackover microbial carbonate and associated facies in Little Cedar Creek field, southwest Alabama, eastern Gulf coastal plain of the United States. American Association of Petroleum Geologists Bulletin, 97(11), pp.2059-2083.

Andrews, I., 2013. The Carboniferous Bowland Shale gas study: geology and resource estimation. London, UK: British Geological Survey for Department of Energy and Climate Change, pp.1-56.

Aplin, A. and Macquaker, J., 2011. Mudstone diversity: Origin and implications for source, seal, and reservoir properties in petroleum systems. American Association of Petroleum Geologists Bulletin, 95(12), pp.2031-2059.

Armstrong, J., Smith, J., D'Elia, V. and Trueblood, S., 1997. The occurrence and correlation of oils and Namurian source rocks in the Liverpool Bay-North Wales area. Geological Society, London, Special Publications, 124(1), pp.195-211.

Avanzini, A., Balossino, P., Brignoli, M., Spelta, E. and Tarchiani, C., 2016. Lithologic and geomechanical facies classification for sweet spot identification in gas shale reservoir. Interpretation, 4(3), pp.SL21-SL31.

Baird, R., 1986. Maturation and Source Rock Evaluation of Kimmeridge Clay, Norwegian North Sea. American Association of Petroleum Geologists Bulletin, 70(1), pp.1-11.

Barnard, P. and Bastow, M., 1991. Hydrocarbon generation, migration, alteration, entrapment and mixing in the Central and Northern North Sea. Geological Society, London, Special Publications, 59(1), pp.167-190.

Bassett, J., Watters, J., Combs, N. and Nikolaou, M., 2013. Lowering Drilling Cost, Improving Operational Safety, and Reducing Environmental Impact through Zonal Isolation Improvements for Horizontal Wells Drilled in the Marcellus Shale. Proceedings of Unconventional Resources Technology Conference. Denver, Colorado, USA.12-14 August.

Behar, F., Beaumont, V. and De B. Penteado, H., 2001. Rock-Eval 6 Technology: Performances and Developments. Oil & Gas Science and Technology, 56(2), pp.111-134.

Bergen, F., Zijp, M., Nelskamp, S. and Kombrink, H., 2013. Shale gas evaluation of the Early Jurassic Posidonia Shale Formation and the Carboniferous Epen Formation in the Netherlands. In: J. Chatellier and D. Jarvie, ed., Critical assessment of shale resource plays. American Association of Petroleum Geologists Memoir 103, 1-24.

Bernard, S. and Horsfield, B., 2014. Thermal Maturation of Gas Shale Systems. Annual Review of Earth and Planetary Sciences, 42(1), pp.635-651.

Bernard, S., Brown, L., Wirth, R., Schreiber, A., Schulz, H., Horsfield, B., Aplin, A. and Mathia, E., 2013. FIB-SEM and TEM Investigations of an Organic-rich Shale Maturation Series from the Lower Toarcian Posidonia Shale, Germany: Nanoscale Pore System and Fluid-rock Interactions. In: Electron Microscopy of Shale Hydrocarbon Reservoirs. American Association of Petroleum Geologists Memoir 102, pp.53-66.

Bernard, S., Horsfield, B., Schulz, H., Wirth, R., Schreiber, A. and Sherwood, N., 2012. Geochemical evolution of organic-rich shales with increasing maturity: A STXM and TEM study of the Posidonia Shale (Lower Toarcian, northern Germany). Marine and Petroleum Geology, 31(1), pp.70-89.

Bowker, K., 2007. Barnett Shale gas production, Fort Worth Basin: Issues and discussion. American Association of Petroleum Geologists Bulletin, 91(4), pp.523-533.

BP plc, 2011. BP Statistical Review of World Energy 2011, International Energy Agency, Special Report: Are We Entering the Golden Age of Gas? [online] Available at::
http://www.bp.com/content/dam/bpcountry/de_de/PDFs/brochures/statistical_review_of_world_energy_full_report_2011.pdf [Accessed 24 May 2016].

British Geological Survey, 2012. The Impact of Shale Gas on Energy Markets. Written evidence submitted by the British Geological Survey (ISG 17) to the UK Commons Select Committee. [online] Available at::

https://publications.parliament.uk/pa/cm201213/cmselect/cmenergy/785/785.pdf [Accessed 9 Mar. 2017].

British Geological Survey, 2013. Bowland Shale Gas Study. [online] DECC Promote. Available at:: https://www.gov.uk/government/publications/bowland-shale-gas-study [Accessed 21 Apr. 2015].

Bryant, I., Stabell, C. and Neumaier, M., 2013. Evaluation of Unconventional Resources Using a Petroleum System Modeling Approach. Proceedings of Unconventional Resources Technology Conference, Denver, Colorado, USA. 12-14 August 2013.

Bustin, A. and Bustin, R., 2012. Importance of rock properties on the producibility of gas shales. International Journal of Coal Geology, 103, pp.132-147.

Caineng, Z., Dong, D., Wang, S., Li, J., Li, X., Wang, Y., Li, D. and Cheng, K., 2010. Geological characteristics and resource potential of shale gas in China. Petroleum Exploration Development, 37(6), pp.641–653.

Caineng, Z., Shizhen, T., Bin, B., Zhu, Z., Yuan, H., ZhangGuosheng, Songtao, W., Zhenglian. P. and Lan, Z., 2015. Differences and Relations between Unconventional and Conventional Oil and Gas. China Petroleum Exploration, 20(1), pp.1-16.

Carvajal-Ortiz, H. and Gentzis, T., 2015. Critical considerations when assessing hydrocarbon plays using Rock-Eval pyrolysis and organic petrology data: Data quality revisited. International Journal of Coal Geology, 152, pp.113-122.

Cayley, G.T., 1987. Hydrocarbon migration in the central North Se. In: : Brooks, J., and Glennie, K.W., ed., Petroleum geology of North West Europe.. Graham & Trotman, London, London, pp.549-556.

Chalmers, G. and Bustin, R., 2012. Geological evaluation of Halfway–Doig–Montney hybrid gas shale–tight gas reservoir, northeastern British Columbia. Marine and Petroleum Geology, 38(1), pp.53-72.

Chalmers, G., Bustin, R. and Power, I., 2012. Characterization of gas shale pore systems by porosimetry, pycnometry, surface area, and field emission scanning electron microscopy/transmission electron microscopy image analyses: Examples from the Barnett, Woodford, Haynesville, Marcellus, and Doig units. Association of Petroleum Geologists Bulletin, 96(6), pp.1099-1119.

Charpentier, R. and Cook, T., 2011. USGS Methodology for Assessing Continuous Petroleum Resources. U.S. Geological Survey Open-File Report 2011–1167.

Chen, Z., Osadetz, K. and Chen, X., 2015. Economic appraisal of shale gas resources, an example from the Horn River shale gas play, Canada. Petroleum Science, 12(4), pp.712-725.

Cooles, G., Mackenzie, A. and Quigley, T., 1986. Calculation of petroleum masses generated and expelled from source rocks. Organic Geochemistry, 10(1-3), pp.235-245.

Cooper, B. S. and Barnard,P.C., 1984. Source rocks and oils of the central and northern North Sea. In: Demaison, G and Murris, R.J, ed., Petroleum geochemistry and basin evaluation:. American Association of Petroleum Geologists Memoir 35, pp.303–314.

Cooper, B. S., Bernard, P.C and Telnaes, N., 1995. The Kimmeridge Clay formation of the North Sea. In: Katz, B. J., ed., Petroleum source rocks:. Berlin, Springer-Verlag, pp.89–110.

Cornford, C., 1984. Source rocks and hydrocarbons of the North Sea. In: Glennie, K. W.,, ed., Introduction to the Petroleum Geology of the North Sea. Blackwell Scientific Publications, Oxford, pp.171-209.

Cornford, C., 1998. Source rocks and hydrocarbons of the North Sea. In: Glennie, K.W, ed., Petroleum geology of the North Sea, 4th ed. London, Blackwell Science Ltd, pp.376–462.

Cornford, C. and Brooks, J., 1989. Tectonic controls on oil and gas occurrences in the North Sea area. In: Tankard, A.J. and Balkwill, H.R, ed., Extensional tectonics and stratigraphy of the North Atlantic margins.

Cornford, C. and Brooks, J., 1989. Tectonic controls on oil and gas occurrences in the North Sea area. In: Tankard, A.J. and Balkwill, H.R., ed., Extensional tectonics and stratigraphy of the North Atlantic margins. American Association of Petroleum Geologists/Canadian, Geological Foundation, pp.46- 641.

Cornford, C., 1994. Mandal-Ekofisk(!) petroleum system in the Central Graben of the North Sea,. In: Magoon, L.B., and Dow, W.G., ed., The petroleum system - From source to trap. American Association of Petroleum Geologists Tulsa, Oklahoma, pp.537-571.

Cornford, C., Birdsong, B. and Groves, G., 2017. Offshore Unconventional Oil from the Kimmeridge Clay Formation of the North Sea: A Technical and Economic Case. Unconventional Resources Technology Conference Proceedings, Denver, CO. August 25-27, 2014.

Cornford, C., Morrow, J.A., Turrington, A., Miles, J.A., and Brooks, J., 1983. Some geological controls on oil composition in the UK. North Sea. In: Brooks, J., ed., Petroleum Geochemistry and Exploration of Europe. Geological Society Special Publication, Blackwell Scientific Publications, Oxford, 12, pp.175-194.

Coward, M., Dewwey, J., Hempton, M., and Mange, M., 2003. Tectonic Evolution. In: Evans,D., Graham, C, Armour, A and Bathurst, P, ed., The Millennium Atlas: petroleum geology of the central and northern North Sea, 1st ed. London: The Geological Society of London, pp.17-33.

Cuadrilla Resources Limited, 2011. Cuadrilla Resources Overview. [online] Available at:: http://www.cuadrillaresources.com/who-we-are/overview/> [Accessed 5 Apr. 2015].

Cuadrilla Resources Limited, 2011. Geomechanical Study of Bowland Shale Seismicity. [online] Available: http://www.cuadrillaresources.com/wp-content/uploads/2012/02/Geomechanical-Study-of-Bowland-Shale-Seismicity_02-11-11.pdf [Accessed 5 Feb. 2015].

Dahl, B., Bojesen-Koefoed, J., Holm, A., Justwan, H., Rasmussen, E. and Thomsen, E., 2004. A new approach to interpreting Rock-Eval S_2 and TOC data for kerogen quality assessment. Organic Geochemistry, 35(11-12), pp.1461-1477.

Davies, R., Foulger, G., Bindley, A. and Styles, P., 2013. Induced seismicity and hydraulic fracturing for the recovery of hydrocarbons. Marine and Petroleum Geology, 45, pp.171-185.

Davies, R.J., O'Donnell, D., Bentham, P.N., Gibson, J.P.C., Curry, M.R., Dunay, R.E. and Maynard, J.R., 1999. The origin and genesis of major Jurassic unconformities within the triple junction area of the North Sea, UK. Geological Society of London, Petroleum Geology Conference Series, 5, pp.117–131.

Department of Energy and Climate Change, 2013. United Kingdom Continental Shelf (UKCS) Geological Basins. [online] Available at:: https://www.gov.uk/oil-and-gas-offshore-maps-and-gis-shapefiles 20140331_UKCS_Geological_Basin [Accessed 22 Apr. 2014].

Department of Energy and Climate Change, 2011) 14th Onshore Licensing Round.. [online] https://www.og.decc.gov.uk/upstream/licensing/onshore_14th/index.htm> [Accessed 22 Jul. 2014].

Department of Energy and Climate Change, 2010. The hydrocarbon prospectivity of Britain's onshore basins.http://og.decc.gov.uk/assets/og/bo/onshore-paper/uk-onshore-shalegas.pdf [Accessed 6 Jun. 2015].

Ding, W.L., Chao, L., Chunyan, L., Changchun, X., Kai, J., Weite, Z. and Liming, W., 2012. Fracture development in shale and its relationship to gas accumulation. Geoscience Frontier, 3, pp.97–105.

Domínguez, R., 2007. Structural evolution of the Penguins Cluster, UK northern North Sea. Geological Society, London, Special Publications, 292(1), pp.25-48.

Dorrick A. V., 1983. Sedimentology of the Brae Oilfield Area, North Sea: a reply. Journal of Petroleum Geology, 6, pp.103-104.

Dow, W., 1977. Kerogen studies and geological interpretations. Journal of Geochemical Exploration, 7, pp.79-99.

Durand, B., 1980. Definition of kerogen in Kerogen: insoluble organic matter from sedimentary rocks.. Technip, Paris, pp.22-33.

Durand, B. and Nicaise, G., 1980. Procedures for kerogen isolation in Kerogen: insoluble organic matter from sedimentary rocks.. Technip, Paris, pp.35-52.

East, J.A., Swezey, C.S., Repetski, J.E and Hayba, D.O., 2012. USGS Scientific Investigations Map 3214: Thermal Maturity Map of Devonian Shale in the Illinois, Michigan, and Appalachian Basins of North America. [online] Pubs.usgs.gov. Available at:http://pubs.usgs.gov/sim/3214/ [Accessed 4 Apr. 2017].

Energy and Climate Intelligence Unit Briefings, 2015. Fracking in the UK. http://eciu.net/briefings/uk-energy-policies-and-prices/does-fracking-have-a-future-in-the-uk [Accessed 7 Jun. 2017].

Energy Information Administration, 2012. U.S. Energy Information Administration (EIA): World Shale Resource Assessments. [online] Eia.gov. https://www.eia.gov/analysis/studies/worldshalegas/ [Accessed 7 Apr. 2017].

Erratt, D., Thomas, G.M. and Wall, G.R.T., 1999. The evolution of the Central North Sea Rift. In: Fleet, A.J. and Boldy, S.A.R., ed., Petroleum Geology of Northwest Europe:. Proceedings of the 5th Conference, pp.63-82.

Erratt, D., Thomas, G.M., Hartley, N.R., Musum, R., Nicholson, P.H and Spisto, Y., 2017. North Sea hydrocarbon systems: some aspects of our evolving insights into a

classic hydrocarbon province. In: Vining, B., and Pickering, S.C, ed., Petroleum Geology: From Mature Basins to New Frontiers. Proceedings of the 7th Petroleum Geology Conference. Geological Society of London, London, England, pp.37-56.

Espitalié, J., and Bordenave, M.L., 1993. Source rock parameters. In: Bordenave, M.L.,, ed., Applied Petroleum Geochemistry, 2nd ed. pp.237-272.

Espitalié, J., Deroo, G., and Marquis, F., 1985. Rock-Eval Pyrolysis and Its Applications (Part Two). Oil & Gas Science and Technology Review IFP 40, pp.755-784.

Espitalié, J., Deroo, G., and Marquis, F., 1985. Rock-Eval Pyrolysis and Its Applications (Part One). Oil & Gas Science and Technology Review, IFP 40, pp.563-579.

Evans, D., Graham, C., Armour, A., and Bathurst, P., 2003. The Millennium Atlas: Petroleum Geology of the Central and Northern North Sea.. London, Geological Society, pp.17-33.

Ewing, T. E., 2009. The ups and downs of the Sabine Uplift and the northern Gulf of Mexico Basin: Jurassic basement blocks, Cretaceous thermal uplifts, and Cenozoic flexure. Gulf Coast Association of Geological Societies Transactions, 59, pp.253– 269.

Færseth, R., 1996. Interaction of Permo-Triassic and Jurassic extensional fault-blocks during the development of the northern North Sea. Journal of the Geological Society, 153(6), pp.931-944.

Fishman, N.S., Egenhoff S.O., Boehlke, A.R. and Lowers, H.A., 2015. Petrology and diagenetic history of the upper shale member of the Late Devonian–Early Mississippian Bakken Formation, Williston Basin, North Dakota. Geological Society of America Special Paper, Denver, CO, pp.125-151.

Fraser, S.I., Robinson, A.M., Underhill, J.R., Kadolsky, D.G.A, Connell, R., Johannessen, E.P., and Ravnas, R., 2003. Upper Jurassic. In: Evans, D., Graham, C.,

Armour, A., and Bathurst, P., ed., The Millennium Atlas: Petroleum Geology of the Central and Northern North Sea. Geological Society, London, pp.157-189.

Furmann, A., Mastalerz, M., Brassell, S., Pedersen, P., Zajac, N. and Schimmelmann, A., 2015. Organic matter geochemistry and petrography of Late Cretaceous (Cenomanian-Turonian) organic-rich shales from the Belle Fourche and Second White Specks formations, west-central Alberta, Canada. Organic Geochemistry, 85, pp.102-120.

Galbraith, K., 2010. Dash for Gas Raises Environmental Worries. [online] Nytimes.com. Available at:: http://www.nytimes.com/2010/07/12/business/energy-environment/12iht-green.html [Accessed 15 Mar. 2017].

Gale, J., Reed, R. and Holder, J., 2007. Natural fractures in the Barnett Shale and their importance for hydraulic fracture treatments. Association of Petroleum Geologists Bulletin, 91(4), pp.603-622.

Gale, J.F.W., Laubach, S.E., Olson, J.E., Eichhubl, P., and Fall, A., 2014. Natural fractures in shale. Association of Petroleum Geologists Bulletin, 98(11), pp.2165-2216.

Galimov, E.M., 2006. Isotope organic geochemistry. Journal of Organic Geochemistry. Journal of Organic Geochemistry, 37(10), p.1200.

Galloway, W. E., 2008. Depositional evolution of the Gulf of Mexico sedimentary basin. In: Miall, A. D., ed., Sedimentary basins of the world 5: The sedimentary basins of the United States and Canada:. Elsevier, Amsterdam, The Netherlands, pp.505–549.

Gas Strategies, 2010. Shale Gas in Europe: A Revolution in the Making?. [online] Available at:: http://www.gasstrategies.com/files/files/euro%20shale%20gas_final.pdf [Accessed 5 Jun. 2017].

Gautier, D. L., 2005. B 2204-C: Kimmeridgian Shales Total Petroleum System of the North Sea Graben Province. [online] Pubs.usgs.gov. Available at:: http://pubs.usgs.gov/bul/2204/c [Accessed 15 Jun. 2014].

Gentzis, T., Goodarzi, F. and Snowdon, L. 1993. Variation of maturity indicators (optical and Rock-Eval) with respect to organic matter type and matrix lithology: an example from Melville Island, Canadian Arctic Archipelago. Marine and Petroleum Geology, 10(5), pp.507-513.

Gilman, J. and Robinson, C. 2011. Success and Failure in Shale Gas Exploration and Development: Attributes that Make the Difference. [online] Adapted from oral presentation at AAPG International Conference and Exhibition, Calgary, Alberta, September 12-15, 2011. http://www.searchanddiscovery.com/documents/2011/80132gilman/ndx_gilman.pdf [Accessed 9 Jul. 2016].

Glennie, K.W. and Underhill, J.R. 1998. Origin, development and evolution of structural styles. In: Glennie, K.W., ed., Petroleum Geology of the North Sea: Basic Concepts and Recent Advances. Blackwell Science, London, pp.42–84.

Goff, J. 1983. Hydrocarbon generation and migration from Jurassic source rocks in the E Shetland Basin and Viking Graben of the northern North Sea. Journal of the Geological Society, 140(3), pp.445-474.

Grathoff, G., Peltz, M., Enzmann, F. and Kaufhold, S. 2016. Porosity and permeability determination of organic-rich Posidonia shales based on 3-D analyses by FIB-SEM microscopy. Solid Earth, 7(4), pp.1145-1156.

Green, C., Styles, P. and Baptie, B. 2012. Preese Hall shale gas fracturing: review and recommendations for induced seismic mitigation. Report for DECC.[online] Available at:: http://www.decc.gov.uk/assets/decc/11/meeting-energy-demand/oil-gas/5055-preese-hall-shalegas-fracturing-review-and-recomm.pdf [Accessed 10 Jul. 2017].

Greenhalgh, E. 2016. The Jurassic shales of the Wessex Area: geology and shale oil and shale gas resource estimation.. British Geological Survey for the Oil and Gas Authority, London, UK.

Hackley, P. and Cardott, B. 2016. Application of organic petrography in North American shale petroleum systems: A review. International Journal of Coal Geology, 163, pp.8-51.

Hackley, P., Fishman, N., Wu, T. and Baugher, G. 2016. Organic petrology and geochemistry of mudrocks from the lacustrine Lucaogou Formation, Santanghu Basin, northwest China: Application to lake basin evolution. International Journal of Coal Geology, 168, pp.20-34.

Hackley, P., Ryder, R., Trippi, M. and Alimi, H. 2013. Thermal maturity of northern Appalachian Basin Devonian shales: Insights from sterane and terpane biomarkers. Fuel, 106, pp.455-462.

Hammes, U., Eastwood, R., McDaid, G., Vankov, E., Gherabati, S., Smye, K., Shultz, J., Potter, E., Ikonnikova, S. and Tinker, S. 2016. Regional assessment of the Eagle Ford Group of South Texas, USA: Insights from lithology, pore volume, water saturation, organic richness, and productivity correlations. Interpretation, 4(1), pp.125–150.

Hartwig, A. and Schulz, H. 2010. Applying classical shale gas evaluation concepts to Germany—Part I: The basin and slope deposits of the Stassfurt Carbonate (Ca2, Zechstein, Upper Permian) in Brandenburg. Chemie der Erde - Geochemistry, 70(S_3), pp.77-91.

Helgeson, D. E. 1999. Structural development and trap formation in the Central North Sea HP/HT play. Geological Society, London 5, pp.1029-1034.

Hemes, S., Desbois, G., Urai, J., Schröppel, B. and Schwarz, J. 2015. Multi-scale characterization of porosity in Boom Clay (HADES-level, Mol, Belgium) using a

combination of X-ray μ-CT, 2D BIB-SEM and FIB-SEM tomography. Microporous and Mesoporous Materials, 208, pp.1-20.

Hodgson, N., Farnsworth, J. and Fraser, A. 1992. Salt-related tectonics, sedimentation and hydrocarbon plays in the Central Graben, North Sea, UKCS. Geological Society, London, Special Publications, 67(1), pp.31-63.

Holditch, S. 2013. Unconventional oil and gas resource development – Let's do it right. Journal of Unconventional Oil and Gas Resources, 1-2, pp.2-8.

Horsfield, B. and Douglas, A. 1980. The influence of minerals on the pyrolysis of kerogens. Geochimica et Cosmochimica Acta, 44(8), pp.1119-1131.

Hunt, J. 1996. Petroleum geochemistry and geology. New York: Freeman.

Husmo, T., Hamar, .G.P, Høiland, O. , Johanessen, E.P., Rømuld, A., Spencer, A.M and Titterton, R 2003. Lower and Middle Jurassic. In: Evans, Graham, Armour and Bathurst,, ed., The Millennium Atlas: Petroleum geology of the Central and Northern North Sea:. Geological Society, London, England, pp.129-155.

Hutton, A. 1987. Petrographic classification of oil shales. International Journal of Coal Geology, 8(3), pp.203-231.

Imber, J., Armstrong, H., Clancy, S., Daniels, S., Herringshaw, L., McCaffrey, K., Rodrigues, J., Trabucho-Alexandre, J. and Warren, C. 2014. Natural fractures in a United Kingdom shale reservoir analog, Cleveland Basin, northeast England. American Association of Petroleum Geologists Bulletin, 98(11), pp.2411-2437.

International Energy Agency (IEA) 2012. Golden Rules for a Golden Age of Gas. World Energy Outlook Special Report on Unconventional Gas. [online] Worldenergyoutlook.org. Available at:: http://www.worldenergyoutlook.org/goldenrules/. [Accessed 1 Sep. 2017].

Isaksen, G.H and Ledje, K.H.I. 2001. Source rock quality and hydrocarbon migration pathways within the greater Utsira High area, Viking Graben, Norwegian North Sea. American Association of Petroleum Geologists Bulletin, 85(5), pp.861–883.

Isaksen, G.H., Patience, R., van Graas, G., and Jenssen, A.I., 2002. Hydrocarbon system analysis in a rift basin with mixed marine and nonmarine source rocks: The South Viking Graben, North Sea. American Association of Petroleum Geologists Bulletin, 86(5), pp.861–883.

Jarvie, D. M 2014. Components and processes affecting producibility and commerciality of shale resource systems. ALAGO 2012 Special Publication, GeologicaActa, 12(, 4,), pp.307-325.

Jarvie, D. M., Brenda L. C., Floyd "Bo" H and John T. B. 2001. Oil and Shale Gas from the Barnett Shale, Ft. Worth Basin, Texas. American Association of Petroleum Geologists National Convention, June 3-6, 2001, Denver, CO. 85, 13 (Supplement), A100.

Jarvie, D., Hill, R., Ruble, T. and Pollastro, R. 2007. Unconventional shale-gas systems: The Mississippian Barnett Shale of north-central Texas as one model for thermogenic shale-gas assessment. American Association of Petroleum Geologists Bulletin, 91(4), pp.475-499.

Jarvie, D.M., 2011. Unconventional Oil Petroleum Systems: Shales and Shale Hybrids. American Association of Petroleum Geologists Search and Discovery Article, #80131.

Jarvie, D.M., 2012. Shale resource systems for oil and gas: part 1 shale-gas resource systems. In: Breyer, J.A., ed., Shale Reservoirs Giant Resources for the 21st Century. American Association of Petroleum Geologists Memoir, 97, pp.pp.69-87.

Jarvis, I., Lignum, J., Gröcke, D., Jenkyns, H. and Pearce, M. (2011). Black shale deposition, atmospheric CO2drawdown, and cooling during the Cenomanian-Turonian Oceanic Anoxic Event. Paleoceanography, 26(3).

Jiao, J., Gan, H. and Wei, Y. 2012. The Impact of Oil Price Shocks on Chinese Industries. Energy Sources, Part B: Economics, Planning, and Policy, 7(4), pp.348-356.

Jinzhou, Z., Yongming, L., Song, W., Youshi, J. and Liehui, Z. 2014. Simulation of complex fracture networks influenced by natural fractures in shale gas reservoir. Natural Gas Industry B, 1(1), pp.89-95.

Johannes, I., Kruusement, K. and Veski, R. 2007. Evaluation of oil potential and pyrolysis kinetics of renewable fuel and shale samples by Rock-Eval analyzer. Journal of Analytical and Applied Pyrolysis, 79(1-2), pp.183-190.

Johannes, I., Kruusement, K., Veski, R., and Bojesen-Koefoed, J., 2006. Characterisation of pyrolysis kinetics by Rock-Eval basic data. Oil Shale, 23, pp.249-257.

Johnson, H., Leslie, A., Wilson, C., Andrews, I. and Cooper, R 2005. Middle Jurassic, Upper Jurassic and Lower Cretaceous of the UK Central and Northern North Sea. British Geological Survey Research Report, RR/03/001, pp.1-44.

Johnson, H.D., and Fisher, M.J., 1998. North Sea plays; geological controls on hydrocarbon distribution. In: Glennie, K.W., ed., Petroleum Geology of the North Sea; Basic Concepts and Recent Advances. Blackwell, Oxford, pp.463-547.

Jones, E., Jones, B., Ebdon C., Ewen, D., Milner, P., Plunkett, J., Hudson, G., Slater, P., Evans, D., Graham, C., Armour, A., and Bathurst, P. 2003. Eocene. In: D. Evans, C. Graham, A. Armour, and P. Bathurst, ed., The MillenniumAtlas; Petroleum Geology of the Central and Northern North Sea. Geological Society, London, pp.261-227.

Justwan, H., Dahl, B. and Isaksen, G. 2006. Geochemical characterisation and genetic origin of oils and condensates in the South Viking Graben, Norway. Marine and Petroleum Geology, 23(2), pp.213-239.

Justwan, H., Isaksen, G. and Meisingset, I. 2005. Quantitative hydrocarbon potential mapping and organofacies study in the greater Balder Area, Norwegian North Sea. In:

A. DoreÅL and B. Vining, ed., Petroleum Geology: North West Europe and Global Perspectives. Proceedings of the 6th Petroleum Geology Conference.

Kavalov, B., Petric, H. and Tzimas, E. 2011. Evolution of the indigenous European oil and gas sources—Recent trends and issues for consideration. Energy Policy, 39(1), pp.487-492.

Kimmeridge Energy 2012. Brother From the Same Mother? The Relationships Between Unconventional and Conventional Oil and Gas Resources. [online] Available at:: http://www.kimmeridgeenergy.com/wp-content/uploads/2012/09/Kimmeridge3.pdf [Accessed 10 Jun. 2017].

King, R. 2015. Modified Method and Interpretation of Source Rock Pyrolysis for an Unconventional World. [online] Available at:: http://www.searchanddiscovery.com/documents/2015/41704king/ndx_king.pdf [Accessed 19 Jun. 2017].

Klaver, J., Desbois, G., Urai, J. and Littke, R. 2012. BIB-SEM study of the pore space morphology in early mature Posidonia Shale from the Hils area, Germany. International Journal of Coal Geology, 103, pp.12-25.

Klemperer, S. and White,, N. 1990. Co-axial stretching or lithospheric simple shear in the North Sea? Evidence from deep seismic profiling and subsidence. In: A. Tankard, and N. Balkwill, ed., Extension tectonics and stratigraphy of the North Atlantic margins. Association for Petroleum Geologists Memoir 46, pp.511--522.

Kubala, M., Bastow, M., Thompson, S., Scotchman, I. and Øygard, K. 2003. Geothermal regime, petroleum generation and migration. In: The Millennium Atlas: Petroleum Geology of the Central and Northern North Sea. Geological Society, London, pp.289-315.

Leythaeuser, D., Radke, M. and Schaefer, R. 1984. Efficiency of petroleum expulsion from shale source rocks. Nature, 311(5988), pp.745-748.

Leythaeuser, D., Schaefer, R. and Radke, M. 1987. On the Primary Migration of Petroleum. Special Paper Proceedings of the 12th World Petroleum Congress, John Wiley & Sons Limited, Chichester, pp.227-236.

Leythaeuser, D., Schaefer, R. and Radke, M. 1988. Geochemical effects of primary migration of petroleum in Kimmeridge source rocks from Brae field area, North Sea. I: Gross composition of C15+-soluble organic matter and molecular composition of C15+-saturated hydrocarbons. Geochimica et Cosmochimica Acta, 52(3), pp.701-713.

Leythaeuser, D., Schaefer,, G. and Yukler, A. 1982. Role of Diffusion in Primary Migration of Hydrocarbons. American Association of Petroleum Geologists Bulletin, 66(4), pp.408-429.

Lombardi, T.E. and Hill D.G. 2002. Fractured Shale Gas Potential in New York. Colorado, Arvada, pp.1–16.

Loucks, R., Reed, R., Ruppel, S. and Hammes, U. 2012. Spectrum of pore types and networks in mudrocks and a descriptive classification for matrix-related mudrock pores. American Association of Petroleum Geologists Bulletin, 96(6), pp.1071-1098.

Loucks, R., Reed, R., Ruppel, S. and Jarvie, D. 2009. Morphology, Genesis, and Distribution of Nanometer-Scale Pores in Siliceous Mudstones of the Mississippian Barnett Shale. Journal of Sedimentary Research, 79(12), pp.848-861.

Luo, D., Dai, Y. and Xia, L. 2011. Economic evaluation based policy analysis for coalbed methane industry in China. Energy, 36(1), pp.360-368.

Mancini, E. and Puckett, T. 2005. Jurassic and Cretaceous transgressive-regressive (T-R) cycles, northern Gulf of Mexico, U.S.A. Stratigraphy, 2, pp.31–48.

Mancini, E., Li, P., Goddard, D., Ramirez, V. and Talukdar, S. 2008. Mesozoic (Upper Jurassic–Lower Cretaceous) deep gas reservoir play, central and eastern Gulf coastal plain. American Association of Petroleum Geologists Bulletin, 92(3), pp.283-308.

Mancini, E.A., Parcell, W. and Ahr, W. 2006. Upper Jurassic Smackover thrombolite buildups and associated nearshore facies, southwest Alabama:. Gulf Coast Association of Geological Transactions, 56, pp.551-563.

Mancini, E., Parcell, W., Ahr, W., Ramirez, V., Llinas, J. and Cameron, M. 2008. Upper Jurassic updip stratigraphic trap and associated Smackover microbial and nearshore carbonate facies, eastern Gulf coastal plain. American Associaton of Petroleum Geologists Bulletin, 88, pp.409-434.

McAuliffe, C. (1980). Oil and Gas Migration Chemical and Physical Constraints. in Roberts III, W.H. and Cordell, R., eds., Problems of Petroleum Migration: American Association of Petroleum Geologists Studies in Geology, 10, pp.89-107.

McCarthy, K., Rojas, K., Niemann, M., Palmowski, D., Peters, K. and Stankiewicz, A. 2011. Basic Petroleum Geochemistry for Source Rock Evaluation. Schlumberger Oilfield Review, 23(2), pp.32-43.

Meckel, L. and Thomasson, M. 2008. Pervasive tight-gas sandstone reservoirs: An overview. In: S. Cumella, K. Shanley, and W. Camp,, ed., Understanding, exploring, and developing tight-gas sands. Vail Hedberg Conference: AAPG Hedberg Series, no. 3, pp.13 –27.

Meyers, P. and Benson, L. 1988. Sedimentary biomarker and isotopic indicators of the paleoclimatic history of the Walker Lake basin, western Nevada. Organic Geochemistry, 13(4-6), pp.807-813.

Meyers, P. and Bernasconi, S. 2005. Carbon and nitrogen isotope excursions in mid-Pleistocene sapropels from the Tyrrhenian Basin: Evidence for climate-induced increases in microbial primary production. Marine Geology, 220(1-4), pp.41-58.

Meyers, P. and Eadie, B. 1993. Sources, degradation and recycling of organic matter associated with sinking particles in Lake Michigan. Organic Geochemistry, 20(1), pp.47-56.

Meyers, P., Leenheer, M., Eaoie, B. and Maule, S. 1984. Organic geochemistry of suspended and settling particulate matter in Lake Michigan. Geochimica et Cosmochimica Acta, 48(3), pp.443-452.

Mikkelsen N. and Hansen J 1982. Hydrocarbon Geological Aspects of Subsidence Curves: Interpretations Based on Released Wells in the Danish Central Graben'. Bulletin Geological Society of Denmark, 31, pp.159-169.

Modica, C. and Lapierre, S. 2012. Estimation of kerogen porosity in source rocks as a function of thermal transformation: Example from the Mowry Shale in the Powder River Basin of Wyoming. American Association of Petroleum Geologists Bulletin, 96(1), pp.87-108.

Moreira de Camargo, T., Merschmann, P., Vasquez Arroyo, E. and Szklo, A. 2014. Major challenges for developing unconventional gas in Brazil – Will water resources impede the development of the Country's industry?. Resources Policy, 41, pp.60–71.

Newport, L. 2016. Petrographic and Geochemical Analysis of the Carboniferous (Namurian) Holywell Shale of northeast Wales. PhD Thesis. Durham University. Available Online: http://etheses.dur.ac.uk/11467. Accessed on 10/04/2017.

Nunn, J. 2012. Burial and Thermal History of the Haynesville Shale: Implication for Overpressure, Gas Generation and Natural Hydrofracture. Journal of Gulf Coast Association of Geological Societies, 1, pp.81-96.

Nunn, J., Scardina, A. and Pilger, R. 1984. Thermal evolution of the north-central Gulf Coast. Tectonics, 3(7), pp.723-740.

Nunn, J. 1984. Subsidence histories for the Jurassic sediments of the northern Gulf Coast: Thermal-mechanical model. In: W. Ventress, D. Bebout, B. Perkins and C. Moore, ed., The Jurassic of the Gulf rim. Proceedings of the 3rd Annual Gulf Coast Section of the Society of Economic Mineralogists and Paleontologists Foundation Research Conference, Houston, Texas, pp.309–322.

Nunn, J. and Sassen, R. 1986. Framework of Hydrocarbon Generation and Migration, Gulf of Mexico Continental Slope: ABSTRACT. Gulf Coast Association of Geological Societies Transactions, 36, pp.257–262.

Oil & Gas UK 2016. Activity Survey 2016. [online] Available at:: http://oilandgasuk.co.uk/wp-content/uploads/2016/02/Oil-Gas-UK-Activity-Survey-2016.pdf [Accessed 10 May 2017].

Okiongbo, K., Aplin, A. and Larter, S. 2005. Changes in Type II Kerogen Density as a Function of Maturity: Evidence from the Kimmeridge Clay Formation. Energy & Fuels, 19(6), pp.2495-2499.

Østvedt, O., Blystad, P. and Magnus, C. 2005. Assessment of undiscovered resources on the Norwegian Continental Shelf. In: A. Doré, and B. Vining, ed., Petroleum Geology: North-West Europe and Global Perspectives. Proceedings of the 6th Petroleum Geology Conference. Geological Society, London, pp.55-64.

Pan, R., Gong, Q., Yan, J. and Jin, J. 2016. Elements and gas enrichment laws of sweet spots in shale gas reservoir: A case study of the Longmaxi Fm in Changning block, Sichuan Basin. Natural Gas Industry B, 3(3), pp.195-201.

Partington, M., Mitchener, B., Milton, N. and Fraser, A. 1993. Genetic sequence stratigraphy for the North Sea Late Jurassic and early Cretaceous: distribution and prediction of Kimmeridgian-Late Ryazanian reservoirs in the North Sea and adjacent areas,. In: J. Parker, ed., Petroleum Geology of Northwest Europe:. Proceedings of the 4th Conference on Petroleum Geology of NW. Europe, at the Barbican Centre, London. Geological Society, London, pp.347-370.

Passey, Q., Creaney, S., Kulla, J., Moretti, F. and Stroud, J. 1990. A Practical Model for Organic Richness from Porosity and Resistivity Logs. American Association of Petroleum Geologists Bulletin, 74, pp.1777-1794.

Peters, K., Walters, C. and Moldowan, J. 2004. The Biomarker Guide. Cambridge: Cambridge University Press, pp.475-1155.

Pilcher, R., Ciosek, J., McArthur, K., Hohman,, J. and Schmitz,, P. 2012. Ranking Production Potential Based on Key Geological Drivers – Bakken Case Study. Paper IPTC 14733 presented at IPTC, Bangkok, Thailand, 7-9, February, 2012.

Pitcher, J., Kwong,, S. and Yarus,, J. 2012. Paper SPE 152579 presented at the SPE/EAGE European Unconventional Resources Conference and Exhibition, Vienna, Austria, 20–22 March 2012.

Pyhäranta, M. 2017. State ownership of petroleum resources: an obstacle to shale gas development in the UK?. The Journal of World Energy Law & Business.

Raji, M., Gröcke, D., Greenwell, C., Gluyas, J. and Cornford, C. 2015. The effect of interbedding on shale reservoir properties. Marine and Petroleum Geology, 67, pp.154-169.

Rexer, T., Mathia, E., Aplin, A. and Thomas, K. (2014). High-Pressure Methane Adsorption and Characterization of Pores in Posidonia Shales and Isolated Kerogens. Energy & Fuels, 28(5), pp.2886-2901.

Richards, P., Lott, G., Johnson, H., Knox,, R. and Riding,, J. 1993. Jurassic of the Central and Northern North Sea. In: R. Knox, and W. Cordey, ed., Lithostratigraphy nomenclature of the UK North Sea.. British Geological Survey, Nottingham, pp.1-252.

Rogers, H. 2013. UK shale gas – hype, reality and difficult questions, The Oxford Institute for Energy Studies. Oxford Energy Comment. [online] Available at:: http://www. oxfordenergy.org/2013/07/uk-shale-gas-hype-reality-and-difficult-questions [Accessed 7 Jul. 2017].

RÖSnnevik, H., Eggen, S. and Vollset, J. 1983. Exploration of the Norwegian Shelf. In: J. Brooks, ed., Petroleum Geochemistry and Exploration of Europe'. Blackwell Scientific, Oxford, pp.71-94.

Ross, D. and Bustin, R. 2007. Impact of mass balance calculations on adsorption capacities in microporous shale gas reservoirs. Fuel, 86(17-18), pp.2696-2706.

Ross, D. and Bustin, R. 2009. Investigating the use of sedimentary geochemical proxies for paleoenvironment interpretation of thermally mature organic-rich strata: Examples from the Devonian–Mississippian shales, Western Canadian Sedimentary Basin. Chemical Geology, 260(1-2), pp.1-19.

Ross, D. and Bustin, R. 2009. The importance of shale composition and pore structure upon gas storage potential of shale gas reservoirs. Marine and Petroleum Geology, 26(6), pp.916-927.

Rundberg, Y. and Eidvin, T. 2005. Controls on depositional history and architecture of the Oligocene–Miocene succession, northern North Sea Basin. In: B. Wandaas, J. Nystuen, E. Eide, and F. Gradstein, ed., Onshore–Offshore Relationships on the North Atlantic Margin. NPF Special Publication, 12, pp.207–239.

Scotland Means Business 2014. Scotland Means Business: Oil & Gas Part Three – Offshore Hydrocarbon Opportunity [online] Available at:: http://www.n56.org/sites/default/files/Scotland%20Means%20Business%20Oil%20%26%20Gas%20Part%203%2030aug14.pdf [Accessed 2 Sep. 2017].

Selley, R. 2011. Shale gas: blessing or curse?. Geoscientist, 21(4), pp.14-19.

Selley, R. 2012. UK shale gas: The story so far. Marine and Petroleum Geology, 31(1), pp.100-109.

Selley, R. 2005. UK shale-gas resources. Petroleum Geology Conference series, 6, pp.707-714.

Sharma, R. and Chopra, S. 2016. Identification of sweet spots in shale reservoir formations. First Break, 34(2136).

Shi, G., Jing, Y., Wang, S. and Zhang, X. 2010. Development status of liquefied natural gas industry in China. Energy Policy, 38(11), pp.7457-7465.

Smith, N., Kirby, G. and Pharaoh, T. 2005. Structure and evolution of the south-west Pennine Basin and adjacent area. Keyworth: British Geological Survey, p.129.

Smith, N., Turner, P. and Williams, G. 2010. UK data and analysis for shale gas prospectivity. In: Vining, B.A. and Pickering, S.C. (eds) Petroleum Geology: From Mature Basins to New Frontiers. Proceedings of the 7th Petroleum Geology Conference: Geological Society of London, pp.1087–1098.

Smith, R., Hodgson,, N. and Fulto,, M. 1993. Salt control on triassic reservoir distribution, UKCS Central North Sea. Geological Society London, 4, pp.547-557.

Smythe, D. 2016. Hydraulic fracturing in thick shale basins: problems in identifying faults in the Bowland and Weald Basins, UK. Solid Earth Discussions, pp.1-45.

Soeder, D. and Kappel, W. 2009. Water Resources and Natural Gas Production from the Marcellus Shale.. U.S. Geological Survey Fact Sheet 2009–3032, p.6.

Sun, X., Zhang, T., Sun, Y., Milliken, K. and Sun, D. 2016. Geochemical evidence of organic matter source input and depositional environments in the lower and upper Eagle Ford Formation, south Texas. Organic Geochemistry, 98, pp.66-81.

Swarbrick, R. and Osborne, M. 1998. Mechanisms that generate abnormal pressures: an overview. In: B. Law, G. Ulmishek, and V. Slavin,, ed., Abnormal Pressures in Hydrocarbon Environments.. American Association of Petroleum Geologist Memoir 70, pp.13-34.

Sweeney, J. and Burnham, A. 1990. Evaluation of a Simple Model of Vitrinite Reflectance Based on Chemical Kinetics (1). American Association of Petroleum Geologists Bulletin, 74.

Sykes, R. and Snowdon, L. 2002. Guidelines for assessing the petroleum potential of coaly source rocks using Rock-Eval pyrolysis. Organic Geochemistry, 33(12), pp.1441-1455.

Sykes, R., Snowdon, L. and Johansen, P. 2003. Rock-Eval-based maturation pathways for humic coals: how well do they represent the natural evolution of oil and gas?. Abstract of EAOG 21st International Meeting on Organic Geochemistry Krakow, Poland.8-12 September 2003.

Thomsen, R., Lerche, I. and Korstgårdt, J. 1990. Dynamic hydrocarbon predictions for the northern part of the Danish Central Graben: an integrated basin analysis assessment. Marine and Petroleum Geology, 7(2), pp.123-137.

Tissot, B. and Welte, D. 2013. Petroleum Formation and Occurrence. Berlin: Springer Berlin.

Trapoil Ltd 2014. Relinquishment Report for Licence P.1938 Blocks 3/2c, 4c, 7d, 9c, 13b, 14h, 14j, 16/12b, 17c, 211/22b, 27d, 28b & 29e, 2014. [online] Available at:: https://itportal.ogauthority.co.uk/web_files/relinqs/nov2015/P1938.pdf [Accessed 10 Jun. 2017].

Turner, C., Cohen, J., Connel, J. and Cooper, D. 1987. A depositional model for the South Brae oilfield. In: J. Brooks, and K. Glennie, ed., Petroleum geology of North West Europe. London: Graham and Trotman, pp.853-864.

Tyson, R. 1996. Sequence-stratigraphical interpretation of organic facies variations in marine siliciclastic systems: general principles and application to the onshore Kimmeridge Clay Formation, UK. Geological Society, London, Special Publications, 103(1), pp.75-96.

Tyson, R. 2004. Variation in marine total organic carbon through the type Kimmeridge Clay Formation (Late Jurassic), Dorset, UK. Journal of the Geological Society, 161(4), pp.667-673.

Tyson, R. 2013. Sedimentary organic matter. [Place of publication not identified]: Springer, pp.151–167.

U.S. Department of Energy 2013. Natural Gas From Shale: Questions and Answers.. [online] Available at:: https://energy.gov/sites/prod/files/2013/04/f0/complete_brochure.pdf [Accessed 4 May 2017].

Underhill, J. 1998. Jurassic. In: K. Glennie, ed., Introduction to the Petroleum Geology of the North Sea. Blackwell Science, pp.245-293.

United States Energy Information Administration 2013. Technically Recoverable Shale Oil and Shale Gas Resources: An Assessment of 137 Shale Formations in 41 Countries Outside the United States. [online] United States Energy Information Administration. Available at:: https://www.eia.gov/analysis/studies/worldshalegas/pdf/overview.pdf [Accessed 5 Feb. 2016].

US Energy Information Administration 2015. Technically Recoverable Shale Oil and Shale Gas Resources: United Kingdom. [Online] Available: https://www.eia.gov/analysis/studies/worldshalegas/pdf/UK_2013.pdf. [Accessed 12 Jun. 2017].

van Krevelen, D. 1950. Graphical-statistical method for the study of structure and reaction processes of coal. Fuel, 29, pp.269-228.

Weijermars, R. 2010. Value Chain analysis of the natural gas industry – lessons from the US regulatory success and opportunities for Europe. Journal of Natural Gas Science and Engineering, 2, pp.86–104.

Weniger, P., Kalkreuth, W., Busch, A. and Krooss, B. 2010. High-pressure methane and carbon dioxide sorption on coal and shale samples from the Paraná Basin, Brazil. International Journal of Coal Geology, 84(3-4), pp.190-205.

Wilhelms, A., Larter, S., Leythaeuser, D. and Dypvik, H. 1990. Recognition and quantification of the effects of primary migration in a Jurassic clastic source-rock from the Norwegian continental shelf. Organic Geochemistry, 16(1-3), pp.103-113.

Winker, C. and Buffler, R. 1988. Paleogeographic Evolution of Early Deep-Water Gulf of Mexico and Margins, Jurassic to Middle Cretaceous (Comanchean). American Association of Petroleum Geologists Bulletin, 72, pp.318–346.

World Energy Resources 2013. A Summary World Energy Council. [online] Available at:: https://www.worldenergy.org/wpcontent/uploads/2013/09/Complete_WER_2013_Survey.pdf [Accessed 12 Jun. 2017].

Yalçın Erik, N., Özçelik, O. and Altunsoy, M. 2006. Interpreting Rock–Eval pyrolysis data using graphs of S_2 vs. TOC: Middle Triassic–Lower Jurassic units, eastern part of SE Turkey. Journal of Petroleum Science and Engineering, 53(1-2), pp.34-46.

Yang, Y. and Aplin, A. 2010. A permeability–porosity relationship for mudstones. Marine and Petroleum Geology, 27(8), pp.1692-1697.

Ziegler, P. 1975. North Sea Basin History in the Tectonic Framework of North-West Europe. In: A. Woodland, ed., Petroleum and the Continental Shelf of North-West Europe, 1st ed. Barking Applied Science Publishers, pp.131-149.

Ziegler, P. 1989. Evolution of Laurussia. London: Kluwer Academic Publishers, p.102.

Ziegler, P. 1990. Tectonic and palaeogeographic development of the North Sea rift system. In: D. Blundell and A. Gibbs, ed., Tectonic Evolution of the North Sea Rifts. Oxford University Press, New York, pp.1-36.

Ziegler, P. 1992. North Sea rift system. Tectonophysics, 208(1-3), pp.55-75.

Chapter 2: Geochemical Database, Sample Collection and Analytical Methods

The main focus of this thesis, as highlighted in Chapter 1, is to evaluate future prospects of offshore unconventional liquid hydrocarbon with the aim to identify producible "sweet-spot" areas for optimum extraction of the remaining residual oil in the South Viking Graben area of the North Sea. In order to evaluate and fully understand the potential of this organic-rich source rock, sweet-spot criteria from North American shale plays have been adapted as analogues for this study (Section 1.6-1.7 in Chapter 1). For application of these sweet-spot criteria from North American shale plays to the assessment of Kimmeridge Clay reservoir properties, it was possible to first of all make a synthesis of all database information presently held in commercial and public databases, as well as literature reviews and particularly the area of interest in the licence blocks held by Trap oil Ltd in Quadrant 16, and 17 in the South Viking Graben area.

Using the available data sets, core samples were selected based on well location, lithology organic matter content and–level of thermal maturation. The selected core samples were examined for a variety of reservoir properties using a wide range of geological, geochemical, petrographical, petrological and porosity analytical methods. The flow chart in Figure 2-1 illustrates the integration of different data types in order to develop a comprehensive evaluation of the Kimmeridge Clay Formation for unconventional resource potential.

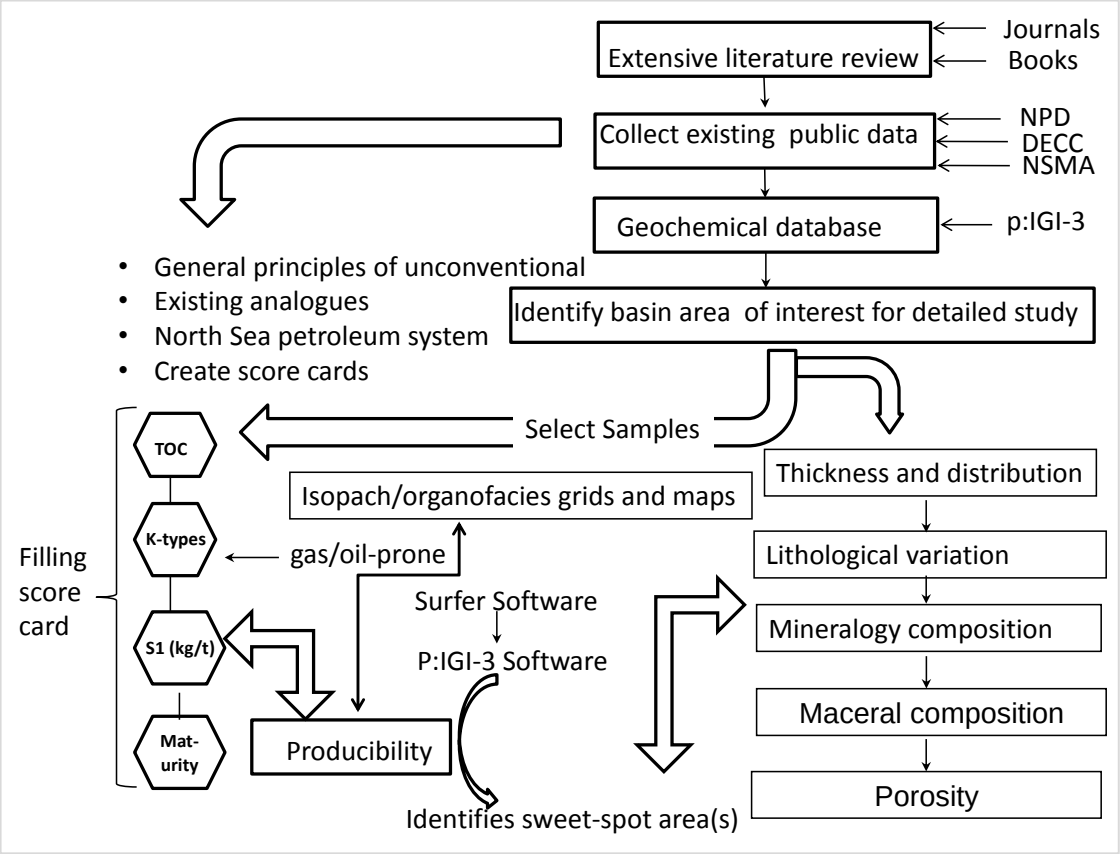

Figure 2-1: Structure and methodology showing flow chart and data integration processes undertaken for research. NPD: Norwegian Petroleum Directorate, DECC: Department of Climate Change, NSMA: North Sea Millennium Atlas, K-types: kerogen types.

2.1: Literature Review

An extensive literature review was undertaken to identify knowledge in the new and actively growing area of unconventional resources and to establish key criteria for successful commercial exploitation. Currently, the literature is almost exclusively from:

1. North America (USA, Canada)
2. UK Onshore, Germany, France

This review identified successful sweet-spots criteria which were placed in score table (Section 1.6 in Chapter 1; Table 1-3-1-5) with factors weighted to allow the basins to be placed in order of their relative importance and similarities to the North Sea graben. These reservoir property criteria were applied to the data-rich offshore area of the North Sea province.

2.2: Published and Public Database

The following data sources were used throughout this thesis.

1. North Sea Millennium Atlas (NSMA): depth to base Cretaceous Unconformity (BCU) and other grids, allowing the creation of the Kimmeridge Clay Formation isopach, organo-facies grids and maps.
2. Department of Energy and Climate Change (DECC) and Norwegian Petroleum Directorate (NPD) websites: basic well formation tops and bases, lithostratigraphic, biostratigraphy and sequence stratigraphy for key wells focussed on the Upper Jurassic in general and Kimmeridge Clay Formation in particular (DECC Oil and Gas well, 2014). The thicknesses of the source rocks were calculated from the mapped formation tops and bases, well formation data grids were created in Trinity 12 software, where isopach and distribution maps were generated.
3. British Geological Survey (BGS): online offshore hydrocarbon wells material database

This database contains hydrocarbon well material from approximately 8000 wells, including over 300 km of drill core and 4.5 million samples of cuttings. For this thesis, visual investigation of sample selection was based on a combination of well name, operator, depth range (m), and a visual estimate of sand-shale content and availability.

2.3: Regional Geochemical Databases Used

The groundwork for this study is a comprehensive geochemical data set provided by Integrated Geochemical Interpretation Limited (IGI Ltd). This geochemical database of Kimmeridge Clay Formation has been compiled from results of proprietary geochemical analyses and from the Fact Pages of the Norwegian Petroleum Directorate (NPD). The assembled dataset were from over 7,000 core and cutting samples with total organic carbon (TOC wt. %, mainly from the LECO method), Rock-Eval pyrolysis (from Rock-Eval II and VI over the years), solvent extract yields and fractions and organic petrography data from various source rock intervals across the South Viking Graben in the UK and Norwegian Continental Shelf available in p: IGI-3

format. The geochemical database formatted in p: IGI-3 is a .NET framework version 3.5.1 containing 687 pre-defined columns, arranged over 17 linked data pages, with additional 300 user-definable columns used to enter any numeric (including equation) or text data that are not standard within p: IGI's pre-defined columns (IGI Ltd, 2017). The database covered wells from UK Quadrant 16 (mainly core samples) and the adjacent Norwegian Quadrants 15, 16 and 17 to the east, which are dominated by cutting sample. Additional geochemical data have been taken from published literature and industry sources. The geochemical database were processed and used to investigate regional variation in Kimmeridge Clay organic-richness, kerogen types, thermal maturation and hydrocarbon potential across the South Viking Graben in Chapter 3 and Chapter 5.

In such a large database, it is inevitable that the analyses were undertaken by many different laboratories using similar but not identical apparatus, and even from the same lab with different apparatus and procedures through time. This analytical 'noise' in the data is considered acceptable. The results from the processing and interpretation of this database together with visual estimates of the sand content of a sub-set of core samples made with the naked eye (thicker sand interbeds) were used to select representative core samples for subsequent geochemical, mineralogy, petrographic and porosity analyses in Chapters 4, 6 and 7

2.3.1: Criterial for Database Sample Selection

The assembled geochemistry dataset from over 5,000 core and cutting samples made available in p: IGI-3 format used for Chapter 3 were selected using a 2% TOC cut off for the Kimmeridge Clay Formation/Draupne sample sets. The organic-lean Heather Formation which typically has < 2 wt. % TOC is grouped with KCF/Draupne and assessed together as the Viking Group because it is limited in the UK sector of the South Viking Graben. A rigorous data quality control was performed on the IGI released database for this project, through comparisons of the values with other public, published and newly generated data to ensure the reliability of the assembled datasets. The database was also routinely updated each year to capture the release of new data in the study area. Compiling and quality assurance of the key well data

used in Chapter 3 from DECC and NPD website was compared with available wireline log data. The depths used are Total Vertical Depth subsea and no depth correction has been undertaken. It should also be noted that the recorded depths for dataset used throughout the thesis are the maximum burial depths. The standard intercept line in some of the p: IGI-3 plots were automatically added by the software and removing these lines automatically removes important plot overlays. Therefore, these standard intercept lines should be ignored on the plots. An overview of the sample preparations and analytical procedures used is given in Section 2.5.

2.4: Sample Strategy and Sample Collection.

Core and outcrop samples collected for this research were prepared for various geochemical, mineralogical, geomechanical and petrographic analyses undertaken at different laboratories. Different sample preparation, database collection and analytical methods and techniques used for each stage of this research are described at the beginning of each of Chapters 3-7.

2.4.1: Sample Strategy

The geochemical database described in Section 2.3 in this chapter was used to select samples based on the variation in the amount of TOC (organic-richness), hydrogen and oxygen Indices (for kerogen types) Rock-Eval T_{max} (for thermal maturation) values. Samples were selected from different wells and different depth intervals that penetrated the Upper Jurassic organic-rich 'hot shale' mudstones with interbedded sandstone in UK Quadrant 16. This was followed by visual estimates of the sand content of a sub-set of core samples made with the naked eye (thicker sand interbeds) from online images to select representative core samples from the British Geological Survey online offshore hydrocarbon wells material database (http://www.bgs.ac.uk/data/offshoreWells/wells.cfc?method=searchWells).

2.4.2: Sample Collection

Samples used for this research were collected from drilled borehole core in the North Sea and some outcrop samples in the south-west part of Britain. Sample types,

location, depth and numbers collected for each stage of this research are further discussed in each chapter (Chapters 4, 6 and 7).

2.4.3: Borehole Core Sampling:

Samples were selected based on wells that penetrated the Kimmeridge Clay Formation in the UKCS Quadrant 16 area of the North Sea using the British Geological Survey online offshore hydrocarbon wells material database. The first set of 17 samples (Table 2-1) was used to study the effects of interbeds on shale reservoir properties and the nature of porosity, in Chapter 4 and Chapter 6, respectively. These samples were selected based on the visual inspection and estimation of the stratigraphy of three lithogies; (typical mudstone dominated (Figure 2-2); typical mudstone with 'tiger-stripe' (Figure 2-3); mudstone-sand mixed (Figure 2-4) colour (for mixed lithologies). Together with depth (for maturity level) from online core images combined with geochemistry results obtained from the p: IGI-3 database. The second set of 27 samples (Table 2-2) which was used to investigate the effect of demineralisation on kerogens in Chapter 7 was collected based on the amount and composition of the organic-matter, level of thermal maturation available in the p: IGI-3 database, and visual investigation of black-olive-grey mudstone dominated core samples on the BGS website.

Table 2-1: List of borehole core sample collected from the BGS core store for TOC, Rock-Eval pyrolysis, stable carbon isotope, Thin-section and XRD analyses in Chapter 4 and 6.

Well	Top-depth (ft.)	Base-depth (ft.)	BGS SSK number	BGS Corebox Barcode Number	Lithology	Sample Type
16/17-14	13779.5	13779.8	SSK47810	S00032751	Sand/shale	drill core
16/17-14	13818	13818.5	SSK47813	S00032757	Sandstone	drill core
16/17-14	13758.5	13759	SSK47814	S00032752	Sand/shale	drill core
16/17-14	13762	13762.5	SSK47815	S00032752	Shale	drill core
16/17-18	12204	12204.5	SSK47825	S00061307	Sand/shale	drill core
16/17-18	12403	12403.6	SSK47830	S00061326	Sand/shale	drill core
16/17-18	12406.3	12406.7	SSK47831	S00061336	Shale	drill core
16/17-18	12411	12411.5	SSK47835	S00061327	Sand/shale	drill core
16/17-19	11654.3	11654.5	SSK47866	S00086169	Sand/shale	drill core
16/17-19	11693.3	11693.8	SSK47870	S00086173	Shale	drill core
16/17-19	11719	11719.4	SSK47873	S00086175	Sand/shale	drill core
16/17-19	11728.3	11728.6	SSK47874	S00086175	Sand/shale	drill core
16/17-19	11754.2	11754.9	SSK47875	S00086178	Shale	drill core
16/18-2	13536.75	13538.38	SSK47839	S00057102	Sand/shale	drill core
16/18-2	13536.75	13537.72	SSK47858	S00057103	Shale	drill core
16/18-2	13542.45	13543	SSK47859	S00057103	Shale	drill core
16/18-2	13541	13541.67	SSK47860	S00057103	Sand/shale	drill core
16/18-2	135445	13545.6	SSK47861	S00057104	Sand/shale	drill core

Figure 2-2: Photographic example of a typical mudstone dominated core sample from the Upper Jurassic Kimmeridge Clay Formation from Well 16/08a-11 and 16/12a-18Z, collected at the British Geological Survey core store in Keyworth. The mudstone-dominated lithologies are black to dark grey, silty, partly laminated with gradational boundaries between the mudstones and the interbedded light-grey thin sand/silt beds.

Figure 2-3: Photographic example of a typical mudstone with 'tiger-stripe' core sample from the Upper Jurassic Kimmeridge Clay Formation from Well 16/17-C5Z collected at the British Geological Survey core store in Keyworth. Typical mudstone with 'tiger stripe' is an intermediate facies of interbedded sands and mudstone and termed the tiger stripe facies comprising an alternating mudstone and fine-grained silt/sand interbeds

Figure 2-4: Photographic examples of typical mudstone-sand mixed core samples of Upper Jurassic Kimmeridge Clay Formation from Well 16/17-14 collected at the British Geological Survey core store in Keyworth. Typical mudstones-sands are massive sand and conglomerates from the main Brae Formation. It is fine-coarse grained grey-brown sandstone with interlaminated dark grey to black mudstone. The formation reaches a maximum drilled thickness of 1000m in Well 16/7a-8 at 3679.5-4271 m, 16/8-1 at 3859-4023 m and 16/7a-16 at 3768-4139 m in the South Viking Graben area.

Table 2-2: List of borehole core sample collected from the BGS core store for whole rock and kerogen isolation analyses in Chapter 7.

Borehole Name/Well Number	BGS SSK number	Depth top (ft.)	Depth base (ft.)	BGS Corebox Barcode number	Lithology	Sample Type
16/12b- 6	61170	15,364.50	15,365	S00051174	Shale	Drillcore
16/12b- 6	61171	15,357	15,357.50	S00051174	Shale	Drillcore
16/12b- 6	61174	15,437	15,438	S00051174	Shale	Drillcore
16/12b- 6	61173	15,379	15,379.50	S00051176	Shale	Drillcore
16/12b- 6	61172	15,395.50	15,396	S00051178	Shale	Drillcore
16/08c- 13	61167	16,055	16,055.80	S00101734	Shale	Drillcore
16/08c- 13	61168	16,096	16,096.50	S00101741	Shale	Drillcore
16/08c- 13	61169	16,097	16,097.50	S00101741	Shale	Drillcore
16/08b- 3	61166	13,146.80	13,147	S00028194	Shale	Drillcore
16/08b- 3	61165	13,143	13,143.50	S00028194	Shale	Drillcore
16/12a- 18Z	61163	13,400	13,400.60	S00094203	Shale	Drillcore
16/12a- 18Z	61164	13,451.50	13,451.70	S00094212	Shale	Drillcore
16/17-5	61162	12,073	12,073.40	S00138188	Shale	Drillcore
16/17- 5	61161	12,075.50	12,075.70	S00138188	Shale	Drillcore
16/17-18	61160	12,288	12,288.30	S00061310	Shale	Drillcore
16/17- 18	61151	12,287.40	12,287.70	S00061315	Shale	Drillcore
16/17- 18	61149	12,263	12,263.40	S00061313	Shale	Drillcore
16/17-19	61148	11,802	11,802.50		Shale	Drillcore
16/17- 19	61147	11,799	11,799.30	S00086181	Shale	Drillcore
16/17- 19	61146	11,826	11,826.50	S00086183	Shale	Drillcore
16/03b- 8Z	61145	14050.3	14051	S00044137	Shale	Drillcore
16/03b- 8Z	61143	14,057	14,057.50		Shale	Drillcore
16/07b- 23	61141	4092.2m	4092.5m	S00031764	Shale	Drillcore
16/07b- 23	61142	4093.26m	4093.60m		Shale	Drillcore
16/08a- 11	61139	13,245	13,245.50	S00073060	Shale	Drillcore
16/08a- 11	61140	13,89.20	13,89.6		Shale	

The selected samples from these boreholes were collected and logged at the British Geological Survey core store in Keyworth, Nottingham in 2014 and 2015. These core samples were carefully laid down on several tables in the core lab according to well

name, top and bottom depth. Another visual investigation and estimations were made and then compared to the online visual investigations. Samples were selected to cover a range of depths and hence maturities, and a range of mudstone types potentially equating to different amounts and types of organic matter. Precautions were taken to avoid samples with obvious drilling mud, yellowish-reddish iron oxides and migrated oil staining to minimise the impact of contamination. Core sample plugs from sections of the selected wells and core were requested from the core store. Typical core plugs collected for analysis were between 30- 120 g for each sample, these samples were weighed, photographed, bagged and labelled in plastic sample bags.

2.4.4: Outcrop Sampling

Outcrop samples in southwest Britain were obtained for the purpose of comparative study of the Lower and Upper Jurassic sequences in terms of their TOC amount, level of maturation and hydrocarbon potential. This was done to compare Upper Jurassic borehole core samples from offshore North Sea with outcrop type sections of Lower-Upper Jurassic sequence exposed in Kilve Pill Month, West Somerset, Lavernock Point, Glamorgan and Pinhay Bay, Lyme Regis, Dorset. Literature review of source rock parameters for the outcrop type sections indicate it varies laterally in terms of lithology, organic content, maturity, maceral composition and hydrocarbon potential between lithologies at a single outcrop, and for similar lithologies from West Somerset to Dorset. These marine limestone-shale sequences also provide a model situation to investigate the effects of mineral matrix on kerogen in terms of TOC, maturity and hydrocarbon potential undertaken in Chapter 7.

The Kimmeridge Clay is widely regarded as the major source rock for North Sea oil (Cornford et al., 1983; Cornford and Brookes, 1989; Cooper and Barnard, 1984; Cooper et al., 1995; Erratt et al., 2010). However, its type locality outcropping onshore is immature, a function of its maximum burial depth having suffered only modest burial (Farrimond et al. 1984; Scotchman, 1987; Ebukanson and Kinghorn, 1986; Sælen et al. 2000). It exhibits a wide range of TOC and maturity (0.3-0.6 %Ro) with TOC content ranging from 0.9-57.2 wt.% and is dominantly marine Type II kerogen with only a

minor contribution of terrestrial material (Gallois, 1979a; Williams and Douglas, 1981; Farrimond et al., 1984; Scotchman, 1987; Ebukanson and Kinghorn, 1986; Sælen et al., 2000). T_{max} values are between 412 °C and 437 °C, indicating the samples are immature and in the immature to early oil window generation (Lewan 1985).

Eight samples (Table 2-3) taken from a number of outcrops and cliff exposures in the south-west region were collected by IGI Ltd as part of a multi- disciplinary study of the Upper Jurassic Kimmeridge Clay. The Lavernock Point samples were taken from the cliff face 200 m west of Lavernock Point in Glamorgan and represented limestone with faint banding and blocky and laminated mudstone (Figure 2-5a). The Pinhay Bay samples were collected as examples of the blocky and laminated mudstone facies from the limestone-shale-limestone cycles to the west of Lyme Regis, Dorset (Figure 2-5b). The Kilve Pill Mouth sample was taken from a cliff below Quantock's Head in West Somerset (Figure 2-5c). The collected samples were photographed, sealed in plastic sample bags, labelled and posted to Durham University for further analyses and to form part of this thesis. An average of 200 g of each sample was split and used for TOC, Rock-Eval, kerogen isolation, petrographic and carbon isotope analysis.

Table 2-3: Sample number, location, lithology age and sample weight of selected outcrop.

Sample ID	Sample Location	Lithology	Stratigraphy	Sample Weight (g)
IGI-2	Lavernock Point, Glamorgan	Laminated Limestone	Hettangian	251.95
IGI-3	Lavernock Point, Glamorgan	Blocky Mudstone	Hettangian	232.58
IGI-4	Lavernock Point, Glamorgan	Blocky Marl	Hettangian	169.23
IGI-5	Lavernock Point, Glamorgan	Laminated Mudstone	Hettangian	139.28
IGI-6	Lavernock Point, Glamorgan	Laminated Marl	Hettangian	248.06
IGI-7	Pinhay Bay, west of Lyme Regis	Laminated Mudstone	Hettangian	154.35
IGI-8	Pinhay Bay, west of Lyme Regis	Blocky Mudstone	Hettangian	155.76
IGI-9	Kilve Pill Mouth, West Somerset	Laminated Marl	Sinemurian	260.11

Figure 2-5A-C: Outcrop samples of (a) Lower Lias limestone/shale cycle in Lavernock Point, Glamorgan, (b) blue Lias limestone/shale cycles in Pinhay Bay, Lyme Regis, Dorset, and (c) laminated black shales (upper), and the blocky mid-grey mudstone (lower) in Kilve Pill Month, West Somerset (images from IGI Ltd).

2.4.5: Sample Preparation and Analytical Techniques

Core and outcrop samples collected for this research were prepared for various geochemical, mineralogical, geochemical and petrographic analyses undertaken at different laboratories. Different sample preparation, database collection and analytical methods and techniques were used for each stage of this research and are described at the beginning of each of Chapters 3-7.

2.4.6: Powdered Sample Preparation and Analyses

Preparation of the powdered samples used for the geochemical techniques (TOC, Rock-Eval Pyrolysis and carbon isotope) was carried out in the mineralogy laboratory at Durham University. All core and outcrop samples were washed with deionised water and dried overnight at room temperature and ground with an agate mortar and pestle. The initial ground powder was then ball milled for 5 mins to obtain a uniform fine powder, which was sieved to minus 20-mesh to achieve homogeneity following standard NIGOGA procedures (Weiss et al., 2000). The remainder of this chapter describes in detail the methodology of the various analytical techniques used in this study.

2.5: Overview of the Analytical Techniques used for Evaluation of the Kimmeridge Clay Formation

A source rock is defined as an organic-rich sedimentary rock, typically comprised of shales or limestones that has generated, or is capable of generating, oil and gas. The quality of source rock is assessed by measuring the total organic carbon (TOC) content in the rock, the origin and type of kerogen, thermal maturity, generation, retention, expulsion, migration and its potential to generate and expel oil and gas if subjected to increased thermal maturation. In the case of unconventional hydrocarbon, the source rocks may also be the reservoir rocks under the right conditions. Assessing and quantifying potential source rock, its maturity, kinetic parameters and its potential to generate oil or gas is done by detailed screening of core or cutting samples using some of the techniques described in this study, *vide infra*.

The geochemical assessment of these source rocks was routinely investigated using LECO/TOC combustion (quantity of the organic matter); programmed Rock-Eval Pyrolysis (quantity, quality, maturity and potential of the organic matter) and carbon isotopic measurements (origin, type of the organic matter and thermal maturation). Organic petrography assessment was carried out by visual kerogen analysis, kerogen isolation, maceral point-counting and vitrinite reflectance for quality, thermal maturation and kerogen distribution. Lithology and mineralogy assessment was investigated by visual estimates (quantity of shale-sand ratio), x-ray diffraction (quantity and quality of minerals) and microscopic thin section (mineralogical composition) analyses. Porosity assessment was carried out using Focused Ion Beam - Scanning Electron Microscope (FIB-SEM) (quantity, nature, type, distribution of pore spaces) analyses.

Both the borehole and outcrop samples were subjected to in-depth analytical techniques following sample collections and preparation. The remainder of this section describes the methodology of the various analytical techniques used in this study.

2.5.1: Geochemical Techniques

Measuring the TOC content of a source is fundamentally important for the evaluation of its potential. This measurement gives information on the richness of the source rocks as defined specially by their total organic carbon contents. The organic carbon content is then used to evaluate the potential hydrocarbon that may be generated. Furthermore, investigation of kerogen by isolating it from its mineral matrixes is very important in the determination of the type and distribution of the maceral end-member present in the organic matter.

Pyrolysis is the thermal decomposition of organic matter by heating in the laboratory in the absence of oxygen. Rock-Eval Pyrolysis is widely used to measure richness, kerogen type and maturity of potential source rocks**.** Carbon isotope ratios are used to classify organic matter into marine and continental (land) plant origins (Meyers, 1994; Galimov, 2006) and for changes in sea level (Gröcke et al., 2006; Jarvis et al., 2011). Carbon and nitrogen (C/N) ratios and organic d^{13}Corg values may be used to place

limits on the source of the organic matter in sediments (Meyers and Eadie, 1993), together with post-depositional changes of the original organic input (Calvert, 2004).

2.5.2: Total Organic Carbon (TOC) Analysis

For accurate measurement of TOC, the LECO®TOC method is commonly used because it can differentiate between organic and inorganic carbon from > 1g of sample (Figure 2-6). This method measures TOC values in samples > 1g by combusting the organic carbon under atmospheric oxygen, any carbon present is converted to CO_2; resulting CO_2 produced is then measured with a non-dispersive infrared (NDIR) detection cell. The mass of the CO_2 is converted to carbon based on the dry sample weight, because the amount of the CO_2 produced is directly proportional to the amount of organic carbon content of the sample (Carvajal and Gentzi, 2015).

Figure 2-6: LECO C230 Carbon Analyser uses an induction furnace and measures carbon with a non-dispersive infrared (NDIR) detection (image from www.ellingtongeologic.com)

For this study, samples for TOC analysis were finely ground and sieved to achieve homogeneity then treated with dilute hydrochloric acid (HCl) to remove carbonate minerals. The samples were rinsed free of the HCl with distilled water, filtered, air-dried and then placed into LECO crucibles. The LECO (C230 and SC-632) Carbon Analyzer instruments (Figure 2-6) were calibrated against standards with known carbon contents. Each calibration standard falls within 3 % of the known carbon content percentage, and the standards were checked against the acceptable range given in NIGOGA standard documentation (Espitalié et al., 1985a; Peters, 1986).

Combustion of both the standards and rock samples was undertaken by heating to 1200 ^{o}C in the presence of excess oxygen. The resulting carbon dioxide was measured by an infrared cell, and the TOC determined as weight percent of the initial rock. LECO-TOC analysis results for Chapter 4 were carried out at Applied Petroleum Technology (APT) Norway using a LECO SC-632 instrument. The analysis for Chapter 7 was carried out by Brian Jarvie at GeoMark Research, Ltd in USA using a LECO C230 instrument.

2.5.3: Kerogen Isolation Analysis

Kerogen was isolated from the mineral matrix by acid digestion. The carbonates were removed by digesting 25–55 g of pulverized sample with 10 % hydrochloric (HCl) acid until the reaction ceased. The residues were then thoroughly washed with distilled water, and subsequently treated with 70% hydrofluoric (HF) acid and oscillated for 4 h to dissolve silicate minerals. The digested samples were centrifuged at 2000 RPM in 50 ml polypropylene test tubes for 5 min. Distilled water was added while vortexing with repeated washing and centrifuging until silicate, clay and carbonate minerals were removed. A few drops of concentrated HCl were added to allow for better pyrite separation. Using only HCl, HF, and distilled water allowed for minimal treatment that might affect organic matter. The TOC of the concentrate can be taken as a measure of the effectiveness of the isolation procedure.

2.5.4: Rock-Eval Pyrolysis analysis

In Rock-Eval Pyrolysis analysis, the organic content is pyrolyzed in the absence of oxygen, then combusted. The amount of hydrocarbons and carbon dioxide released is measured. This is done in the laboratory by subjecting source rock to very high temperature (400 °C- 500 °C) in an inert atmosphere (helium or nitrogen) to artificially mature the kerogens. It measures the quantity of free hydrocarbon as the S_1 peak and hydrocarbon that can be potentially generated after maturation as S_2 peak in a given sample (Behar et.al. 2001).

For this study, each pulverized sample (> 60 mg) was placed in an isothermal oven temperature of 300 °C for 3 mins, and the free hydrocarbons detected by Flame

Ionization Detector (FID) were then volatized and measured as the S_1 peak on the standard Rock-Eval pyrogram. The measured S_1 value can be used as a direct measurement of amount and extent of the oil generated by the source rock (in milligrams of hydrocarbon per gram of rock). In the second phase of volatilization, the temperature of the oven was then increased from 300 °C to 550 °C at a rate of 25 °C per minute. This phase decomposes kerogen into hydrocarbon vapor, as well as cracking of non-volatile organic matter. It measures the volume of hydrocarbon formed, and it is used to estimate the remaining hydrocarbon generation potential should burial and maturation continue in a given sample. The total hydrocarbon released during this thermal cracking is detected and measured as the S_2 peak. The CO_2 released from the kerogen cracking is trapped between 300-390 °C, the oxygen-bearing kerogen compounds decomposes and the mass is measured as S_3 in milligrams CO_2 per gram of rock (Tissot and Welte, 1984). This is the measurement of the amount of organic oxygen in the sample during the cooling of the pyrolysis oven detected on a thermal conductivity detector (TCD) and is used to calculate the oxygen index (OI) as OI = S_3 (mg)/TOC (g) x 100. The OI measures the O/C ratio of a given sample, where high OI indicates oxidized or contaminated organic matter which usually corresponds to lower hydrogen index (HI).

T_{max} is an estimated temperature for maximum S_2 yield, reflecting the lab temperature required to create additional pyrolysate given the natural temperature (maturation) experienced by the sample during burial. It is directly associated with the activation energy of "live carbon" in a kerogen which relates with the maximum rate of S_2 when hydrocarbon is released during the second phase of volatilization (Pimmel and Claypool, 2001; Nordeng, 2012). The Hydrogen Index (HI) measures the relative amount of "live carbon" as HI = S_2 (mg)/TOC (g) x 100 and is used to characterize the origin of the organic matter in a given sample. Evolution level of the organic matter can be characterize by the Production Index (PI) as PI = S_1/ (S_1 + S_2), it is the ratio of the amount of oil relative to the amount of "live carbon" in a given sample. It can be used to determine the amount of hydrocarbon that already produced from the kerogens.

The basics of the Rock-Eval technique is shown in Figure 2-7 where the primary data comprise S_1 (kg free oil/tonne rock), S_2 (kg pyrolysate oil/tonne rock) and (sometimes) S_3 (kg CO_2/tonne rock). Derivative ratios comprise the Hydrogen index (HI = S_2/TOC, mg/g TOC), the Oxygen Index (OI = S_3/TOC, mgCO_2/g TOC) and the Production Index (PI = S_1/ (S_1+S_2)).

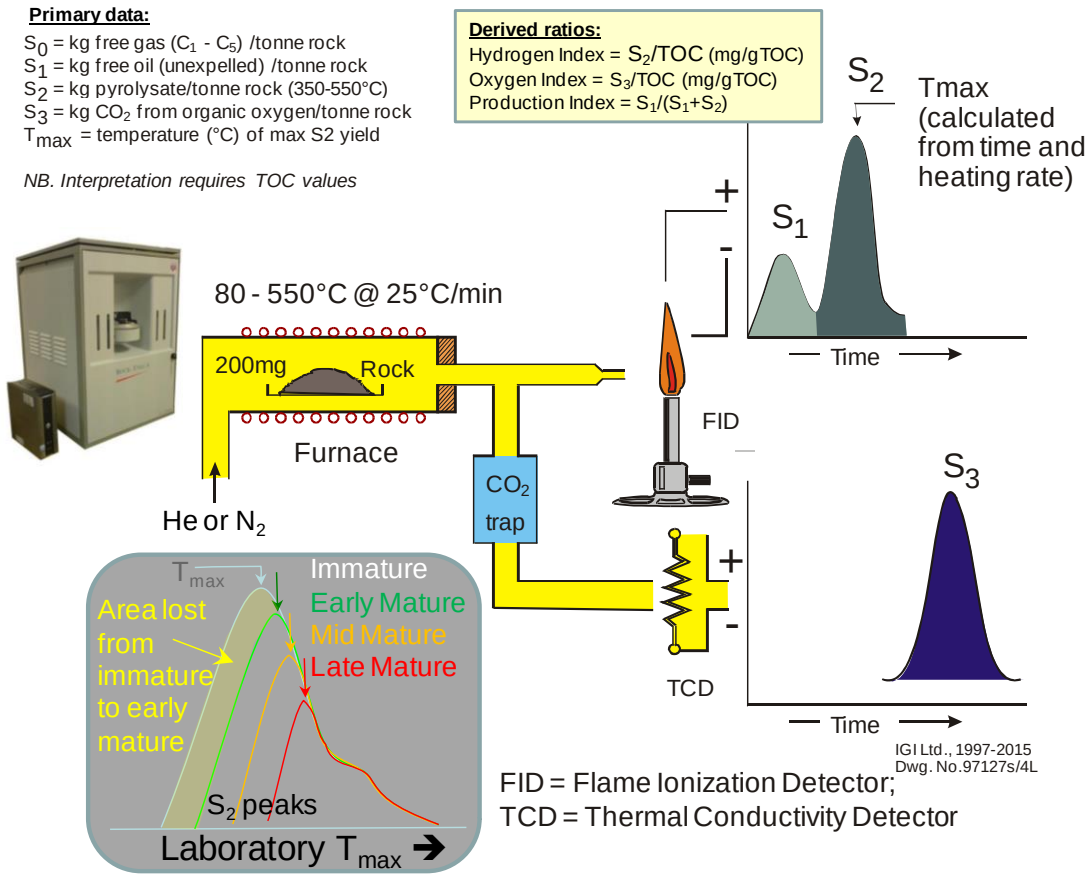

Figure 2-7: Schematics of the Rock-Eval apparatus and the primary and derived parameters. Inset (bottom left) shows the changes in the S_2 peaks with maturity leading to changes in T_{max} as a maturity parameter (Cornford et al., 2014).

2.5.5: Carbon Isotopic Analysis

In this study, stable-isotope measurements were performed on whole rock samples in Chapter 4 and isolated kerogen samples in Chapter 7 at Durham University using a Costech Elemental Analyser (ECS 4010) coupled to a ThermoFinnigan Delta V Advantage. Powdered samples were treated in 3 M of hydrochloric acid for decalcification, samples were then rinsed 5 x in de-ionised water until neutral pH was achieved. The samples were subsequently dried overnight in an oven at 60 °C.

Further preparation for the isotope analysis involved weighting about 0.2-0.5 mg of powdered samples placed within a 6 mm x 4 mm capsule tin foil and dropped into a furnace where they were completely combusted. The resulting gases were passed through a gas chromatography column for separation and then measured in succession by the TCD detector. Carbon-isotope ratios are corrected for ^{17}O contribution and reported in standard delta (δ) notation in per mil (‰) relative to the Vienna Pee Dee Belemnite (VPDB) scale. Data accuracy is monitored through routine analyses of in-house standards, which are stringently calibrated against international standards (e.g., USGS 40, USGS 24 and IAEA 600). Analytical uncertainty for $\delta^{13}C_{org}$ measurements is typically ±0. 1 ‰ for replicate analyses of the international standards and typically <0.2 ‰ on replicate sample analysis (e.g., USGS 40, USGS 24, and IAEA 600). In addition to the LECO analysis mentioned above, total organic carbon was obtained as part of the isotopic analysis using an internal standard (i.e., glutamic acid, 40.82 %C).

2.6: Petrographic and Mineralogical Techniques

The objective of the petrographic thin-section was to investigate rock types and properties (mineralogy, rock fabric, texture, structures, fractures and fossil contents), depositional environment and diagenesis of the rocks. X-ray Diffraction analyses were used to investigate the amount, abundant and proportions of the different mineral present in each given sample. It can also be used for quantitative identification and quantification of clay fraction, clay volume and clay/silt ratio.

An organic petrographic analysis allows the ability to identify the various types of maceral end-members in organic matter. It allows the determination of thermal maturation parameter (vitrinite reflectance) in order to evaluate the organic matter type and quantity. It can also be used to investigate the origin and primary sources (marine algae, lacustrine algae and land plant materials) in organic matter

2.6.1: Thin Section Preparation and Analysis

Petrographic thin-sections analyses were carried out following the visual estimate of core samples for lithofacies and the abundance of sand-shale ratio for each sample.

Samples were cut into 20 mm slices with a bench-mounted circular disc with a fine diamond saw and ground optically flat. Samples were then mounted on a glass slide and impregnated with low viscosity blue epoxy under vacuum, and the epoxy was forced into pore spaces by pressure with an inert gas. The cut rock sections were polished to approximately 20 μm in thickness using a flat glass surface with a 9.5 μm aluminum oxide paste. The samples were then covered with cover slips for optical petrographic and scanning electronic microscopic analyses. Petrographic analyses were performed under transmitted and crossed light using a Leica DM 1B02 polarizing microscope. Quantitative observation of rock fabric, texture, fracture; lithology and mineral compositions were made, and images were captured using the attached Leica DFC 320 digital camera at small-higher magnifications (5* to 100*). Thin-section preparation was done at the Earth Science Department of Durham University by Ian Chaplin, Thin Slide Technician.

2.6.2: X-ray Diffraction (XRD) Analysis

For this study, a Bruker D8 Advanced diffractometer set to Bragg-Brentano geometry reflection mode was used to record the X-ray diffraction pattern of powdered samples. Each 5-10 g of pulverised sample were prepared and dried at 60 °C overnight and then mounted on a dry slide glass and held in a sample holder. The sample holders were then placed into the X-ray Diffractometer, the X-ray radiation was Cu Kα (1.54056 nm) and the sample was scanned between 5 and 65° 2θ angle with a 0.02° 2θ step size (Moore & Reynolds, 1997). Peak analysis was manually done with MS Excel using known diffraction patterns from the Inorganic Crystal Structure Database (ICSD). The X-ray diffraction (XRD) analysis was undertaken at the Chemistry Department of Durham University by Manohar G.V.

2.7: Organic Petrography Analysis

Macerals are defined as microscopically homogenous aggregates of organic substances with distinctive chemical and physical properties occurring naturally in sedimentary rocks. Different kerogen types contain different macerals, and kerogen generates oil and /or gas based on type and maturation of these macerals.

For this study, splits of each whole-rock (40–50 g) and kerogen (20–30 mg) sample were crushed to minus 20-mesh (841 μm or 0.85 mm size) with a mortar and pestle. Each sample was mixed with the appropriate ratios of epoxy resin and hardener (Buehler EpoxyCure 2) in a paper cup and poured into 2.5 cm diameter phenolic ring forms glued to a foiled glass plate and allowed to cure overnight (Figure 2-8). Due to the small amount of isolated kerogen, a small diameter (~0.5 cm) hole was drilled into an epoxy blank pellet, and the kerogen/epoxy mix was poured into the cavity and allowed to cure (Figure 2-8). Each sample was then labelled; additional epoxy was poured over the label to complete the pellets, which were again left to cure overnight.

Figure 2-8: Pellets of whole rock and isolated kerogen samples prepared for organic petrographic.

The surface of the cured pellets (Figure 2-8) was ground and polished using a Buehler Automet 250 (Figure 2-9), following a stepwise procedure using 320 grit, 400 grit and 600 grit Carbimet paper. The grinding was followed by polishing with 1 μm Buehler Micropolish II alumina powder and 0.06 μm Buehler Mastermet 2 colloidal silica suspension for 2 min. Distilled water was used throughout as the lubricant, and each pellet was rinsed in a Branson 3510 ultrasonic bath in between each grinding and polishing steps to remove grit and polishing compound. Finally, the pellets were thoroughly washed with distilled water and air-dried.

Petrographic observations of the polished whole-rock and kerogen samples were performed using a Leica DM 2500P reflected-light microscope, equipped with 12V 100W white-light (halogen) source and a Prior Lumen 200 blue-light source (metal halide) for fluorescence excitation. Samples were viewed using a 50x/0.85 oil immersion objective providing an overall magnification of *500 with 10* eye-pieces. Vitrinite reflectance measurements were calculated as the mean of 30 measurements on vitrinite particles per sample as described in ASTM D7708-14 using a Leica DM 2500P reflected-light microscope equipped with J & M Analytik TIDAS hardware and software (Figure 2-10). The organic petrology preparation and analysis was performed at the Kerogen Lab of Southern Illinois University, Carbondale, Illinois, USA.

Figure 2-9: The Buehler Automet 250 Micropolish used to ground and polish the cured pellets up to 0.06 μm before microscopic observations.

Petrographic observations of the polished whole-rock and kerogen samples were performed using a Leica DM 2500P reflected-light microscope, equipped with 12V 100W white-light (halogen) source and a Prior Lumen 200 blue-light source (metal

halide) for fluorescence excitation. Samples were viewed using a 50x/0.85 oil immersion objective providing an overall magnification of *500 with 10* eye-pieces. Vitrinite reflectance measurements were calculated as the mean of 30 measurements on vitrinite particles per sample as described in ASTM D7708-14 using a Leica DM 2500P reflected-light microscope equipped with J & M Analytik TIDAS hardware and software (Figure 2-10). The organic petrology preparation and analysis was performed at the Kerogen Lab of Southern Illinois University, Carbondale, Illinois, USA.

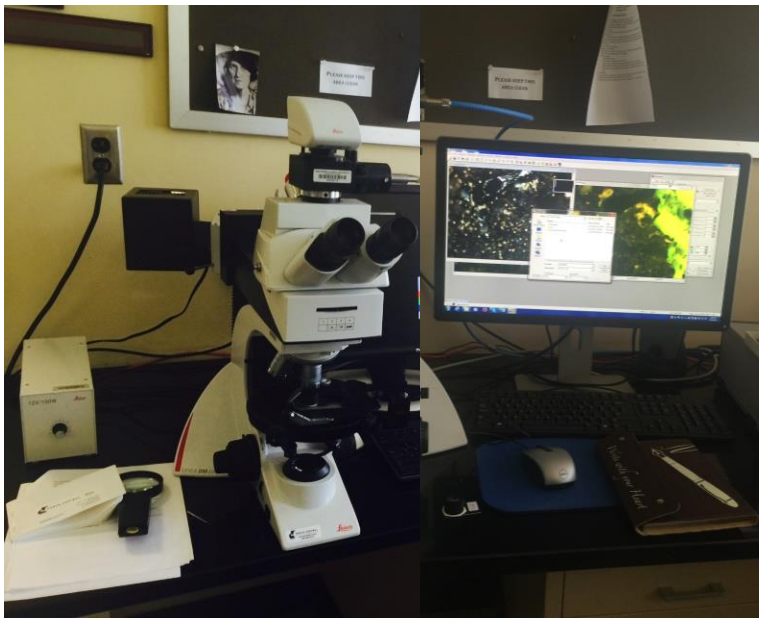

Figure 2-10: A Leica DM 2500P reflected-light microscope equipped with J & M Analytik TIDAS hardware and software

2.8: Porosity Analysis

Porosity is the volume of void space in a rock between rock grains (inorganic porosity and micro-porosity), within organic matter (organic porosity) occupied by water, oil or gas in a given reservoir or source rock expressed as percentages. It is important to know the porosity of the different lithologies in both nanometer and micrometer scale, to identify the pore network, size, distribution and connectivity of the porosity. Laminated fine-grained mudstones typically have low porosity usually measured in nanometer scale, while pores within sandstone are in micrometer scale. The porosity of source rocks is very important in the assessment of its potential for unconventional

resources; pores of less than 5 μm can be identified in mudstone samples (Reed and Loucks, 2007).

2.8.1: Focused Ion Beam -Scanning Electron Microscope (FIB-SEM)

For this study, Scanning Electron Microscope (SEM) equipped with an Oxford Instruments energy dispersive X-ray spectroscopy (EDS) microanalysis system (INCA Energy 700) was used at University of Durham GJ Russell Microscopy Facility. For the FIB-SEM/EDS analyse, thin-sectioned samples were polished by an Argon ion mill with two ion sources. The polished samples were mounted on a flat aluminium stage using a conductive carbon tape and then lightly carbon-coated with a carbon sputter coater. Focused ion beam milling and SEM imaging was conducted using an FEI Helios Nanolab G3 DualBeam™ system. FIB milling provides accurate cross-section surface of any area of interest to an approximately 1 mm in width. The technique involves sputtering platinum (2 to 3 μm thick) at both 0° and 52° to protect the site of interest. The Ga+ ion beam was then used at a high voltage and current (30 kV, 9.3 nA) to mill a trench 25 μm * 18 μm *18 μm in order to image a 10 μm * 10 μm image. Then the sample is tilted to 0° to mill the site of interest and SEM images were captured and saved.

2.8.2: Energy Dispersive X-ray Spectroscopy (EDS)

In Energy Dispersive X-ray Spectroscopy (EDS), an electron beam impinges on the sample and generates x-rays collected by a detector; the energy of the generated x-ray gives information on the quantification of the elemental composition in the sample. EDS maps were obtained using AZtecEnergy EDS software for mineral phase identification, and the mineral phases obtained were divided into several mineral groups such as quartz, plagioclase, mica, muscovite, biotite, siderite, anatase, chlorite, kaolinite and illite/smectite. Multiple 2D SEM and EDS images, maps were obtained. Backscattered electron (BSE) of each sample (3072 * 2304 pixels) were collected at 20 kV acceleration voltage, 4000 nA beam current, 30 μm aperture size and a 15 mm free working distance. BSE is the elastically-scattered beam electrons that escapes from the samples back to the surface.

2.8.3: Microtomography (Micro-CT) analysis

X-ray computer tomography (CT) is a non-destructive technique for visualizing interior features within a given sample, and for obtaining digital information on their internal 3-D geometries and structural properties. A CT image is created by directing X-rays through the slice plane from multiple orientations and measuring their resultant decrease in intensity. A specialized algorithm is then used to reconstruct the distribution of X-ray attenuation in the slice plane. Micro-tomography was taken from small cylindrical sample with dimensions of 10 mm in diameter and 15 mm in height using a Zeiss XRadia-410 CT scanner. The X-ray source was set to 80 kV and 140 μA, a Bremsstrahlung filter was used to enhance the performance of the detector for the X-ray photons to acquire 3201 projections of 2048 pixel for 24 hours. The projections were typically reconstructed to a 3-dimensional (3D) raw tomogram, with a voxel size of 1.03 μm/voxel resolution. The analysed samples were selected to represent predominantly mudstone and sand-mudstone interface ratios. High resolution 3D Micro-CT images were obtained for these samples, images processing and visualization and interpreted was done using Avizo™ 9 software. Identification of surface and pore mineral phases were further used to understand the nature of porosity, pore size distribution, pore connectivity and hydrocarbon flow path in this hybrid reservoir system.

2.9: Implications of Analytical Methods used in Evaluation of the Kimmeridge Clay Formation

The analytical methods described in this chapter were systematically employed to evaluate and characterise the potential of Upper Jurassic Kimmeridge Clay source rock for unconventional resources. Data and sample collections with the combination of these analytical methods used for this thesis were chosen for identification of sweet-spot parameters described in Chapter 1.

TOC analyses were carried out to measure the amount and quality of organic matter in the source rock. Total organic carbon richness of the source rock is an important parameter in the evaluation of hydrocarbon potential of the Kimmeridge Clay Formation. For the evaluation of source rock maturity, kerogen types and

hydrocarbon generative potential the Rock-Eval Pyrolysis technique and the relationship between pyrolysis parameters were considered. Carbon isotope analyses were used to differentiate and characterise the source rock origin into marine and non-marine (terrestrial) organic matter. For the identification and composition of the mineral phases, thin-section and X-ray diffraction techniques were used. Kerogen isolation procedures were performed to chemically isolate the kerogens from the mineral matrix in order to understand the effect of demineralisation on quality of organic matter, kerogen type, thermal maturation and generative potential. To investigate the nature and type of porosity within the source rock focused ion beam-scanning electron microscopy analyses were employed. All of these analyses and their derivative parameters used for sweet-spot identification are detailed in subsequent chapters.

2.10: References

Behar, F., Beaumont, V. and De B. Penteado, H. 2001. Rock-Eval 6 Technology: Performances and Developments. Oil & Gas Science and Technology, 56(2), pp.111-134.

British Geological Survey 2016. Offshore Hydrocarbon Wells | British Geological Survey (BGS).[online] Bgs.ac.uk. Available at:: http://www.bgs.ac.uk/data/offshoreWells/wells.cfc?method=searchWells [Accessed 28 Mar. 2014].

Calvert, S. 2004. Beware intercepts: interpreting compositional ratios in multi-component sediments and sedimentary rocks. Organic Geochemistry, 35(8), pp.981-987.

Carvajal-Ortiz, H. and Gentzis, T. 2015. Critical considerations when assessing hydrocarbon plays using Rock-Eval pyrolysis and organic petrology data: Data quality revisited. International Journal of Coal Geology, 152, pp.113-122.

Cooper, B. S. and Barnard,P.C. 1984. Source rocks and oils of the central and northern North Sea. In: G. Demaison and R. Murris, ed., Petroleum geochemistry and basin evaluation. American Association of Petroleum Geologists Memoir, 35, pp.303–314.

Cooper, B. S., Bernard, P.C and Telnaes, N 1995. The Kimmeridge Clay formation of the North Sea. In: B. Katz, ed., Petroleum source rocks. Berlin, Springer-Verlag, pp.89–110.

Cornford, C and Brooks, J. 1989. Tectonic controls on oil and gas occurrences in the North Sea area. In: Tankard, A.J. and Balkwill, H.R, ed., Extensional tectonics and stratigraphy of the North Atlantic margins. American Association of Petroleum Geologists/Canadian, Geological Foundation, pp.46- 641.

Cornford, C. 1998. Source rocks and hydrocarbons of the North Sea. In: Glennie, K.W., ed., Petroleum geology of the North Sea. London, Blackwell Science Ltd, pp.376–462.

Cornford, C., Birdsong, B. and Groves, G. 2014. Offshore Unconventional Oil from the Kimmeridge Clay Formation of the North Sea: A Technical and Economic Case. Unconventional Resources Technology Conference Proceedings, Denver, CO. August 25-27, 2014.

Department of Energy and Climate Change 2013. Public Wellbore Search - UK Oil Portal. [online] Itportal.ogauthority.co.uk. Available at:: https://itportal.ogauthority.co.uk/edufox5live/fox/edu/WONS_WELLBORE_SEARCH_PUBLIC [Accessed 12 Mar. 2014].

Department of Energy and Climate Change 2013. United Kingdom Continental Shelf (UKCS) Geological Basins. [online] Available at:: https://www.gov.uk/oil-and-gas-offshore-maps-and-gis-shapefiles 20140331_UKCS_Geological_Basin [Accessed 12 Mar. 2014].

Ellington and Associates Inc. 2017. Total Organic Carbon(TOC-LECO)Analysis. [online] Ellingtongeologic.com. Available at:: http://www.ellingtongeologic.com/total-organic-carbon-TOC-LECO.html [Accessed 2 May 2017].

Erratt, D., Thomas, G.M., Hartley, N.R, Musum, R., Nicholson, P.H. and Spisto, Y. 2010. North Sea hydrocarbon systems: some aspects of our evolving insights into a classic hydrocarbon province. In: Pickering, S.C. and Vining, B., ed., Petroleum Geology: From Mature Basins to New Frontiers. Proceedings of the 7th Petroleum Geology Conference. Geological Society of London, London, England, pp.37-56.

Espitalie, J., Deroo, G. and Marquis, F. 1985. La pyrolyse Rock-Eval et ses applications. Première partie. Revue de l'Institut Français du Pétrole, 40(5), pp.563-579.

Galimov, E. 2006. Isotope organic geochemistry. Organic Geochemistry, 37(10), pp.1200-1262.

Gröcke, D., Ludvigson, G., Witzke, B., Robinson, S., Joeckel, R., Ufnar, D. and Ravn, R. 2006. Recognizing the Albian-Cenomanian (OAE1d) sequence boundary using plant carbon isotopes: Dakota Formation, Western Interior Basin, USA. Geology, 34(3), p.193.

Jarvis, I., Lignum, J., Gröcke, D., Jenkyns, H. and Pearce, M. 2011. Black shale deposition, atmospheric CO2drawdown, and cooling during the Cenomanian-Turonian Oceanic Anoxic Event. Paleoceanography, 26(3), p.n/a-n/a.

Leythaeuser, D., Radke, M. and Schaefer, R. 1984. Efficiency of petroleum expulsion from shale source rocks. Nature, 311(5988), pp.745-748.

Meyers, P. 1994. Preservation of elemental and isotopic source identification of sedimentary organic matter. Chemical Geology, 114(3-4), pp.289-302.

Meyers, P. and Eadie, B. 1993. Sources, degradation and recycling of organic matter associated with sinking particles in Lake Michigan. Organic Geochemistry, 20(1), pp.47-56.

Moore, D. M. and Reynolds, R. C. 1997. X-Ray diffraction and the identification and analysis of clay minerals. 2nd ed. Oxford University Press, New York.

NIGOGA (n.d.). The Norwegian Guide to Organic Geochemical Analyses. [online] Available at:: http://www.npd. no/engelsk/nigoga/default.htm [Accessed 10 May 2014].

Norwegian Petroleum Directorate (NPD) (n.d.). Home - Norwegian Petroleum Directorate. [online] Npd.no. Available at:: http://www.npd.no/en/ [Accessed 18 Apr. 2014].

Peters, K. 1986. Guidelines for Evaluating Petroleum Source Rock Using Programmed Pyrolysis. American Association of Petroleum Geologists Bulletin, 70.

Raji, M., Gröcke, D., Greenwell, C., Gluyas, J. and Cornford, C. 2015. The effect of interbedding on shale reservoir properties. Marine and Petroleum Geology, 67, pp.154-169.

Reitsema, R. H. 1983. Geochemistry of North and South Brae areas, North Sea. In: Brooks, J., ed., Petroleum Geochemistry and Exploration of Europe,. Geological Society, London, Special Publication, 12, pp.203-212.

Richards, P., Lott, G.K., Johnson, H., Knox, R.W and Riding, J.B. 1993. Jurassic of the central and northern North Sea. Nottingham: British Geological Survey on behalf of the UK Offshore Operators Association.

Roberts, M. J. 1991. The South Brae Field, Block 16/7a, U.K. North Sea. In: Abbotts, I. L., ed., United Kingdom Oil and Gas Fields 25 Years Commemorative Volume. . Geological Society, London, Memoir, 14, pp.55-62.

Rooksby, S.K 1991. The Miller Field, Blocks 16/7B, 16/8B, UK North Sea. Geological Society, London, Memoirs 4, pp.159-164.

Stow, D. 1983. Sedimentology of the Brae Oilfield Area, North Sea: A Reply. Journal of Petroleum Geology, 6.

Turner, C.C., Cohen, J.M., Connell, E.R. and Cooper, D.M. 1987. A depositional model for the South Brae Oilfield. In: Brooks, J. and Glennie, K.W., ed., Petroleum Geology of North West Europe, .. Graham and Trotman, London, pp.853-864.

Weiss, H.M., Wilhelms, A., Mills, N., Scotchmer, J., Hall, P.B., Lind, K., and Brekke, T. 2000. NIGOGA – The Norwegian Industry Guide to Organic Geochemical Analyses. [online] Available at:: http://www.npd.no/Global/Norsk/5-Regelverk/Tematiske-veiledninger/Geochemical-analysis_e.PDF [Accessed 7 Jul. 2015].

Ziegler, P.A. 1990. Tectonic and palaeogeographic development of the North Sea rift system. In: Blundell, D.J. and Gibbs, A.D, ed., Tectonic Evolution of the North Sea Rifts. Oxford University Press, New York, pp.1-36.

Chapter 3: The relationship between source rock thickness and organo-facies of the South Viking Graben

This chapter is based on a paper in preparation for submission to Journal of the Geological Society, London: Raji, M., Gröcke, D. R., Greenwell, C. H. and Cornford, C.

In this chapter, a large geochemical database of over 5,000 source rock cores and cutting samples from the British Geological Survey (BGS) and Norwegian Petroleum Directorate (NPD) were used to characterise the Upper Jurassic- Lower Cretaceous source rocks in the South Viking Graben area of the North Sea. The main objective of this study is to systematically map thickness, source rock quality, organofacies as well as hydrocarbon potential of these source rocks and to understand the controls on the unconventional source rock potential in the South Viking Graben area. It presents the initial results from the database on source rock analysis and uncovers regional variations in hydrocarbon potential across the study area.

3.1: Abstract

The South Viking Graben is a thermally mature North Sea depocenter that accumulated the organic-rich Kimmeridge Clay (Draupne), and Heather Formation collectively called the Viking Group source rocks in the Late Jurassic and Early Cretaceous period. The source facies and quality of these source rocks varies stratigraphically and regionally across the South Viking Graben in the UK and Norway due to the topography of the seafloor, nutrient supply, widespread anoxia conditions, bottom water stratification, preservation of the organic matter and siliciclastic dilution effect. This study was undertaken to systematically map out the source rock thicknesses and distributions in order to evaluate the source rock quality and unconventional hydrocarbon potential of these organic-rich intervals.

The average thickness of the Upper Jurassic Kimmeridge Clay -Draupne Formation is about 85 m, and up to 600 m thick in the north-western part towards the graben centre, where it gradually thins to between 0-200 m towards the south eastern area. The Heather Formation is up to 70 m, and thins towards Norway, with thicker sedimentation in the south-west and north-west part of the area, and up to 800 m in

graben centre. The average total organic carbon (TOC) values for the Viking Group is up to 5 wt. % with a maximum TOC of 11 wt. % (< 2 wt. % for Heather Formation) indicating a good to very good organic-richness source rock.

The kerogen types as reflected by Rock-Eval HI, T_{max} values predominantly consist of Type II and Type III kerogens as end members. The onset of oil generation as shown by the T_{max} /Depth plot suggests early oil window generation started at 2700-3350 m while the mid oil window began at 3500 m with peak oil generation and expulsion at 4200-4800 m. Organic petrology data interpretation indicates the maceral composition is dominated by liptinite and vitrinite with some inertinite. Correlation between Rock-Eval HI and liptinite suggests that the high HI facies contain a higher percentage of liptinite macerals comprising algae (plankton) together with amorphous Type II kerogen where the algal biomass has been subjected to bacterial degradation. The deepest sediments accumulating in the most anoxic part of the graben contain–the richest amount of organic matter. These variations in source facies, source quality and maceral composition show that the basin-ward area are generally oil-prone and have better quality of organic content and source potential for unconventional hydrocarbon in the South Viking Graben area.

3.2: Introduction

To date, 16 billion barrels of commercial reserves have been discovered in conventional reservoirs in the UK Viking Graben area with 29 billion barrels discovered in the Norwegian sector to the east (Norwegian Ministry of Petroleum and Energy, 2005). However, the principal UK hydrocarbon province has reached the mature phase of conventional exploration, leading to a growing interest in unconventional hydrocarbon in the UK onshore. Due to the high organic carbon of the Kimmeridge Clay Formation as a world-class source rock, it could also be a very good target for the first offshore unconventional resource in the North Sea. A significant part of the remaining and future potential of oil in this region is anticipated to be retained in the actively generating Kimmeridge Clay Formation (KCF) source rocks buried below 3400-4300 m in the South Viking Graben area (Cornford et al., 2014).

The Upper Jurassic to Lower Cretaceous Kimmeridge Clay Formation (KCF) in UK waters (or Draupne Formation in Norway) comprises the upper part of the Viking Group, and is the major source rock in the North Sea region with the Heather Formation as the lower part of the Viking Group (Miller, 1990; Cornford, 1998; Kubala et al., 2003; Justwan and Dahl, 2005). The source facies and quality of these source rocks vary considerably across the South Viking Graben (Kubala et al., 2003; Justwan and Dahl, 2005).

The main focus of this study is on the upper part of the Viking Group since it contains the major source rocks in the North Sea region (Miller, 1990; Cornford, 1998; Kubala et al., 2003; Justwan and Dahl, 2005). Limited well and geochemical data are available for the lower Viking Group. The main aim of this chapter is to produce thickness and distribution maps and to define the quality of the Upper Jurassic-Early Cretaceous source rocks as a potential unconventional resource in the South Viking Graben area of the North Sea.

The generated maps were used to describe the lateral and vertical variation in both thicknesses and distributions of the source rocks based on stratigraphic information from well logs. Geochemical data such as total organic carbon (TOC) and Rock-Eval data were used to investigate regional variation in source rock quality, organofacies and hydrocarbon potential across the area. Petrographic data combined with visual kerogen description was used to determine the overall variation in the amount, composition and origin of the macerals in the organic matter.

Isopach and organofacies maps are important for source rock evaluation and have been used by several authors for qualitative and quantitative study of basin formation, hydrocarbon generation and accumulation (Cornford, 1998; Justwan et al., 2005; Justwan and Dahl, 2005; Guan et al., 2017), source rock characterisation and potential (Wu et al., 2012) lithofacies changes, (Ramadan et al., 2014) maturation and organofacies variation (Fisher and Miles, 1983; Pearson and Watkins, 1983; Baird, 1986; Dahl et al., 2003). Isopach mapping enables a more reliable model of source rock quality, distribution and potential across a regional area.

3.3: Methodology and Dataset

A large dataset assembled from over 5,000 samples with total organic carbon (TOC), Rock-Eval and organic petrography data was made available in p: IGI-3 format. This database has been compiled by Integrated Geochemical Interpretation Limited (IGI Ltd) from the Fact Pages of the Norwegian Petroleum Directorate (NPD) and other proprietary data source. Equivalent UK data was generated for this project by analyzing core and cutting samples from the British Geological Survey core store by IGI Ltd. The database covered UK Quadrant 16 (mainly core samples) and the adjacent Norwegian Quadrants 15, 16 and 17 to the east, which are dominated by sample cuttings (Figure 3-1). The workflow for this project is designed around integrating lithostratigraphy and source rock geochemistry by mapping key surfaces and thicknesses of the Upper Jurassic and Lower Cretaceous (Figure 3-2).

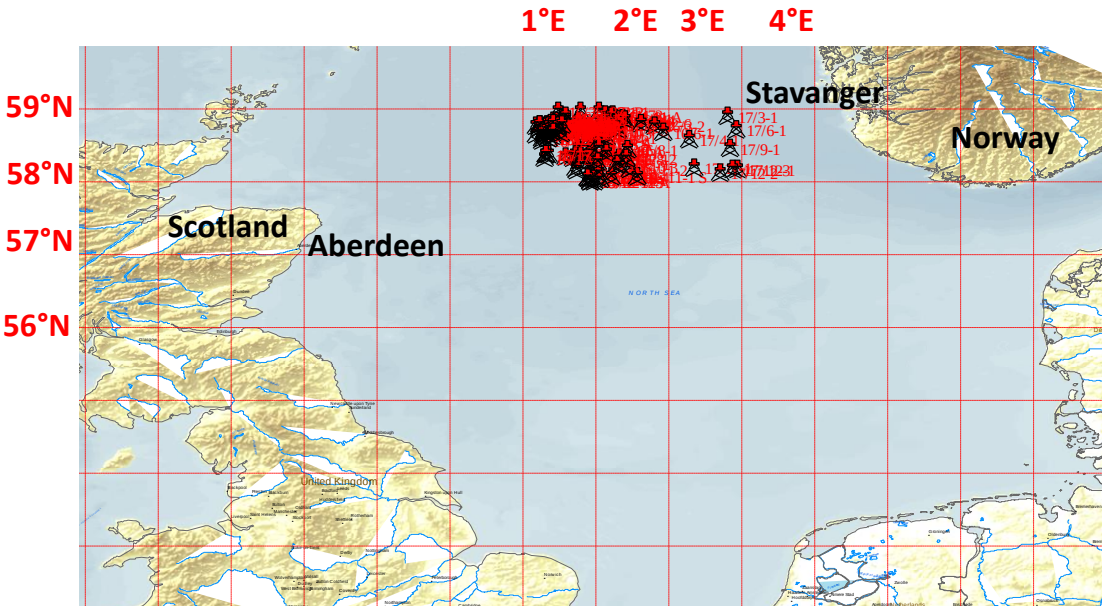

Figure 3-1: Map of the North Sea showing location of selected well and samples across the UK and Norwegian blocks of the South Viking Graben.(modified from p:IGI-3 database).

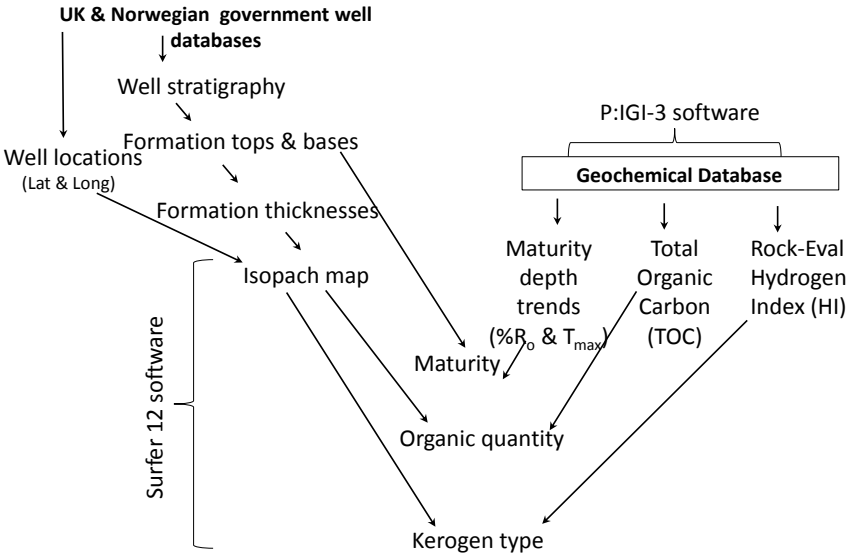

Figure 3-2: Project workflow showing data sources and the integration of stratigraphic, mapping and geochemical data to define organic matter quality, thermal maturity, kerogen and kerogen types in this study.

Mapping for this study was based on grids from the Millennium Atlas (Evans et al., 2003), with the Base Cretaceous Unconformity (BCU) grid being the best defined. Subsequent surfaces were produced by correlation from well tops/bases from 310 wells that penetrated the Upper Jurassic and Lower Cretaceous KCF/Draupne Formation, together with the underlying Oxfordian Heather Formation from 85 wells. Well formation data grids were created in Trinity software, where thickness and distribution maps for the KCF/Draupne Formation and Heather Formation were generated. Thicknesses calculated from these mapped tops and bases were used to investigate the lateral distribution of the source rock across the study area.

To investigate the source rock quality and thermal maturation and hydrocarbon potential, geochemical analyses data was compiled. The geochemical analyses used for this study are Total Organic Carbon (TOC wt. %, mainly from the LECO method described in Chapter 2.5), Rock-Eval pyrolysis (from Rock-Eval 2 and 6 over the years, also described in Chapter 2.5). All available geochemical data were used to investigate the variation in organo-facies of these source rocks. For selected samples,

sand/shale ratios at the millimetre-decimetre level were used to characterise lithofacies. Interpretation and plotting of the geochemical data was undertaken using p: IGI-3 software. Isopach, distributions, TOC and vitrinite reflectance maps were created using Trinity software.

3.4: Geology and Stratigraphy of South Viking Graben

The Viking Graben is a major N-S linear trough approximately located along the junction between the UK and Norwegian sectors of the northern North Sea (Figure 3-3). The graben is flanked by the Shetland Platform to the west, the Utsira High and Horda Platform to the east. This graben is part of the North Sea post-Caledonian rift system developed during two major phases of extension Permo-Triassic period (Glennie, 1986; Ziegler, 1990; Faerseth, 1996; Justwan et al., 2005; Johnson et al., 2005; Erratt et al., 2010). During the Lower Triassic period, arenaceous mudstones of the Smith Bank Formation with sandy alluvial fan deposits of Skagerrak Formation were deposited in the graben, these Triassic rocks are widely distributed in the northern North Sea (Fisher and Mudge, 1998; Goldsmith et al., 2003). Lower Jurassic sediments are sporadically encountered in the South Viking Graben area due to the broad doming and erosion of Lower Jurassic strata in the early–mid Jurassic (Richard et al., 1988). This sediment was transported to the north from the dome centre in the Central North Sea, where it sourced the Middle Jurassic clastic reservoir sediments (Ziegler, 1992).

In the Middle Jurassic (Callovian-Oxfordian), marine transgression together with structural extension, and continuous rapid subsidence resulted in the deposition of thick sediments in the South Viking Graben (Cornford, 1998). These processes combined to produce an isolated deep- water basin which became relatively sediment-starved in the Upper Jurassic. With a distal connection to the Boreal seaway far to the north and in the reduction of circulation, the basin accumulated organic-rich marine sediments of the KCF/Draupne Formation (Cornford, 1998). The organic rich oil and gas-prone shales of the Heather and Draupne Formations were deposited during a sea-level rise in the Late Jurassic. Heather Formation sandstones are widely developed along the western margin of the UK sector (Figure 3-4), and also act as

reservoirs in the South Viking Graben area (Justwan et al., 2005). Three principal palaeo-environmental models have been proposed for the depositional environment of the KCF/Draupne Formation; the productivity model (Gallois, 1974, 1976); the preservation model (Tyson, 1987, 1989; Tyson et al., 1979) and the palaeoceanography model (Oschmann, 1988 and Miller, 1990).

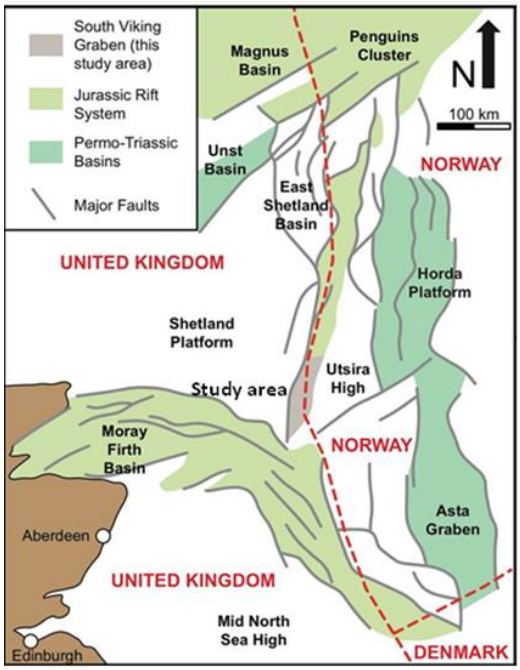

Figure 3-3: Overview map of the North Sea showing an outline of the Jurassic Rift System and the study area in the South Viking Graben. (modified from Dominguez, 2007)

In the Middle Jurassic (Callovian-Oxfordian), marine transgression together with structural extension, and continuous rapid subsidence resulted in the deposition of thick sediments in the South Viking Graben (Cornford, 1998). These processes combined to produce an isolated deep- water basin which became relatively sediment-starved in the Upper Jurassic. With a distal connection to the Boreal seaway far to the north and in the reduction of circulation, the basin accumulated organic-rich marine sediments of the KCF/Draupne Formation (Cornford, 1998). The organic rich oil and gas-prone shales of the Heather and Draupne Formations were deposited during a sea-level rise in the Late Jurassic. Heather Formation sandstones are widely developed along the western margin of the UK sector (Figure 3-4), and also act as reservoirs in the South Viking Graben area (Justwan et al., 2005). Three principal palaeo-environmental models have been proposed for the depositional environment

of the KCF/Draupne Formation; the productivity model (Gallois, 1974, 1976); the preservation model (Tyson, 1987, 1989; Tyson et al., 1979) and the palaeoceanography model (Oschmann, 1988 and Miller, 1990).

The KCF/Draupne Formation, together with the Heather Formation, is collectively called the Upper and Lower Viking Group respectively (Justwan and Dahl, 2005). The Viking Group includes the upper and lower 'hot shale' members, locally separated by the 'cold shale' or, locally, coarse clastics of the Brae Sandstone Member (Figure 3-4). The lower part of the Viking Group is formed by the Heather Formation shales and the upper part is the KCF/Draupne Formation, which forms the major source rock for the North Sea hydrocarbon (Cornford and Brookes, 1989; Cornford, 1998; Gautier, 2005; Justwan and Dahl, 2005). There is little contribution from the Heather Formation as a source rock in the North Sea because it is organic-lean (Cornford, 1998; Justwan and Dahl, 2005) but it also has the potential for oil and gas generation (Cooper and Barnard, 1984; Cooper et al., 1993; Cornford, 1998). The boundary between the organic-rich Kimmeridge Clay Formation and organic- lean Heather Formation is generally picked based on electric log responses (natural gamma ray, density, sonic velocity).

The major unconformity between the Upper Jurassic sediment and Lower Cretaceous is termed the Base Cretaceous Unconformity (BCU), which is most clearly viewed on seismic lines where the final stages of Ryazanian rifting in the Early Cretaceous caused erosion on the crests of uplifted (rotated) fault blocks (Vollset and Doré, 1984; Cooper et al., 1993; Cornford, 1998; Kubala et al., 2003; Coward et al., 2003). In the graben, away from the faulted regions, the BCU is a prominent seismic marker due to the sonic velocity contrast between the underlying organic- rich Kimmeridge Clay Formation and the organic- poor Cromer Knoll shales deposited as shallow marine mudstones (Vollset and Dore, 1984; Oakman and Partington, 1998; Cooper et al., 1993; Cornford, 1998; Kubala et al., 2003; Coward et al., 2003). Though termed the BCU, the seismic marker in fact cuts down into the Triassic, with recommencement of sedimentation in the early-mid Ryazanian (Coward et al., 2003).

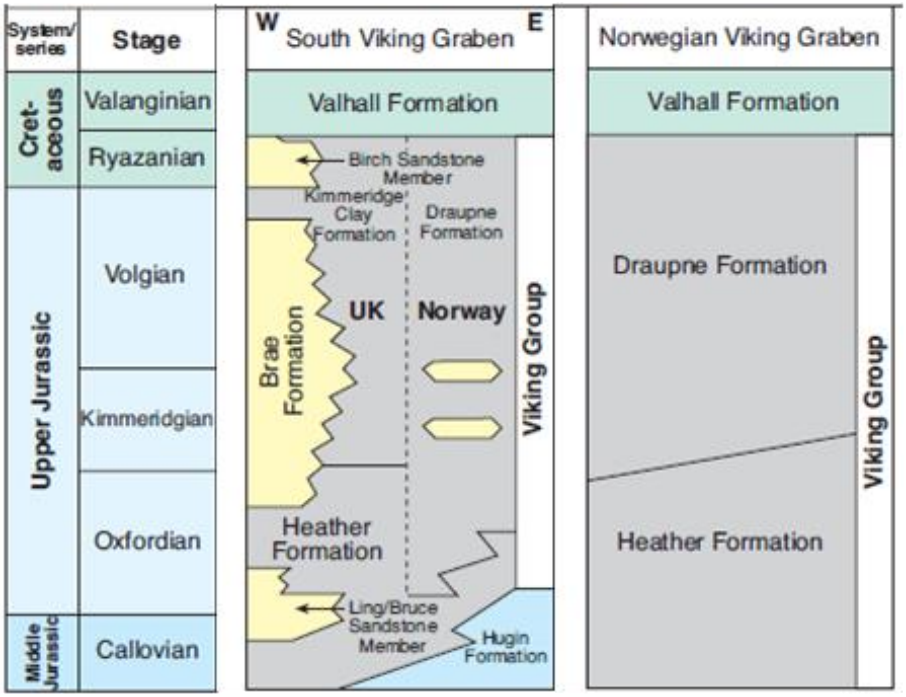

Figure 3-4: Local litho-stratigraphic terms used for the Late Jurassic and Early Cretaceous in the UK and Norwegian sectors of the South Viking Graben. The schematic boundary between the KCF (Draupne) Formation and the Heather Formation is diachronous, and denotes the changes from oxic to anoxic marine mudstone facies (From Coward et al., 2003).

3.5: Source Rocks Distribution and Thicknesses

3.5.1: The Heather Formation

The Heather Formation is Bathonian – Late Oxfordian in age and diachronously overlies Middle Jurassic Brent and Vestland Group sediments (Vollset and Dore' 1984; Norwegian Ministry of Petroleum and Energy, 2005; Justwan and Dahl, 2005). It comprises of organic-lean grey, silty mudstones with interbedded limestone bands deposited as syn-rift sediments under oxic bottom water conditions following the Bathonian transgression of the Brent Delta system (Vollset and Dore´ 1984).

In this study, the thickness and distribution of the formation across the South Viking Graben area thins towards Norway, with thicker sedimentation in the south-west and north part of the area (Figure 3-5 & 3-6). The observed average thickness of the Heather Formation is about 70 m with up to 800 m in the graben centre, and is thickest in the northwest area (Figure 3-5 & 3-6), but mostly absent over eroded fault

block in the UK wells. Figure 3-5 shows contours restricted to the UK acreage, where only 20 wells in the north east penetrate the Heather Formation.

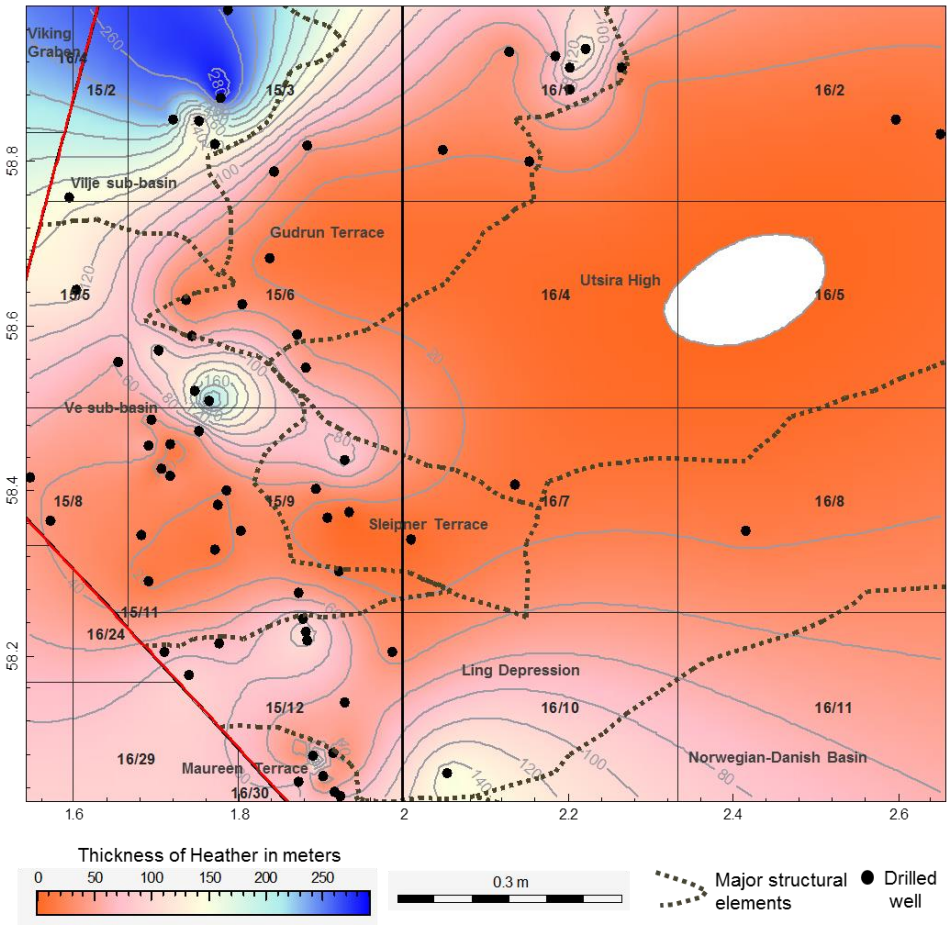

Figure 3-5: Isopach map for Heather Formation in showing well locations and structural elements in the South Viking Graben. The thicknesses were derived from formation top and base from 84 wells that penetrated the Heather Formation.

The maximum recorded thickness is 297 m in Well 15/3-3, with > 200 m recorded in Wells 15/3-2 R, 15/3-1 S, 15/6-5, 15/12-14 and 15/9-19 B, all of which are in the Norwegian group of wells with a gradual decrease in thickness towards the Utsira High in the east. As with all lithostratigraphic units and particularly those with diachronous boundaries some of the variation in thickness may be due to the definition of the top and base of the formation and its transgressive nature (Figure 3-4). Modelled sedimentation rate in the Heather Formation ranges from 1 m/Ma to over 50 m/Ma, with an average value of around 20 m/Ma (Justwan, et.al. 2005)

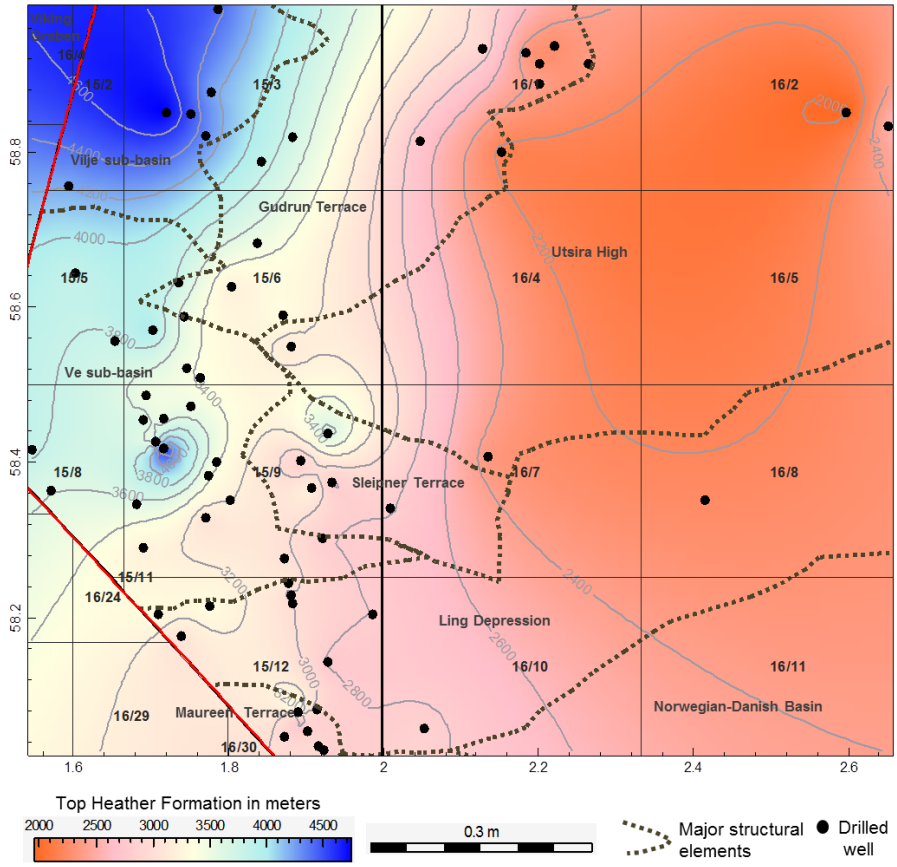

Figure 3-6: Distribution of Top Heather Formation showing well locations and structural elements in the South Viking Graben. Well Formation tops were derived from 84 wells that penetrated the Heather Formation.

3.5.2: The Kimmeridge Clay / Draupne Formation

The Upper Jurassic KCF/Draupne Formation is a major source rock in the North Sea (Barnard and Cooper 1981; Dorè et al., 1985; Cooper et al., 1995; Cornford 1998). The KCF/Draupne Formation has widespread distribution with varying thickness throughout the South Viking Graben, and may be locally absent in places due to erosion. This formation diachronously overlies the Heather Formation, and ranges in age from Kimmeridgian (Volgian) to Ryazanian (Figure 3-4). Late Jurassic global rise in sea-level followed by a marine transgressive event in the Late Oxfordian to Early Kimmeridgian marked the transition from the Heather Formation to the KCF/Draupne Formation (Rawson and Riley 1982; Cornford, 1998; Justwan and Dahl, 2005). The KCF/Draupne Formation occurred in a shallow sea with persisted anoxic bottom water conditions through much of the time of deposition, resulting in

accumulation of very thick intervals of organic-rich mudstones in the graben (Cornford and Brookes, 1989; Cooper et al., 1995; Cornford, 1998; Erratt et al., 2010). The shale of the Kimmeridge Clay Formation is broadly described as black to dark-olive-grey, mainly calcareous-non-calcareous, 'carbonaceous 'silty mudstones, though in detail there can be significant local variation (Cornford, 1998; Justwan and Dahl, 2005; Raji et al., 2015). In terms of paleogeography, these sediments were deposited in a restricted marine embayment of the Boreal Seaway in the north, resulting from crustal stretching and formation of the three main North Sea grabens which includes the South Viking Graben (Cornford and Brookes, 1989; Cooper et al., 1995; Erratt et al., 2010).

In the UK South Viking Graben, three major facies have been recognized: (1) Kimmeridge Clay hot shale (both upper and lower members); (2) an intermediate facies of interbedded sands and mudstones termed the tiger stripe facies; and (3) massive sand and conglomerates of the Brae Formation. The tiger stripe facies is locally found below the Upper "hot shale" but mainly towards the base of the main Brae Member, and comprises an alternating mudstone and fine-grained sand interbeds (Huc et al., 1985; Isaksen and Ledje, 2001; Cornford et.al., 2014; Raji et.al., 2015). It is interpreted to have been deposited by low-density turbidity currents on the outer submarine fan, inter-fan and in the basin plain environments (Reitsema, 1983; Stow, 1983; Leythaeuser et al., 1984; Turner et al., 1987; Roberts, 1991; Rooksby, 1991). To the east of the Norwegian acreage, and away from the fan facies, this interval is represented by a 'cold shale' Member sandwiched between the two 'hot shale' members (Norwegian Ministry of Petroleum and Energy, 2005). In practice, the divisions into members have not been common practice in the standard operator's Final Well Reports, as made available by government agencies. The Brae Member sands contain a greater amount of reworked terrestrial organic matter (Justwan and Dahl, 2005) and form important reservoirs in the South Viking Graben area (Underhill, 1998; Isaksen and Ledje, 2001; Isaksen et al., 2002).

In this study, the thickness of the KCF/Draupne Formation varies considerably in both the UK and Norway, with a thickness of up to 600 m in the north-western part

towards the graben centre and from about 0-200 m in south eastern part with an average thickness of 85 m (Figure 3-7). The maximum recorded thickness of 807 m is observed in Well 15/3-1 S (the Gudrun discovery). Further noticeable examples of thickness include 453 m thick in Well 15/3-7, 541 m thick in Well 15/3-8 and 347 m in Well 15/3-9 all located in the Norwegian acreage in the deepest part of the graben (Figure 3- 7). A decrease in thickness is observed towards the Utsira High. The base of the formation is diachronous which reflects subsidence or transgression, and also gradational into the organic leaner Heather Formation in places (Miller, 1990).

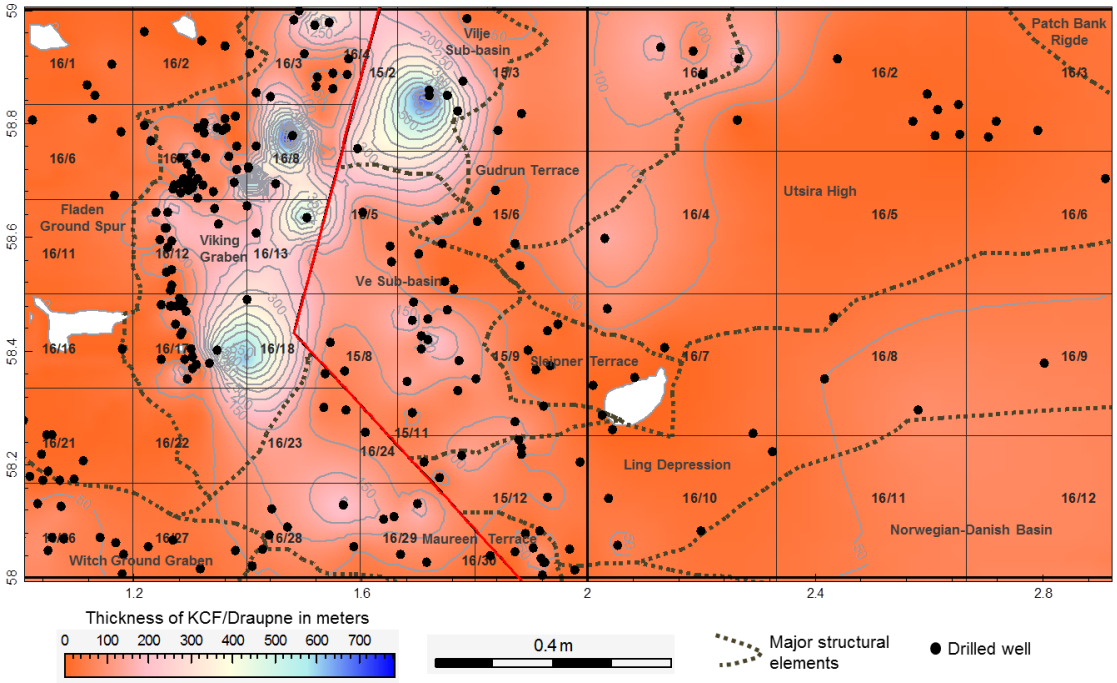

Figure 3-7: Thickness Isopach map for KCF/Draupne Formation showing well locations and structural elements in the South Viking Graben. The thicknesses were derived from formation top and base from 310 wells that penetrated the Kimmeridge/Draupne Formation.

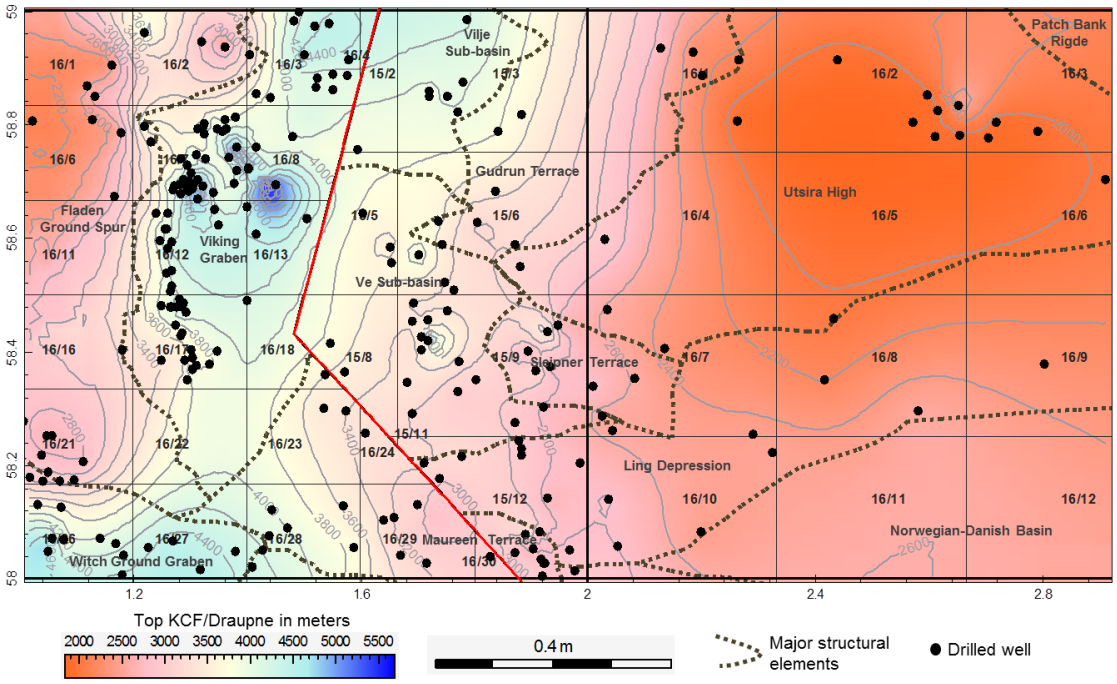

Figure 3-8: Distribution of Top KCF/Draupne-Depth Base Cretaceous showing well locations and structural elements in the South Viking Graben. Formation top and base were derived from 310 wells that penetrated the Kimmeridge/Draupne Formation.

Based on the organo-facies model, the deepest sediments accumulating in the most anoxic part of the basin are predicted to contain the richest amount of organic matter due to greatly improved preservation of the organic matter in these shales (Cornford and Brookes, 1989; Tyson, 2004). With the closing of the Boreal–Tethyan seaway, high sedimentation rates, elevated organic matter productivity (probably controlled by nutrient supply) and increased water depths (up to 600 m) all promoted stratified anoxic bottom waters (Cornford, 1998, Justwan and Dahl, 2005). Rapid subsidence and burial favours the maturation of the accumulated source rocks with minimal siliciclastic dilution (Cornford, 1998). Due to the tectonic influence in the South Viking Graven area; the organic matter may have be controlled in the Late Jurassic: (1) basin-centre sediments will be richer in organic matter due to improved preservation of the organic matter under stronger anoxic conditions which gives higher TOC values; and (2) clastic dilution from high sediment supply resulted in leaner organic matter contents which gives low TOC values (Cornford and Brookes, 1989; Cooper et al., 1995; Cornford, 1998; Tyson, 2004; Erratt et al., 2010). The higher sedimentation rate

of the more basinal settings is also thought to have led to more enhanced preservation of organic matter (Myers and Wignall, 1987).

An average sedimentation rate of 15 m/Ma deposited for 18 Ma with an average thickness of 155 m reflecting diachronous or transgressive base of the KCF/Draupne have been proposed by Miller, 1990. However, Justwan et al., 2005 proposed the sedimentation rates for the KCF/ Draupne Formation are between 1 and 47 m/Ma with an average of 11.7 m/Ma, reaching a maximum of 20 m/Ma in the deep graben and around 1 m/Ma for the condensed sections on the Utsira High, with an average of only 7 m/Ma. In this study, the shallower sediments are relatively thinner, with thicker sedimentation accumulating in the deepest part of the graben (Figure 3-9). After KCF/ Draupne deposition, the stagnant warm bottom brine was replaced by a cold southward-flowing bottom current (Cooper et al., 1995). This introduced sufficient oxygen to prevent the preservation of any further organic material, although the degree of oxygenation appears to decrease from the lower to the upper Draupne Formation (Justwan and Dahl, 2005).

3.6: Organo-facies and Source Rock Potential

Organo-facies and potential source quality of the Upper Jurassic- Early Cretaceous source rocks (Viking Group) vary both laterally and vertically in the study area. These variations in the hydrocarbon potential of these facies are related to the dilution of organic matter by clastic sandstone transported by gravity flow into the main anoxic basin of the South Viking Graben (Partington et al., 1993). Organic-richness was investigated using measured total organic carbon content together with kerogen types and maturities as determined using Rock-Eval pyrolysis from the p: IGI-3 database. In addition, a limited amount of available vitrinite reflectance and organic petrography data were used to augment maturity and kerogen type respectively.

3.6.1: Organic-richness of the Viking Group

Previous authors recorded typical TOC values between 2–12 wt.% (Cooper et al., 1995; Cornford, 1998; Kubala et al., 2003) for The KCF/Draupne Formation , 5-10 wt % (Miller, 1990) and TOC values < 2 wt. % for the Heather Formation (Cooper and

Barnard 1984; Cornford, 1984, 1998; Isaksen et al., 1998). Mean TOC values of 5.6 wt % from 2,600 – 3,200 m and 4.9 wt % from 3,250-3,650 m were also reported from the Kimmeridge Clay Formation in the Viking Graben (Goff, 1983). Fuller (1980) also found an average of 3.25 wt % in sediments from the Kimmeridge Clay Formation in general.

In this study, the Heather Formation which typically has < 2 wt.% TOC is grouped with KCF/Draupne and assessed together as the Viking Group because it is limited in the UK sector of the South Viking Graben. The mean TOC values recorded for this Viking Group assymetric mean is about 5 wt. %; with a maximum TOC of 11 wt. % indicating a good to very good quality organic matter-richness (Figure 3-9 and 3-10). These values suggest that the source rocks contain a high amount of organic matter, which has been shown to be adequate for shale oil generation (Jarvie, 2012). As shown on the histogram (Figure 3-9) for the Norway samples, quadrant 15 and 16 wells appear to have poor to very good source rock whereas good to very good source rock is observed in the quadrant 17 wells, this is due to the clastic dilution effect (Miller, 1990). In the UK wells, samples from the north appear to be fairly to very good source rocks and good to very good source rocks and in the south (Figure 3- 9).

On individual well by well basis in both the UK and Norway, TOC values shows large lateral and vertical variations in source quality especially in the variations in the basin depocentre where sediment accumulation is much higher (Figure 3-10). It has been described that there is a distinct difference in source facies of the KCF/Draupne and Heather Formation. As a result, the KCF/Draupne Formation has better source rock quality and organic-richness and is dominated by Type II kerogens, while the Heather Formation has poor organic-richness and a higher amount of Type III kerogen that decreases upwards (Cooper and Barnard 1984; Cornford, 1984, 1998; Isaksen et al., 1998; Isaksen and Ledje, 2001; Isaksen et al., 2002; Kubala et al., 2003).

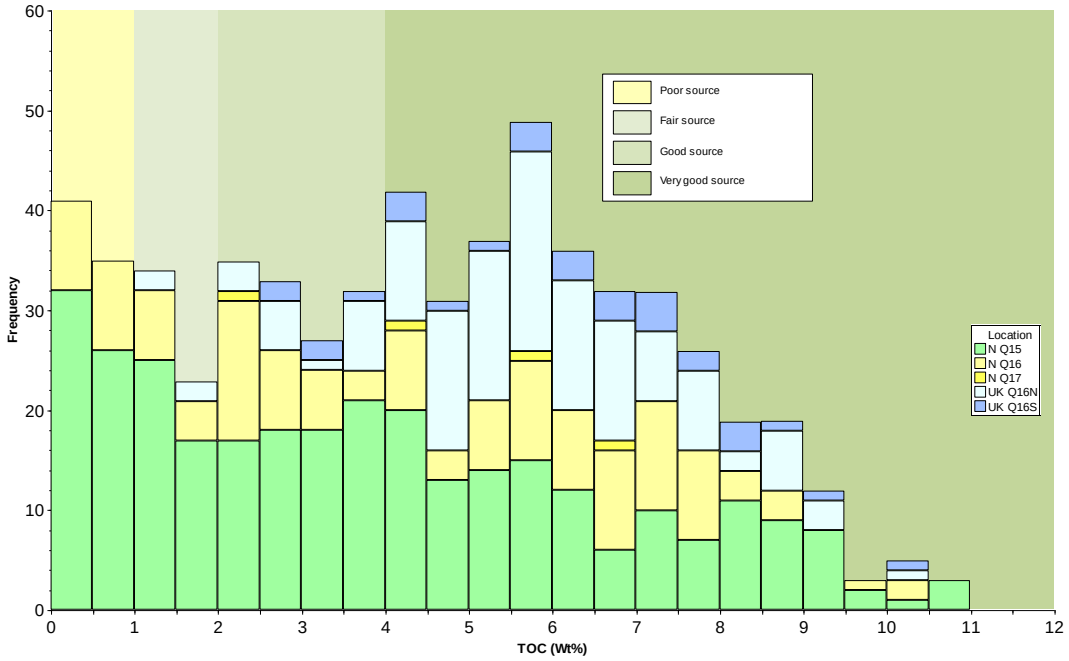

Figure 3-9: TOC range and distribution of the Viking Group showing the organic-richness of each quadrant in the study area. Note: The Viking Group consists of the Heather Formation and Kimmeridge/Draupne Formation.

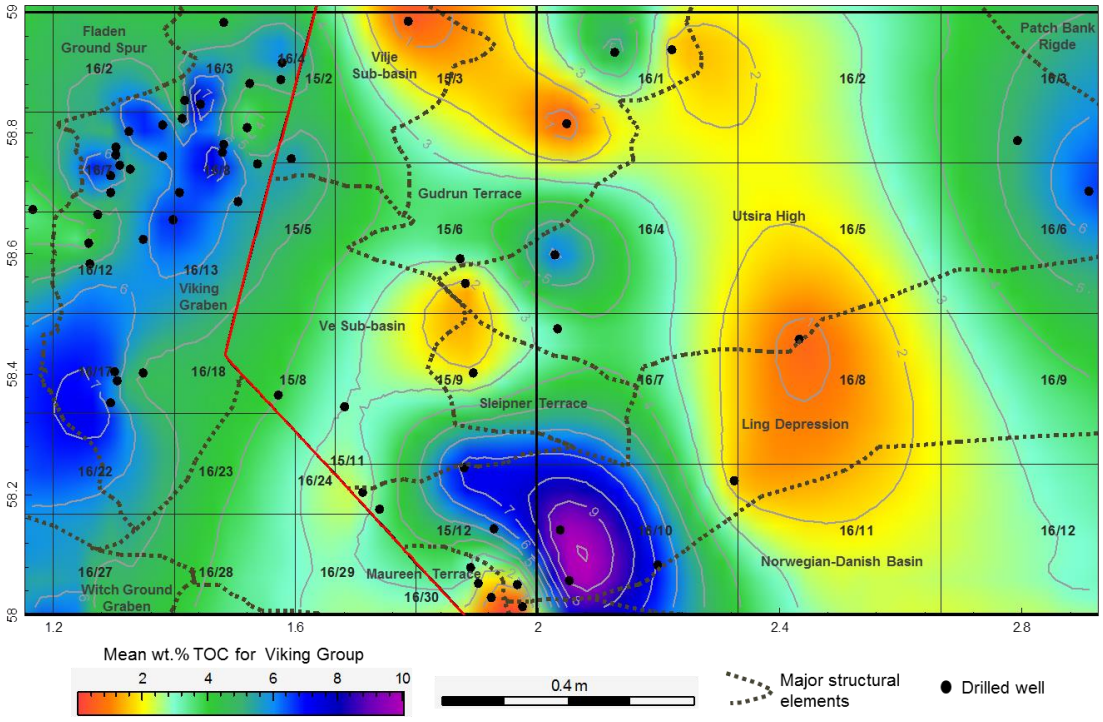

Figure 3-10: Quantitative source rock map of mean TOC distribution of the Viking Group. Note: The Viking Group consists of the Heather Formation and Kimmeridge/Draupne Formation.

There is a better correlation between TOC and thickness in the Norwegian wells (mainly cutting samples) compared with the UK wells (mainly selected cores and

perhaps unrepresented). In most part, the TOC distribution may be related to the preservation of the organic matter (Cornford, 1998); but, in the northern part of UK Quadrant 16, the deep graben area appears to show some lower TOC values. This may be due to the lower average geothermal gradient of 30.02 °C/km (Cornford, 2014) or the topography of the area, and its proximity to Utsira High and Shetland Platform where mass flow transportation of silica-clastic sediment may have diluted more of the preserved organic matter leading to the observed decrease in TOC. These mass flows were caused by the rifting activity in the Middle Jurassic, and are typically encountered in the syn-rift section. This area is to the north of the Brae Field, which is generally dominated by coarse grained reservoir sandstones of the Brae Formation (Stow, 1983; Underhill, 1998). In this area, the high TOC content is not related to rapid sediment (thick KCF =low TOC) but may be related to; (1) nutrient supply; (2) preservation with anoxia conditions; (3) topography of the sea floor maximum anoxia in deep graben; and (4) bottom water stratification (Cooper and Barnard, 1984; Cornford, 1998; Field, 1985; Thomas etal., 1985; Scotchman, 1991; Gormly et al., 1994; Isaksen et al., 2002).

3.7: Thermal Maturity for the Viking Group

The Viking Graben exhibits a wide range of maturities as a function of Hydrogen Index (HI) and the burial depth, the HI versus depth plot (Figure 3-11) has been described as a very good indicator for maturity. The shallower and hence immature samples (2500–3000 m) give an average Hydrogen Index (HI) of 305 mg/g TOC with a maximum value of 720 mg/g TOC in the graben centre. However, with increasing depth the deeper samples give–some anomalously low HI values, with a gradual decrease seen below 4500 m (Figure 3-11). This decrease in HI values is taken to reflect maturation of the kerogen and the conversion of Rock-Eval S_2 to S_1 (Cornford et al., 1998b) or it may be due to turbiditic influxes of terrestrial organic matter with synchronised refill of the pore-water sulfate (Miller, 1990).

Using other maturity parameters (depth, temperature, T_{max} and $\%R_o$; since T_{max} is both a maturity (depth, temperature) and facies (TOC, HI) parameter), the deviation of T_{max} away from the 'pure' maturity trend can be used to predict organofacies. In

addition to depth, T_{max} values together with vitrinite reflectance (%R_o) are also used to define maturity to comparisons made with TOC (symbol size) and HI as a measure of kerogen type (Figure 3.11).

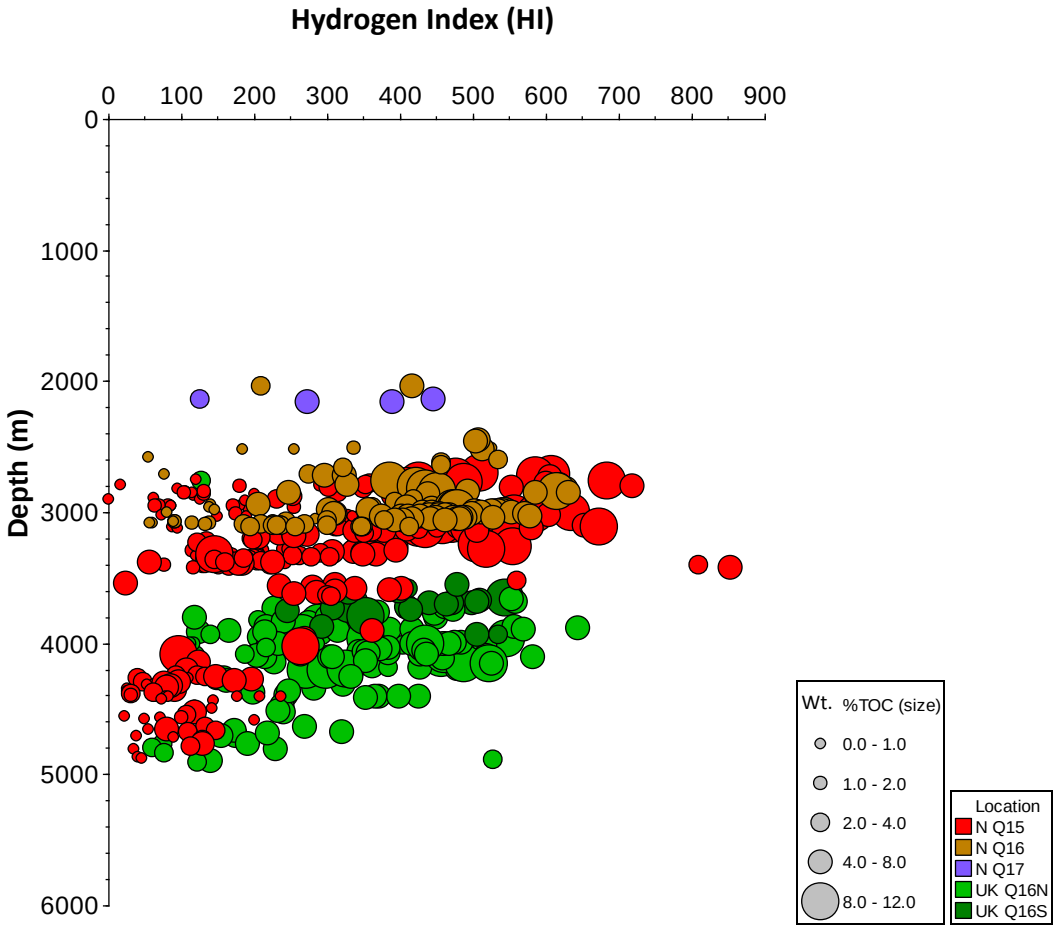

Figure 3-11: Hydrogen Indices (HI) versus sample depth maturity plot for Viking Group samples. Note: The Viking Group consists of the Heather Formation and Kimmeridge/Draupne Formation.

The T_{max} versus depth plot is a good indicator for the onset of oil generation (Cornford, 1998; Kubala et al., 2003; Justwan and Dahl, 2005). The T_{max} values range from 415-465 °C, and arguably show an increase in TOC values from 8-12 wt.% then a progressive decrease in TOC values is observed to about 4 wt. % at 455 °C (Figure 3-12). The onset of oil generation as shown by the T_{max} /Depth plot suggest early oil window generation started at 2700-3350 m while the mid oil window began at 3500 m with peak oil generation at 4200-4800 m (Figure 3-12). The observed maturity trend in this study is similar to the 0.62 % R_o of oil window recorded at an average depth of 3500 m (Kubala et al., 2003; Justwan et al., 2006), 3400 m (Isaksen and Ledje, 2001) and

3340 m (Baird, 1986) for Viking Group samples in the South Viking Graben area. Figure 3-12 shows that peak oil generation and the onset of oil expulsion occurred at 4200-4800 m, this is similar to the estimated depth of 4000-4100 m for the KCF/Draupne Formation (Petersen et al., 2002), and 4200 m for the Heather Formation (Justwan et.al. 2005).

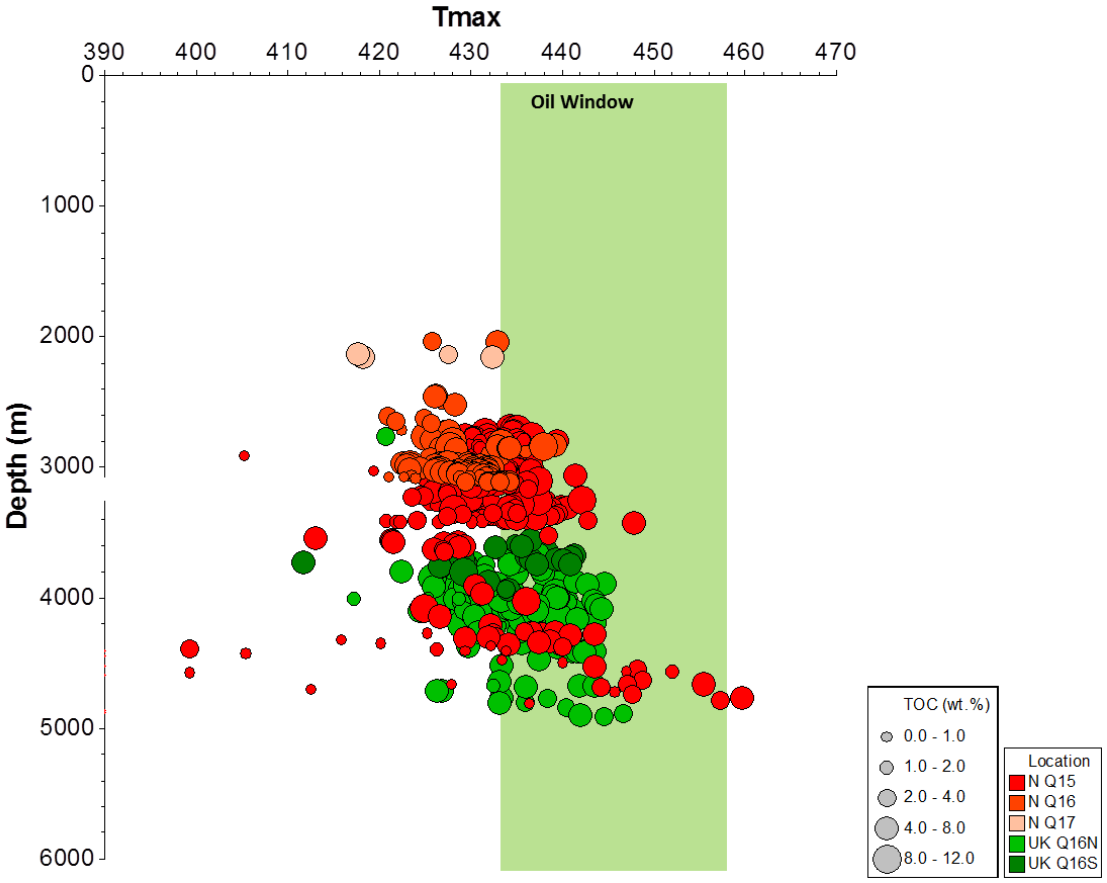

Figure 3-2: T_{max} versus sample depth maturity plot for Viking Group samples. Note: The Viking Group consists of the Heather Formation and Kimmeridge/Draupne Formation.

A relationship between TOC (wt.%) and sample depth (metres), T_{max} (°C) and vitrinite reflectance (%Ro) is showed where T_{max} values (°C) decrease with increasing TOC (gradients from 2.25-4.10 °C/1 wt.% TOC), thus T_{max} is both a maturity and facies parameter (Figure 3-13). TOC and vitrinite reflectance show a decrease from ~8 % TOC at 0.5 %Ro to about 4 wt.% TOC by the 0.9 %Ro (mid oil mature) level. The corresponding depth trend for the Viking Group T_{max} values shows increase but again with considerable spread from 2500 to 5000 m (Figure 3.12). In the shallower part of the section, higher TOC samples (symbol size) have lower T_{max} values which suggest that the high TOC samples produce an S_2 peak which maximises at a lower pyrolysis temperature.

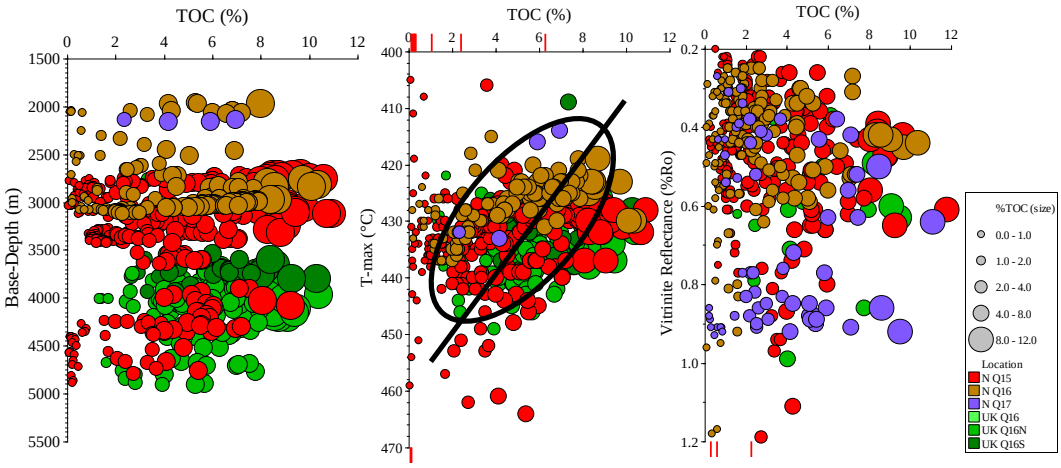

Figure 3-13: Relationship between TOC (wt. %) and sample depth (metres), T_{max} **(°C) and vitrinite reflectance (%R_o) for the Viking Group samples from UK Quad 16 and Norway Quad 15, 16 and 17. Note: The Viking Group consists of the Heather Formation and Kimmeridge/Draupne Formation.**

Using the mass balance argument, the source rock may have lost half of its total organic carbon content in the oil generation window. This distribution suggest that the high TOC values mapped by projection in the main graben to be an under-estimation due to maturation rather than an over estimate due to dilution.

The vitrinite reflectance versus depth plot placed the samples within immature (< 0.34 %R_o) to Early mature (~ 0.6 %R_o) to Late mature (> 0.9 %R_o) oil window (Figure 3-14). The distribution of the vitrinite reflectance across the area shows that immature samples (0.35- 0.45 %R_o) occurred in the east, while the early mature (0.5-0.6 %R_o) occurred towards the northwest with the mid mature to late mature samples in the main graben centre (Figure 3-15). This observation is in good agreement with the recorded Rock-Eval T_{max} /depth maturity plot in Figure 3-12. For locating "sweet-spot "area in both unconventional oil and unconventional gas, the fine-grained rocks should contain mid (0.6 %Ro, 442 °C) to late mature (0.9 %Ro) organic matter (Jarvie, 2012; Cornford, et al., 2014). These vitrinite reflectance values shows that early mature (~ 0.6 %R_o) to late mature (> 0.9 %R_o) oil window maturity of the Viking Group to be adequate for shale oil generation.

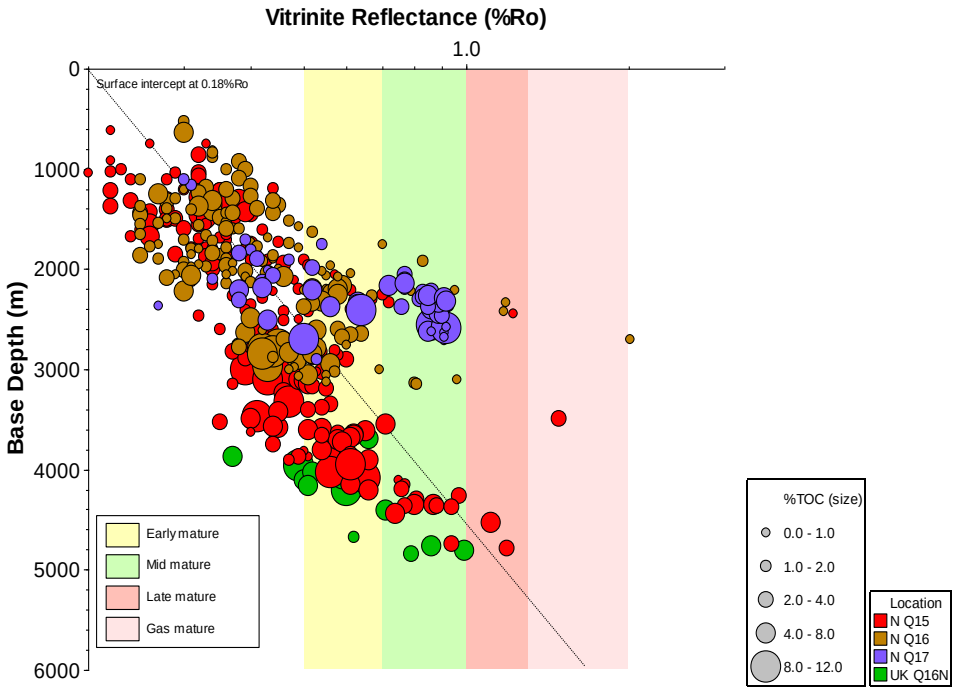

Figure 3-14: Vitrinite Reflectance (%R_o) versus sample depth oil window maturity plot for Viking Group samples. Note: The Viking Group consists of the Heather Formation and Kimmeridge/Draupne Formation. The standard surface intercept line automatically added in p: IGI-3 software).

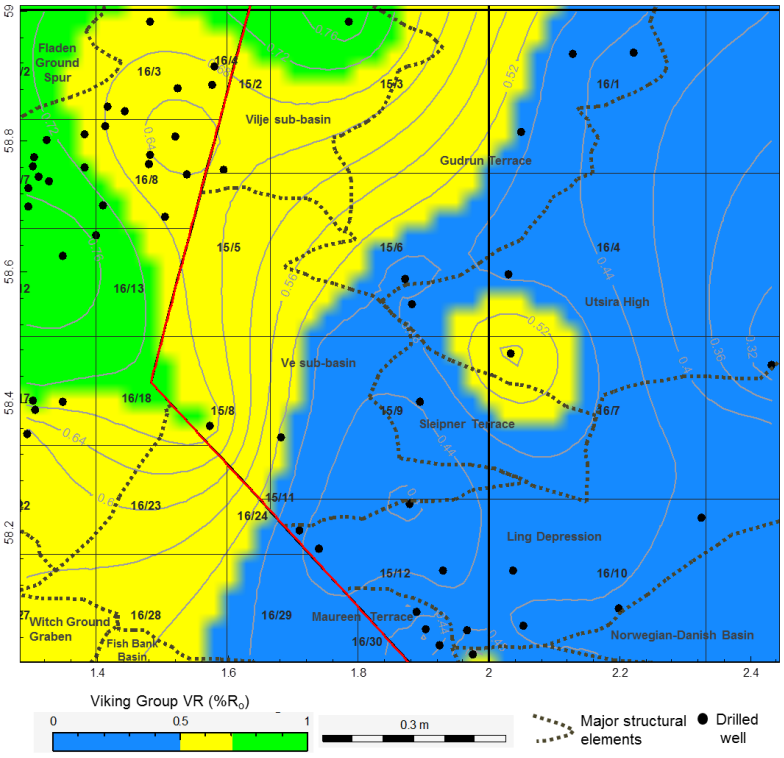

Figure 3-15: Vitrinite Reflectance (%R_o) maturity distribution for Viking Group samples. Note: The Viking Group consists of the Heather Formation and Kimmeridge/Draupne Formation.

3.8: Kerogen-Types for the Viking Group

The T_{max} versus HI (HIT) plot is a good indicator of the kerogen type (Cornford, 1998; Kubala et al., 2003; Justwan and Dahl, 2005). In this study the Viking Group source rocks predominantly consist of Type II and some Type III kerogens as end members, with the mixture of Type II/III kerogen, in addition a few samples show Type I kerogen (Figure 3-16). The predominant classic Type II (oil & gas-prone) kerogen types recorded are mostly derived from marine bacterially degraded algae with terrigeneous input (Cornford, 1998). The terrestrial sourced Type III kerogen decreases towards the deep basinal area with increasing TOC and Hydrogen Indices (Figure 3-16) whilst marine-sourced Type II kerogen increases with high TOC are deposited in the centre of the graben. Type III kerogen is higher close to the flanks where transported mass flow sands and reworked organic matter from the East Shetland Platform and the Utsira High occurred.

These variations in organic-richness and hydrocarbon quality show that the basin-ward area is generally oil-prone and has better quality of organic content and source potential. Selectively, the kerogen type in the Heather Formation is Type II kerogen with the majority of the samples having lower HI dominated with Type II/III kerogen. Type II kerogen have the best characteristics for unconventional exploration compared to Type I and Type III; because they are oil prone and highly generative, though similar to Type I, but retain a high proportion of oil and gas in the source rock (Jarvie, 2011; Kimmeridge Energy, 2012). These values show the kerogen types in the Viking Group to be adequate for shale oil generation (Jarvie, 2012).

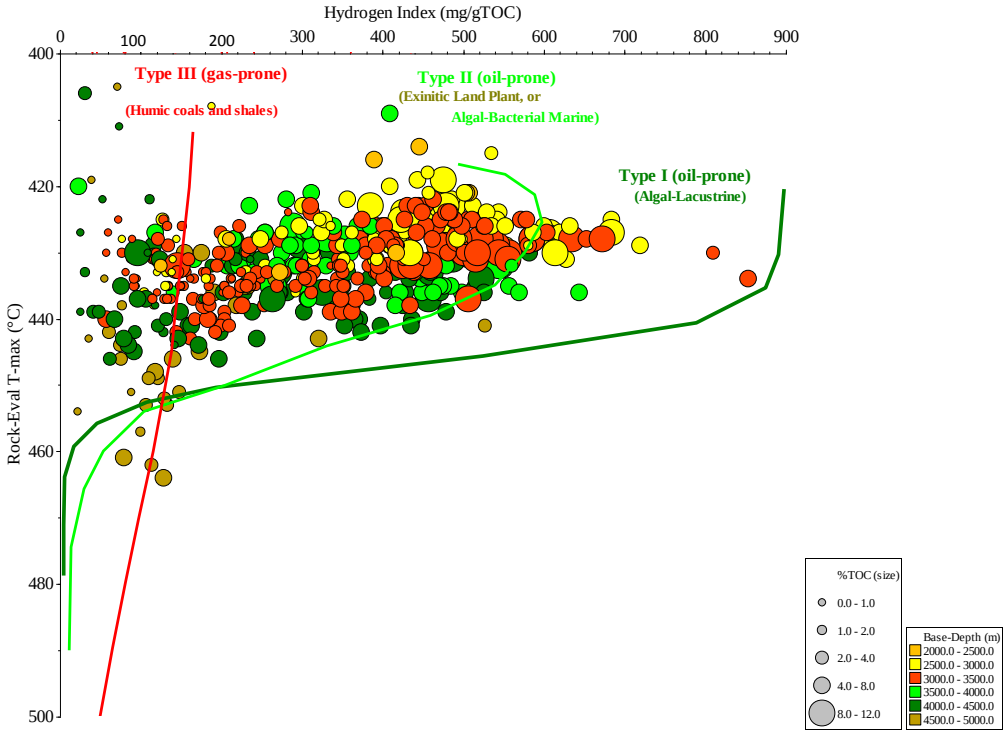

Figure 3-16: Relationship between Rock-Eval Tmax and Hydrogen Index showing kerogen type and maturity, coloured by depth (left) for Viking Group samples in Quadrants UK16, N15, N16 and N17). (Note: the kinetically defined maturity pathways are after equations by Banerjee et al (2004) automatically added in p: IGI-3 software). Note: The Viking Group consists of the Heather Formation and Kimmeridge/Draupne Formation.

3.9: Organic Petrology

Application of organic petrographic techniques has been used in the past for the classification of kerogen type, thermal maturity and hydrocarbon generation potential (Tissot and Welte, 1984; Bustin et al., 1985; Falcon and Snyman 1986; Teichmüller 1983; Sweeney and Burnham, 1990; Suárez-Ruiz and Prado, 1995; Taylor et al., 1998; Wilkins and George, 2002). This is determined by using reflected, fluorescence and transmitted light microscopy by identifying various discrete and diverse components of the kerogen mixtures. Recently, investigations of organic facies, thermal maturity has become an even more important factor in the evaluation of hydrocarbon potential in the shale petroleum system (Loucks and Ruppel, 2007: Hackley et al., 2015, 2016; Hackley and Cardott, 2016).

In this study, the Viking Group sample is dominated by liptinite and vitrinite with some inertinite, where the main grouping of the samples falls near the Liptinite apex of the triangle (Figure 3-17a). The inertinite macerals encountered in this area are mostly reworked terrestrial organic matter derived from the Utsira High and transported through mass flows from the East Shetland Platform (Huc et al., 1985; Isaksen and Ledje, 2001; Isaksen et al., 2002; Kubala et al., 2003). A comparison on the relationship of maceral abundance with Rock-Eval HI results on a sample by sample basis shows that there is a positive correlation between the Hydrogen Index (HI) of the source rocks and their maceral composition (Figure 3.17b-d). Figure 3.17b suggests that the high HI facies contain a higher percentage of liptinite macerals comprising algae (plankton) together with amorphous Type II kerogen where the algal biomass has been subjected to bacterial degradation (Cornford, 1998). In contrast a negative correlation is seen between HI and vitrinite equating to Type III kerogen derived from ligno-cellulose tissues of land plants (Figure 3.17c), Inertinite and the combustion products thereof (Figure 3.17d).

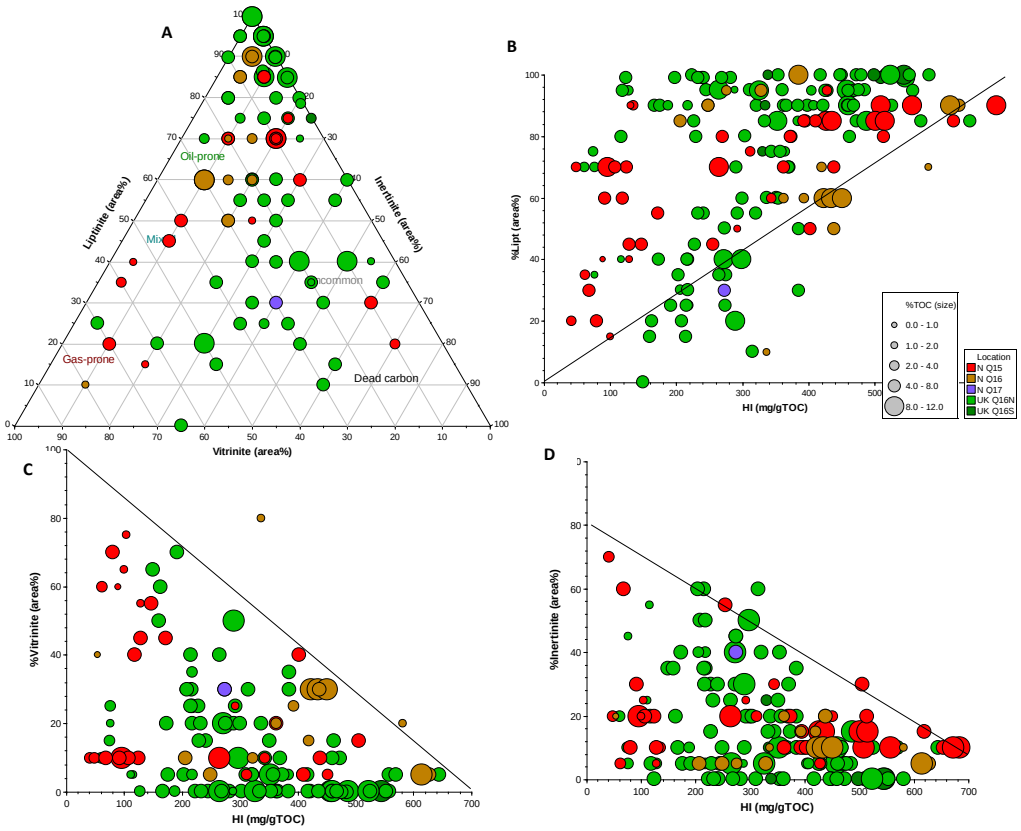

Figure 3-17: Relationship between pyrolysis HI and Liptinite, Vitrinite and Inertinite defining kerogen types in Viking Group samples from UK Quadrant 16 and Norwegian Quadrants 15, 16 and 17. Note: The Viking Group consists of the Heather Formation and Kimmeridge/Draupne Formation.

The percentage of the inertinite decreases upwards with increase in HI; this suggests that the amount of dilution by reworked terrestrial material decreases, and the preservation of oil prone Type II organic matter dominate. Since HI is calculated from S_2/TOC, a change in HI results from the change of S_2 relative to TOC. In the most oil-prone kerogens (Type I or pure alginite); the loss of S_2 during generation can be (almost) balanced by the decrease in TOC, leading to little or no change in HI. Thus the better quality the kerogen, the lower the decrease in HI despite decreases in S_2 and TOC. There is no significant correlation between the maceral content and Oxygen Index (OI).

3.10: Conclusions

The Upper Jurassic KCF-Draupne Formation is up to 600 m thick in the graben centre, and an average thickness of 85 m representing post-rift sediment deposited in deep

anoxic basin. The Heather Formation is up to 70 m, and thins towards Norway, with thicker sedimentation in the south-west and north-west part of the area, and up to 800 m in graben centre. The deepest sediments accumulating in the most anoxic part of the basin contain the richest amount of organic matter due to sediment supply, sea-floor topography and improved preservation under anoxic conditions. In terms of source rock quality, the average TOC values recorded for the Viking Group is up to 5 wt.%, with a maximum TOC of 11 wt. % (< 2 wt.% for Heather Formation) indicating a good to very good organic-richness. This variation is related to the dilution of organic matter by clastic sediment transported by gravity flow into the main anoxic basin of the South Viking Graben.

The kerogen types as reflected by Rock-Eval HI, T_{max} values shows both vertical and lateral variation, they predominantly consist of Type II and Type III kerogens as end members, with the mixture of Type II/III kerogen dominating. The predominant Type II (oil & gas-prone) kerogen types are mostly derived from marine bacterially degraded algae with terrigeneous input. The terrestrial sourced Type III kerogen decreases towards the deep basinal area with increasing TOC and Hydrogen Indices whilst marine-sourced Type II kerogen increases with high TOC. Type III kerogen is higher close to the flanks where transported mass flow sands and reworked organic matter from the East Shetland Platform and the Utsira High occurred. These variations in organic-richness and hydrocarbon quality show that the basin-ward area are generally oil-prone and have better quality of organic content and unconventional source potential in the South Viking Graben area.

The onset of oil generation as shown by the T_{max} /Depth plot suggests early oil window generation started at 2700-3350 m while the mid oil window began at 3500 m with peak oil generation and expulsion at 4200-4800 m. The maceral composition is dominated by liptinite and vitrinite with some inertinite, where the main grouping of the samples falls near the Liptinite apex of the triangle. The inertinite macerals encountered in this area are mostly reworked terrestrial organic matter derived from the Utsira High and transported through mass flows from the East Shetland Platform. A comparison of macerals abundance with Rock-Eval HI results on a sample by

sample basis shows that there is a positive correlation between the Hydrogen Index (HI) of the source rocks and their maceral composition.

3.11: References

Baird, R. A. 1986. Maturation and source rock-evaluation of Kimmeridge Clay, Norwegian North Sea. American Association of Petroleum Geologists Bulletin, 70, pp.1–11.

Barnard, P. C., and Cooper, B. S. 1981. Oils and source rocks of the North Sea area, in L. V. Illing and G. D. Hobson, ed., Petroleum geology of the Continental Shelf of northwest Europe: Heyden, London, Institute of Petroleum, pp.169–175.

Bernard, P. C., Collins, A.G. and Cooper, B.S., 1981. Identification and distribution of kerogen facies in a source rock horizon—examples from the North Sea basin, in Brooks, J., ed., Organic maturation studies and fossil fuel exploration: London, Academic Press, pp.271–282.

Bustin, R.M., Cameron, A.R., Grieve, D.A., Kalkreuth, W.D., 1985. Coal Petrology, its principles, methods and applications. Geological Association of Canada, Short Course Notes, 2nd ed., Victoria, British Columbia 3, pp.230.

Cooper, B. S., and Barnard,P.C. 1984. Source rocks and oils of the central and northern North Sea, in G. Demaison and R. J. Murris, ed., Petroleum geochemistry and basin evaluation. American Association of Petroleum Geologists Memoir 35, pp.303–314.

Cooper, B. S., Bernard, P.C and Telnaes, N. 1995. The Kimmeridge Clay Formation of the North Sea, in B. J. Katz, ed., Petroleum source rocks: Berlin, Springer-Verlag, pp.89–110.

Cornford, C. 1984. Source rocks and hydrocarbons of the North Sea. In: Glennie, K. W., (ed.) Introduction to the Petroleum Geology of the North Sea. London, Blackwell Science Ltd, pp. 171-209.

Cornford, C. 1998. Source rocks and hydrocarbons of the North Sea. In: Glennie, K.W., ed., Petroleum geology of the North Sea. London, Blackwell Science Ltd, pp. 376–462.

Cornford, C., Gardner, P., Burgess, C., 1998b. Geochemical truths in large data sets. I: Geochemical screening data. Organic Geochemistry, 29 (1-3), pp. 519-530.

Cornford, C and Brooks, J. 1989. Tectonic controls on oil and gas occurrences in the North Sea area. In: Tankard, A.J. and Balkwill, H.R, ed., Extensional tectonics and stratigraphy of the North Atlantic margins. American Association of Petroleum Geologists/Canadian, Geological Foundation, pp. 46- 641.

Cornford, C., Birdsong, B. and Groves, G. 2014. Offshore Unconventional Oil from the Kimmeridge Clay Formation of the North Sea: A Technical and Economic Case. Unconventional Resources Technology Conference Proceedings, Denver, CO. August 25-27, 2014.

Coward, M. P., Dewey, J. F., Hempton, M. & Holroyd, J. 2003. Regional tectonics. In: Evans, D., Graham, C., Armour, A. & Bathurst, P. ed., The Millennium Atlas: Petroleum Geology of the Central and Northern North Sea. Geological Society of London, pp. 17-33.

Dahl, B., Bojesen-Koefoed, J., Holm, A., Justwan, H., Rasmussen, E. and Thomsen, E. 2003. Analysing Rock Eval Pyrolysis S_2 and TOC data for source rock property modelling. In: Book of Abstracts Part I, 21st International Meeting of Organic Geochemistry, Krakow. Society of Research on Environmental Changes "Geosphere", Krakow, pp. 307–308.

Dore′, A. G., Vollset, J. & Hamar, G. P. 1985. Correlation of the offshore sequences referred to the Kimmeridge Clay Formation; relevance to the Norwegian sector. In: Thomas, B.M., Dore′, A.G., Eggen, S. S., Home, P. C. and Larsen, R.M., ed., Petroleum Geochemistry in Exploration of the Norwegian Shelf. Grahamand Trotman, London, pp. 27–38.

Erratt, D., Thomas, G.M., Hartley, N.R, Musum, R., Nicholson, P.H. and Spisto, Y. 2010. North Sea hydrocarbon systems: some aspects of our evolving insights into a classic hydrocarbon province. In: Pickering, S.C. and Vining, B., ed., Petroleum Geology: From Mature Basins to New Frontiers. Proceedings of the 7th Petroleum Geology Conference. Geological Society of London, London, England, pp. 37-56.

Evans, D. Graham, C., Armour, A. and Bathurst, P. 2003. The Millennium Atlas: Petroleum geology of the central and northern North Sea. The Geological Society of London, pp. 105-128.

Faerseth, R. B. 1996. Interaction of Permo-Triassic and Jurassic extensional fault blocks during the development of the northern North Sea. Journal of Geological Society of London, 153, pp. 931 – 944.

Falcon, R.M.S., Snyman, C.P., 1986. An introduction to coal petrography: Atlas of petrographic constituents in the bituminous coals of Southern Africa. The Geological Society of South Africa. Review Paper, 2. Kelvin House, 2 Hollard Street. (Johannesburg).

Gallois, R.W. and Cox, B.M. 1974. Stratigraphy of the Upper Kimmeridge Clay of the Wash area. Bulletin of the Geological Survey of Great Britain, 47, pp. 1-28.

Gallois, R.W. and Cox, B.M. 1976. Stratigraphy of the Lower Kimmeridge Clay of Eastern England. Proceedings of the Yorkshire Geological Society, 41,pp.13-26.

Gautier, D. L., 2005. Kimmeridgean Shales Total Petroleum System of the North Sea Graben Province: U.S. Geological Survey Bulletin 2204-C, p. 24. Available at:: http://pubs.usgs.gov/bul/2204/c [accessed June 15, 2014].

Glennie, K.W. 1986. Development of northwest Europe's southern Permian gas basin. In: Brooks, J., Goff, J.C. and van Hoorn, B., ed., Habitat of Palaeozoic gas in NW Europe. Geological Society, London, Special Publication, 23, pp. 3-22

Goff, J. C. 1983. Hydrocarbon generation and migration from Jurassic source rocks in the East Shetland Basin and Viking Graben of the northern North Sea: Journal of the Geological Society, 140, pp. 445–474.

Goldsmith, P. J, Hudson, G. & van Veen, P. 2003. Triassic. In: Evans, D. Graham, C., Armour, A. and Bathurst, P., (ed., The Millennium Atlas: Petroleum geology of the central and northern North Sea. The geological society of London, pp. 105-128.

Guan, D., Xu, X., Li, Z., Zheng, L., Tan, C., Yao, Y. 2017. Theory and Practice of Hydrocarbon Generation within Space-Limited Source Rocks. Springer Singapore, pp.69-80

Fisher, M.J. and Miles, J.A., 1983. Kerogen types, organic maturation and hydrocarbon occurrences in the Moray Firth and South Viking Graben, North Sea basin. In: Brooks, J. ed., Petroleum geochemistry and exploration of Europe. Geological Society of London Special Publication, 12, pp.195-201.

Fisher, M. J. and Mudge, D. C. 1998. Triassic. In: Glennie, K. W., ed., Petroleum Geology of the North Sea. London, Blackwell Science Ltd, pp. 212-244.

Hackley, P.C., Araujo, C.V., Borrego, A.G., Bouzinos, A., Cardott, B., Cook, A.C., Eble, C., Flores,D., Gentzis, T., Gonçalves, P.A., Mendonça Filho, J.G., Hámor-Vidó, M., Jelonek, I., Kommeren, K., Knowles, W., Kus, J., Mastalerz, M., Menezes, T.R., Newman, J., Oikonomopoulos, I.K., Pawlewicz, M., Pickel, W., Potter, J., Ranasinghe, P., Read, H.,Reyes, J., Rodriguez, G.D.L.R., Fernandes de Souza, I.V.A., Suarez-Ruiz, I., Sýkorová, I.,Valentine, B.J., 2015. Standardization of reflectance measurements in dispersed organic matter: results of an exercise to improve interlaboratory agreement. Journal of Marine and Petroleum Geology. 59, pp. 22–34.

Hackley, P.C., Fishman, N., Wu, T., Baugher, G., 2016. Organic Petrology and Geochemistry of Mudrocks from the Lacustrine Lucaogou Formation, Santanghu Basin, Northwest China: Application to Lake Basin Evolution. International Journal of Coal Geology, 168, pp. 20-34.

Hackley, P.C. and Cardott, B.J. 2016. Application of organic petrography in North American shale petroleum systems: A review. International Journal of Coal Geology 163, pp. 8–51.

Isaksen, G.H., Curry, D.J., Yeakel, J.D. and Jenssen, A.I. 1998. Controls on the oil and gas potential of humic coals. Journal of Organic Geochemistry, 29, pp. 23-44.

Isaksen, G.H. and Ledje, K.H.I. 2001.Source rock quality and hydrocarbon migration pathways within the greater Utsira High area, Viking Graben, Norwegian North Sea. American Association of Petroleum Geologists Bulletin, 85, 5, pp. 861–883.

Isaksen, G.H., Patience, R., van Graas, G. and Jenssen, A.I. 2002. Hydrocarbon system analysis in a rift basin with mixed marine and non-marine source rocks; the South Viking Graben, North Sea. American Association of Petroleum Geologists Bulletin, 86 (4), pp. 557–591.

Johnson, H., Leslie, A. B., Wilson, C. K., Andrews, I. J., and Cooper, R. M., 2005. Middle Jurassic, Upper Jurassic and Lower Cretaceous of the UK Central and Northern North Sea. British, Geological Survey Research Report, RR/03/001, pp. 42.

Justwan, H., Dahl, B. 2005. Quantitative hydrocarbon potential mapping and organofacies study in the Greater Balder Area, Norwegian North Sea. Geological Society, London, Petroleum Geology Conference series 2005, 6, pp. 1317-1329

Justwan, H., Dahl, B. and Isaksen G.H. 2006.Geochemical characterization and genetic origin of oils and condensates in the South Viking Graben, Norway. Journal of Marine and Petroleum Geology, 23, pp. 213–239.

Justwan, H., Dahl, B., Isaksen, G.H. and Meisingset, I., 2005. Late to Middle Jurassic source facies and quality variations, South Viking Graben, North Sea. Journal of Petroleum Geology, 28 3, pp. 241–268.

Justwan, H. and Dahl, B. 2005. Quantitative hydrocarbon potential mapping and organofacies study in the greater Balder Area, Norwegian North Sea. In: DoreÅL, A.G. and Vining, B., ed., Petroleum Geology: North West Europe and Global Perspectives – Proceedings of the 6th Petroleum Geology Conference.

Kubala, M., Bastow, M., Thompson, S., Scotchman, I. C. and Oygard, K. 2003. Geothermal regime, petroleum generation and migration. In:Evans, D., Graham, C., Armour, A. & Bathurst, P., ed., The Millennium Atlas: Petroleum Geology of the Central and Northern North Sea. Geological Society, London, pp. 289–316.

Leythaeuser, D., Radke, M. and Schaefer, R. (1984). Efficiency of petroleum expulsion from shale source rocks. Nature, 311(5988), pp.745-748.

Loucks, R.G., Ruppel, S.C., 2007. Mississippian Barnett Shale: lithofacies and depositional setting of a deep-water shale-gas succession in the Fort Worth Basin, Texas. American Association of Petroleum Geologists Bulletin 91, pp. 579–601.

Miller, R.G., 1990. A paleoceanographic approach to the Kimmeridge Clay Formation. In: Huc, A.Y. (ed.), Deposition of organic facies. Association of Petroleum Geologists Studies in Geology 30, pp.13-26.

Myers, K.J. and Wignall, P.B. 1987. Understanding Jurassic organic-rich mudrocks-new concepts using gamma ray spectrometry and palaeoecology: examples from the Kimmeridge Clay of Dorset and the Jet Rock of Yorkshire. Leggett, J.K. and Zuffa, G.G. ed., Marine clastic environments: concepts and case studies, London, Graham & Trotman pp. 175-192.

Norwegian Petroleum Directorate, 2005. Factmaps. [18 April 2015]. Available online at: <http://217.68.117.237/ website/NPDGIS/viewer.htm>[Accessed 18 Apr. 2015]

Norwegian Petroleum Directorate well data (NPD) (Available online: http://www.npd.no/en/ [Accessed 18 Apr. 2015]

Oakman, C. D. & Partington, M. A. 1998. Cretaceous. In: Glennie, K. W., ed., Petroleum Geology of the North Sea; Basic Concepts and Recent Advances. Blackwell Science Geology&Petroleum Geology, Oxford, pp.294–349.

Oschmann, W. 1988. Kimmeridge Clay sedimentation - a new cyclic model.Palaeogeography, Palaeoclimatology, Palaeoecology, 65, pp.217-251.

Partington, M.A., Mitchener, B.C., Milton, N.J. and Fraser, A.J., 1993. Genetic sequence stratigraphy for the North Sea Late Jurassic and early Cretaceous: distribution and prediction of Kimmeridgian-Late Ryazanian reservoirs in the North Sea and adjacent areas, in: Parker, J.R. ed., Petroleum Geology of Northwest Europe: Proceedings of the 4th Conference on Petroleum Geology of NW. Europe, at the Barbican Centre, London. Geological Society, London, pp.347-370.

Pearson, M. J. and Watkins D. 1983. Organofacies and Early Maturation Effects in Upper Jurassic Sediments from the Inner Moray Firth Basin, North Sea. Geological Society, London, Special Publications, 12, pp.147-160.

Petersen, H.I., Bojesen-Koefoed, J.A. and Nytoft, H.P., 2002. Source rock evaluation of Middle Jurassic coals, Northeast Greenland, by artificial maturation; aspects of petroleum generation from coal. American Association of Petroleum Geologist Bulletin 86, pp.233-256.

Ramadan, F.S., El Nady, M.M., Eysa, E.A. and Abdel Wahed, N.M. (2014). Subsurface Geology and Potential Capability of Oil Generation of some Jurassic and Lower Cretaceous Source Rocks in North Western Desert, Egypt. Journal of Petroleum Science and Engineering 4(2), pp.300-317.

Raji, M., Gröcke, D.R., Greenwell, H.C., Gluyas, J.G and Cornford C, (2015). The effect of interbedding on shale reservoir properties. Journal of Marine and Petroleum Geology, 67, pp.154-169.

Rawson, P. F. & Riley, L. A. 1982. Latest Jurassic-early Cretaceous events and the 'Late Cimmerian Unconformity' in North Sea area. American Association of Petroleum Geologist Bulletin 66, pp.2628-2648.

Reitsema, R. H. 1983. Geochemistry of North and South Brae areas, North Sea. In: Brooks, J. (ed) Petroleum Geochemistry and Exploration of Europe, Geological Society, London, Special Publication, 12, pp.203-212.

Richards, P.C., Lott, G.K., Johnson, H., Knox, R.W.O'B. and Riding, J.B. 1993. Jurassic of the Central and Northern, North Sea. In: Knox, R.W.O'B and Cordey, W.G., ed., Lithostratigraphy nomenclature of the UK North Sea. British Geological Survey, Nottingham, pp.1-252.

Richards, P.C., Brown, S., Dean, J.M. and Anderton, R. 1988. Short Paper: A new paleogeographic reconstruction for the Middle Jurassic of the northern North Sea. Journal of the Geological Society, 145, pp. 883-886.

Roberts, M. J. 1991. The South Brae Field, Block 16/7a, U.K. North Sea. In: Abbotts, I. L. ed., United Kingdom Oil and Gas Fields 25 Years Commemorative Volume. Geological Society, London, Memoir, 14, pp.55-62.

Rooksby, S.K. 1991. The Miller Field, Blocks 16/7B, 16/8B, UK North Sea. Geological Society, London, Memoirs, 4,159-164.

Stow, D. A. V. 1983. Sedimentology of the Brae oilfield, North Sea: a reply. Journal of Petroleum Geology, 6, pp.103-104.

Suárez-Ruiz, I. and Prado, J. G., 1995. Characterization of Jurassic black shales from Asturias(Northern Spain): Evolution and petroleum potential. In: Snape, C., ed., Composition, Geochemistry and Conversion of Oil Shales, NATO A.S.I. Series,Series C: Mathematical and Physical Sciences 455, pp. 387-395.

Sweeney, J.J., Burnham, A.K., 1990. Evaluation of a simple model of vitrinite reflectance based on chemical kinetics. The American Association of Petroleum Geologists Bulletin 74, pp.1559–1570.

Taylor, G.H., Teichmuller, M., Davis, A., Diessel, C.F.K., Littke, R. and Robert, P., 1998. Organic petrology. Gebrüder Borntraeger. Berlin. pp.704

Teichmüller, M., Durand, B., 1983. Fluorecence microscopical rank studies on liptinite and vitrinite in peat and coals and comparison with results of the Rock-Eval pyrolysis. International Journal of Coal Geology 2, pp.197-230.

Tissot, B.P., Welte, D.H., 1984. Petroleum Formation and Occurrence. 2nd Edition. Berlin, Springer Verlag, pp.699.

Turner, C. C., Cohen, J. M., Connel J. R. and Cooper, D. M. 1987. A depositional model for the South Brae oilfield. In: Brooks, J. and Glennie, K. W., ed., Petroleum geology of North West Europe,London, Graham and Trotman, pp.853-864.

Tyson, R.V., Wilson, R.C.L. and Downie, C. 1979. A stratified water column model for the type Kimmeridge Clay. Nature, 277, pp.377-380.

Tyson, R.V. 1987. Genesis and palynofacies of marine petroleum source rocks.In: Marine Petroleum Source Rocks, ed., Brooks, J. and Fleet, A.J. Geological Society Special Publication 26, pp.47-67.

Tyson, R.V. 1989. Late Jurassic palynofacies trends, Piper and Kimmeridge Clay Formations, UK onshore and northern North Sea. In: European Micropalaeontology and Palynology, ed., Batten, D.J. and Keen, M.C. Ellis Horwood Ltd., Chichester, pp.136-172.

Tyson, R.V. 2004. Variation in marine total organic carbon through the type Kimmeridge Clay Formation (Late Jurassic), Dorset, UK. Journal of the Geological Society, 161, pp.667-673.

Underhill, J.R. 1998. Jurassic. In: Glennie, K. ed., Introduction to the Petroleum Geology of the North Sea London, Blackwell Science Ltd,pp.245-293.

Vollset, J. and Dore, A.G., 1984. A revised Triassic and Jurassic Lithostratigraphic Nomenclature of the Norwegian North Sea. Norwegian Petroleum Directorate Bulletin. 59, pp.53.

Wilkins, R.W.T. and George, S.C., 2002. Coal as a source rock for oil: a review. International Journal of Coal Geology 50, pp.17– 361.

Wu, L., Liao, Y., Fang,Y., and Geng, A. 2012.The study on the source of the oil seeps and bitumens in the Tianjingshan structure of the northern Longmen Mountain structure of Sichuan Basin, China Marine and Petroleum Geology, 37, pp.147–161.

Ziegler, P.A. 1990. Tectonic and palaeogeographic development of the North Sea rift system. In: Blundell, D.J. and Gibbs, A.D, ed., Tectonic Evolution of the North Sea Rifts. Oxford University Press, New York, pp.1-36.

Ziegler, P.A. 1992. North Sea rift system. Tectonophysics, 208, pp.55-75.

Chapter 4: The Effect of Interbedding on Shale Reservoirs Properties

This chapter is based on a paper published in the Journal of Marine and Petroleum Geology. **Raji, M.,** Gröcke, D. R., Greenwell, C. H., Gluyas, J. G. and Cornford, C., 2015. The Effect of Sand Interbedding on Shale Reservoir Properties. Journal of Marine and Petroleum Geology 67, 154-169.

This paper investigated the effect of sand Interbedding on shale reservoir properties using geochemical and mineralogy data collected from analyses of core samples from wells that penetrated the Upper Jurassic Kimmeridge Clay Formation in the South Viking Graben area.

4.1: Abstract

North Sea oil is overwhelmingly generated in shales of the Upper Jurassic – basal Cretaceous Kimmeridge Clay Formation. Once generated, the oil is expelled and ultimately migrates to accumulate in sandstone or carbonate reservoirs. The source rock shales, however, still contain the portion of the oil that was not expelled. As a consequence such shales and juxtaposed non-source lithofacies can form the targets for the exploration for 'unconventional oil'.

In this paper, we examined part of the Kimmeridge Clay source rock as a 'hybrid 'shale resource system within which 'hot shale' and organic-lean sandstone and siltstone intervals are intimately interbedded. This hybrid system can contain a greater volume of oil because of the increased storage capacity due to larger matrix porosities of the sand-silt interbeds, together with a lower adsorptive affinity in the interbedded sandstone. The relationship between the estimated volume percentages of sand and mudstone and the free oil determined from Rock-Eval® S_1 yields is used to place limits on the drainage of oil from source mudstone to reservoir sand at the decimeter scale. These data are used to determine oil saturations in interbedded sand-mudstone sequences at peak oil maturity. Higher values of free hydrocarbon (as evidenced by the S_1 value in mudstone) suggest that more oil is being retained in the mudstone, while higher S_1 values in the interbedded sands suggest the oil is being

drained to saturate the larger pore spaces. High silica content in the interbeds confirms the brittleness in this mudstone-sandstone lithofacies, an important factor to be considered for fracture stimulation to successfully work in this hybrid system. The key points of this hybrid unconventional system are the thickness, storage capacity and the possibility to capture a portion of the expelled as well as retained oil.

4.2: Introduction

The Upper Jurassic – basal Cretaceous Kimmeridge Clay Formation of the North Sea is an actively, generating source rock for conventional oil and gas (Barnard and Cooper, 1981; Barnard et.al., 1981; Goff, 1983; Cooper and Barnard, 1984 ; Cornford, 1984, 1998), with further potential as an unconventional hydrocarbon reservoir. It may be something of a paradox that the Kimmeridge Clay Formation is neither Kimmeridgian (it is mainly Volgian-Ryazanian in age) nor is it a claystone, with silt-sized particles dominating as demonstrated below. A recent re-evaluation of the extensive Kimmeridge Clay Formation source rock and interbedded silicate-rich intervals has located potential for unconventional resource sweet-spots in terms of thickness, organic-richness, oil quality, maturity together with appropriate lithology, mineral content and natural fractures in the South Viking area of the North Sea (Cornford et.al., 2014).

The present study focuses on 4 selected wells in UK Quadrant 16 in the southern part of the South Viking Graben area of the North Sea (Figure 4-1). The South Viking Graben is located within the United Kingdom (UK) and Norwegian sectors of the northern North Sea, and is bounded by the East Shetland Platform to the west and the Utsira High to the east. The 4 sampled wells lie in the UK sector of the Southern Viking Graben, with 3 of the wells (16/17-14, 16/17-18 and 16/17-19) drilled in the area where the Upper 'hot shale' Member is underlain by the fault-related clastic fans of the Brae Member of the Kimmeridge Clay Formation (Figure 4-2). The fourth well (16/18-2) was drilled in a more axial position where the hot shales are underlain by a more distal facies of the Brae Member fans.

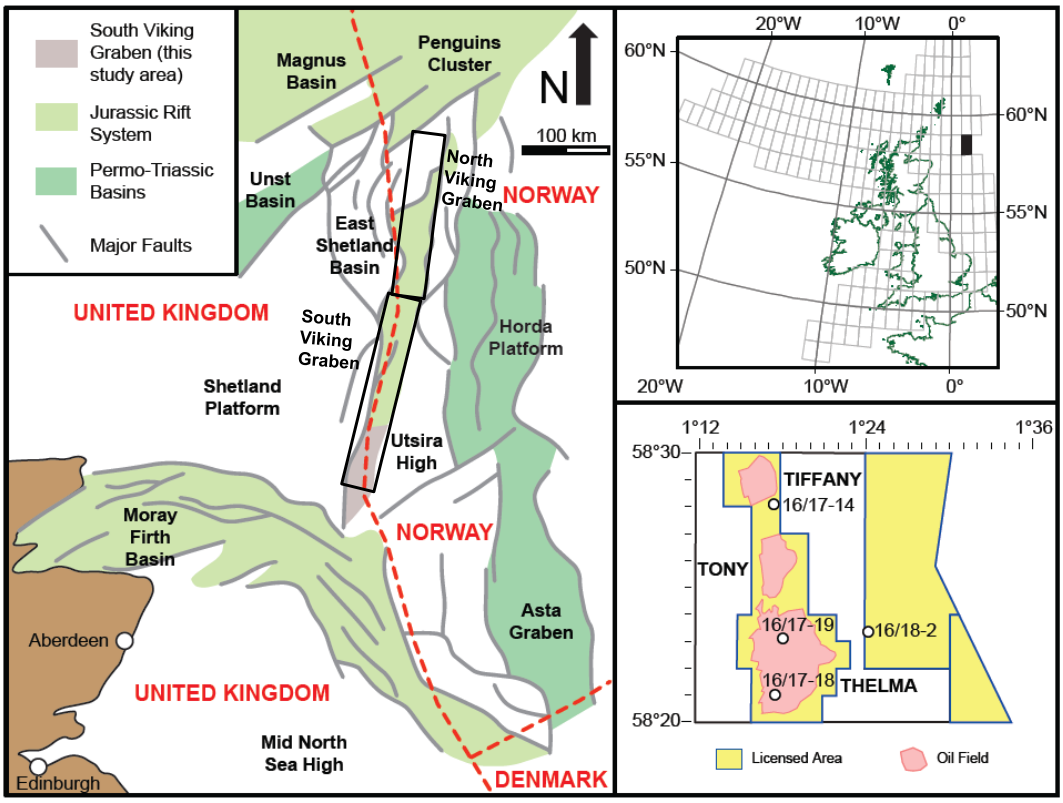

Figure 4-1: Structural elements of the North Sea showing the structural framework of the Viking Graben (modified from Dominguez, 2007) with inset of UK Quadrant 16 showing the location of wells studied (modified from DECC, 2013).

The formation of the Viking Graben was initiated during the Permo-Triassic from different phases of extension followed by regional subsidence (Glennie, 1986; Erratt et al., 2010). During the Middle Jurassic a domal uplift in the central area of the North Sea Basins arguably initiated the development of the Central and Viking grabens. In the late Jurassic-early Cretaceous, block faulting and tilting created the grabens, together with some strike-slip movements offsetting the graben margin faults. These offset zones played a key role in focussing coarse clastics into the deep water of the grabens, which forms the submarine fans of the Brae Member in UK Quadrant 16 (Stow 1983; Turner et al., 1987).

Separation of the Viking Graben into northern and southern sectors occurred during structural development in the Jurassic (Richards et al., 1993). In the Middle Jurassic (Callovian-Oxfordian), marine transgression and sea level rise resulting from both-structural extension, is evidenced by continuous rapid subsidence in these grabens, These two processes combined to produce a relatively isolated deep water basin

which became relatively sediment-starved in the Upper Jurassic. With a distal connection to the Boreal seaway far to the north and in the absence of water circulation, the deep restricted basins accumulated marine Kimmeridge Clay sediments rich in organic matter (Cornford and Brookes, 1989; Gautier, 2005).

Rapid subsidence, and burial favours the maturation of the accumulated source rocks with oil generation beginning in the Cretaceous and peak generation during the Tertiary. During the Upper Jurassic to Early Cretaceous (Kimmeridgian to Ryazanian), the active western graben margin fault shed beds of coarse clastics Brae Formation conglomerates and sands into deep water trough of the south Viking Graben (Partington et al., 1993). These pebbly to fine sandstones Brae Formation are interpreted as proximal deep-water slope apron fans derived from the East Shetland Platform and Fladen Ground Spur (Underhill, 1998; Justwan et al., 2005; Stow, 1983).The organic-rich mudstone and interbedded fan sands, together with distal and inter-fan areas forms the basis of a sweet spot for a hybrid Unconventional petroleum system (Figure 4-2).

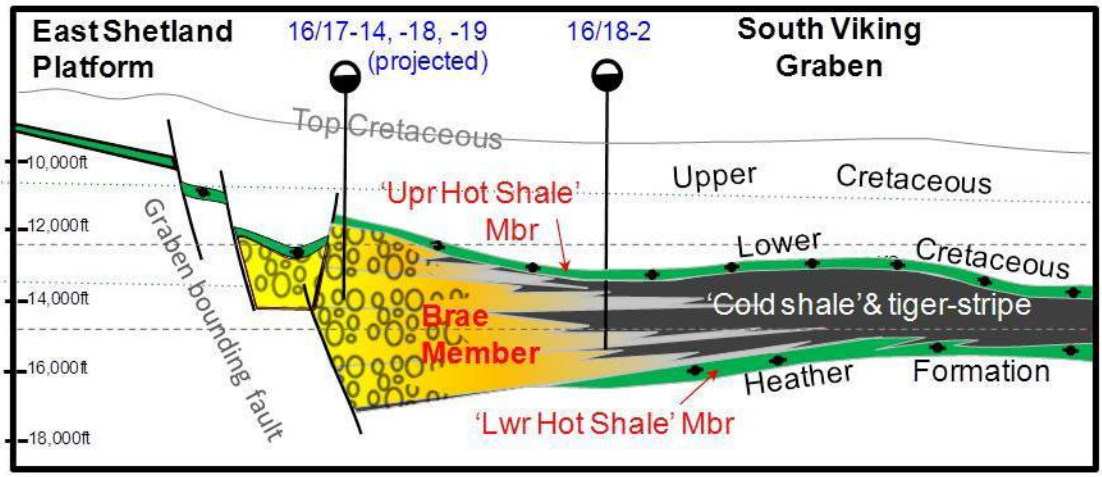

Figure 4-2: Schematic cross section of the Southern Viking Graben showing the facies relationships between the Upper & Lower Hot Shale and Brae members of the Kimmeridge Clay Formation.

Though deep water persisted, bottom water oxygenation returned in the early Cretaceous as the graben became the connecting seaway between the Boreal Ocean to the north and the Tethys Ocean to the south (Cornford and Brookes, 1989). By late Cretaceous, rifting in the North Sea region essentially ceased, with regional thermal

subsidence most prominent near the axis of the abandoned rift resulting in basin depocenters for the syn- and post-rift sediments (Cornford and Brookes 1989; Ziegler, 1990; Cooper et al., 1995; Faerseth, 1996; Gautier, 2005; Johnson et al., 2005; Erratt et al., 2010).

The Kimmeridge Clay Formation is a mature source rock for both oil and gas in the graben centre. This interpretation is based on measured maturity parameters such as vitrinite reflectance and Rock-Eval T_{max} (Cornford et.al., 2014) , thermal modelling (Schlakker et.al., 2012), direct measurement of oil generation within the source rock from solvent extraction and Rock-Eval S_1 yields (Schaefer et.al., 1990) and oil/source rock correlations based on molecular maturity parameters (Cornford et al., 1983). Burial history modelling, calibrated against measured parameters, suggest a burial depth deeper than 3,200 m below sea bed for maturity and generation from the typical Type II oil-prone kerogen, (Cornford, 1998).

As well as oil generation, deep burial of the mudstones leads to loss of porosity (mainly by compaction) and permeability (assisted by diagenetic cementation). Inter-granular pore system within interbedded sandstone from Miller and Kingfisher Fields in UK Quadrant 16 average up to about 10 vol. % (Gluyas et. al., 2000; Marchand, et.al., 2002; Spence and Kreutz, 2003). The porosity of the mudstones is less well constrained; however, Cornford et al., (2014) reported bulk volumes in range of 5 %BV for mudstone core plugs, with some porosity possibly associated with organic particles (kerogen).

Unconventional oil and gas is defined as oil and gas exploitable by directly drilling and fracturing of low permeability fine grained rocks acting as both source and reservoir (Jarvie et al., 2007; Abrams et. al., 2014). For both unconventional oil and unconventional gas, the fine-grained rocks should be sufficiently thick and contain mid to late mature organic matter. Based on experience in the USA, for either an oil or gas play, oil prone kerogen is the preponderant source material. Decomposition of organic-rich kerogen (and probably the related bitumen) yields liquid and gas, as well as potential for organic-hosted porosity as shown by numerous Scanning Electron Microscope (SEM) images (Loucks et al., 2009; Bernard et al., 2013). Combinations of

some reservoir properties for unconventional resource assessment include; lithology, thickness, organic matter-richness, kerogen types, thermal maturation, burial/uplift history, timing, mineralogy, fracture networks, fluid properties (density, viscosity, water saturation, phase behaviour) and expulsion efficiency (Jarvie et al., 2007; 2013; Abrams et.al., 2014). Optimum combinations of these properties can be used to predict and identify sweet spots, though the controlling processes seem to vary from basin to basin. There is limited compensation within these properties, for example, a lack of maturity cannot be compensated by a greater thickness. However, whether oil or gas is produced from unconventional resources is largely a function of the source rock maturity rather than kerogen type (Jarvie et al., 2007).

Shale oil resources are defined as a source rocks (organic-rich mudstones with juxtaposed organic-lean sandstone, silt) that have generated, expelled and retained oil at mostly lower thermal maturity, hence lower temperature and pressure conditions than shale gas. The retained oil is either stored in the mudstone itself or is expelled into interbedded thin non-source facies. The term *"hybrid system" i*s used to describe this type of organic-rich mudstone with juxtaposed (interbedded, underlying and/or overlying) organic-lean non-source lithofacies (Jarvie, 2012 and Cornford et.al., 2014). This organic-lean non-source lithofacies has less affinity for oil so it produces more readily leading to higher recovery of the original oil in place (OOIP). In contrast, the organic-rich mudstone tends to retain more oil due to sorptive affinity and lower permeability (Jarvie, 2012).

At this early stage of the exploitation cycle, there are no reliable indicators for identifying commercial shale oil productivity in the UK, with the potential and resource estimates being largely based on the criteria obtained from shale oil production in the North America. Examples of hybrid systems in North America, both organic-rich, low permeability intervals and interbedded, organic-lean intervals are presently being explored in late Devonian-early Mississippian Bakken Formation and the late Cretaceous Niobrara Formation (Jarvie et al., 2007; Jarvie, 2012) and arguably in the Triassic Montney Formation of British Columbia (Chalmers et al., 2012; Chalmers and Bustin, 2012).

4.3: North Sea Kimmeridge Clay Formation

The Upper Jurassic Kimmeridge Clay Formation is the main source rock for the North Sea oil and gas fields in the Central and Viking Grabens. The dark, olive -grey calcareous to non-calcareous organic- rich mudstones in the Viking Graben area range in age from Volgian to Ryazanian. These sediments were deposited in a restricted marine embayment of the Boreal seaway in the north, resulting from crustal stretching and formation of the three main North Sea grabens (Cornford and Brookes, 1989; Cooper et al., 1995; Erratt et al., 2010). Sediment accumulation followed the widespread subsidence that occurred during the late Jurassic to early Cretaceous rifting episodes. Concomitant global sea-level rise led to the late Jurassic marine transgression event, resulting in the Oxfordian Heather Formation, comprising organically lean mudstones deposited under oxic bottom water conditions. With the closing of the Boral-Tethyan connection, high sedimentation rates, elevated organic matter bioproductivity (probably controlled by nutrient supply) and increased water depths all promoted stratified anoxic bottom waters. With greatly improved organic matter preservation, this resulted in the deposition of the thick, organic-rich Kimmeridge Clay Formation (Cornford and Brookes, 1989; Tyson, 2004).

During the Upper Jurassic, conglomerates and sands were periodically transported as submarine fans by gravity flow across the uplifted graben edge of the Shetland Platform and in to the main graben (Partington et al., 1993). These sands were fed into the basin via graben-edge'notches' formed over ramps/transfer zones (transform fault lineations) which breached the uplifted footwall. These coarse clastics sediments, called the 'Brae Member' were deposited into the anoxic basin of the main South Viking Graben, where they are found interbedded with the mudstones of the Kimmeridge Clay Formation (Leythaeuser et al., 1984, 1987; Turner et al., 1987). This sediment association (Figure 4-2) forms the target for this present study.

The Kimmeridge Clay Formation can be assessed as a potential shale oil reservoir since it contains actively generating source rocks and significant quantities of residual oil in the fully mature areas of the North Sea (Cornford et.al., 2014). A maximum thickness of 1,100 m is recorded for the Kimmeridge Clay Formation in the South

Viking Graben (Gautier, 2005), with the maturity and lithofacies of these source rocks varying laterally and vertically across the study area (Figure 4 -3). This illustration emphasises the need to overlap aspects of thermal maturity (upper) and of organo-facies (lower) to identify the optimal 'sweet spots' for drilling unconventional wells. The interaction of facies and maturity are optimized where total organic content (TOC) values are high and the kerogen type is oil-prone. Where oil saturation is high, asphaltene contents are extremely low and resins are reduced, and the interval lies in the volatile oil window where API gravities are generally > 40°API and gas/oil ratios (GORs) are in the range of 1000 to 15000 scf/stb (standard cubic feet of gas/barrel of oil) (Jarvie, 2012).

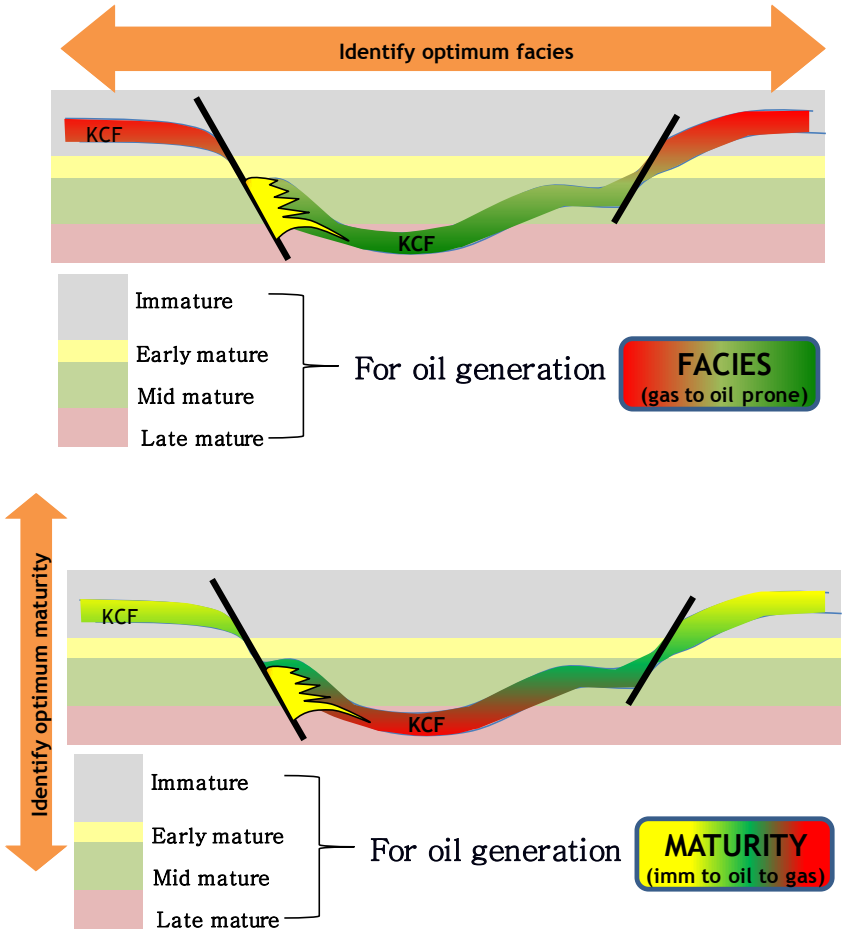

Figure 4-3: Identification of optimum facies (lateral), and maturity (vertical) for extracting unconventional liquids from the Kimmeridge Clay Formation (KCF) of the Southern Viking Graben, North Sea.

In the South Viking Graben, the formation generally thickens towards the basin margin fault and thins over the crest of the intra-basinal fault blocks (Richards et al.,

1993). The thickening into faults is less prominent for the Upper and Lower Hot Shale mudstones, than for the pebbly to fine sands of the Brae Formation (Figure 4-2). Three gross facies are recognized: Kimmeridge Clay "Hot Shale" (both Upper and Lower), an intermediate facies of interbedded sands and mudstones termed the Tiger Stripe facies, and massive sand and conglomerates of the Brae Formation (Figure 4-2). The Tiger Stripe facies is mainly found below the Upper "hot shale" and above the main Brae Formation, and comprises an alternating mudstone and fine-grained sand interbeds. It is interpreted to have been deposited by low-density turbidity currents on the outer submarine fan, inter-fan and in the basin plain environments (Reitsema, 1983; Stow, 1983, Leythaeuser et al., 1984; Turner et al., 1987; Roberts, 1991; Rooksby, 1991). Lithological and compositional heterogeneity of the mudstone-sandstone interbeds is caused in part by variation in organic richness (TOC) and kerogen type as evidenced by the core samples in the study area (Huc et al., 1985; Isaksen and Ledje, 2001).

4.4: Methods: Sampling and Analytical Procedures

4.4.1: Sampling

In this paper, eighteen core plugs from four south Viking Graben wells (16/17-14, 16/17-18, 16/17-19, 16/18-2) drilled between 1984- 1991 were sampled from the British Geological Survey core storage in Keyworth, Nottingham UK (Figure 4-4, right). The samples were selected based on the visual inspection of slabbed cores and estimates of percentage of mudstone and sandstones at different intervals from each well (Figure 4-4, right). The first three wells lie on the western margin of the graben along the Tiffany-Toni-Thelma field trend, and the latter (16/18-2) is in the trough axis to the east near the UK-Norwegian boundary (Figure 4-1 and Figure 4-2).

In terms of depth (metres sub-Kelly Bushing), the cores from the 16/17-19 well are the shallowest (3,552-82 m) followed by those from 16/17-18 at 3,720-83 m. The cores from the other two wells are substantially deeper with the 16/18-2 having a short cored interval of 4,126.5-28.7 m and 16/17-14 at 4,193.7-4,211.9 m (Table 4-1). Since they represent the upper part of the sequence (Upper hot shale and Tiger Stripe), the units sampled are taken to be Volgian to Ryazanian in age, and consists of mudstone

Table 4-1: : TOC and Rock-Eval Pyrolysis data for 18 core plug samples from the Kimmeridge Clay Formation of the Southern Viking Graben, UK North Sea. #Visual estimate of area, error taken as ±5%; samples marked c reacted with HCl and hence contained significant carbonate.

Well	Depth (m)	S_1 (mg/g)	S_2 (mg/g)	S_3 (mg/g)	T_{max} (°C)	PP	PI ((SI/Si+S_2))/2)	HI (mg/gTOC)	OI (mg/gTOC)	TOC (wt. %)	Sandstone (%)#
16/17-14	4200	3.61	7.11	0.2	437	11	0.34	132	4	5.37	30
16/17-14	4211.7	1.86	5.69	0.1	439	7.6	0.25	245	4	2.32	50c
16/17-14	4193.6	2.7	3.74	0.18	427	6.4	0.42	340	16	1.1	90 c
16/17-14	4194.7	5.42	11.1	0.25	437	17	0.33	152	3	7.32	10
16/17-14	Average	3.4	6.91	0.182	435	10.5	0.335	217.25	6.75	4.02	
16/17-18	3719.8	5.51	12.3	1.06	428	18	0.31	221	19	5.54	10
16/17-18	3780.4	2.5	3.09	0.15	431	5.6	0.45	151	7	2.04	50
16/17-18	3781.4	4.53	10.9	0.34	435	15	0.29	167	5	6.51	30
16/17-18	3782.9	1.2	2.32	0.24	431	3.5	0.34	329	34	0.71	90c
16/17-18	Average	3.43	7.152	0.4475	431	10.52	0.34	217	16.25	3.7	
16/17-19	3552.2	1.68	2.34	0.16	427	4	0.42	257	18	0.91	70
16/17-19	3564.1	3.99	15.3	0.4	430	19	0.21	291	8	5.25	30
16/17-19	3572	4.27	21.4	0.1	430	26	0.17	354	2	6.06	10c
16/17-19	3574.8	2.72	6.34	0.16	433	9.1	0.3	334	8	1.9	90
16/17-19	3582.7	3.42	4.64	0.47	432	8.1	0.42	243	25	1.91	50
16/17-19	Average	3.2	10	0.258	430	13.24	0.3	295.8	12.2	3.2	
16/18-2	4126	3.19	33.1	0.48	436	36	0.09	368	5	8.99	10
16/18-2	4126.2	1.54	22.5	0.2	434	24	0.06	352	3	6.38	50
16/18-2	4127.7	1.87	14.6	0.49	432	17	0.11	311	10	4.7	70
16/18-2	4127.4	1.32	4.92	0.12	434	6.2	0.21	286	7	1.72	90
16/18-2	4128.4	2.38	14	0.08	429	16	0.15	276	2	5.08	30
16/18-2		2.06	17.82	0.27	433	19.84	0.124	318.6	5.4	5.37	

sequences with interbedded sandstone (Figure 4-2). The percentage of the mudstone and sandstone were visually estimated from full cores and core plugs initially, with the estimates being substantiated by observing thin sections under an optical microscope.

The composition of the sandstone-mudstone mineralogy and porosity distribution were derived from petrographic thin sections, X-ray diffraction (XRD) and visual core descriptions. Geochemical analyses were carried out to determine the source rock potential, kerogen-type, maturity, carbon-isotope composition and retained hydrocarbon yield.

4.4.2: Petrography

Eighteen petrographic thin-sections were analyzed for mineralogy, rock fabric, texture, fractures and fossil contents. Rock sections were polished to approximately 20 μm in thickness. In terms of simple lithofacies, the abundance of sand in the mudstone was estimated from the thin sections, with each sample being placed in one of five categories (Figure 4-.4, right).

4.4.3: X-ray diffraction (XRD)

A Bruker D8 Advanced diffractometer set to Bragg-Brentano geometry reflection mode analysis was used to record the X-ray diffraction pattern of powdered samples. The samples were prepared and mounted on a dry slide glass and held in a sample holder. The X-ray radiation was Cu K_α (1.54056 nm) and the sample was scanned between 5 and 65° 2θ angle with a 0.02° 2θ step size (Moore & Reynolds, 1997).

4.4.4: Total Organic Carbon and Pyrolysis Analysis

Thermal vaporization and pyrolysis analysis of powdered samples was carried out using a Rock-Eval 6 Instrument to obtain information on hydrocarbon generation, potential, type and maturity of organic matter in the samples. Norwegian Petroleum Directorate (NPD) rock standard, Jet-Rock 1 (JR-1) standard was used to analyze every tenth sample and checked against the acceptable range given in NIGOGA standard documentation (Espitalié et al., 1985a; Peters, 1986; Lafargue et al., 1998;

Weiss et al., 2000). The TOC (total organic carbon) content of the samples was measured on a Leco SC-632 instrument as weight percent of the initial rock sample. Prior to TOC analysis samples were treated with dilute hydrochloric acid to remove carbonates.

4.4.5: Sample Preparation for Stable Isotope Analysis

Each sample was ground into fine powder using a Retsch RM100 mill. The powdered samples were placed in 50 ml centrifuge tubes, 40 ml of 3M HCl were poured onto the samples for decalcification and left to stand overnight. Only four samples (from 3,572.0 m in well 16/17-19, and 3,782.9 m in well 16/17-18 and from 4,211.7 m and 4,193.6 m in well 16/17-14,) showed visible moderate to violent reaction to HCl, indicating high $CaCO_3$ content. All the samples were rinsed five times with de-ionised water to remove any residual HCl. The samples were then dried for 24 hours at 50–60 °C, and then ground again using an agate mortar and pestle. Each sample was accurately weighed into a tin capsule (Gröcke, et. al., 2011; Brett et. al., 2014)

Stable-isotope measurements were performed at Durham University using a Costech Elemental Analyser (ECS 4010) coupled to a ThermoFinnigan Delta V Advantage. Carbon-isotope ratios are corrected for ^{17}O contribution and reported in standard delta (δ) notation in per mil (‰) relative to the Vienna Pee Dee Belemnite (VPDB) scale. Data accuracy is monitored through routine analyses of in-house standards, which are stringently calibrated against international standards (e.g., USGS 40, USGS 24 and IAEA 600). Analytical uncertainty for $\delta^{13}C_{org}$ measurements is typically ±0.1 ‰ for replicate analyses of the international standards and typically <0.2 ‰ on replicate sample analysis (e.g., USGS 40, USGS 24, and IAEA 600). In addition to the Leco analysis mentioned above, total organic carbon was obtained as part of the isotopic analysis using an internal standard (i.e., glutamic acid, 40.82 % C).

4.5: Results and Discussions

4.5.1: Mudstone and Sandstone Mineralogy

Observations from 18 thin-sections suggest that, generally, the interbedded sandstones are fine-medium grained, silty with high organic carbon content in the

mixed sandstone/mudstones interface and lower organic carbon content in the purer sandstone facies (Figure 4-4A-E). The mudstone-dominated lithologies are black-dark grey, silty, partly laminated with gradational boundaries between the mudstones and the interbedded light-grey sandstones (Figure 4-5A, B and D). At this magnification it is clear that even the mudstone-rich samples contain mainly silt (2-63 μm) and there is not much clay-sized fraction (< 2 μm) apparent.

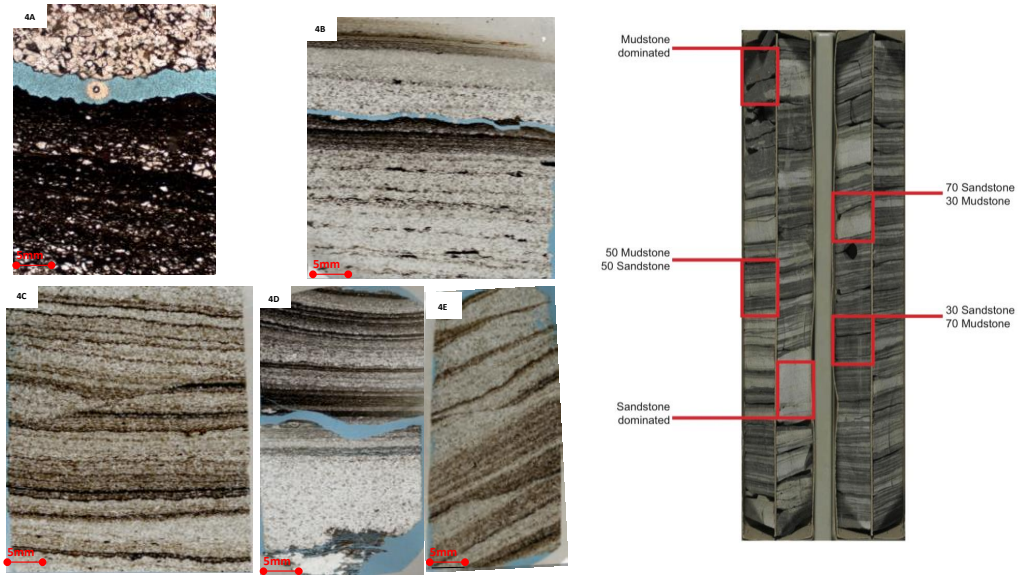

Figure 4-4: Thin-section photomicrographs of sand-dominated mudstone interbeds: (A) Sandstone-dominated photomicrograph thin section images from 4,127.4m (well 17/18-2); (B) Sandstone alternating with organic-rich mudstone layers, impregnated with blue-dyed resin showing breakage at the contact boundary between sandy and muddy layer (probably core disintegration during drilling and sampling); (C) Organic-rich 70/30 sandstone / mudstone from 3,552 m (well 16/17-19); (D) 50/50 sandstone/mudstone with desiccation fractures from 4,126.2 m (well, 16/18-2);(E) organic-rich sandstone-mudstone from 3, 582.9 m (well 16/17-19).

X-ray diffraction (XRD) results suggest these samples are dominated by quartz, clay, organic matter and pyrite (Figure 4-6). Kaolinite, illite/smectite and some chlorite are the dominant clay minerals identified in all samples. In general, a more intense XRD peak for quartz is observed in the sandstone dominated samples, though fine quartz is also a significant fraction of the mudstones. Brittleness measures the amount of stored energy within the grains prior to failure, which is controlled by the temperature, effective stress from burial, diagenesis texture, total organic carbon content and fluid type. The abundance and preservation of silicate minerals (Figure 4-6) in the sand-rich samples suggest little diagenetic alteration, as expected given the

limited depth range, with the primary quartz content likely to exert control on the brittleness of the interbedded sandstone and mudstone.

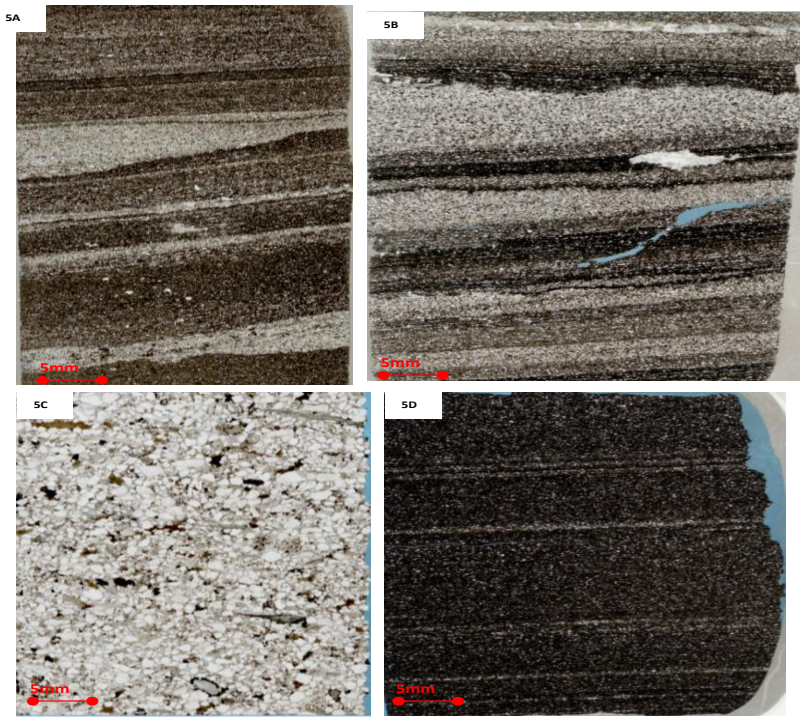

Figure 4-5: Thin-section photomicrographs of hybrid shale system displaying various mudstone-sandstone interbeds: (A) 30/70 sandstone/mudstone fine-medium sandstone, dark-grey, sub-angular-sub-rounded, moderately sorted from 3, 564.1m (well 16/17-19); (B) 50/50 sandstone/mudstone with darker organic-rich layers from 3,780.4 m (well 16/17-18); (C) Sandstone dominated sample with visible shell fragments and woody (Type II kerogen) remnants from 4,193.6m (well 16/17-14); (D) mudstone-dominated samples from 4, 194.7 m (well 16/17-14), the light-grey colour within the mudstone are thin siliceous sandstone layers, some only one grain thick.

Kaolinite, a non-swelling clay and is able to absorb petroleum while illites are able to absorb pore water which increases the wettability of these samples (Arduini et. al., 2009). However, smectite (swelling clay) hinders the flow of fluid in the pore space leading to low permeability and reduced the porosity in these samples (Kwon et. al., 2004; Arduini et. al., 2009). The ratio of illite-smectite can be used to estimate the level of maturity (%R_o) and hence oil generation during burial relating to diagenesis and catagenesis. However, smectite to illite conversion is more sensitive to time than temperature compared with changes in vitrinite reflectance (Hillier et al., 1995). Diagenetic alteration of clay minerals during burial in the South Viking Graben (well 16/22-2) is reported by Pearson et al., (1983), and shows an initial increase of 70 % to 100 % smectite (Oligocene-Eocene; 1,500-2,500 m), followed by an abrupt increase

back to 70 % in the Paleocene (2,500-2,800 m) and then little change to 3,500 m (Paleocene – Campanian). Below this depth a decrease to 20 % smectite is observed from the Campanian through to the Middle Jurassic at and below 4,000 m. This non-linear trend illustrates a combination of the effects of lithofacies for shallow (cool) samples, and a dominance of catagenesis at depth. Given the proximity of the well reported by Hillier at al., (1995) and the likelihood of a similar thermal profile, the presence of smectite in the samples of the present study from below 4,000 m suggest control from the former rather than the latter process.

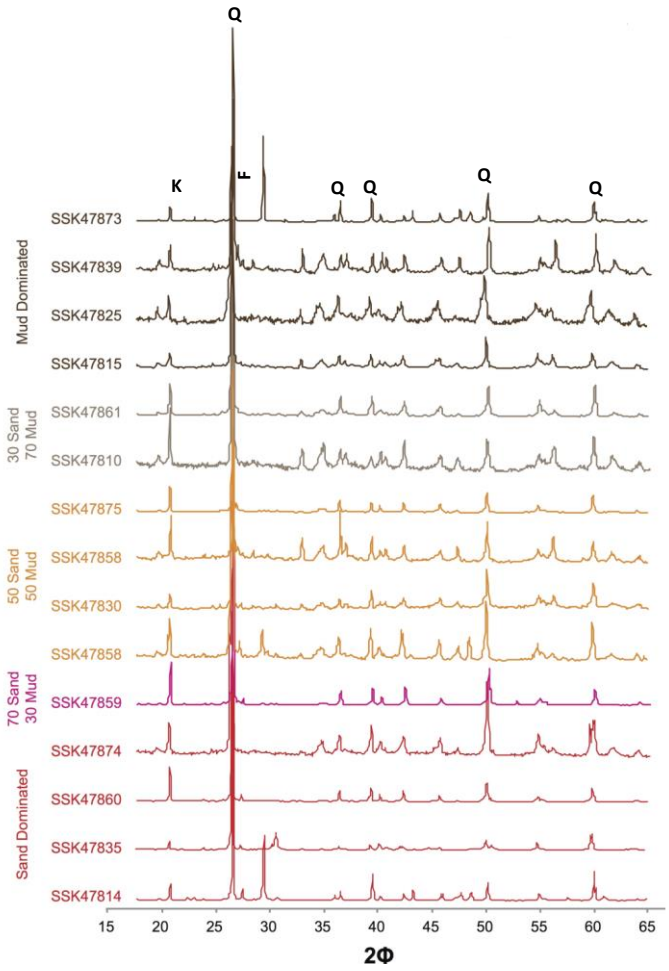

Figure 4-6: X-Ray Diffraction (XRD) pattern (Cu Kα radiation) of sandstone and mudstones samples. Q= Quartz, K=Kaolinite, F= Plagioclase Feldspar.

The XRD trends for the clay minerals are similar to the Kimmeridge Clay type-section in Dorset, which is much lower maturity, deposited in shallower water and is co-eval with the Lower and not the Upper Hot Shale of the grabenal setting (Hallam et.al, 1991; Hesselbo et al., 2009; Farrimondet al., 1984). The observed mineralogy from these present samples is comparable to the recorded Nordland Shale mineralogy from

UK quadrant 16 and Norwegian Quadrant 16 (Lothe and Zweigel, 1999; Kemp et al., 2001). Finding an area in this hybrid system that is brittle may be a key factor in creating vertical fracture pattern that are large enough to connect the highest amount of rock volume during hydraulic fracturing stimulation

4.5.2: Carbon Isotope Composition of the kerogens

Carbon isotope ratios are used to classify the origin of organic matter in terms of marine (aquatic) or continental (land) plant origins (Meyers, 1994 ; Galimov, 2006), with stratigraphically restricted deviations based on global climate variation (Jarvis et al., 2011) and on changes in sea level (Gröcke et.al., 2006). Carbon and Nitrogen (C/N) ratios and $\delta^{13}C$ values may be used to place limits on the source of the organic matter in sediments (Meyers and Eadie, 1993), together with post-depositional changes of the original organic input (Calvert, 2004). The $\delta^{13}C$ values for the investigated samples range from -29.73 ‰ to -26. 88 ‰, these values being characteristic of marine organic matter (Meyer et.al., 1984a; Meyer and Benson, 1988) or *n*-alkanes derived from land plant leaf waxes (Gunter and Mensing, 2005; Meyers, 1994).

For the Quadrant 16 samples, both sandstones and mudstones have a common projected origin of 30 ‰ VPDB for the plot of TOC vs kerogen stable carbon isotope values (Figure 4-7). Different gradients are noted for mudstone-dominated and sandstone-dominated samples from the 4 wells. The sandstone gradient of 1.33 ‰ VPDB units/1 %TOC suggests the increase in TOC derives from the addition of an isotopically heavy macerals, such as vitrinite. This is consistent with the particulate kerogen seen in the sand-dominated thin section shown in Figure 4-5c. This suggests that isotopically heavy land plant fragments fromthe Shetland Platform, presumably carried by the rivers transporting the fan sand, is the main contributors to the TOC values in the sandstones.

In contrast the mudstones form a cluster of 8 high TOC samples (mean TOC = 6.43 %), and their kerogens have mid-range isotope values (mean $\delta^{13}C$ = -28.15 ‰). At 0.3 ‰ VPDB units per 1% TOC, the mudstone gradient in Figure 4-7 is much lower than the sandstones suggesting the mixing and preservation of an isotopically light end member is controlling the gross kerogen properties. Such values probably reflect

bacterially degraded algal kerogens found in North Sea Kimmeridge Clay mudstones (Galimov, 2006).

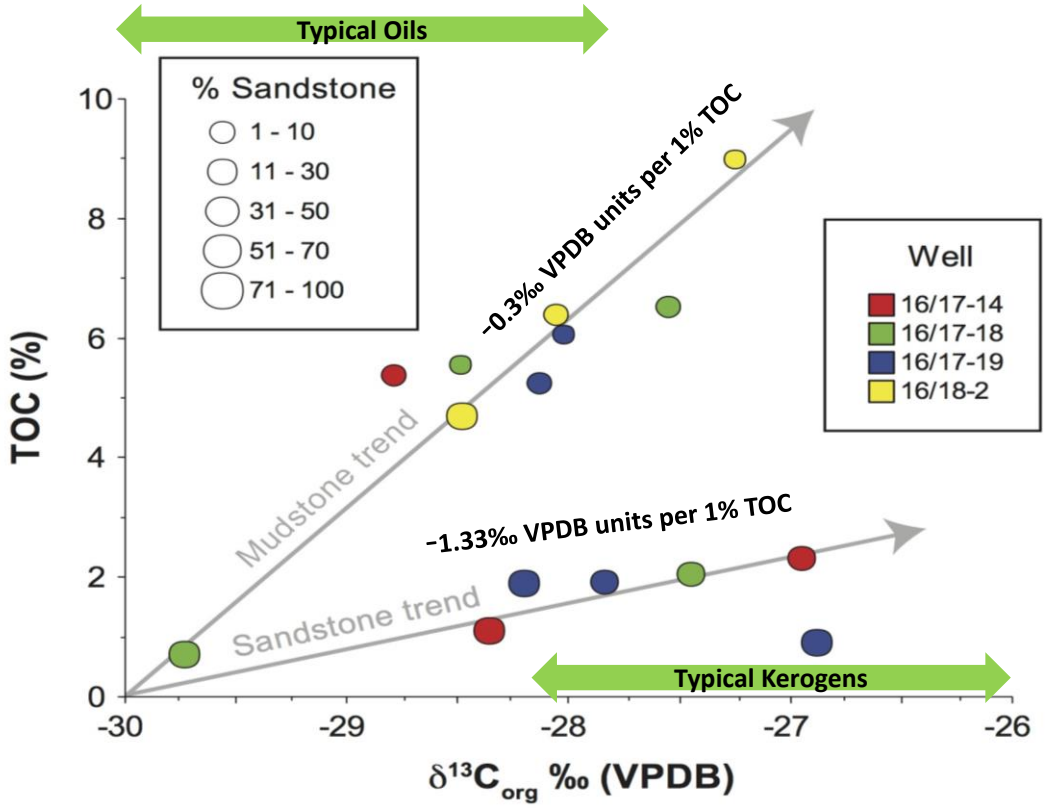

Figure 4-7: Relationship of TOC and δ ^{13}C of the kerogen between sandstone and mudstone samples for the Upper Jurassic of UK Quadrant 16.

This interpretation is supported by the relationship between the kerogen carbon isotopes and the Hydrogen Index (HI) used as an indicator of kerogen type at comparable maturities (Figure 4-8). The majority of the data in Figure 4-8 show that low HI samples (gas prone and presumably vitrinite rich) have isotopically heavier carbon, and the higher HI samples are isotopically lighter. The sandstone-rich samples show similar kerogen isotopes, this fitting with the background data from Viking Group shales from adjacent wells (Figure 4-8).

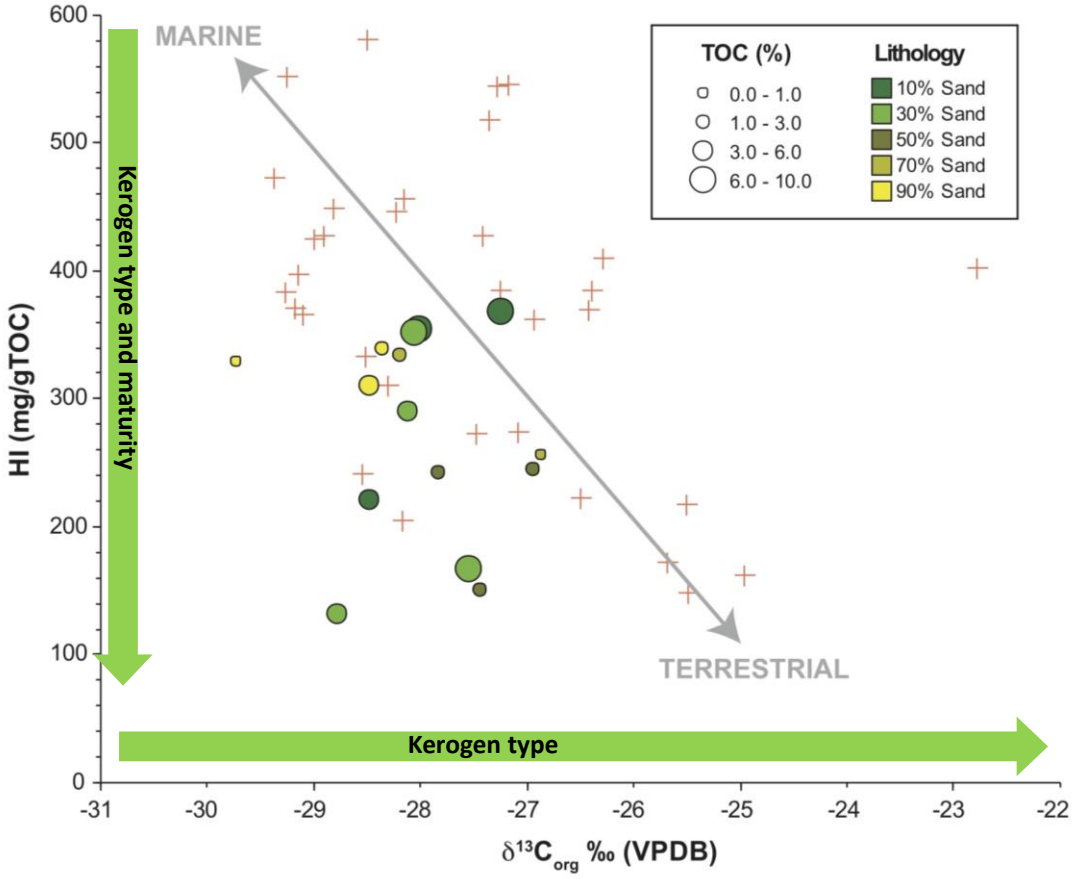

Figure 4-8: Decreasing HI (kerogen and maturity dependent) correlating with isotropically heavier carbon (kerogen type dependent) in the maturity of kerogens from cores from 3,500-4,300 m (UK Quadrant 16, South Viking Graben), and (red crosses) equivalent public data from adjacent Norwegian wells (NPD 2015).

The trends for C/N (atomic ratios) against TOC show a steep increase in C/N ratio for the mudstone rich samples, but a shallower gradient for the sand-rich samples (Figure 4-9). This points to the kerogens in the sandstones being nitrogen (i.e. protein) deficient, as expected for land plant kerogens. High organic carbon content and high C/N values from the mudstone-rich samples suggest that there is enhanced preservation of algal-bacterial carbon, and/or relative depletion of nitrogen rich proteinaceous material (Jenium and Arthur, 2007).

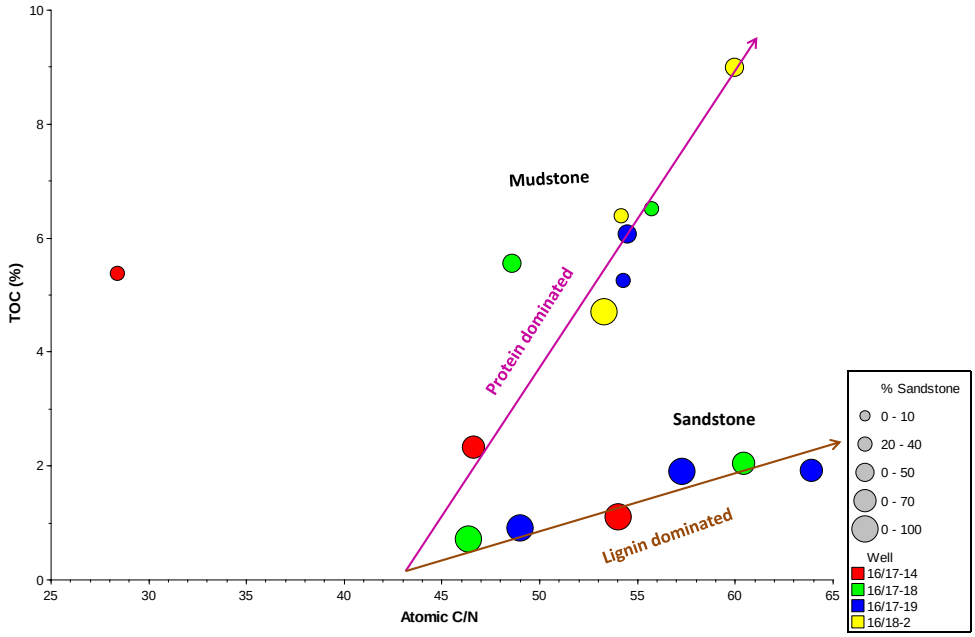

Figure 4-9: Relationship between TOC and C/N ratio showing different trends for sandstone-dominated and mudstone-dominated samples for core plugs from 4 UK Quadrant 16 wells.

Generally, the kerogen type in both the mudstones and sandstones is predominantly a classical Type II oil (and associated gas) prone kerogen. However, based on isotope bulk properties such as $\delta^{13}C_{kerogen}$ and ratios of C/N_{atomic} for the kerogens, separate trends against TOC are noted for sandstones and for mudstones. This can be explained by a uniform background of bacterially degraded algal kerogen, with the isotope and nitrogen composition reflecting the residue of different bacterial metabolic pathways (sulphate-reducing versus methane-generating bacteria). The mudstone-dominated samples, with low sedimentation rates, show mildly increasing (heavier) isotope values per 1% increase in TOC, which would be consistent with a dominance of sulphate-reducing bacterial degradation. Carbon loss will be dominated by isotopically heavier bacterial CO_2, leaving an isotopically lighter residue.

In contrast, the sandstone-dominated samples, with higher sedimentation rates, show strongly increasing (heavier) kerogen isotope values per 1% increase in TOC, suggesting degradation dominated by methanogenesis. Carbon loss will be dominated by isotopically light bacterial CH_4, leaving an isotopically heavier residue. Thus in both cases the Type II kerogen is bacterially degraded, but with different bacterial metabolisms dominating.

4.6: Richness, source and maturity of organic matter in the Kimmeridge Clay interbeds

TOC content and Rock-Eval pyrolysis measurement values for these samples are recorded in Table 4-1, and are shown plotted against depth in Figure 4.10. No consistent depth trends are seen with most variation, particularly for TOC and S_2 values, correlating with the sandstone/mudstone ratio for each well.

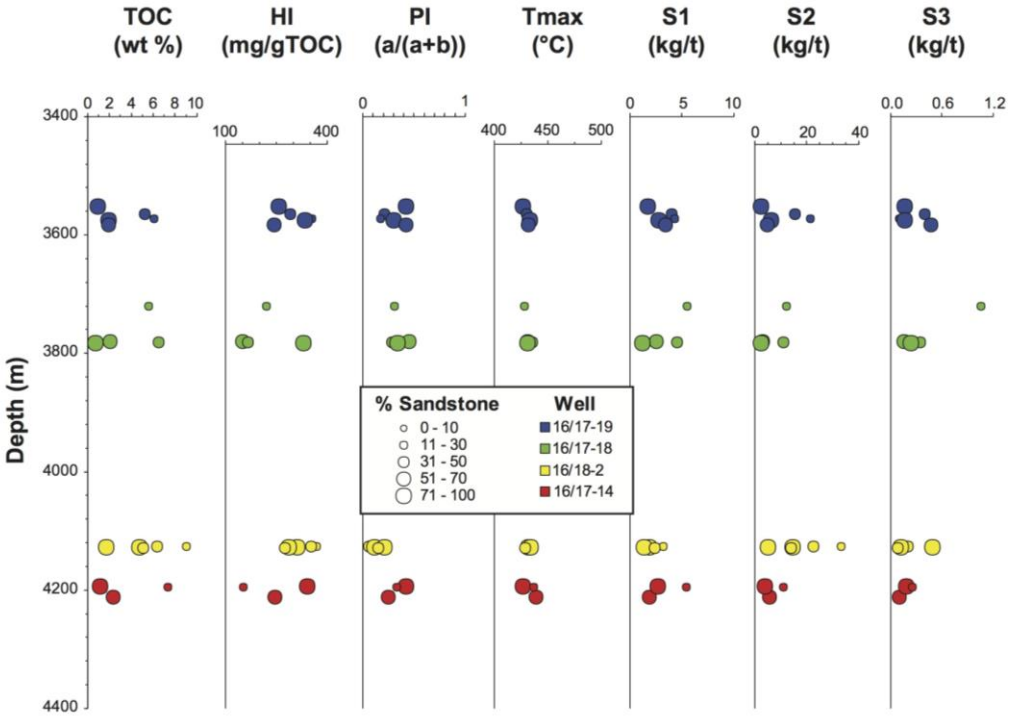

Figure 4-10: Relationships between TOC and Rock-Eval parameters versus depth for core plugs from the Kimmeridge Clay Formation intersected by four wells at different depths within UK Quadrant 16, South Viking Graben.

In terms of the overall organic richness, the samples containing a high proportion of mudstone (70 % or more of mudstone) have good to very good TOC values by industry standards (Cornford, 1998). Nine of these samples are characterized by TOC values ranging from 5.08-8.99 wt. % (Mean = 6.28 wt %TOC; standard deviation = ±1.25 wt %). A plot of the *% sandstone* values *versus TOC* (Figure 4-11) shows a steeper gradient for the sandier samples (≥50 % sand) projecting to ~0.5 % TOC for 100 % sand. In contrast, there is more scatter and a lower gradient for the mud-dominated samples, with a poorly defined trend projecting to 8-10 %TOC for a pure mudstone end member (Figure 4-11).

In well 16/18-2 at 4127.7 m.kb, a sample with a dominance of sandstone (70 % sandstone) recorded a TOC value as high as 4.7 wt % (Figure 4-11). Accepting the high TOC value and given it comes from a more basinal well, the 'normal' Hydrogen and Oxygen indices (Table 4-1) suggest that the kerogen type is of the marine bacterial-algal Type II composition. This points to 70 % of relatively clean sand containing little land plant kerogen interbedded with 30 % of particularly organic rich mudstones.

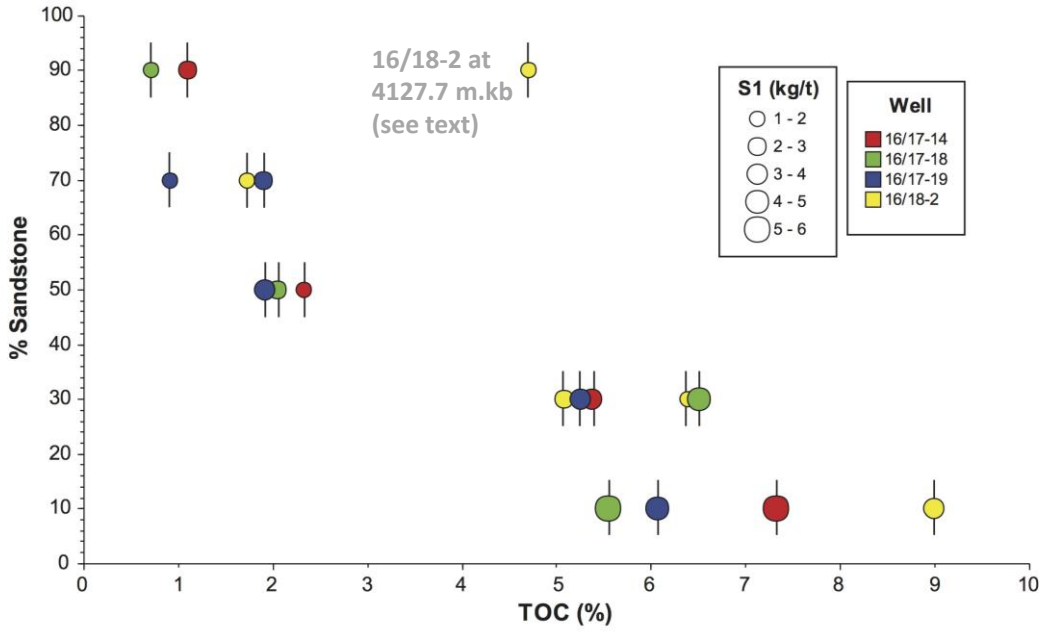

Figure 4-11: Total Organic Carbon (TOC) as a function of sandstone/mudstone ratio showing two trends and projecting an average 0.5 wt. % TOC for a 100% sandstone end member and ~9wt %TOC for a 100 % mudstones end member.

The measured TOC values in this study are similar to those previously reported in North Sea data, For example, Isaksen et al. (2002) recorded TOC values that range from 3-10 wt % in the Upper Draupne (Kimmeridge Clay) Formation, and 2-5 wt % for organically leaner Lower Draupne and Heather Formation in Norway. Average TOC values of 5.6 wt % from 2,600 – 3,200 m and 4.9 wt % from 3,250-3,650 m were also reported from the Kimmeridge Clay Formation in the Viking Graben (Goff, 1983). Fuller (1980) also found an average of 3.25 wt % in sediments from the Kimmeridge Clay Formation in general. These values suggest that the source rocks contain very rich amount of organic matter, which has been shown to be adequate for shale oil generation (Jarvie, 2012).

Origin and types of organic matter were determined mainly from Rock-Eval analysis, using plots of Hydrogen Index (HI) versus T_{max} , HI versus Oxygen Index (OI), and TOC versus S_2 (remaining petroleum generation potential). The new UK Quadrant 16 values are plotted in the context of the public access data on the website of the Norwegian Petroleum Directorate (NPD), with the Upper Jurassic Viking Group samples from the adjacent Norway Quadrant 15 being shown as small crosses in the background of the figures (Figure 4-12).

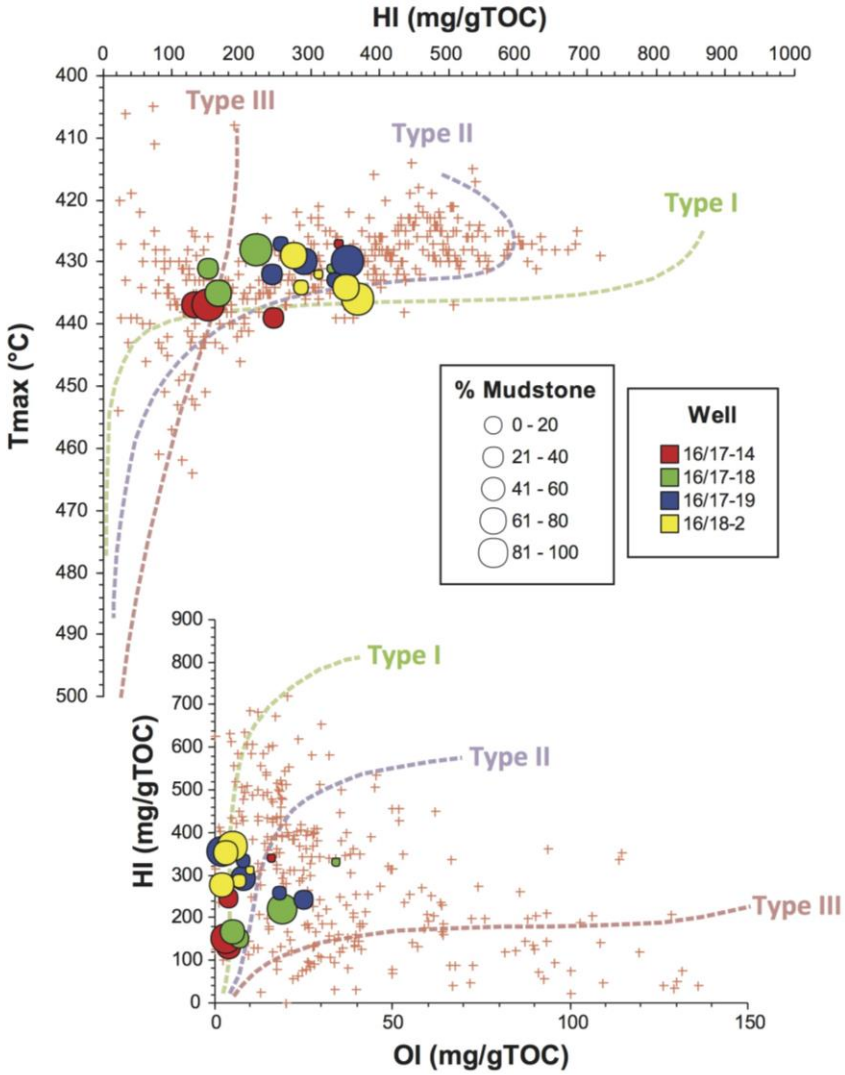

Figure 4-12: Kerogen type and maturity from Rock-Eval pyrolysis: the Hydrogen Index vs T_{max} (HIT) plot (upper) and pseudo-van Krevelen Oxygen Index (OI) and Hydrogen Index (HI) plot (lower). (Note: the kinetically defined maturity pathways are after equations by Banerjee et al (2004) automatically added in p: IGI-3 software).

The Hydrogen Index *vs* T_{max} (HIT) plot (Figure 4-12, upper) shows the new data to both fit with the regional maturity trend from Norway Quadrant 15 (N15) and with a typical Type II kerogen trend based on the maturity trends. Fitting with the well-defined Norwegian trend indicates that the initial kerogen was Type II containing bacterially degraded algal kerogen, with a few samples plotting towards Type I kerogens containing better preserved algae (Cornford, 1998). The relationship between HI *vs* OI, a pseudo-van Krevelen plot (Figure 4-12, lower), suggests that most of the UK samples are more a mix of Type I (mainly algal) and Type II (bacterially-degraded algal) kerogens, though this assignation is based largely on low Oxygen Indices. In contrast to TOC (Figure 4-11), the sand-rich and mudstone-rich samples plot together in terms of kerogen type for both these graphs shown in Figure 4-12.

The contrasting of kerogen quantity being linked to sand-mudstone ratio while kerogen type is independent is shown by the standard S_2 *vs* TOC plot (Figure 4-13). Whilst the sand rich samples plot with low S_2 and TOC values, they fall on the same diagonal (iso-HI line = 300 mg/gTOC) as the majority of the richer samples. The extent to which the sand-rich samples fall below the HI = 300 mg/gTOC line reflects the amount of terrigenous Type III kerogen in the mix. This discrepancy in kerogen type assignment may also occur because the S_2 versus TOC plot overlay is based on immature organic matter, and not mature samples such as those from the deep wells sampled in UK Quadrant 16 (Table 4-1).

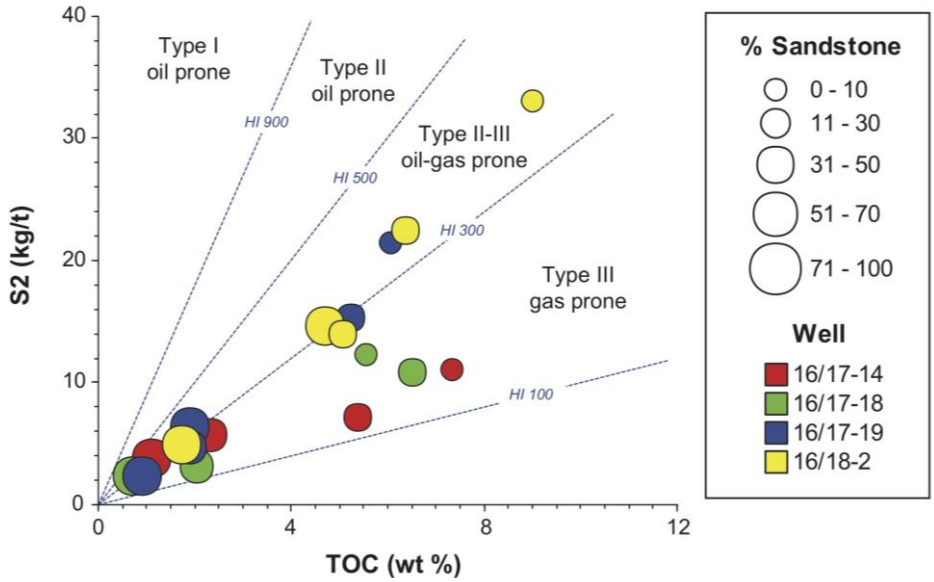

Figure 4-13: Relationship between Total Organic Carbon (TOC) and Rock-Eval S_2 (kg pyrolysate/tonne of rock) where the diagonals are Hydrogen Index (S_2/TOC, mg pyrolysate/gTOC). (Note: the kinetically defined maturity pathways are after equations by Banerjee et al (2004) automatically added in p: IGI-3 software).

4.6.1: Interpretation of Maturation and Quantification of Generated Oil

Rock-Eval T_{max} values were used as a thermal maturity indicator, these values range from 427 °C (late immature-early mature) to 439 °C (mid-mature) with an average of 432 °C (Table 4.1). The samples cover a depth interval from 3552.2 m to 4212.0 m. To make literature comparisons, the T_{max} values were converted to vitrinite reflectance (Ro), using Jarvie's equation: $Ro = (T_{max} \times 0.018) - 7.16$ (Jarvie, 2001; Peters et al., 2005). The converted T_{max} -based Ro values range from 0.526- 0.742 % R_o with an average of 0.62 % R_o suggesting that the majority of the samples are in the early- to mid-mature oil window (Figure 4-14).

The maturity is similar to the 0.62 % R_o of oil window recorded at an average depth of 3500 m (Justwan et.al., 2006), 3400 m (Isaksen and Ledje, 2001) and 3340 m (Baird, 1986) for the South Viking Graben area confirming that the Quadrant 16 sampled intervals are currently just in the oil generation window (Figure 4-14).

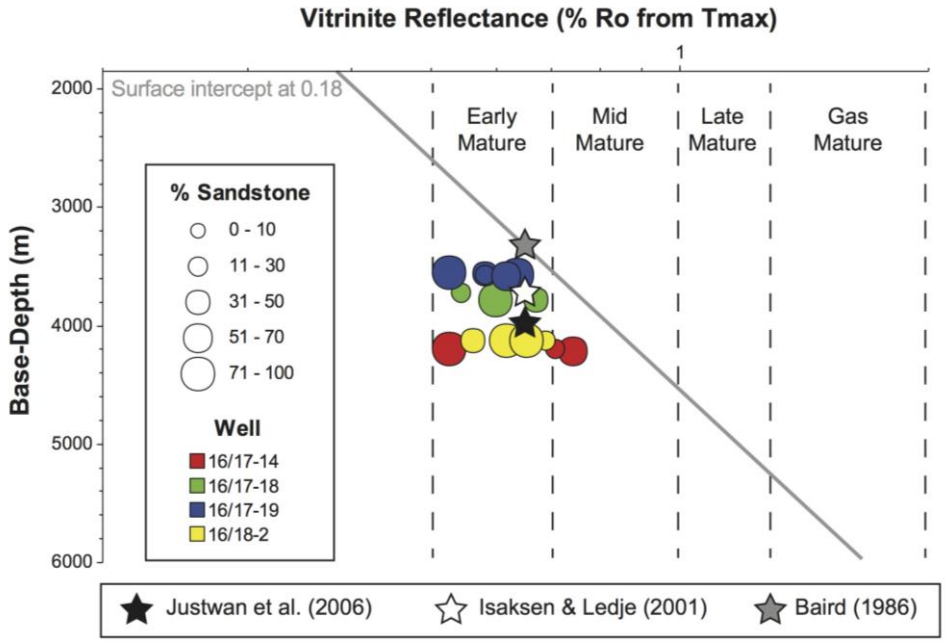

Figure 4-14: Thermal maturity depth plot showing early-mid oil generation window based on vitrinite reflectance values converted from Rock-Eval T_{max} compared with similar maturity/depth values recorded by Baird, 1986, Justwan et.al, 2006 and Isaksen and Ledje (2001). Note: standard surface intercept line automatically added in p:IGI-3 software).

The lithological differences between the mudstones and sandstones are reflected in the Rock-Eval Production Index (PI) values (Table 4.1), where the PI is calculated as the ratio of $S_1/ (S_1+S_2)$. In general PI tracks the transformation of kerogen into free hydrocarbons (S_1 kg / *tonne* of rock). In addition, PI is generally higher in poorly drained source rocks and lower in well drained source rocks (Cornford, 1998). In the case of the UK Quadrant 16 samples, the abundance of sandy layers would be expected to define drainage. However, the relationship between PI and T_{max} suggest these bulk samples (i.e. analyzing the sandstone-mudstone mix as a single sample) to be poorly-drained source rocks (Figure 4-15). This implies that the sandier samples have retained rather than drained oil, and hence that they may enhance the potentially producible oil in the mudstones.

The conventional interpretation of PI as an indicator of generation and retention is shown by the interpretation lines in Figure 4.15. The samples covering a relatively narrow range of maturity (T_{max} = 427-439 °C) show a wide range of PI values (0.06-0.45). Figure 4-15 suggests that there is a consistent variation by well and that the PI

values are independent of sandstone content. At the same maturity level based on T_{max}, the 16/18-2 well (5 samples from 13,358-13,546 ft.) has consistently low PI values and the 16/17-18 well (4 samples from 12,205-12,412 ft.) has consistently higher PI values.

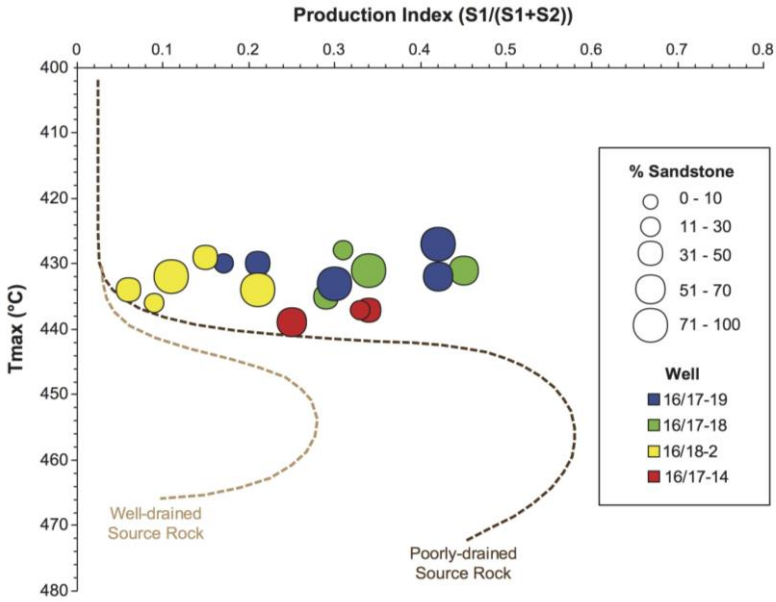

Figure 4-15: Rock-Eval Production Index (PI) versus T_{max} plot with interpretation based on organic rich mudstones. Comparison with the trends may indicate the effects of drainage and retention by the interbedded sandstones.

The relationship of PI (S_1/ (S_1+S_2)) with sand content (Figure 4.16) is further investigated to test whether the sandstone layers offer storage for the oil generated in the interbedded mudstone layers. The mean PI value for each lithology group is shown as well as the individual measurements on each sample. Where mudstone dominates (<30% sand), the average PI values are low (0.21-0.23), suggesting a low retention of generated oil. Where sandstones dominate (>70 % sand), the average PI values are intermediate (0.29-0.31). The changes seen for PI for these essentially iso-maturity samples (Figure 4-14) are broken down into the influence of Rock-Eval S_2 and S_1 (Figure 4-16 lower left and right respectively). From these plots it seems that the increase in PI is more to do with a systematic decrease in S_2 (generation from kerogen) than the increase in S_1 (retention of generated oil). The stratigraphically equivalent public database from adjacent UK and Norwegian wells (shown as red + symbols) confirms that these trends also derive from routine cuttings samples from

numerous exploration wells (Figure 4-16). It can be concluded that the sand-rich samples have closely grouped low S_2 values but more scattered, higher S_1 values (Figure 4.16, bottom right circled cluster) in contrast to the interbedded mudstone-rich samples.

The anomalous individual PI value of 0.42 is observed at 4,193.6 m in well 16/17-14, and suggests either the migration of oil into the pore spaces of the sandstones (oil staining), or because the sandstone has reduced kerogen (1.1 %TOC). Migration of oil from the mudstone into the interbedded sandstone involves a short vertical distance from the source to storage in the interbeds (Turner et al., 1987; Reitsema, 1983; Roberts, 1991). Thus the conclusion is that free oil (S_1) has migrated into the sandy layers of these finely layered sedimentary units.

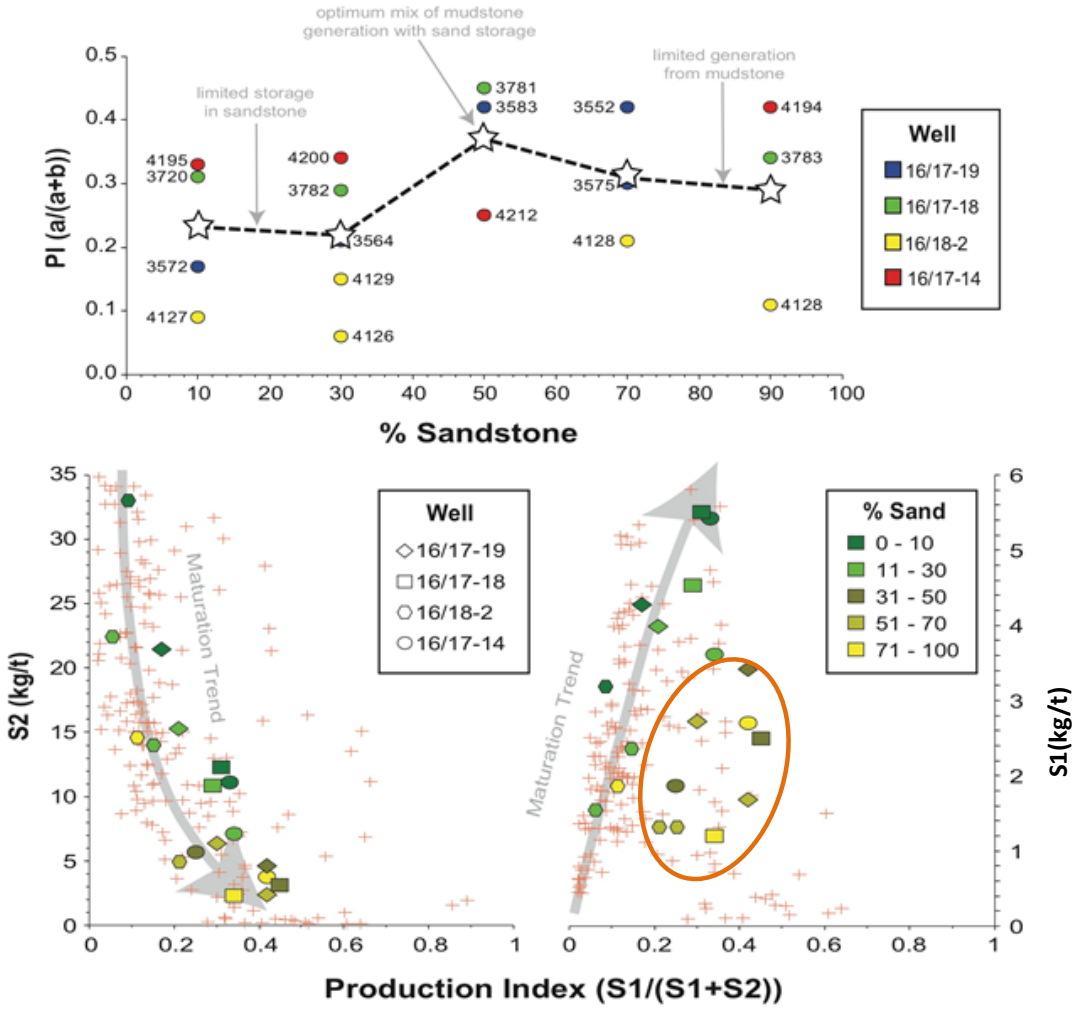

Figure 4-16: Relationship between sandstone content and Production Index (Upper) and the breakdown of Production Index into contributions from S_2 (lower left) and S_1 (lower right) yields. For the latter circled cluster = higher PI values for sands with lower S_1 yields.

4.6.2: Effect of Sand Content on Free Oil in Sediments

Rock-Eval S_1 is used to measure the quantity of free oil in mg 'oil' /g of source rock in the sampled cores. Plotted against sample depth, and in the context of the local Viking Group mudstones, the core plug Rock-Eval data (Table 4-1) confirm a deeper zone of high S_1 values (Figure 4-17, left). Plotted against lithology, the sandstone-dominated samples have lower S_1 (free oil) values (1-3 kg/t) than the mudstone-rich samples with S_1 values of 3-6 kg/t (Figure 4-17, right). A consistent, but poor correlation is observed independent of the well from which the samples were taken. The negative correlation (high S_1 = low % sand) suggests that the sandstone lithofacies has a lower affinity to absorb the expelled free oil (S_1) while the organic-rich mudstone has a higher

adsorptive affinity for S_1 oil (Figure 4-17). In the sample intervals the mudstone S_1 values may be considered as 'in situ' free oil, and the sandstone S_1 values may be considered as 'migrated', where the migration distance is between 0.01 and 10mm (Figure 4-3 and Figure 4-4).

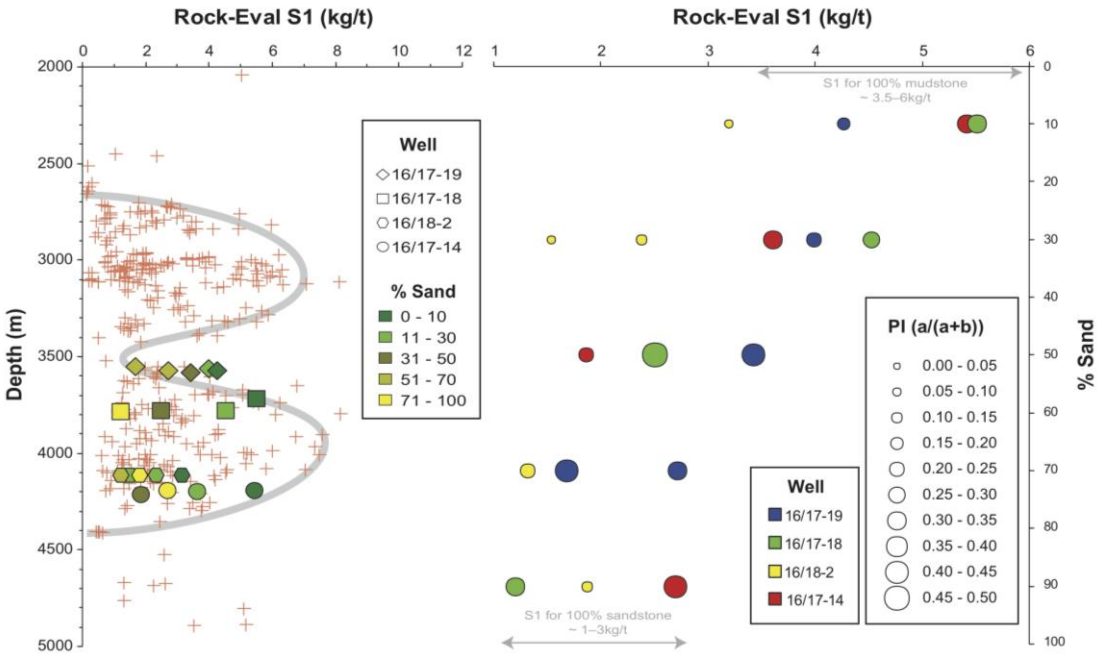

Figure 4-17: Correlation between sandstone and S_1 (free oil).

Jarvie's (2012) plot of S_1 versus TOC (Figure 4.18) discriminates between unconventional productive and unproductive S_1 values, and suggests that it is not the absolute value of S_1 but the amount of S_1 relative to TOC that controls unconventional oil productivity. In this plot, the axes units are TOC in weight % and S_1 in parts per thousand (kg/tonne), so the 1:1 diagonal line for S_1/TOC (= ‰/%) may be labeled as 1 or 10. For the UK Quadrant 16 samples, the Jarvie plot places the sand-rich samples on the productive side of the diagonal boundary (S_1/TOC ratio of 1.0), with none of the samples falling clearly within the 'oil shows' region of the plot. The sand-poor samples plot in the 'low oil production' area (Figure 4-18) though they actually contain higher S_1 values than the sand-dominated samples (Figure 4-17 right). Other than the obvious greater storage capacity of the sandstones, this may be due to evaporative losses during core storage or sample preparation, contamination into the sands from drilling fluid, the lack of adsorption of sandstones or the type of oil

(lighter oils or volatile). Adsorption affinity is an important factor in hydrocarbon storage, as organic -rich shales tend to hold onto hydrocarbon better than either organic lean rocks (Jarvie, 2014) or rocks with predominantly quartz and carbonate minerals (Schettler and Parmely, 1991). Another technical factor to be considered is that the Rock-Eval 6 instrument has been shown to yield lower S_1 values compared to other Rock-Eval instruments (Jarvie, 2014). Thus, samples with S_1/TOC <1 may still be productive. The shale samples co-plotted with a larger background data set of cuttings (symbol = +) from the UK Quadrant 16 and Norwegian Quadrant 15 over a similar depth range (Viking Group samples from 3.5-4.5 km).

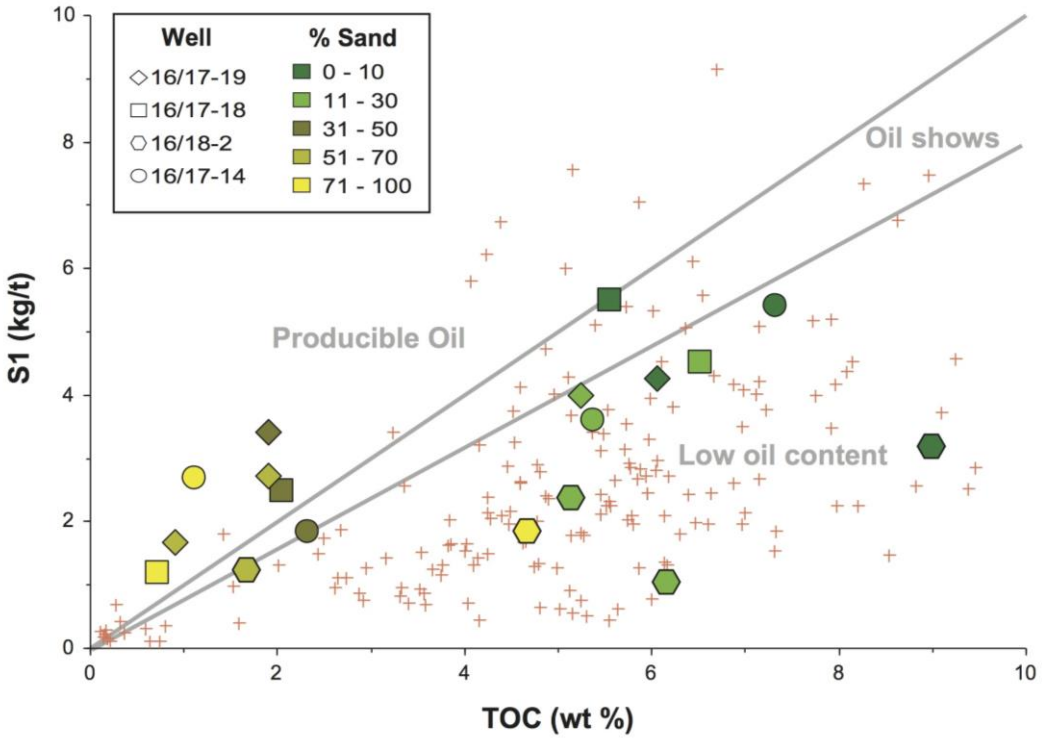

Figure 4-18: TOC (wt %) vs. S_1 (kg/tonne) plot (after Jarvie 2012) showing the producible oil content in UK Quadrant 16 samples to be in the sand-rich samples. Note that in this plot, the axes units are TOC in weight % and S_1 in parts per thousand (‰ or kg/tonne), so the 1:1 diagonal line for S_1/TOC (= ‰/%) may be labeled as 1 or 0.1 (where free oil is 1/10th of the TOC by weight).

This interpretation suggests that the optimal unconventional samples have > 50 % sand and TOC values in the 1-2 % range (Figure 4-16 upper and Figure 4-18).The ratio of S_1/TOC forms the Oil Saturation Index (OSI = S_1 kg/tonne/ (%TOC/100) as defined by Jarvie (2012) which shows higher OSI values for sandstone-rich samples relative to the mudstones (Figure 4-19). Jarvie (2012) proposes that values greater than 100 (e.g.

TOC = 3 %, S_1 = 3 kg/t) are prospective for shale oil exploitation, which again is confined to samples with > 50 % sandstone for the UK Quadrant 16 sample set.

At an early stage of maturation, the oil generated from kerogen in the mudstones will start to saturate any available porosity. With increasing maturation, the mudstone porosity will be filled and, subject to adequate permeability, localised expulsion will start to fill the open pore spaces of sandstones in close proximity. The mudstones will contain the retained oil prior to, during and after expulsion, the expected volumetric situation being shown schematically in Figure 4-20. This also emphasises that the new S_1 data broadly fit the distribution from cuttings samples of Viking Group shales taken from numerous wells in adjacent areas.

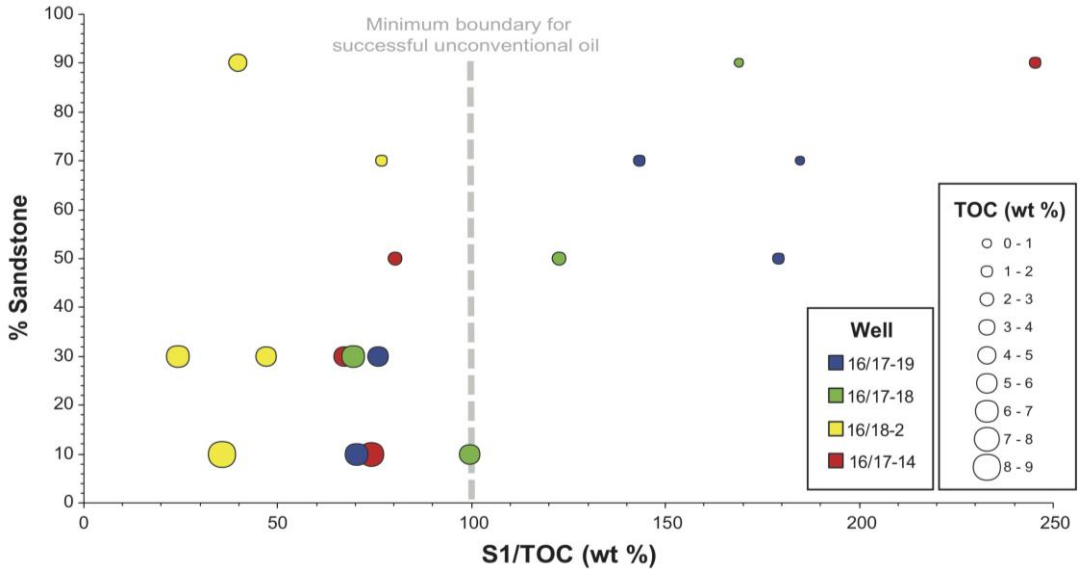

Figure 4-19: Relationship between the Oil saturation Index (S_1/TOC; mgHC/gTOC) vs. estimated % sandstone showing samples predicted to contain producible oil when OSI is greater than 100mg/gTOC. This boundary restricts unconventional oil productivity to the more sand-prone and lower TOC samples: however, it is noted that the Rock-Eval 6 machine has been reported to generate lower S_1 yields than other Rock-Eval instruments (Jarvie, 2014).

This simple calculation shows that, given the typical densities (ϱ_{Rock} =2.65 g/cc; $\varrho_{Kerogen}$ =1.40 g/cc; ϱ_{Oil} =0.86 g/cc), 6 wt. % TOC occupies about 11 volume % of the sediment, and that the S_1 value of 5 kg/tonne (typical for pure Kimmeridge Clay shales at this maturity level – see Figure 4-14) occupies about 1.54 volume% of the rock. Measuring the porosities of fine grained rocks is problematic depending on the method of

determination, grain size, mineralogy and burial depth (Swarbrick & Osborne, 1998). Based on lab measurements of helium porosity and QEMScan electron microscopy of Kimmeridge Clay mudstone core plugs from UK Quadrant 16, Cornford et al. (2014), reported mean porosity values of 2.58±1.14 % (n=15) and 1.62±1.41 % (n=34), respectively, for the two methods. Taking an average of 2 % volume 'available' porosity (where 'available' excludes residual water saturation and closed porosity), and S_1 values of 1.5 % volume, the 'oil' saturation of the porosity of the sampled mudstone is about 75 %. Gas and light hydrocarbon loss from S_1 during sampling and sample preparation may make this value up to 100 % as expected for samples taken in the oil expulsion window. This analysis indicates that for pure mudstone, full saturation of the 'available' porosity limits the retained oil available for unconventional exploitation.

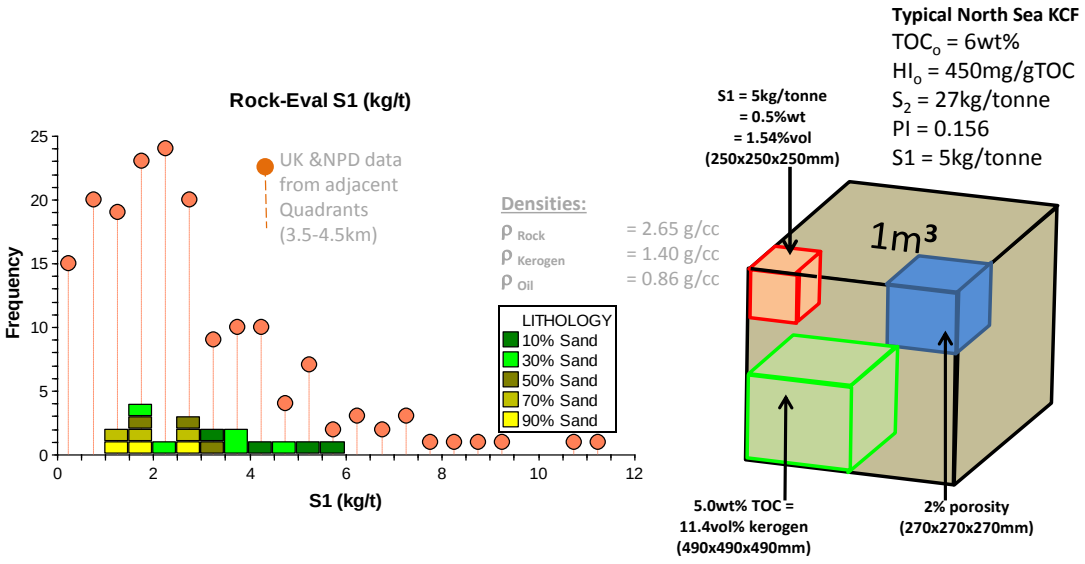

Figure 4-20: Distribution of S_1 (free oil) values for the project core plug samples and Viking Group cuttings from adjacent UK and Norwegian wells in the 3.5-4.5km range (orange pins) with schematics of expected volumetric.

The expulsion process results in some changes in the chemical composition through geo-chromatography fractionation leading to the expulsion of less polars and asphaltenes and more saturates in the expelled oil (Leythaeuser et.al., 1984) leaving the retained 'residual' oil conversely enriched. Geo-chromatographic fractionation of the expelled oil would likely occur as the oil undergoes expulsion and migration from the source rock into non-source rocks. In this process, the heavy oil with more polar

hydrocarbon components is retained in the mudstones (? adsorbed on the clay mineral surfaces), while the lighter oil is drained into the interbedded sandstones.

These organic-lean, but oil mature interbedded sandstones would be expected to have free oil (S_1) stored in their pores resulting in high productivities due to the short distances required for the migration of weakly adsorbed oil within the porous intervals (Leythaeuser et al., 1982, 1984, 1987). The lower S_1 values in the sandstone-rich samples (Figures 16 and 19) may derive from a number of processes:

1. The oil failed to move from the shales into the sands, possibly due to overpressure developed in isolated sand lenses reducing the pressure potential gradient
2. During drilling of the cores, oil was more effectively flushed from the sand compared to the mudstone interbeds
3. Migration into sandstone may also have occurred because these wells were drilled 'on structure' and hence are plumbed into the main migration path (drained sand). As such, the oil may have locally migrated into the sandstones from the mudstones a few cm away, or migrated from deeper in the basin, and then up dip to the basin margin structures.

All of these three factors will arguably have had some influence on the oil saturation of the sand layers. With reference to Figures 4-16 and 4-20, if the initial S_2 potential of 27 kg/ton is eventually converted to oil (S_1) and only 5 kg/ton is retained, then 22 kg/ton (2.2 wt %) or 6.82 %volume oil will be lost from fully mature mudstones. Taking a cubic metre of oil mature 50 % mudstone /50 % sandstone, and given the observed porosity range of 5-10 % for Brae Formation sandstones at 4 km (Cornford et al., 2014), the expelled oil volume of 6.8% equates approximately to a mid-range porosity for an equal volume of sandstone (Figure 4-20).

4.7: Conclusions

Integration of geochemical and mineralogy data from oil-mature core samples from wells in the UK North Sea Quadrant 16 demonstrate some of the effects of sand interbeds on the likely unconventional shale reservoirs properties. North Sea Kimmeridge Clay Formation with interbedded mudstones and sandstones contains

significant amount of expelled oil in the sands, as well as retained oil in the muds. Distal and inter-fan areas allow development of a hybrid system (frack production from both mudstones and sandstones), and selection of optimum sand-shale ratio for unconventional oil exploitation.

The abundance and preservation of silicate minerals in the sand-rich samples suggest little diagenetic alteration which is likely to exert control on the brittleness of the interbedded sandstone and mudstone. Finding an area in this hybrid system that is brittle may be a key factor in creating vertical fracture pattern that are extensive enough to connect and drain the optimum rock volume during hydraulic fracturing stimulation.

The amount of kerogen, as measured by TOC, is higher in the mudstone-dominated samples (6.28 wt.% average) than in the sandstone dominated samples (1.36 wt.% average), with projected pure end members being 9 wt.% and 0.5 wt.% respectively. In the deep water largely pelagic environment of the late Jurassic graben, this is interpreted as the dilution of the kerogen-mudstone background sedimentation by sand. A dilution model is confirmed by the surprising uniformity of the bulk kerogen type as measured by Rock-Eval Hydrogen Indices, based on HI-T_{max} trends and confirmed by a larger data set of cuttings analyses from adjacent Norwegian wells. The kerogen type in both the mudstones and sandstones is predominantly a classical Type II oil (and associated gas) prone kerogen. The mudstone-dominated samples, with low sedimentation rates, show mildly increasing (heavier) isotope values per 1% increase in TOC, which would be consistent with a dominance of sulphate-reducing bacterial degradation. In contrast, the sandstone-dominated samples, with higher sedimentation rates, show strongly increasing (heavier) kerogen isotope values per 1% increase in TOC, suggesting degradation dominated by methanogenesis. Rock-Eval T_{max} values of 432 °C (early mature) to 439 °C (mid-mature) equate to the 3-4 km interval placing the samples in a limited range of early oil window maturation for the sampled mudstones and sandstone interbeds. Based on US analogues, this maturity level is lower than claimed as optimum for extraction of 'volatile oil' by hydraulic fracking.

Migration of free oil (S_1) from the mudstone into the interbedded sandstone involves a short lateral distance through the sandstone pores from the source to storage in the interbeds resulting in high productivities. Thus the conclusion is that free oil (S_1) has migrated into the sandy layers, this implies that the sandier samples have retained rather than drained oil, and hence that they may enhance the potentially producible oil content in the study area. The abundance of sandy layers would be expected to define drainage. However, the relationship between PI and T_{max} suggest these bulk samples to be poorly-drained source rocks at the maturity levels encountered.

The Oil Saturation Index (OSI = S_1/TOC) shows higher values for sandstone-rich samples relative to the mudstones, and higher values for lower TOC samples at the encountered early-mature level of maturation. These data suggest that the optimal unconventional samples have ~50 % sand and TOC values in the range of 1-2 %. The key points of this hybrid system are the thickness, storage capacity and the possibility to capture a portion of the expelled as well as retained oil.

4.8: Acknowledgements

The authors would like to thank Trapoil and Two Fields Consulting (TFC) for supporting this research. HCG thanks the Royal Society for an Industry Fellowship. MR acknowledges receipt of a Durham University Doctoral Scholarship (DDS). We are grateful to the British Geological Survey (BGS) for providing the core samples for this study, and Applied Petroleum Technology (APT) for rapid analyses of these samples. Special thanks to Integrated Geochemical Interpretation Limited (IGI Ltd) for the use of their p: IGI-3 software for the geochemical interpretation of the results.

The authors wish to acknowledge important contributions and review by Dan Jarvie, and an anonymous reviewer.

4.9: References

Abrams, M.A., Dieckmann, V., Curiale, J.A. and Clark, R. 2014. Hydrocarbon Charge Considerations in Liquid-Rich Unconventional Petroleum Systems. American Association of Petroleum Geologists Search and Discovery Article, #80366.

Arduini, M., Golfetto, F. and Ortenzi, A. 2009. The Chlorite-Bearing Reservoirs: Effects of the Main Petrographic Parameters on Reservoir Quality. Search and Discovery Article #50178.Posted 27/04/2009

Baird, R. A. 1986. Maturation and source rock-evaluation of Kimmeridge Clay, Norwegian North Sea. American Association of Petroleum Geologists Bulletin, 70, pp.1–11.

Barnard, P. C., and Cooper, B. S. 1981. Oils and source rocks of the North Sea area, in L. V. Illing and G. D. Hobson, ed., Petroleum geology of the Continental Shelf of northwest Europe: Heyden, London, Institute of Petroleum, pp.169–175.

Bernard, P. C., Collins, A.G. and Cooper, B.S., 1981. Identification and distribution of kerogen facies in a source rock horizon—examples from the North Sea basin, in Brooks, J., ed., Organic maturation studies and fossil fuel exploration: London, Academic Press, pp.271–282.

Bernard, S., Brown, L., Wirth, R., Schreiber, A., Schulz, H.-M., Horsfield, B., Aplin, A.C., Mathia, E.J., 2013. FIB-SEM and TEM Investigations of an Organic-rich Shale Maturation Series from the Lower Toarcian Posidonia Shale, Germany: Nanoscale Pore System and Fluid-rock Interactions. American Association of Petroleum Geologists Memoir: Electron Microscopy of Shale Hydrocarbon Reservoirs 102, pp.53-66.

Brett, M.J., Baldini, J.U.L. and Gröcke, D.R. 2014. Environmental controls on stable isotope ratios in New Zealand Podocarpaceae: implications for palaeoclimate reconstruction. Global and Planetary Change 120: pp.38-45.

Calvert, S.E. 2004. Beware intercepts: interpreting compositional ratios in multicomponent sediments and sedimentary rocks. Organic Geochemistry 35, pp.981–987.

Chalmers, G.R.L., Bustin, R.M. and Bustin, A.A.M. 2012. Geological controls on matrix permeability of the Doig-Montney hybrid shale-gas–tight-gas reservoir, northeastern British Columbia (NTS 093P); in Geoscience BC Summary of Activities 2011, Geoscience BC, Report 2012-1, pp.87–96.

Chalmers, G.R.L. and Bustin, R.M., 2012. Geological evaluation of Halfway–Doig–Montney hybrid gas shale–tight gas reservoir, northeastern British Columbia. Marine and Petroleum Geology 38, pp.53-72.

Cooper, B. S., and Barnard,P.C. 1984. Source rocks and oils of the central and northern North Sea, in G. Demaison and R. J. Murris, ed., Petroleum geochemistry

and basin evaluation. American Association of Petroleum Geologists Memoir 35, pp.303–314.

Cooper, B. S., Bernard, P.C and Telnaes, N. 1995. The Kimmeridge Clay Formation of the North Sea, in B. J. Katz, ed., Petroleum source rocks: Berlin, Springer-Verlag, pp.89–110.

Cornford, C. 1984. Source rocks and hydrocarbons of the North Sea. In: Glennie, K. W., (ed.) Introduction to the Petroleum Geology of the North Sea. London, Blackwell Science Ltd, pp. 171-209.

Cornford, C. 1998. Source rocks and hydrocarbons of the North Sea. In: Glennie, K.W., ed., Petroleum geology of the North Sea. London, Blackwell Science Ltd, pp. 376–462.

Cornford, C and Brooks, J. 1989. Tectonic controls on oil and gas occurrences in the North Sea area. In: Tankard, A.J. and Balkwill, H.R, ed., Extensional tectonics and stratigraphy of the North Atlantic margins. American Association of Petroleum Geologists/Canadian, Geological Foundation, pp. 46- 641.

Cornford, C., Birdsong, B. and Groves, G. 2014. Offshore Unconventional Oil from the Kimmeridge Clay Formation of the North Sea: A Technical and Economic Case. Unconventional Resources Technology Conference Proceedings, Denver, CO. August 25-27, 2014.

Cornford, C., Morrow, J.A., Turrington, A., Miles, J.A., Brooks, J., 1983. Some geological controls on oil composition in the UK. North Sea, in: Brooks, J. ed., Petroleum Geochemistry and Exploration of Europe. Geological Society Special Publication, Blackwell Scientific Publications, Oxford, 12, pp.175-194.

Department of Energy and Climate Change (DECC) 2013. United Kingdom Continental Shelf (UKCS) Geological Basins, (Available online: https://www.gov.uk/oil-and-gas-offshore-maps-and-gis-shapefiles 20140331_UKCS_Geological_Basin (Accessed March 12, 2014).

Dominguez, R. 2007. Structural evolution of the Penguins Cluster, UK Northern North Sea Geological Society of London, Special Publications, pp.292, 25-48, doi 10.1144/SP292.2.

Erratt, D., Thomas, G.M., Hartley, N.R, Musum, R., Nicholson, P.H. and Spisto, Y. 2010. North Sea hydrocarbon systems: some aspects of our evolving insights into a classic hydrocarbon province. In: Pickering, S.C. and Vining, B., ed., Petroleum Geology: From Mature Basins to New Frontiers. Proceedings of the 7th Petroleum Geology Conference. Geological Society of London, London, England, pp. 37-56.

Espitalié, J., Deroo, G. and Marquis, F. 1985. La pyrolyse Rock-Eval etses applications. Première Partie. Revue de l'InstitutFrançais du Pétrole 40, pp.563-579.

Faerseth, R. B. 1996. Interaction of Permo-Triassic and Jurassic extensional fault blocks during the development of the northern North Sea.Journal of Geological Society of London, 153, pp. 931 – 944, doi,10.1144/gsjgs.153.6.0931.

Farrimond, P., Comet, P., Eglinton, G., Evershed, R.P., Hall, M.A., Park, D.W.and Wardroper, A.M.K., 1984. Organic geochemical study of the Upper Kimmeridge Clay of the Dorset type area. Marine and Petroleum Geology 1, pp.340-354.

Fuller, J. G. C. M. 1980. Progress report on fossil fuels—exploration and exploitation. In Proceedings of Yorkshire Geology Society, (eds) Jones J. M., Scott P. W. 33:581–593

Galimov, E.M. 2006. Isotope Organic Geochemistry, Journal of Organic Geochemistry, 37, 10, pp.1200-1262

Gautier, D. L., 2005. Kimmeridgean Shales Total Petroleum System of the North Sea Graben Province: U.S. Geological Survey Bulletin 2204-C, p. 24. Available at:: http://pubs.usgs.gov/bul/2204/c [accessed June 15, 2014].

Glennie, K.W. (1986). Development of northwest Europe's southern Permian gas basin. In: Brooks, J., Goff, J.C. and van Hoorn, B., ed., Habitat of Palaeozoic gas in NW Europe. Geological Society, London, Special Publication, 23, pp. 3-22

Gluyas, J., Garland, C., Oxtoby, N.H., & Hogg, A.J.C., 2000. Quartz cement: the Miller's tale. In: Worden, R.H., Morad, S. ed., Quartz Cementation in Sandstones. International Association of Sedimentology Special Publication, 29, pp.199 – 218.

Goff, J. C. 1983. Hydrocarbon generation and migration from Jurassic source rocks in the East Shetland Basin and Viking Graben of the northern North Sea: Journal of the Geological Society, 140, pp. 445–474.

Gröcke, D. R.; Ludvigson, G. A.; Witzke, B. L.; Robinson, S. A.; Joeckel, R. M.; Ufnar, D. F. and Ravn, R. L. 2006. Recognizing the Albian-Cenomanian (OAE1d) sequence boundary using plant carbon isotopes: Dakota Formation, Western Interior Basin, USA, Geology, 34, pp.193-196.

Gröcke, D.R., Hori, R.S., Trabucho-Alexandre, J., Kemp, D.B. and Schwark, L. 2011. An open ocean record of the Toarcian oceanic anoxic event. Solid Earth: An Interactive Open Access Journal of the European Geosciences Union 2(2), pp.245-257

Gunter, F. and Mensing, T.M. 2005. Isotopes: Principles and applications (3rd ed.): Hoboken, New Jersey, John Wiley & Sons, Inc.

Hallam, A., Grose, J. A. and Ruffell, A. H. 1991.Palaeoclimatic significance of changes in clay mineralogy across the Jurassic–Cretaceous boundary in England and France.Palaeogeography, Palaeoclimatology, Palaeoecology, 81, pp.173–87.

Hallam, A. 1995. Oxygen-restricted facies of the basal Jurassic of North West Europe. Historical Biology, 10, pp.247–257.

Hesselbo, S., Deconinck, J.-F., Huggett, J.M., and Helen, S. 2009. Late Jurassic palaeoclimatic change from clay mineralogy and gamma-ray spectrometry of the Kimmeridge Clay, Dorset, UK: Journal of the Geological Society, 166, pp.1123-1133.

Hillier S, Matyas J, Matter A. and Vasseur, G. 1995. Illite/smectite diagenesis and its variable correlation with vitrinite reflectance in the Pannonian Basin.Clays and Clay Minerals, 43(2), pp.174-83.

Huc, A.Y., Irwin, H. and Schoell, M.1985. Organic matter quality changes in an Upper Jurassic shale sequence from the Viking Graben. In: Thomas, B.M., Dore′, A.G., Eggen, S.S., Home, P.C. & Larsen, R.M. ed., Petroleum Geochemistry in exploration of the Norwegian Shelf. Graham and Trotman, London, pp.179–183.

Isaksen, G.H. and Ledje, K.H.I. 2001.Source rock quality and hydrocarbon migration pathways within the greater Utsira High area, Viking Graben, Norwegian North Sea. American Association of Petroleum Geologists Bulletin, 85, 5, pp. 861–883.

Isaksen, G.H., Patience, R., van Graas, G. and Jenssen, A.I. 2002. Hydrocarbon system analysis in a rift basin with mixed marine and non-marine source rocks; the South Viking Graben, North Sea. American Association of Petroleum Geologists Bulletin, 86 (4), pp. 557–591..

Jarvie, D. M., Brenda L. C., Floyd "Bo" H. and John T. B, 2001. Oil and Shale Gas from the Barnett Shale, Ft. Worth Basin, Texas, AAPG National Convention, June 3-6, 2001, Denver, CO, American Association of Petroleum Geologists Bulletin 85, 13 (Supplement), A100.

Jarvie, D.M., Hill, R.J., Ruble, T.E. and Pollastro, R.M. 2007. Unconventional shale gas systems: the Mississippian Barnett Shale of north-central Texas as one model for thermogenic shale gas assessment. American Association of Petroleum Geologists Bulletin, 91, pp.475-499.

Jarvie, D.M., 2012. Shale resource systems for oil and gas: part 1 shale-gas resource systems. In: Breyer, J.A, ed., Shale Reservoirs Giant Resources for the 21st Century, American Association of Petroleum Geologists Memoir, 97, pp.69-87

Jarvie, D. M. 2014. Components and processes affecting producibility and commerciality of shale resource systems, ALAGO 2012 Special Publication, GeologicaActa, 12, 4, pp.307-325.

Jarvis I., Lignum J. S., Gröcke D. R., Jenkyns H. C and Pearce, M. A, 2011. Black shale deposition, atmospheric CO2 drawdown, and cooling during the Cenomanian-Turonian Oceanic Anoxic Event. Paleoceanography, 26(3)

Johnson, H., Leslie, A. B., Wilson, C. K., Andrews, I. J., and Cooper, R. M., 2005. Middle Jurassic, Upper Jurassic and Lower Cretaceous of the UK Central and Northern North Sea. British, Geological Survey Research Report, RR/03/001, p. 42.

Junium, C.K. and Arthur, M.A. 2007. Nitrogen cycling during the Cretaceous, Cenomanian-Turonian Oceanic Anoxic Event II. Geochemistry, Geophysics, Geosystems, 8, 3, doi:10.1029/2006GC001328.

Justwan, H., Dahl, B. and Isaksen G.H. 2006.Geochemical characterization and genetic origin of oils and condensates in the South Viking Graben, Norway. Journal of Marine and Petroleum Geology, 23, pp. 213–239.

Justwan, H., Dahl, B., Isaksen, G.H. and Meisingset, I., 2005. Late to Middle Jurassic source facies and quality variations, South Viking Graben, North Sea. Journal of Petroleum Geology, 28 3, pp. 241–268..

Justwan, H. and Dahl, B. 2005. Quantitative hydrocarbon potential mapping and organofacies study in the greater Balder Area, Norwegian North Sea. In: DoreÅL, A.G. and Vining, B., ed., Petroleum Geology: North West Europe and Global Perspectives – Proceedings of the 6th Petroleum Geology Conference.

Kemp, S.J., Bouch, J. and Murphy, H.M. 2001. Mineralogical characterisation of the Nordland Shale, UK Quadrant 16, northern North Sea.British Geological Survey Commissioned Report, CR/01/136, 52.

Kwon, O., Herber, B.E. and Kronenberg, A. K. 2004. Permeability of illite-bearing shale: 2. Influence of fluid chemistry on flow ad functionally connected pores, Journal of Geophysical Research, B10206, doi:10,.1029/2004B003055.

Lafargue, E., Marquis, F. and Pillot, D. 1998. Rock-Eval 6 applications in hydrocarbon exploration, production, and soil contamination studies. Revue de l'InstitutFrançais du Pétrole, 53, pp.421-437.

Leythaeuser, D., R., Schaefer, G. and Yukler, A. 1982. Role of Diffusion in Primary Migration of Hydrocarbons, American Association of Petroleum Geologists Bulletin 66, 4, pp.408-429.

Leythaeuser, D., Radke, M. and Schaefer, R. 1984. Efficiency of petroleum expulsion from shale source rocks. Nature, 311(5988), pp.745-748.

Leythaeuser D., Schaefer R.G .and Radke M. 1987. On the Primary Migration of Petroleum. Special Paper Proceedings of the 12th World Petroleum Congress, John Wiley & Sons Limited, Chichester, pp.227-236.

Leythaeuser, D.,Schaefer, R.G. and Radke, M. 1988. Geochemical effects of primary migration of petroleum in Kimmeridge source rocks from Brae field area, North Sea, 1: gross composition of C-15 + soluble organic matter and molecular composition of C- 15+ saturated hydrocarbons: Geochimica et CosmochimicaActa, 52, pp.701-713.

Lothe, A.E. and Zweigel, P. 1999. Saline Aquifer CO2 Storage (SACS). Informal annual report 1999 of SINTEF Petroleum Research's results in work area 1 'Reservoir Geology'. SINTEF Petroleum Research report 23.4300.00/03/99, 54.

Loucks, R.G., Reed, R.M., Ruppel, S.C. and Jarvie, D.M., 2009.Morphology, Genesis, and Distribution of Nanometer-Scale Pores in Siliceous Mudstones of the Mississippian Barnett Shale. Journal of Sedimentary Research 79, pp.848-861.

Marchand, A.M.E., P. Craig Smalley, P.C., Haszeldine, R.S.and Fallick, A.E. 2002. Note on the Importance of Hydrocarbon Fill for Reservoir Quality Prediction in Sandstones. American Association of Petroleum Geologists Bulletin, 86, 9, pp.1561-1571.

Meyers, P.A., Leenheer, M.J., Eadie, B.J. and Maule, S.J. 1984. Organic geochemistry of suspended and settling particulate matter in Lake Michigan. Geochimica et Cosmochimica Acta, 48, 443-452.

Meyers P. A. and Benson L. V. 1988. Sedimentary biomarker and isotopic indicators of the paleoclimatic history of the Walker Lake basin, western Nevada.Organic Geochemistry. 13, pp.807-813

Meyers, P. A. and Eadie, B. J. 1993. Sources, degradation and recycling of organic matter associated with sinking particles in Lake Michigan. Organic Geochemistry, 20, pp.47–56.

Meyers, P.A. 1994. Preservation of source identification of sedimentary organic matter during and after deposition. Chemical Geology, 144, pp.289–302.

Moore, D. M. and R. C. Reynolds, J. (1997). X-Ray diffraction and the identification and analysis of clay minerals. 2nd Ed. Oxford University Press, New York.

NIGOGA: The Norwegian Guide to Organic Geochemical Analyses. Available online: http://www.npd.no/engelsk/nigoga/default.htm. (Accessed 10.05. 2014)

Norwegian Petroleum Directorate well data (NPD). Available online: http://www.npd.no/en/ [Accessed 18 Apr. 2015]

Partington, M.A., Mitchener, B.C., Milton, N.J. and Fraser, A.J., 1993. Genetic sequence stratigraphy for the North Sea Late Jurassic and early Cretaceous: distribution and prediction of Kimmeridgian-Late Ryazanian reservoirs in the North Sea and adjacent areas, in: Parker, J.R. ed., Petroleum Geology of Northwest Europe: Proceedings of the 4th Conference on Petroleum Geology of NW. Europe, at the Barbican Centre, London. Geological Society, London, pp.347-370.

Pearson, M. J. and Watkins D. 1983. Organofacies and Early Maturation Effects in Upper Jurassic Sediments from the Inner Moray Firth Basin, North Sea. Geological Society, London, Special Publications, 12, pp.147-160..

Peters, K. E. 1986. Guidelines for evaluating petroleum source rock using programmed pyrolysis: American Association of Petroleum Geologists Bulletin, 70, pp.328-329.

Peters, K.E., Walters, C.C. and Moldowan, J.M., 2005. The Biomarker Guide, 2nd edition, Cambridge University Press, Cambridge, UK.

Reitsema, R. H. 1983. Geochemistry of North and South Brae areas, North Sea. In: Brooks, J. (ed) Petroleum Geochemistry and Exploration of Europe, Geological Society, London, Special Publication, 12, pp.203-212.

Richards, P.C., Lott, G.K., Johnson, H., Knox, R.W.O'B. and Riding, J.B. 1993. Jurassic of the Central and Northern, North Sea. In: Knox, R.W.O'B and Cordey, W.G., ed., Lithostratigraphy nomenclature of the UK North Sea. British Geological Survey, Nottingham, pp.1-252.

Richards, P.C., Brown, S., Dean, J.M. and Anderton, R. 1988. Short Paper: A new paleogeographic reconstruction for the Middle Jurassic of the northern North Sea. Journal of the Geological Society, 145, pp. 883-886.

Roberts, M. J. 1991. The South Brae Field, Block 16/7a, U.K. North Sea. In: Abbotts, I. L. ed., United Kingdom Oil and Gas Fields 25 Years Commemorative Volume. Geological Society, London, Memoir, 14, pp.55-62.

Rooksby, S.K. 1991. The Miller Field, Blocks 16/7B, 16/8B, UK North Sea. Geological Society, London, Memoirs, 4,159-164.

Schaefer, R.G., Schenk, H.J. and Harms, R. 1990. Determination of gross kinetic parameters for petroleum formation from Jurassic source rocks of different maturity levels by means of laboratory experiments. Advances in Organic Geochemistry, 3, 16, I-3, pp.115-120.

Schettler Jr., P.D. and Parmely, C.R. 1991. Contributions to total storage capacity in Devonian shales, Society of Petroleum Engineers, 23422, 9.

Schlakker,A., Csizmeg, J., Pogácsás, G. and Horti, A., 2012. Burial, Thermal and Maturation History in the Northern Viking Graben (North Sea).American Association of Petroleum Geologists Search and Discovery Article #50545.Poster presentation at AAPG International Convention and Exhibition, Milan, Italy, October 23-26, 2011.

Spence, S. and Kreutz, H. 2003. The Kingfisher Field, Block 16/8a, UK North Sea. Geological Society, London, Memoirs, 20, pp.305-314.

Stow, D. A. V. 1983. Sedimentology of the Brae oilfield, North Sea: a reply. Journal of Petroleum Geology, 6, pp.103-104.

Swarbrick, R.E. and Osborne, M.J. 1998. Mechanisms that generate abnormal pressures: an overview, In: Law, B.E., Ulmishek, G.F., Slavin, V.I. ed., Abnormal Pressures in Hydrocarbon Environments. American Association of Petroleum Geologist Memoir, 70, pp.13-34.

Turner, C. C., Cohen, J. M., Connel J. R. and Cooper, D. M. 1987. A depositional model for the South Brae oilfield. In: Brooks, J. and Glennie, K. W., ed., Petroleum geology of North West Europe,London, Graham and Trotman, pp.853-864.

Tyson, R.V. 1995. Sedimentary organic matter: organic facies and palynofacies. Springer, pp.151–167.

Tyson, R.V. 1996. Sequence-stratigraphic interpretation of organic facies variations in marine siliciclastic systems: general principles and application to the onshore Kimmeridge Clay Formation, UK. In: Hesselbo, S. P. and Parkinson, D. N, ed., Sequence Stratigraphy in British Geology. Special Publication Geological Society London, 103, pp. 75-96.

Tyson, R.V. 2004. Variation in marine total organic carbon through the type Kimmeridge Clay Formation (Late Jurassic), Dorset, UK. Journal of the Geological Society, 161, pp.667-673.

Underhill, J.R. 1998. Jurassic. In: Glennie, K. ed., Introduction to the Petroleum Geology of the North Sea London, Blackwell Science Ltd,pp.245-293.

Weiss, H.M., Wilhelms, A., Mills, N., Scotchmer, J., Hall, P.B., Lind, K. and Brekke, T., 2000. NIGOGA - The Norwegian Industry Guide to Organic Geochemical Analyses [online]. Edition 4.0 Published by Norsk Hydro, Statoil, GeolabNor, SINTEF Petroleum Research and the Norwegian Petroleum Directorate, 102 (Available online http://www.npd.no/engelsk/nigoga/default.htm) [Accessed 10 May2014].

Ziegler, P.A. 1990. Tectonic and palaeogeographic development of the North Sea rift system. In: Blundell, D.J. and Gibbs, A.D, ed., Tectonic Evolution of the North Sea Rifts. Oxford University Press, New York, pp.1-36.

Chapter 5: Pyrolysis, Porosity and Productivity in Unconventional Mudstone Reservoirs: 'Free' and 'Adsorbed' Oil

This chapter is based on a paper published in the Proceedings of the Unconventional Resources Technology Conference held in San Antonio, Texas, USA, 20-22 July 2015. Raji, M., Gröcke, D. R., Greenwell, C. H., and Cornford, C., 2015. Pyrolysis, Porosity and Productivity in Unconventional Mudstone Reservoirs: 'Free' and 'Adsorbed' Oil. Proceedings of the Unconventional Resources Technology Conference held in San Antonio, Texas, USA, 20-22 July 2015.

This paper uses a large accessible public geochemical database of rock properties from the UK and Norwegian sectors of the South Viking Graben to investigate where the 'retained oil' is located at peak oil maturity for unconventional hydrocarbon potential in the Viking Graben area. The geochemical database comprises of total organic carbon (mainly from the LECO method), Rock-Eval pyrolysis (from Rock-Eval II and VI over the years) and solvent extract yields and fractions.

5.1: Abstract

Rock-Eval pyrolysis analysis of unconventional mudstone reservoirs uses the S_1 peak (kg free liquid per tonne of rock) to determine the volume of oil that can be potentially produced by hydraulic fracking. The data presented in this paper were obtained from a study of the unconventional oil potential of the marine Upper Jurassic Kimmeridge Clay Formation of the southern Viking Graben area of the UK and Norwegian sectors of the North Sea. Typical marine silty mudstones with > 2 wt.%TOC contains < 1 kg/t (0.1 wt. %) of free oil when immature at depths < 2.5 km and T_{max} < 420 °C. The peak saturation of free oil rises to values of 12 kg/t, with a typical peak average of ~6 kg free oil/tonne of rock (0.6 wt.%). Such average values are reached when mature at depths of 3.4km and T_{max} values of 435 °C in the North Sea. Converting Rock-Eval S_1 yields to volume percent, the average mature mudstone contains about 1.8 vol% of 'Free oil'. How does this compare with the accessible porosity of the mudstone?

Conventional log analysis for porosity measures everything that is not mineral grains as pore space, but fluid injection methods (mercury, helium) measure the effective porosity, a more realistic measure of open pores that are available to petroleum. In the case of log-derived porosities, closed porosity and structured (fixed) water are counted, but appear not to be open to Rock-Eval free oil (S_1) and hence for 'saturation'. Comparing typical peak S_1 volumes (1.8 vol. %) against mudstones porosities (1.62 vol. %), suggests, within error, that the open porosity is fully saturated with oil at peak maturity. Also, the distributions of porosity and S_1 yields are similar.

However, if the S_1 yield at peak maturity is totally a function of porosity; the S_1 yield should be independent of the amount or type of kerogen. This is not so. Plotting S_1 yield against TOC shows a strong positive correlation, with a gradient of 0.7 kg/t per 1 wt. %TOC and an intercept of about 1 wt.%TOC. This gradient indicates that the S_1 'oil' is partitioned between the kerogen and the porosity. Given the size of the molecules relative to the micro-porosity of the largely amorphous kerogen, the oil is likely to be absorbed onto the kerogen surface. This explains the asymmetry (or shoulders) seen on the pyrograms of S_1 peaks, the main peak representing easily liberated liquids in open porosity and the shoulder the more strongly adsorbed liquids. The additional adsorbed liquid is more efficiently recovered and can be quantified by solvent extraction of the mudstones, where saturates + aromatics are shown to be over twice the Rock-Eval S_1 yield. Thus, like Unconventional gas, this evidence suggests that Unconventional liquids too may be derive from 'free' and 'adsorbed oil' and that both are mainly stored within organic (kerogen) porosity.

5.2: Introduction

During the investigation of the commerciality of extracting unconventional offshore oil from the Upper Jurassic Kimmeridge Clay Formation (KCF) of the North Sea (Cornford et al., 2014; Raji et.al, 2015), a large database of rock properties was assembled. This paper uses this database to investigate where the retained oil is located within these actively generating oil-prone source rocks. A key aspect of potentially exploiting these mid-graben source rocks is that the basin continues to

subside to the present day, and hence wells are drilled into actively generating source rocks.

5.3: Database

The project database mainly comprises publicly accessible data for the UK and Norwegian sectors of the South Viking Graben, mainly from UK Quadrant 16 and Norwegian Quadrants 15, 16 and 17 (Figure 5-1). These wells all penetrated the late Jurassic – earliest Cretaceous organic-rich 'Hot shale' mudstones, termed the Kimmeridge Clay Formation (KCF) in the UK and the Draupne Formation in Norwegian waters. Together with the underlying Oxfordian mudstones, these units comprise the Viking Group, into which course clastic fans were injected mainly from the western boundary fault during the Oxfordian-Kimmeridgian. These fan sands form the reservoir of the main Brae group of fields and are termed the Brae Member of the KCF.

The majority of the database has been assembled from well geochemical reports available from the Norwegian Petroleum Directorate (NPD) website. Additional data have been taken from published literature and industry sources.

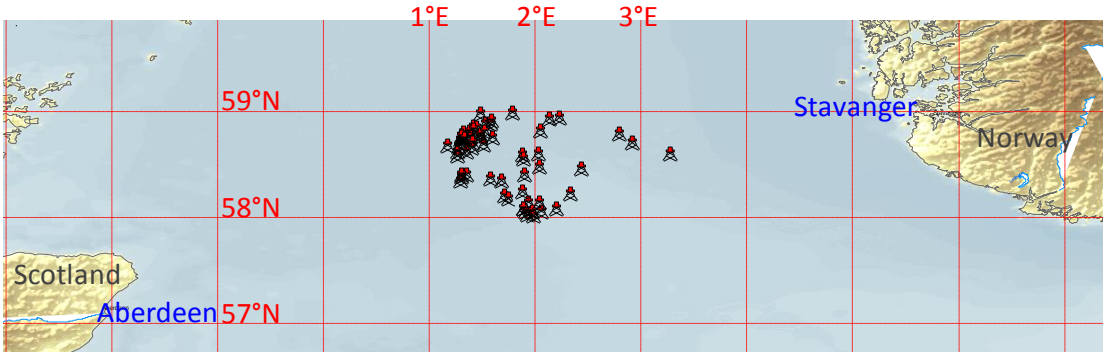

Figure 5-1: Location of the sampled well across the UK and Norwegian blocks of the South Viking Graben.

5.4: Data Analyses

The analyses used for this study are total organic carbon (TOC wt. %, mainly from the LECO method), Rock-Eval pyrolysis (from Rock-Eval II and VI over the years), and solvent extract yields and fractions. The basics of the Rock-Eval technique is shown in

Figure 5-2 where the primary data comprise S_1 (kg free oil/tonne rock), S_2 (kg pyrolysate oil/tonne rock) and (sometimes) S_3 (kg CO_2/tonne rock). T_{max} is an estimated temperature for maximum S_2 yield, reflecting the lab temperature required to create additional pyrolysate given the natural temperature (maturation) experienced by the sample during burial (Figure 5-2, inset). Derivative ratios comprise the Hydrogen index (HI = S_2/TOC, mg/gTOC), the Oxygen Index (OI = S_3/TOC, mgCO_2/gTOC) and the Production Index (PI = S_1/ (S_1+S_2)).

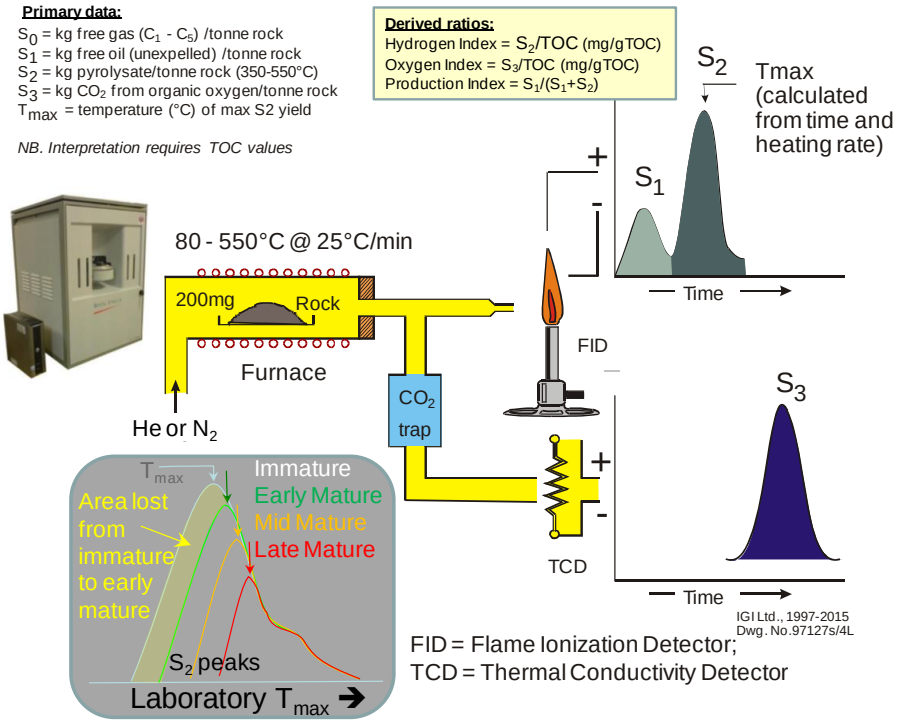

Figure 5-2: Schematics of the Rock-Eval apparatus and the primary and derived parameters. Inset (bottom left) shows the changes in the S_2 peaks with maturity leading to changes in T_{max} as a maturity parameter (From Cornford et al., 2014).

In such a large database, it is inevitable that the analyses were undertaken by many different laboratories using similar but not identical apparatus, and even from the same lab with different apparatus and procedures through time. This analytical 'noise' in the data is considered acceptable.

Visual estimates of the sand content of a sub-set of core samples were made with the naked eye (thicker sand interbeds) or with a low power binocular microscope where thin beds, ripples or sandy wisps were encountered.

5.5: Results

Taking the Viking Group with TOC values in the 0-12 % range, 620 samples derived from 65 Norwegian and UK wells. Of these, 552 samples also had basic Rock-Eval data (S_1, S_2, HI, PI, T_{max}), and only 445 samples reported S_3 and hence Oxygen Index ratios. No samples reported S0, the free gas peak. Solvent extraction yields data are available for 106 Viking Group samples with 94 samples reporting a Saturate/Aromatic ratio, and 83 samples a carbon-normalised extract (CNE) value (mgExtract/gTOC).

Detailed analyses of lithology (sand/shale ratios), helium porosity and light oil permeability were carried out on 34 samples from 6 wells in UK Quadrant 16. The initial expectation was that the S_1 yields (kg 'free oil'/tonne rock) would; (a) increase with visual estimates of sand content in the sample, (b) increase with sample depth (and hence T_{max}) as S_2 pyrolysate yields decrease, (c) be essentially similar to extract yields, and (d) be independent of TOC once a threshold value (e.g. 2 wt.% TOC) has been reached. However, the data fail to support these expectations.

Plotting 115 samples from 24 wells show no clear correlation with the visual estimate of the sand content of the core samples (Figure 5-3). For the cores with few or no visible sand layers, the S_1 yields range widely from 0.5-30 kg free oil/tonne rock, while with higher sand contents the S_1 yields converge on 1-4 kg/tonne. A cluster of higher maturity samples (coloured red) show low S_1 values even for 0 % sands. The two high values in 100 % sand samples correlate with oil staining and not indigenous kerogen-derived S_1 yields.

The expected trend of increase in S_1 yield with increasing sample depth is confirmed but less so than with increasing T_{max} (Figure 5-4). The increase in Production Index (PI) with falling S_1 and S_2 appears to be more controlled by a decrease in S_2 than any increase in S_1 (Figure 5-4). The lack of low PI values below 4,250 m (= 440 T_{max}) is as significant and argues for the re-naming of the Production Index (S_1/ [S_1+S_2]) as the Retention Index (Figure 5-4).

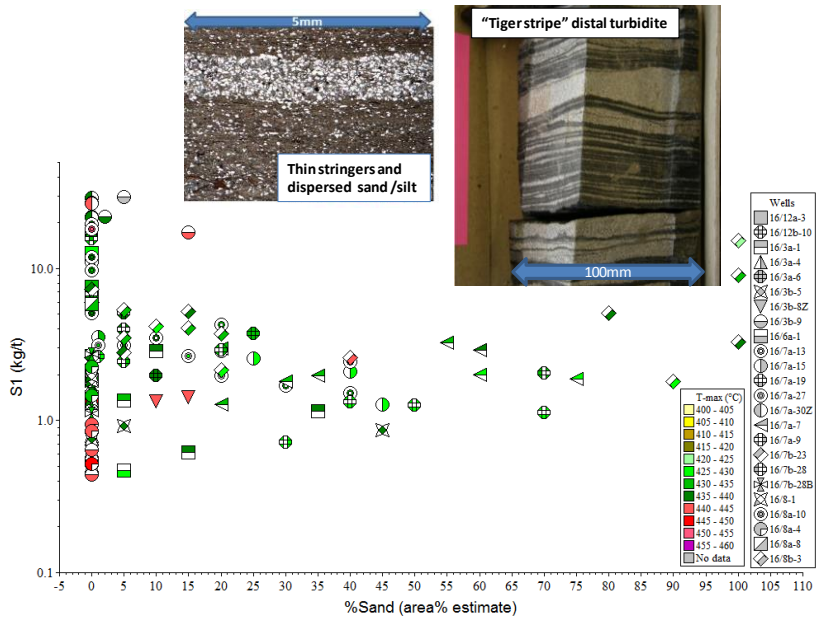

Figure 5-3: Lack of correlation between Rock-Eval S_1 yields from 115 samples from 24 South Viking Graben wells with the visual estimate of the sand content of the core samples.

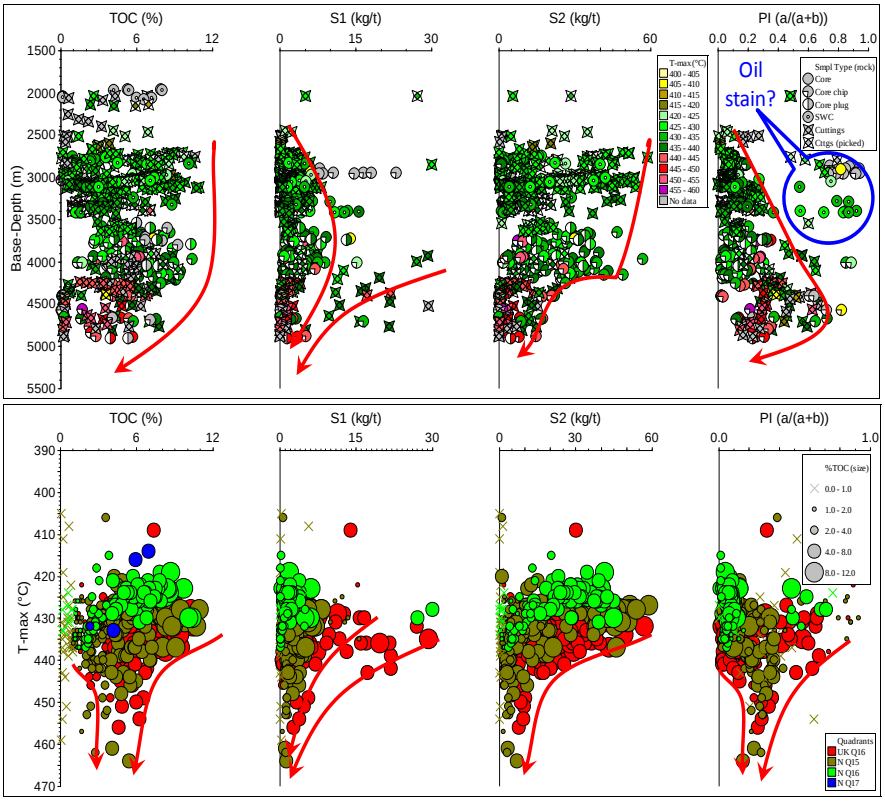

Figure 5-4: Maturity trends for TOC (wt. %) plus Rock-Eval S_1, S_2 and Production Index using depth (upper) using T_{max} (lower) as proxies for generation. (Note: red line used for showing sample trends)

The relationship of the solvent extract yield with the thermal extract yield (i.e. Rock-Eval S_1) is poor (Figure 5-5) showing the sum of the Saturates and Aromatics fractions yields (Sats+Aroms, kg/tonne) to be between 3 x and 10 x higher than the Rock-Eval S_1 yields. This suggests that while 'thermal extraction' to about T_{max} = 350 °C releases the 'free oil', the solvent extraction also removes adsorbed hydrocarbons, and possibly solvent swelling releases petroleum trapped in closed porosity.

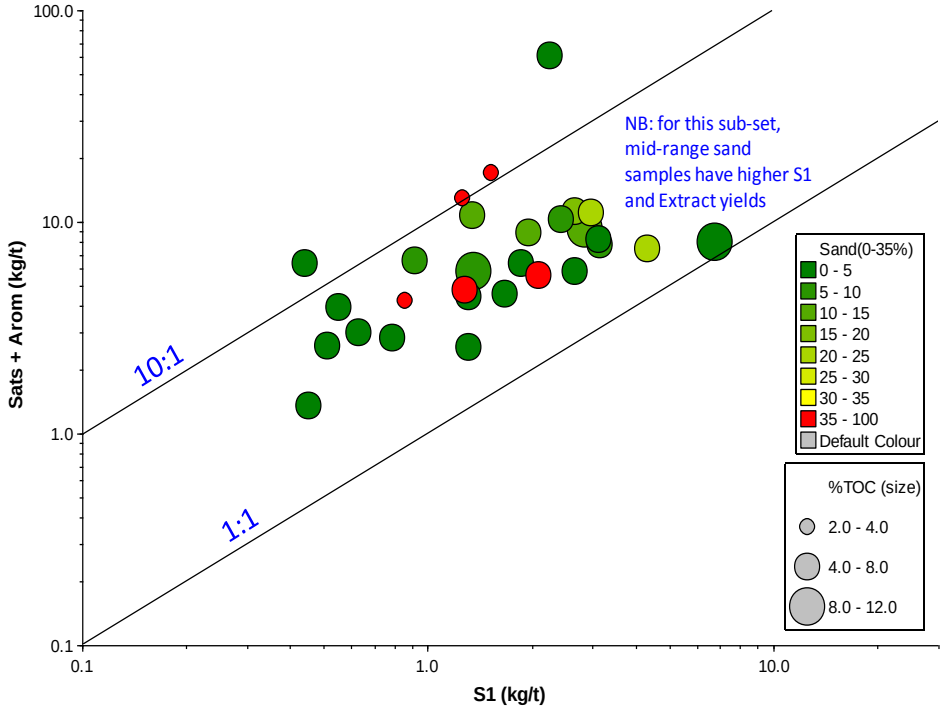

Figure 5-5: Relationship between solvent extract yields and thermal extract yields (i.e. Rock-Eval S_1) for Viking Group samples from wells in the South Viking Graben. (Note: standard surface intercept line automatically added in p:IGI-3 software).

A number of previous publications discussed the cross plot of Rock-Eval S_1 against TOC (Lopatin et al., 2003; Jarvie 2012; Abrams, 2014; Raji et.al., 2015). The relationship of S_1 with TOC is more revealing (Figure 5.6), where the majority of > 2 wt.%TOC samples (89.5 %) fall below the cross-over line of Generation Index = 100 (Jarvie, 2012) and are hence less likely to give high unconventional oil yields on fracking. A best-fit line through the main data cluster gives a gradient of 0.7 kg/t / 1 wt.%TOC (GI = 70). The very high S_1 yields with low TOC values (GI = ~900) formed a trend characteristic of staining by migrated oil.

Comparison with a much smaller database of solvent extract fractions (Saturates + Aromatics) drawn on the same axes (Figure 5-6, lower), shows a higher percentage of samples (51 %) falling above the GISA=100 line. For both the S_1 and the Sats+Aroms yield data, the UK Quadrant 16 samples are richer than the Norwegian samples. This may be simply because the UK samples are dominated by cores and the Norwegian database by cuttings.

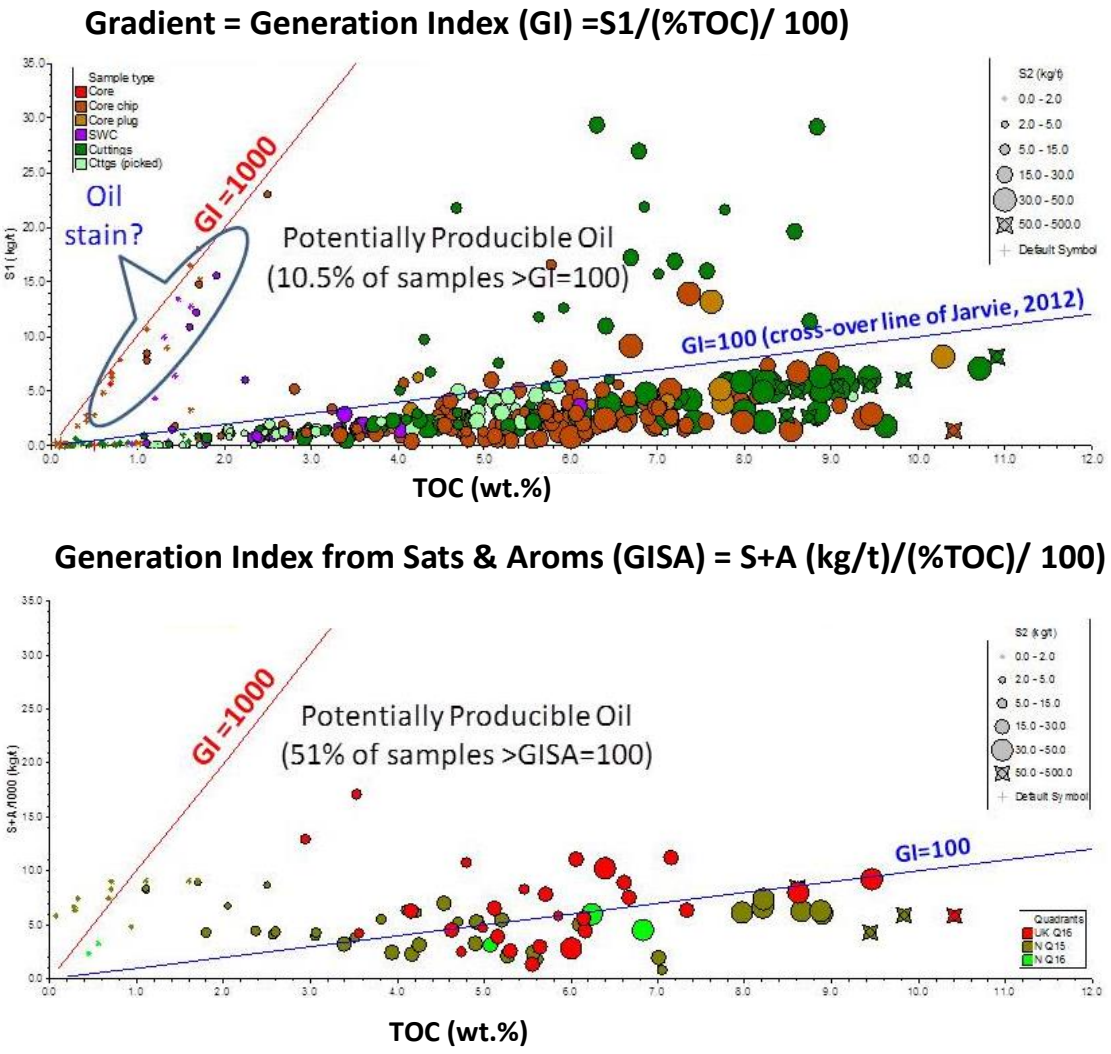

Figure 5-6: Generation index plots from Rock-Eval S_1 vs. TOC (upper) and extract Saturate + Aromatics fractions vs. TOC (lower), with Jarvie's (2012) cross-over line shown in blue.

5.6: Discussions

Rock-Eval pyrolysis analysis of unconventional mudstone reservoirs uses the S_1 peak (kg free liquid per tonne of rock) to determine the volume of oil that can be

potentially produced by hydraulic fracking of an appropriately mature organic-rich mudstone. In addition, solvent extracts also give a measure of free oil, though solvent evaporation removes the light oil components, typically $<C_{12}$ molecules. Our discussion is based on a subset of samples with > 2 wt.%TOC.

As indicated above, the initial expectation was that the S_1 yields (kg 'free oil'/tonne rock) would increase with maturity, i.e. sample depth (and hence T_{max}) as S_2 pyrolysate yields decrease. However, the data (Figure 5-4) show that both S_1 and S_2 decrease over the oil window (depth > 4 km, T_{max} > 430 °C), more coherently for the T_{max} trends then the depth trends. Thus the increase in the Production Index ($S_1/S_1 + S_2$) with maturity (depth or T_{max}) is, in fact, far from 'production' but is the result of the S_1 decreasing less than S_2.

Mass balance arguments indicate that the decrease in S_2 is a correct indication of 'generation', and the measured S_1 value is more an indication of 'retention' than 'production'. This suggests that the increase in S_1 is indicative of an increase in available 'storage' of 'free oil' (storage as defined for gas in the Barnett Shale by Jarvie et al., 2007).Hence its decrease is related to a loss of 'storage' (= collapsing porosity or decrease in the adsorptive surface area). A similar argument is put forward by Modica and Scott (2012) for the kerogens of the Mowry Shale of the Powder River Basin, where a maturity-related "intra-particle organic nanopore system" controls retained oil. These authors claimed that the conventional matrix or mineral porosity has little to do with hydrocarbon storage capacity in fine-grained, organic-rich source rocks.

This concept is quantified in Table 5-1, where S_1 and S_2 values (mean and standard deviation) average is calculated for 5 °C maturity steps of Rock-Eval $T_{max.}$ Then δS_1 and δS_2 are calculated as the increments in these yields for each T_{max} 5 °C (maturity) step, and the difference between the decrease in S_2 and the increase in S_1 is calculated as $\Delta\delta S_1\text{-}S_2$. Irregular decreasing positive values from T_{max} = 420 °C to T_{max} = 460 °C ($\Delta\delta S_1\text{-}S_2$ = 4.41 ➔ 0.11) indicate that the decrease in S_2 (= generation) is not balanced against a corresponding increase in S_1 (retention), and hence is indicating expulsion.

Based on a conventional porosity model, the threshold value of TOC (e.g. ~2 wt.% TOC) would be required to saturate the maturing source rock and initiate expulsion when in the main oil window. However, as shown in Figure 5-6 (upper), the strongest correlation of S_1 (free oil) is with the abundance of organic matter as measured by total organic carbon (TOC wt. %). This is also true of the extract yields (sats + aroms, Figure 5-6, lower), and points to the kerogen and not the mineral phase as containing the greatest liquid storage capacity for the Kimmeridge Clay mudstones of the South Viking Graben.

Table 5-1: Summary of Rock-Eval S_1 and S_2 yields for 5°C T_{max} intervals (410-465°C) based on 481 samples of the Viking Group shales of the Southern Viking Graben, North Sea. δS_1 and δS_2 are the difference between the mean values at T_{max} and T_{max} - 5°C, i.e. the increase or decrease in S_1 and S_2 at each 5°C step in T_{max}. N = number of samples per 5°C T_{max} interval.

T_{max}	S1 (kg/tonne)			S2 (kg/tonne)		N	δS1	δS2	ΔδS1-S2
	Mean	Max	SD	Mean	SD				
405-410	5.15	13.97	8.13	6.38	14.64	4			
410-415	0.15			0.14		1	-5.00	-6.24	1.24
415-420	1.00	1.90	0.88	27.39	12.91	4	0.85	27.25	-26.41
420-425	3.35	34.86	5.90	25.33	11.64	37	2.35	-2.06	4.41
425-430	3.56	32.03	4.70	23.34	14.46	134	0.21	-1.98	2.20
430-435	3.37	27.14	4.10	17.86	14.03	145	-0.19	-5.48	5.29
435-440	3.69	29.24	5.32	14.46	11.33	97	0.31	-3.40	3.72
440-445	2.78	21.83	4.38	8.91	7.15	36	-0.91	-5.55	4.65
445-450	2.36	5.58	1.56	6.08	3.16	10	-0.42	-2.82	2.40
450-455	2.16	4.73	1.59	5.36	3.45	8	-0.21	-0.72	0.52
455-460	1.55	2.63	1.53	4.64	4.18	2	-0.61	-0.72	0.11
460-465	1.17	1.30	0.16	4.44	2.17	3	-0.38	-0.19	-0.18

Plotting S_1 yield against TOC shows a strong positive correlation (for geology), with a gradient of 0.7 kg/t yield for every 1%TOC and an intercept of about 1%TOC for zero yields. Given the size of the molecules relative to the micro-porosity of the largely amorphous kerogen, the oil is likely to be partly absorbed onto the kerogen surface. The gradient indicates that the S_1 'free oil' is partitioned between the kerogen and the porosity.

It was expected that S_1 and extract yields (expressed as sats + aroms in mg/gRock) should be similar, with Rock-Eval S_1 expected to have lost light ends (say C1-C5 molecules) during sample handling, while solvent evaporation following extraction and fractionation typically loses all C1-C12 molecules. However, the data (Figure 5-5)

fail to support these expectations, with sats + aroms extract yields being consistently higher than S_1 yields. If storage is in mineral porosity both thermal and solvent extraction should give similar results. That solvent extraction liberates more 'oil' suggests the additional 'oil' occupies pores made more accessible by the presence of solvents. This effect is noted during solvent swelling of kerogens (Kelemen et al., 2006), with both swelling and retention decreasing with maturity through the oil window defined as %EasyRo = 0.75 – 1.00 (Wei et al., 2012). Both thermal and solvent extraction supports the concept that kerogen porosity dominates the storage capacity of these shales.

At onset, it was assumed that matrix (mineral or inter-granular) porosity controls storage and that the abundance of S_1 will be related to sand content in the South Viking Graben samples. The data (Figure 5-3) do not support this assumption. For these data there is a little correlation of sand content with Rock-Eval S_1 yields, with a wide spread of yields for pure mudstones (> 95 % mudstone), falling to S_1 values in the 1-3 kg/tonne range for samples with > 40 % sandstone. For the pure mudstones, the higher S_1 values derive from cuttings (which may be contaminated), while the cores consistently return lower yields. It is thus concluded that storage has little to do with sand in general and inter-granular porosity specifically.

Considering it is core and cuttings samples, typical marine silty mudstones contains < 1 kg/t (0.1 wt.%) of free oil when immature (depths < 2.5 km and T_{max} < 420 °C) while peak saturation of free oil rises to values of 12 kg/t (Figure 5-7). A typical peak average of ~6 kg free oil/tonne of rock (0.6 wt.%) is reached when mature at depths of 3.4 km and T_{max} values of 435 °C in the North Sea (Figure 5-4 and Figure 5-7).

When converted to volumes, i.e. multiply by (rock density/oil density), the mean mature pyrolysis yield contains about 1.8 vol.% of 'free oil'. In Figure 5-7 this free oil volume is compared with the porosity available to contain it. On this basis, an average Helium porosity of 1.62 % at 3.5-4.0 km (= available porosity) equates to an average mean S_1 at the same depth of 2.86 kg/tonne and hence 0.87 % by volume. This suggests that the S_1 yield occupies 0.87/1.62 ≈ 54 % of the available porosity at maximum retention. It is noted in Figure 5-7 that the maximum S_1 of 6 kg/tonne

equates to 1.8 vol% and is almost exactly the average porosity at this depth. Higher porosities are observed using logs and SEM (quantified using QEMscan mode) which cover the upper range of Helium porosities.

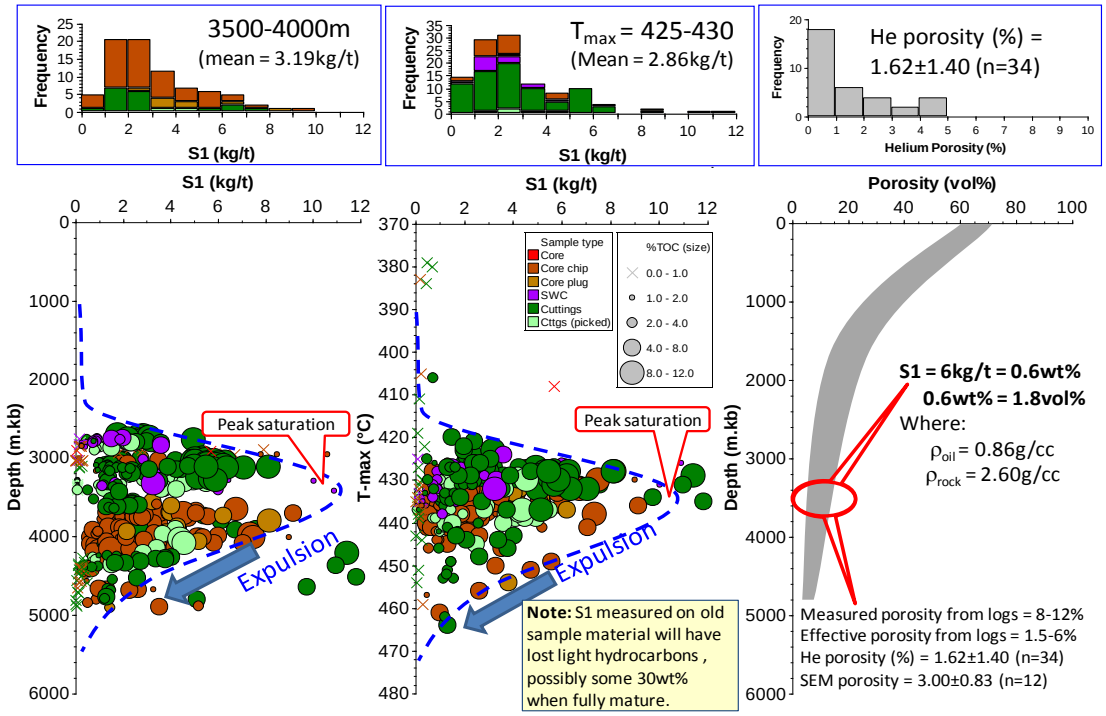

Figure 5-7: Maturity (depth and T_{max}) trends for Rock-Eval S_1 (bottom left and centre) and histograms (top row) of yields at peak retention (3,500 m- 4,000 m and T_{max} =425-430 °C respectively) compared with a generalised porosity-depth trend (bottom right) and a smaller porosity database for selected samples (top right).

Conventional log analysis for porosity measures everything that is not mineral grains as pore space, but fluid injection methods (mercury, helium) measure the effective porosity, a more realistic measure of the open pores that are available to petroleum. In the case of log-derived porosities, closed porosity and structured (fixed) water are counted, but appear not to be open to Rock-Eval free oil (S_1) and hence for 'saturation'. Comparing typical peak S_1 volumes (1.8 vol.%) against mudstones porosities (1.62 vol. %), suggests, within error, that the open porosity is fully saturated with oil at peak maturity. In addition, the distributions of porosity and S_1 yields are similar (Figure 5-7 top row). As discussed earlier, the S_1 storage and hence porosity appear to be within the kerogen (intra-kerogen porosity) rather than between the grains (inter-granular mineral porosity). Thus, like unconventional gas (Jarvie 2012; Abrams, 2014), this evidence suggests that unconventional liquids too may derive

mainly from kerogen porosity/surface area and hence from both 'free oil' and 'adsorbed oil'. Mapping these two unconventional oil 'habitats' arguably allows an improved identification of 'sweet spot' targets for optimum liquids production.

5.7: Conclusions

The data presented in this paper reports the characterization of typical organic-rich "Hot shale" mudstone with interbedded tiger stripe clastic sandstones from the South Viking Graben area of UK Quadrant 16 and Norway Quadrant 15, 16 and 17. These data suggest that Upper Jurassic – earliest Cretaceous organic-rich 'hot shale' mudstones progressively increases in thermal maturation with depth. The relationship between; TOC, Rock-Eval S_1, T_{max} and helium porosity and the formation of organic porosity at peak oil maturity accounts for the observed oil storage in terms of Rock-Eval S_1 and solvent extract yields. The difference between thermal and solvent yields suggests that organic porosity is saturated with both free and adsorbed liquids. This study highlights the importance of Rock-Eval S_1 as a key factor to determine retention, and drainage of oil in the mudstone as well as expelled oil in the interbeds.

5.8: Acknowledgements

IGI would like to thank their database team lead by Michelle Dart for assembly and quality assurance of the databases used in this study. The authors would like to thank Trapoil and Two Fields Consulting (TFC) for supporting this research. HCG thanks the Royal Society for an Industry Fellowship. MR acknowledges receipt of part funding of Durham University Doctoral Scholarship (DDS).

5.9: References

Abrams, M.A. 2014. Petroleum System Charge Analysis for Liquid-Rich Unconventional Plays. Unconventional Resources Technology Conference Proceedings, August 25-27, 2014.

Cornford, C., Birdsong, B. and Groves-Gidney 2014. Offshore Unconventional Oil from the Kimmeridge Clay Formation of the North Sea: A Technical and Economic Case. Unconventional Resources Technology Conference Proceedings, August 25-27, 2014.

Jarvie, D.M., 2012. Shale Resource Systems for Oil and Gas: Part 2 - Shale-oil Resource Systems. American Association of Petroleum Geologist Memoir 97, pp.89-119.

Jarvie, D.M., Hill, R.J., Ruble, T.E., Pollastro, R.M., 2007. Unconventional shale-gas systems: The Mississippian Barnett Shale of north-central Texas as one model for thermogenic shale-gas assessment. American Association of Petroleum Geologist Bulletin 91, 475-499.

Lopatin, N.V., Zubairaev, S.L., Kos, I.M., Emets, T.P., Romanov, E.A. and Malchikhina, O.V., 2003. Unconventional Oil Accumulations in the Upper Jurassic Bazhenov Black Shale Formation, West Siberian Basin: A Self-Sourced Reservoir System. Journal of Petroleum Geology 26, pp.225-244.

Kelemen, S.R., Walters, C.C., Ertas, D., Kwiatek, L.M., Curry, D.J., 2006. Petroleum expulsion Part 2. Organic matter type and maturity effects on kerogen swelling by solvents and thermodynamic parameters for kerogen from Regular Solution Theory. Energy and Fuels 20, pp.301-308.

Modica, C.J., Lapierre, S.G., 2012. Estimation of kerogen porosity in source rocks as a function of thermal transformation: Example from the Mowry Shale in the Powder River Basin of Wyoming. American Association of Petroleum Geologist Bulletin 96, pp.87-108.

Norwegian Petroleum Directorate (NPD) (Available online: http://www.npd.no/en/ (Accessed 18.04, 2014)

Raji, M., Gröcke, D.R., Greenwell, C., Gluyas, J. and Cornford, C. 2015. The Effect of Interbedding on Shale Reservoirs Properties. Journal of Marine and Petroleum Geology

Wei, Z., Zou, Y.-R., Cai, Y., Wang, L., Luo, X., Peng, P.A., 2012. Kinetics of oil group-type generation and expulsion: An integrated application to Dongying Depression, Bohai Bay Basin, China. Organic Geochemistry 52, pp.1-12.

Chapter 6: The Nature of Porosity in Selected Mudstone-Sandstone Interbeds of the Upper Jurassic Kimmeridge Clay Formation, South Viking Graben, North Sea.

In this chapter, selected core samples from three wells from the South Viking Graben have been described visually and microscopically as well as analysed by X-ray Diffraction in order to study their lithological variation and mineralogy.

The geochemical analyses used to obtain information on quantity, type and maturity of organic matter in this study are total organic carbon (TOC wt. %) and programmed pyrolysis (Rock-Eval). The study in this chapter has major implications for identifying potential sweet-spot area (s) in terms of mineralogy and porosity from a reservoir evaluation perspective. This chapter emphasizes the fact that a better and improved understanding of type and distribution of porosity in Upper Jurassic Kimmeridge Clay Formation is required for optimal identification of sweet spot areas.

6.1: Abstract

Scanning electron microscope (SEM) and focused ion beam (FIB) analyses of core samples from the Upper Jurassic Kimmeridge Clay Formation were performed to evaluate the nature and type of porosity in these organic-rich mudstones. Three distinct types of porosity of varying shapes and sizes were observed across all samples: organic pores within the organic matter in organic-rich mudstone dominated samples with higher total organic carbon (TOC) content; interparticle pores between mineral grains and inter-crystalline pyrite; and intraparticle pores within the mineral grains in all samples. The dominant porosities in the Kimmeridge appear to be interparticle and intraparticle pores occurring mostly within and between mineral grains for sandstone-rich and clay-rich mudstone samples. The combination of these pores on the overall total porosity of hydrocarbon storage reservoirs can be significant and may contribute to the permeability and connectivity of hydrocarbon flow pathways in the Kimmeridge hybrid shale reservoir.

X-ray diffraction (XRD) and Energy Dispersive X-ray Spectroscopy (EDS) results suggest these samples are dominated by quartz, clay, organic matter, mica and pyrite. Kaolinite and illite/smectite are the dominant clay minerals identified in all samples. High silica content in the interface and the sandstone-rich samples confirms the brittleness in this mudstone-sandstone lithofacies, an important factor to be considered for fracture stimulation to successfully work in this hybrid system. The amount of organic matter, as measured by total organic carbon (TOC), is higher in the mudstone-dominated samples (5.25- 7.32 wt.% TOC) than in the sandstone dominated samples (1.1-1.72 wt.% TOC). The kerogen type in both the mudstones and sandstones is predominantly a classical Type II oil-prone (and associated gas) kerogen. Rock-Eval T_{max} values of 427 °C (early mature) to 439 °C (mid-mature) equate to the 3-4 km interval placing the samples in early-mid mature oil window of maturation for the sampled mudstones and sandstone interbeds. Rock-Eval S_1 (free oil) values recorded for the sandstone-dominated samples range from 1.32-2.77 mg/g, suggesting that that free oil (S_1) has migrated into the pores of sandy layers. Migration of generated oil from the mudstone into the interbedded sandstone involves a short vertical distance from the source to storage in the interbeds. However, the mudstones will still contain the retained oil within sub-nanometer micropores in the kerogen prior to, during and after expulsion, and the sandstone will absorb the expelled free oil (S_1).

6.2: Introduction

The Kimmeridge Clay Formation is a sequence of organic-rich black-grey mudstones interbedded with clastic sandstone source rock deposited in a deep restricted basin and along the active western margin faults of the South Viking Graben area during the Upper Jurassic to early Cretaceous (Cornford and Brookes, 1989; Partington et al., 1993; Gautier, 2005). The Kimmeridge mudstones in the graben centre are considered to be a mature source rock for both oil and gas (Barnard and Cooper, 1981; Barnard et al., 1981; Goff, 1983; Cooper and Barnard, 1984; Cornford, 1984, 1998) based on measured maturity parameters such as vitrinite reflectance and Rock-Eval T_{max} (Cornford et al., 2014; Raji et al., 2015); thermal modelling (Schlakker et al., 2012); direct measurement of oil generation within the source rock from solvent extraction

and Rock-Eval S_1 yields (Schaefer et al., 1990) and oil/source rock correlations from molecular maturity parameters (Cornford et al., 1983). When the oil is generated within these organic-rich mudstones some of the generated oil is then expelled and ultimately migrates into juxtaposed clastic non-source sandstone lithofacies (Jarvie et al., 2007; Cornford et al., 2014; Raji et al., 2015). However, following expulsion and migration into the interbedded sandstone, the source rock still contains retained oil, that is not yet expelled. These organic-rich source rocks with intimately interbedded sandstones are termed the "Hybrid Shale System" (Jarvie et al., 2007; Cornford et al., 2014). This hybrid shale reservoir can contain a greater volume of oil because of the increased storage capacity due to larger matrix porosities of the sand-silt interbeds, together with a lower adsorptive affinity in the interbedded sandstone (this is discussed in more detail in Chapter 4). The previous study in Chapter 4 shows that this hybrid shale system can contain a greater volume of expelled as well as retained oil and thus forms a potential target for unconventional shale oil in the North Sea area (Raji et al., 2015).

The study in this chapter was undertaken to understand the type, nature and distribution of porosity in this hybrid shale reservoir. The main objective of this study is to systematically classify the distribution and types of porosities of organic-rich Kimmeridge Clay Formation mudstone and sandstone interbeds at different levels of organic-richness and maturity. Previous work has been carried out by several authors on the identification and classifications of the different types of pores in mudstone in shale reservoirs (e.g. Davies et al., 1991; Loucks et al., 2009, 2010; Passey et al., 2010; Schieber, 2010; Curtis et al., 2010, 2012; Heath et al., 2011; Bernard et al., 2012 Klaver et al., 2015; Robinet et al., 2015; Bertier et al., 2016; Schurig et al., 2016; Lanzirotti et al., 2016; Desbois et al., 2016; Kaufhold et al., 2016; Welch et al., 2016; Marschall et al., 2016; Aplin and Moore, 2016). These authors classified the types of porosity in fine-grained mudstone into three different categories based on their relationship to the mineral matrixes and organic matter: (1) organic porosity occurred within the organic matter (OM); (2) inter-particle porosity occurred between the sand and mineral grains and; (3) the intra-particle porosity occurred within the grains and the organic matter

(Kwon et al., 2004; Desbois et al., 2009; Fishman et al., 2012; Loucks et al., 2009, 2010; Curtis et al., 2010; Milliken and Reed, 2010; Lu et al., 2011).

In the work presented in this Chapter, scanning electron microscope (SEM) combined with focused ion beam (FIB) milling have been employed to assess the nature of the porosity in the organic matter (kerogen), mineral matrixes and at the interface between mudstone-rich and sandstone-rich samples of the Kimmeridge. Conceptually, as interbeds become finer, the properties of the reservoir would reflect the dominant/hybrid phase. This study focused on six drill core samples from wells that penetrated the Kimmeridge Clay Formation in the South Viking Graben area of the North Sea. Emphasis was placed on samples representing a range of lithologies exhibiting variable levels of richness of organic matter and thermal maturity. The analysed samples presented in this chapter are from three different wells that have been previously studied for effects of sand interbeds on shale reservoir properties (in Chapter 4), where organic-richness, kerogen types and maturity were determined before this study.

6.3: Sampling

For this study, six drilled cores from Wells 16/17-14, 16/17-19 and 16/18-2 drilled between 1984- 1991 in the South Viking Graben area were sampled and collected using an idealised stratigraphic column of sand-mudstone, mudstone and sandstone ratio (the stratigraphic column is described in Chapter 4, Section 4.3.1) from the British Geological Survey (BGS) core store in Keyworth, Nottingham. The first two wells lie on the western margin of the graben along the Tiffany-Toni-Thelma field trend, and the latter (16/18-2) is in the trough axis to the east near the UK-Norwegian boundary (Figure 6-1).

The samples were selected based on the visual inspection of slabbed cores and estimates of percentage of mudstone and sandstones at different intervals from each well (Figure 6-2). In terms of depth (metres sub-Kelly Bushing), the cores from the 16/17-19 well are the shallowest (3,552-82 m),the cores from the other two wells are substantially deeper with the 16/18-2 having a short cored interval of 4,126.5-28.7 m and 16/17-14 at 4,193.7 - 4,211.9 m.

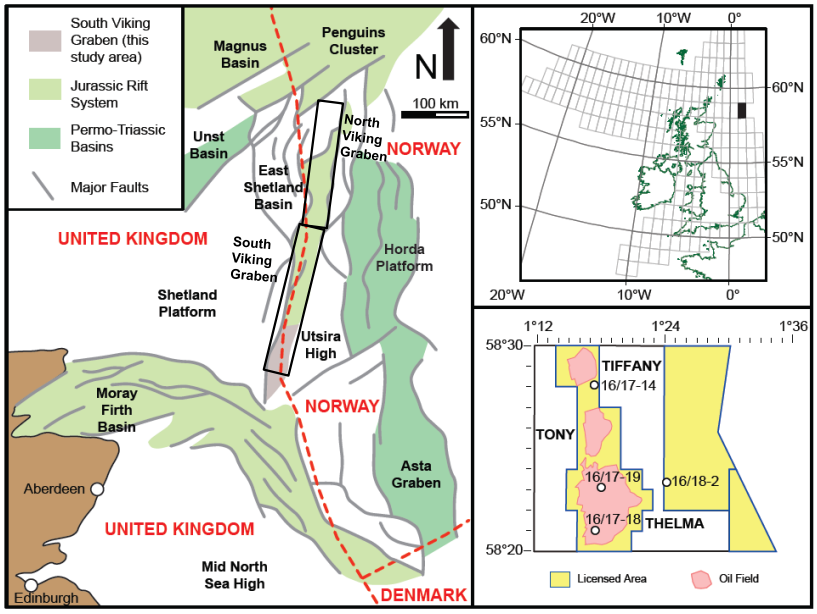

Figure 6-1: Structural elements of the North Sea showing the structural framework of the Viking Graben (modified from Dominguez, 2007) with inset of UK Quadrant 16 showing the location of wells studied (modified from DECC, 2013).

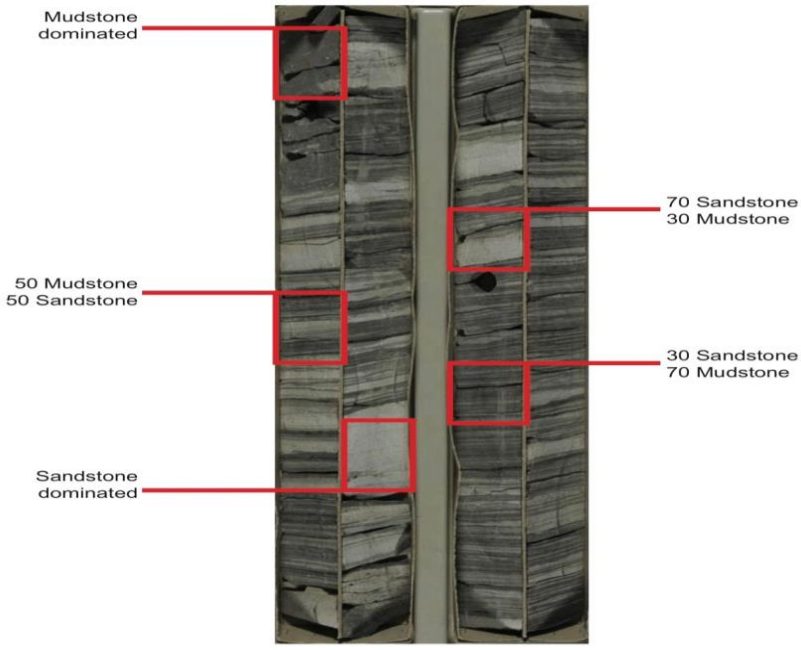

Figure 6-2: Core slab of idealized stratigraphic sampling of sand-mudstone, mudstone and sandstone ratio collected from the BGS core store in Nottingham.

The units sampled consist of mudstone sequences with interbedded sandstone and as they represent the upper part of the sequence (Upper hot shale and tiger stripe) they are considered to be Volgian to Ryazanian in age (Goff, 1983; Cooper and Barnard,

1984; Cornford, 1984, 1998). These samples were selected using the percentage of mudstone and sandstone initially estimated visually from full cores and core plugs and subsequently substantiated via observation of thin sections under an optical microscope. These six subsamples were chosen to represent a range of; mudstone-dominated, sandstone-dominated, 50/50 sandstone/mudstone and the interfaces between mudstone and sandstone samples throughout the Kimmeridge Clay Formation.

6.4: Analytical Methods

Total organic carbon (TOC), Rock-Eval pyrolysis and X-ray diffraction analyses were performed on the selected samples for organic matter quality, kerogen type, thermal maturity, hydrocarbon potential and mineral composition. To investigate the nature, types and distribution of porosity in the samples and the interface between sand and shale of the Kimmeridge Clay Formation; SEM-FIB milling and energy dispersive X-ray spectroscopy (EDS) microanalysis was undertaken on selected subsamples of the suite previously analysed by XRD, TOC and Rock-Eval pyrolysis in Chapter 4.

6.4.1: TOC, Rock-Eval Pyrolysis, Thin-Section and X-ray Diffraction (XRD) Analyses

The total organic carbon (TOC) quantity, Rock-Eval pyrolysis and XRD results for this Chapter are taken from the results of the analyses performed on 18 Kimmeridge Clay Formation samples in Chapter 4. Background to methods for the analytical procedures used for this chapter are described in more details in Chapter 2, Section 2.4.5-2.6.3 and in Chapter 4, Section 4. 3- 4.3.4.

6.4.2: Scanning Electron Microscope (SEM) and Focused Ion Beam (FIB) Milling

Standard petrography thin-sections were polished to approximately 20 μm in thickness for all the samples. These polished thin sections were carbon-coated using a Cressington 108 carbon/A to a coating thickness of about 20 nm-25 nm. These thin sections were first examined using a Hitachi SU-70 high-resolution analytical SEM with a Schottky field emission gun (FEG), equipped with an Oxford Instruments

energy dispersive X-ray (EDX) and microanalysis system (INCA Energy 700). The SEM has a secondary electron (SE) detector which utilises the low energy (50 eV) electrons emitted from the sample when bombarded with a high-voltage electron beam (20 kV). The SE images give information about surface topography, grain edges and pore structures. The SEM also has a backscattered electron (BSE) detector which uses high energy beam electrons which are scattered back from the surface of the sample. The number of electrons backscattered depends on the sample composition reflecting its atomic number; this gives information on the mineral composition, grain distribution, size, roundness and the sphericity of the individual grains within the samples.

Focused ion beam (FIB) milling with SEM was carried using an FEI Helios Nanolab G3 DualBeam™ system at University of Durham, GJ Russell Microscopy Facility in the Physics Department. The FIB imaging system uses positively charged Ga^+ ions instead of negatively charged electrons similar to the SEM. In the FEI Helios Nanolab G3 DualBeam™ system, the electron column is at 0 ° for imaging, and the ion column is at 52 °. The technique involves sputtering platinum (2 to 3 μm thick) at both 0 ° and 52 ° to protect the site of interest. The Ga^+ ion beam was then used at a high voltage, and current source operated at 30 kV, 9.3 nA to mill a trench 25 μm × 18 μm x 18 μm to image a 10 μm x 10 μm image. Each milling step used a 50 % focus, and the sample is tilted to 0 ° to mill the site of interest. Electron images were collected every 1 μm slice through an area of interest 10 μm

6.4.3: Energy Dispersive X-ray Spectroscopy (EDS)

Energy dispersive X-ray spectroscopy (EDS) microanalysis was conducted on SEM samples using an Oxford Instruments X-MaxN silicon drift detector (SDD) to give qualitative and semi-quantitative elemental composition of each sample. This technique uses a high energy electron beam which impinges on to the sample surface causing two types of x-rays to be generated. Each atom has unique energy levels which occur in electron transfer leading to the wavelengths of the X-rays emitted from a distinct length to be able to characterise each atom. These X-rays are collected

by a detector and turned into an electronic signal, and the X-ray counts at a given energy allow quantification of the elemental composition (Goldstein et al., 2003).

6.5: Results and Discussion

Geochemical analyses were carried out to determine the source rock potential, kerogen-type, maturity and retained hydrocarbon yield. Results from TOC, Rock-Eval and XRD analyses are discussed in more detail in Chapter 4, Section 4.4. The lithology and composition of the sandstone-mudstone mineralogy were derived from petrographic thin sections, X-ray diffraction (XRD) and visual core descriptions. Nature and type of porosity distribution was investigated with focused ion beam (FIB) milling with SEM equipped with an Oxford Instruments energy dispersive X-ray (EDX) and microanalysis system.

6.5.1: Organic Matter and Thermal Maturation

TOC and Rock-Eval pyrolysis analyses for these samples were obtained from the previous study undertaken in Chapter 4 and the results for the six selected samples are given in the table (Table 6-1). In terms of organic-richness, the samples containing a high proportion of mudstone (70 % or more of mudstone) have a TOC content range of 5.25- 7.23 wt.%, and samples with a high proportion of sandstone have a TOC content range of 1.1-1.72 wt.% (Table 6-1). As expected, these values suggest that the mudstones contain higher amounts of organic matter in contrast to the dominant sandstone samples. The Hydrogen Index vs. T_{max} (HIT) plot shows the kerogen type to be a typical Type II based on maturity trends (Figure 6-3). Rock-Eval T_{max} values were used as a thermal maturity indicator; these values range from 427 °C (late immature-early mature) to 439 °C (mid-mature) with an average of 434 °C (Table 6-1). Burial history modelling of the South Viking Graben area calibrated against measured parameters, suggests a burial depth deeper than 3,200 m below sea bed for maturity and generation (Cornford, 1998), this is consistent with the maturity results from the previous study in Chapter 4 and this Chapter.

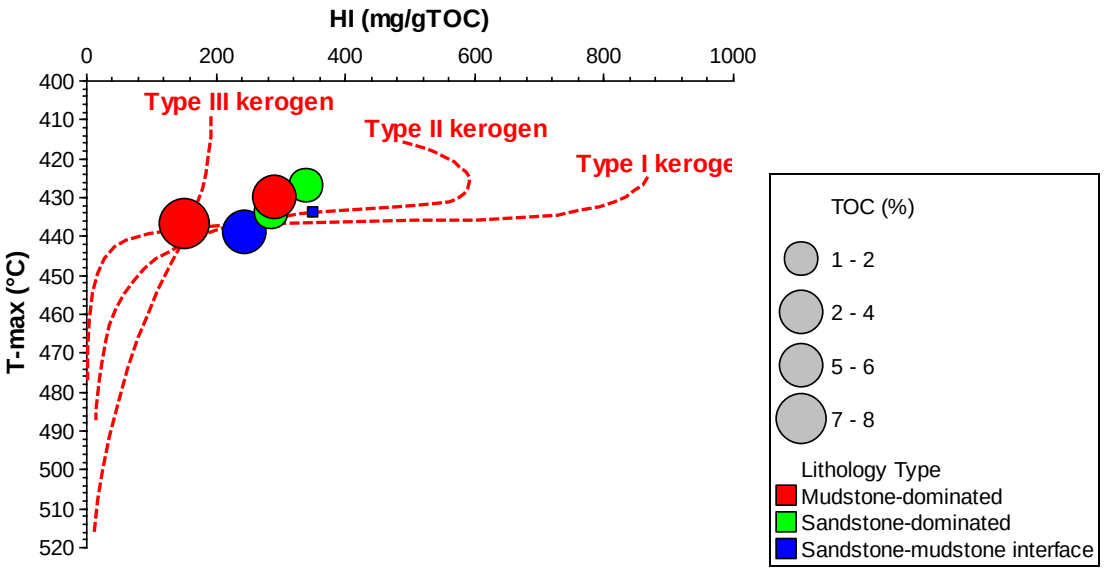

Figure 6-3: Kerogen type and maturity from Rock-Eval pyrolysis: the Hydrogen Index vs T_{max} (HIT) plot. (Note: the kinetically defined maturity pathways are after equations by Banerjee et al (2004) in automatically added in p: IGI-3 software).

To make literature comparisons, the T_{max} values were converted to vitrinite reflectance (R_o), using Jarvie's equation: $R_o = (T_{max} \times 0.018) - 7.16$ (Jarvie, 2001; Peters et al., 2005). The converted T_{max} -based Ro values range from 0.52- 0.742 % R_o with an average of 0.65 % R_o suggesting that the majority of the samples are in the early- mid-mature oil window (Table 6-1). Rock-Eval S_1 is used to measure the quantity of free oil in mg 'oil' /g of source rock in the sampled cores. For the sample set, the sandstone-dominated samples have lower S_1 (free oil) values (1.32-2.77 mg/g) than the mudstone-rich samples with S_1 values of 3.99-5.42 mg/g (Table 6-1), suggesting that organic-rich mudstone has a higher adsorptive affinity for S_1 oil compare to the sandstone lithofacies. The TOC and Rock Eval results (Table 6-1) in this Chapter are consistent with the regional organic-richness and maturity trend of the Kimmeridge Clay Formation throughout the UK (Cornford and Brookes, 1989; Partington et al., 1993; Gautier, 2005; Barnard and Cooper, 1981; Barnard et al., 1981; Goff, 1983; Cooper and Barnard, 1984; Cornford, 1984, 1998), and in the other studies of this thesis (discussed in details in Chapters 3, 4, 5 and 7).

Table 6-1: TOC and Rock-Eval Pyrolysis data for 6 core plug samples from the Kimmeridge Clay Formation of the Southern Viking Graben, UK North Sea.

Well	Sample ID	Top-depth (m)	TOC (wt. %)	S_1 (mg/g)	S_2 (mg/g)	S_3 (mg/g)	T_{max} (°C)	PP	PI ((SI/Si+S_2))/2)	HI (mg/gTOC)	OI (mg/gTOC)	%R_o	Mudstone (area %)	Sand (area %)
16/17-14	SSK47813	4211.7	2.32	1.86	5.69	0.1	439	7.55	0.25	245	4	0.742	50	50
16/17-14	SSK47814	4193.6	1.1	2.7	3.74	0.18	427	6.44	0.42	340	16	0.526	10	90
16/17-14	SSK47815	4194.7	7.32	5.42	11.1	0.25	437	16.52	0.33	152	3	0.706	90	10
16/18- 2	SSK47858	4126.2	6.38	1.54	22.46	0.2	434	24	0.06	352	3	0.652	50	50
16/18- 2	SSK47860	4127.4	1.72	1.32	4.92	0.12	434	6.24	0.21	286	7	0.652	10	90
16/17-19	SSK47870	3564.1	5.25	3.99	15.3	0.4	430	19.29	0.21	291	8	0.58	70	30

6.5.2: Lithology and Mineralogy

The lithological variations of the Kimmeridge Clay Formation were determined by visual inspection of core slabs and microscopic examination of thin-section slides, mineral constituents were determined by X-ray diffraction. Observations from both visual and thin-sections examination suggest that–in general, mudstone-dominated lithologies are black-dark grey, silty, partly laminated and with gradational boundaries between the mudstone and the interbedded light-grey sandstone-(Figure 6-4A and Figure 6-4B). At this magnification it is clear that even the mudstone-rich samples contain mainly silt (2-63 μm) and there is not much clay-sized fraction (< 2 μm) obvious (Figure 6-4C).

The mudstone-dominated samples are tightly packed and appear to be poorly sorted, with little or no interconnectivity between grains. The sandstone-dominated lithologies are greyish-dark-brownish-whitish, silty, sandy, and moderate-poorly sorted; varying in grain sizes and shapes from rounded, angular to sub-angular grains and mostly tightly packed grains (Figure 6-4D and Figure 6-4E). The interbedded sandstones are fine-medium grained, dark-grey, sub-angular-sub-rounded, moderately sorted—and silty with high organic carbon content in the mixed sandstone/mudstones interface and lower organic carbon content in the purer sandstone facies (Figure 6-4E and Figure 6-4F). X-ray diffraction (XRD) results from previous studies (Section 4.4.1 in Chapter 4) and the present SEM studies suggest these samples are dominated by quartz, clay, K-feldspar, calcite, organic matter (OM), pyrite and titanium.

In general, a more intense XRD peak for quartz is observed in the sandstone dominated samples and in the interface, though fine quartz with clay is also a significant fraction of the mudstones. Kaolinite and illite/smectite are the dominant clay minerals identified in all the six samples. Kaolinite is a non-swelling clay and is able to absorb petroleum while illites are able to absorb pore water which increases the wettability of these samples (Arduini et al., 2009). However, smectite (swelling clay) hinders the flow of fluid in the pore space leading to low permeability and reduces the porosity in these samples (Kwon et al., 2004; Arduini et al., 2009). The clay

mineral appears to be silty, clayey and with compaction bending occurring around the grains in the mudstone dominated samples (Figure 6-5).

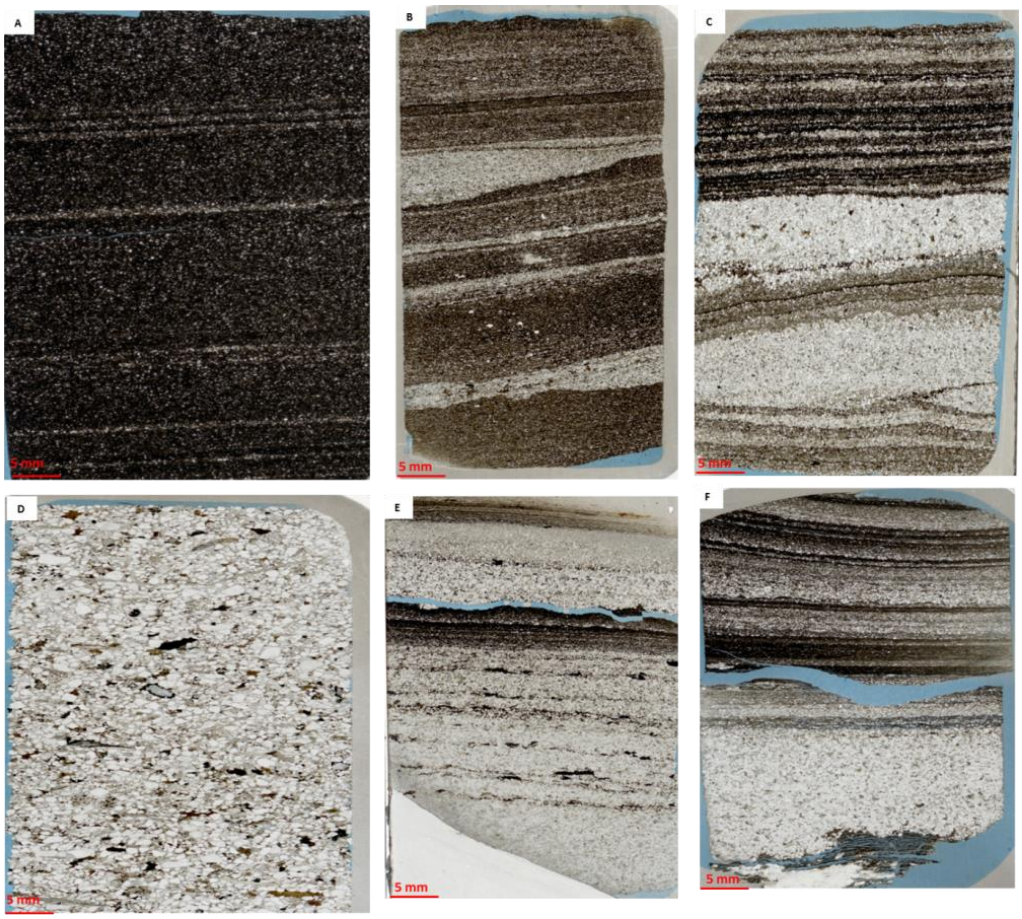

Figure 6-4: Thin-section photomicrographs of hybrid shale system displaying various mudstone-sandstone interbeds: (A) mudstone-dominated samples (SSK47815) from 4, 194.7 m (Well 16/17-14), the light-grey colour within the mudstone are thin siliceous sandstone layers, some are grain thick, TOC is 7.32 wt.% with maturity R_o value of 0.70 %; (B) 30/70 sandstone/mudstone fine-medium sandstone, dark-grey, sub-angular-sub-rounded, moderately sorted sample (SSK47870) from 3, 564.1 m (Well 16/17-19), TOC is 5.29 wt.% with maturity R_o value of 0.58 %; C) 50/50 sandstone/mudstone sample (SSK47813) with darker organic-rich layers from 4,211.7 m (Well 16/17-14), TOC is 2.32 wt. % with maturity R_o value of 0.74 %; (D) sandstone dominated sample (SSK47814) with visible shell fragments and woody (Type II kerogen) remnants from 4,193.6 m (Well 16/17-14), TOC is 1.1 wt.% with maturity R_o value of 0.52 %; (E) sandstone-dominated alternating with organic-rich mudstone layers (SSK47860), impregnated with blue-dyed resin showing breakage at the contact boundary between sandy and muddy layer (probably core disintegration during drilling and sampling) from 4,127.4 m (Well 16/18- 2), TOC is 1.72 wt. % with a maturity R_o value of 0.65 %; (F) 50/50 sandstone/mudstone interface sample (SSK47858) with darker organic-rich layers and desiccation fractures from 4,126.2 m (Well 16/18- 2), TOC is 6.38wt. % with maturity R_o value of 0.65 %.

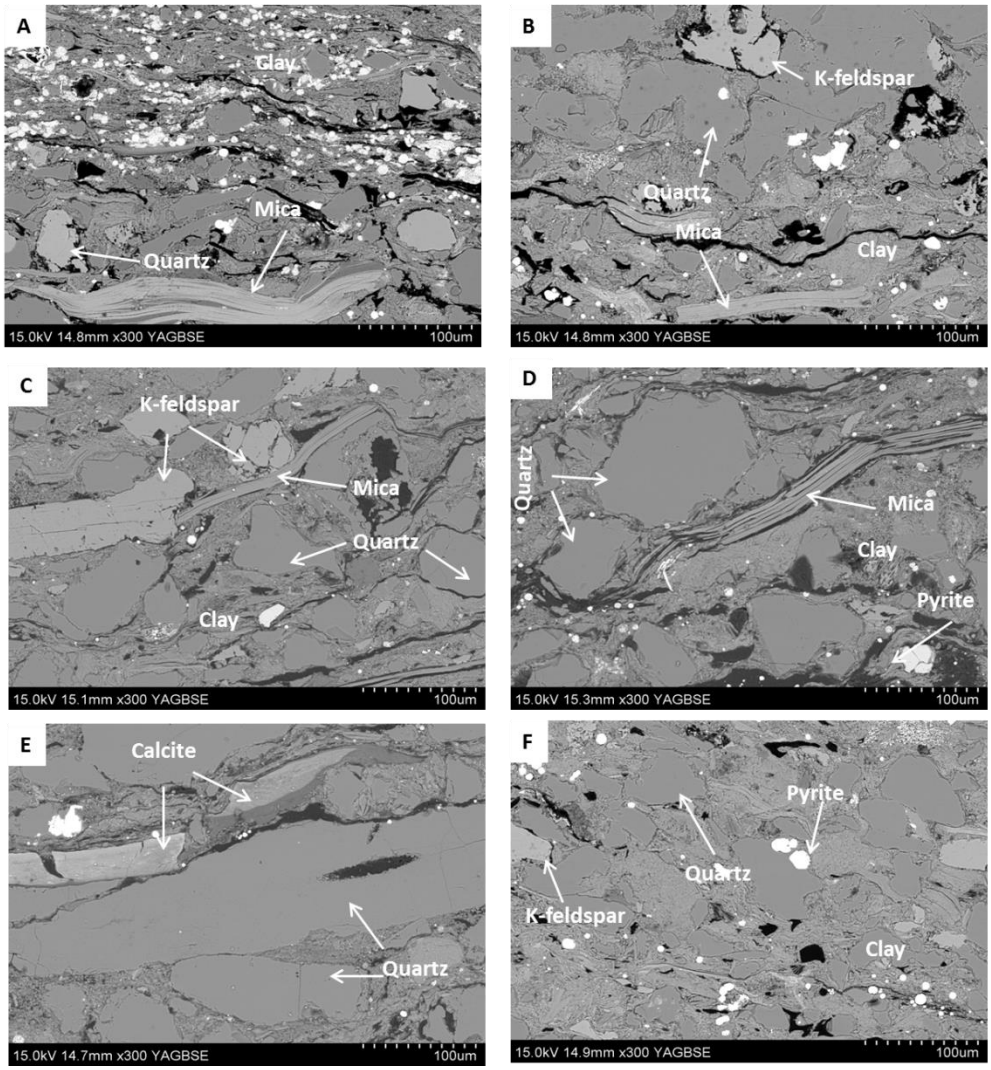

Figure 6-5: SEM back-scattered images of selected sites of interest to illustrate the nature of the mudstone dominated samples and the interfaces between mudstones-sandstone of Kimmeridge Clay Formation at 4, 193.6 m from Well 16/17-14 (A-C) and at 3, 564.1 from Well 16/17-19 (D-F). (A) mudstone-rich silt-grade clay particles, the rigid grains are predominantly quartz, with some K-feldspar and some mica and pyrite; (5B) tightly packed sandstone with quartz grains surrounding K-feldspar and clay mineral; (C) clay-rich mudstone with quartz and mica grain occurring between clay in mudstone-rich sample; (D) mudstone-rich sample showing poorly sorted and fractured quartz grain with clay-rich matrix and pyrite; (E) clay mineral in between elongated quartz and calcite grains in mudstone-rich sample; (F) detrital grains of quartz, pyrite and K-feldspar within a fine clay matrix. Note: The black areas in the images are resin-filled organic matter.

Further mineralogical observations were made using energy-dispersive X-ray analysis (EDS), a very good mapping tool used to identify mineral phases and their relative proportion in sediment. Abundance and preservation of silicate minerals is observed in the sand-rich samples (Figure 6-6A-Figure 6-6F), suggesting little diagenetic alteration.

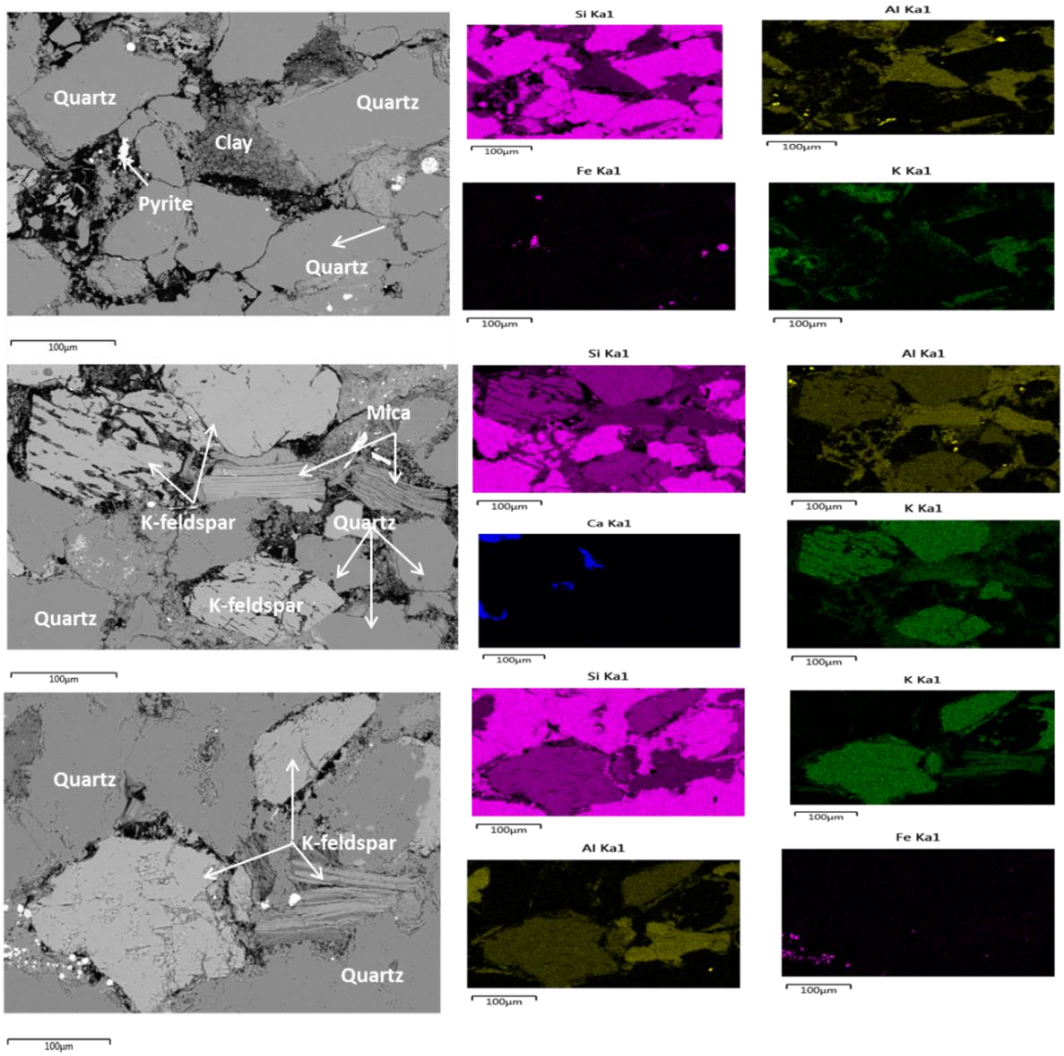

Figure 6-6: SEM back-scattered imaging and EDS mapping of selected site of interest to illustrate the different sandstone dominated samples of the Kimmeridge Clay Formation at 4,193.6m in well 16/17-14 (A) and at 4, 127.4m in well 16/18-2 (B and C). The Kimmeridge Clay samples are dominated by siliciclastic quartz, K- feldspar, elongated and flaky micas and pyrite. The black areas in the images are resin-filled organic matter at the interface between sandstone and mudstone with compaction bending of clay around large quartz grains; the white fine-grains are pyrite. (A) angular-shaped quartz-rich grain in sandstone samples surrounding K-rich clay minerals at grain interfaces and non K-rich minerals containing clay in pores (B) moderately-sorted sandstone with compaction bending of clay around large K-feldspar and quartz grains (C) Tightly-packed sandstone sample dominated by quartz grains surrounding K-feldspar and clay minerals. Note: in the EDS mapping, Fe= pyrite, AI=clay, Si= Quartz, Ca=carbonate, K=K-feldspar.

As expected given the limited depth range, the primary quartz content is likely to infer control on the brittleness of the interbedded sandstone and mudstone. Brittleness measures the amount of stored energy within the grains prior to failure, which is controlled by the temperature, effective stress from burial, diagenetic texture,

total organic carbon content and fluid type (Jarvie, 2007). SEM observations suggest that most of the quartz is detrital with silty sand-grade quartz grains associated with clay matrices; quartz grains appear to be angular, rounded and sub-rounded and are moderate-poorly sorted (Figure 6- 5 - Figure 6-7).

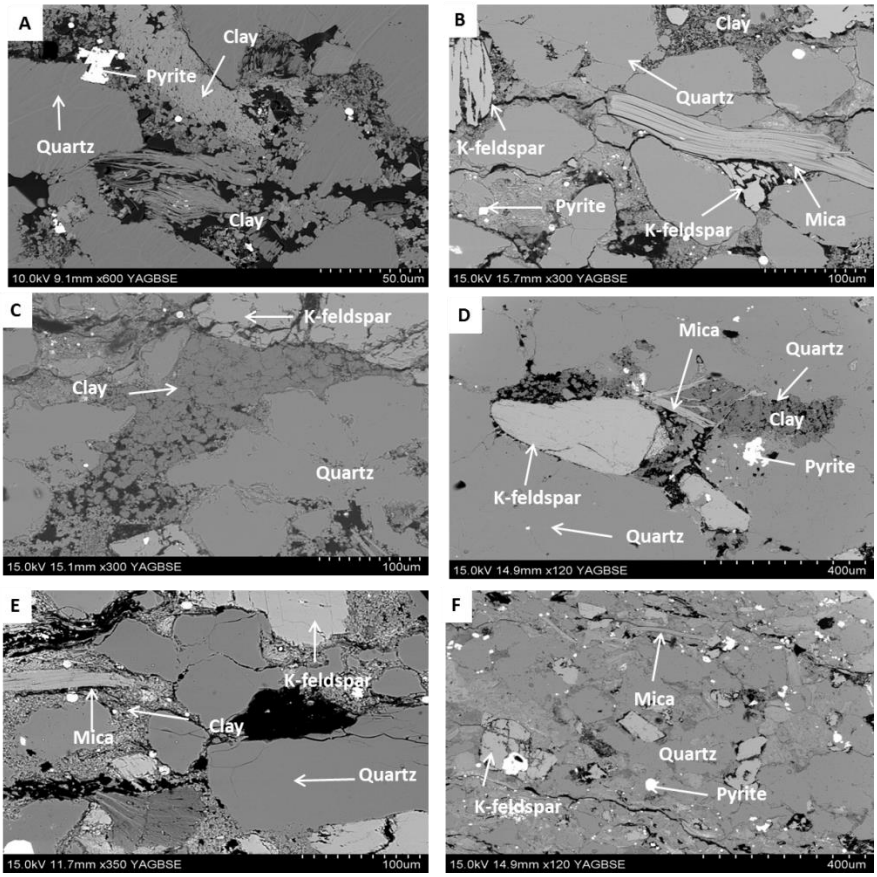

Figure 6-7: SEM back-scattered imaging of selected site of interest to illustrate the sandstone-mudstones interface samples of the Kimmeridge Clay Formation at 4, 211.7 m in Well 16/17-14 and at 4,126.2 m in Well 16/18-2. These samples are dominated by siliciclastic quartz; (7A) sample with large detrital quartz and pyrite grains in clay-silt rich matrix; (B) K- feldspar with elongated and flaky micas and pyrite at the edge of the interface between sand-mudstone. (C) clay-rich with abundant quartz and some K-feldspar; (D) large grain of K-feldspar in surrounded by tightly packed quartz, mica and clay mineral in the interface between sand-mudstone; (E) large quartz and K-feldspar grains occurring in clay-rich matrix; (F) sand/silt sized detrital grains of quartz within a fine clay-rich matrix.

It is apparent from Figure 6-5 and Figure 6-6 that the observed clays are both authigenic and detrital and are much the same as seen elsewhere comprising clay-grade to silt-grade particles and platelets in all samples. K-rich clays are observed at grain interfaces whereas non K-rich clay (kaolinite or smectite) is seen in the pores (Figure 6-6). Clay-rich matrix that is relatively loosely packed with moderate amounts

of micropores (< 1 μm) is evident in some of the samples (Figure 6-.6A and Figure 6-6B). Tightly packed clay particles with no significant intraparticular microporosity are observed in the sandstone-mudstone interface samples (Figure 6-7). The tight packing of the quartz and clay in the interface suggest limited interconnectivity between mineral grains (Figure 6-7).

Mica is the most abundant phyllosilicate minerals evident in these samples (Figure 6-5 and 6-6), more notably in samples from Well 16/17-14 and 16/17-19 (Figure 6-5) and Well 16/18-2 (Figure 6-6B). Some of the samples contain large voids at the sample surface, which are interpreted to represent the pulling of coarser grade grains during sample preparation in the lab. Authigenic framboidal and disseminated pyrite present in all samples varies in content between the three wells (Figure 6-5, 6-.6 & 6-7), more pyrite is observed in the shallowest sample (3,564.1 m) from Well 16/17-19 (Figure 6-5). Samples that are clay-dominated correlate with high TOC and S_1 (free oil) values such as sample SSK47814 (Well 16/17- 14) which has a TOC value of 7.32 wt. % and S_1 value of 5.42 mg/g and sample SSK47870 (Well 16/17-19) with a TOC value of 5.25 wt. % and S_1 values of 3.99 mg/g (Table 6-1). These values suggest that these organic-rich mudstone has a higher amount of organic matter and free S_1 oil compared to the sandstone lithofacies. The mineralogy of the samples analysed in this chapter is broadly comparable with previously published mineralogical analyses of the Kimmeridge Clay Formation (Pearson et al., 1983; Kemp et al., 2001; Hillier et al., 1995; Lothe and Zweigel, 1999). Finding an area in this hybrid system that is very brittle (more quartz) may be a key factor in creating vertical fracture patterns that are large enough to connect the maximum amount of rock volume during hydraulic fracturing stimulation.

6.6: Nature of Pores in the Kimmeridge Clay Formation

Mudstone displays a greater range of textural and compositional variation than sandstone, however; porosity in mudstone and sandstone is controlled by post-depositional mechanical and chemical processes such as compaction, dissolution, cementation, replacement and fracturing (Curtis et al., 2010; Loucks et al., 2010, 2012). Compaction processes are the most controlling factor in porosity reduction in both

mudstone and sandstone (Loucks et al., 2010), and given the burial history of the Kimmeridge Clay Formation, these may differ significantly across the study area. The nature of porosity in mudstones and its connectivity framework is also controlled by organic matter, thermal maturity (Loucks et al., 2010), the original matrix mineralogy, the arrangement of grains, sizes, distribution and grain sorting (Kwon et al., 2004; Curtis et al., 2010; Loucks et al., 2010, 2012). Studies of storage of hydrocarbons in shale reservoirs show that hydrocarbon is stored as free oil and gas within the pore system and as adsorbed oil and gas associated with organic matter (Montgomery et al., 2005; Loucks et al., 2009; Gasparik et al., 2012; Jarvie 2012; Fishman et al., 2012; Rexer et al., 2013; Chapter 5 of this thesis).

In this study, three types of porosity were observed from the results of the SEM-FIB analyses of the six selected Kimmeridge Clay samples (Figure 6-4). Pores of various sizes and shapes are observed; (1) within organic matter in the organic-rich samples (referred to as organic pores); (2) between detrital and authigenic mineral grains (referred to as interparticle pores); and (3) within detrital grains and pyrite crystals (referred to as intraparticle pores) following the pore type nomenclature and classification by Loucks et al., (2009). This pore classification is similar to the pore subdivision scheme used in describing sandstone reservoirs (Pittman. 1979), though much smaller in scale in mudstones (Loucks et al., 2012).

The pores observed within organic matter appears to be related to samples that are higher in organic matter (SSK47870, SSK47815 and SSK47858) in the three wells (Table 6-1). The non-organic pores (interparticle and intraparticle) appears to be found within framboids of pyrite crystals, between quartz and other mineral grains and within grain boundaries in all samples. Similar types of organic, interparticle and intra-particle porosities have been previously documented for the organic-rich samples of the Kimmeridge Clay Formation by Curtis et al., (2010) and Fishman et al., (2012). Porosity is generally low in unconventional reservoirs owing to the fine grained nature of the minerals and high kerogen content. Since unconventional shale systems have been become significantly expoitable commericially, extensive research on the characterisation of mudstone porosity has been conducted over the years and

these results have contributed to our understanding of the nature of pores on the microscale and nanoscale in these mudstones. Advances in drilling techniques and stimulation methods such as hydraulic fracturing and horizontal drilling have made possible the commercial exploration for natural oil and gas locked up in these porosity/low permeability fine-grained organic-rich shales. Previous studies that have looked at pores in fine- grained shales reservoirs include:(Kwon et al., 2004; Yang and Aplin, 2007; Desbois et al., 2009; Loucks et al., 2009; Milliken and Reed, 2010; Milner et al., 2010; Sondergeld et al., 2010; Schieber 2010; Lu et al., 2011; Klaver et al., 2015; Robinet et al., 2015; Bertier et al., 2016; Schurig et al., 2016; Lanzirotti et al., 2016; Desbois et al., 2016; Kaufhold et al., 2016; Welch et al., 2016; Marschall et al., 2016; Aplin and Moore, 2016; Ma et al., 2016, 2017). These authors were able to characterised, measured the full pore size and distribution of different pore system in shale reservoirs.

The main focus of this chapter is to investigate the pore types that occur in the mudstone dominated, sandstone dominated and the sandstone-mudstone interface in samples of the Kimmeridge Clay Formation. Percentages and quantification of porosity were not determined from the SEM-FIB analyses because the six selected subsamples are too few for significant statistics and SEM-FIB analysis does not give an accurate measurement of the effective porosity such as mercury or helium injection methods used in Chapter 5. Other techniques for quantitative characterisation of porosity such as; N2 physisorption (Bertier et al., 2016); gas adsorption (Kaufhold et al., 2016); nitrogen adsorption/desorption measurements (Marschall et al., 2016), mercury intrusion, or small-angle neutron scattering (Mastalerz et al., 2013; Bahadur et al., 2015) is beyond the scope of this thesis. These quantitative pore characterisation techniques cannot differentiate the different pore type in fine-grained mudstone; this requires high resolution imagining techniques such as SEM-FIB (Löhr et al., 2015) used in this study.

6.6.1: Organic Porosity in the Kimmeridge Clay Formation

Organic porosity in organic-rich mudstone is largely a function of TOC and thermal maturity, which means organic pores develop with increases in thermal maturity

during the thermal transformation of kerogen into hydrocarbon (Loucks et al., 2009, 2012). TOC quality significant influences the total volume of organic pores and maturity controls the formation of intra-organic pores (Ma et al., 2017). As hydrocarbon is generated and subsequently expelled from the kerogen structure, organic pores are formed within the void (Loucks et al., 2012; Curtis et al., 2012; Milliken et al., 2013; Schieber, 2013).

In this study, organic pores occurring within the organic matter (kerogen) are more commonly observed in the organic-rich mudstone-dominated samples (SSK47815 and SSK47870) (Figure 6-8), suggesting a greater potential for hydrocarbon storage may exist in higher TOC mudstone-rich intervals which are dependent on pore connectivity.

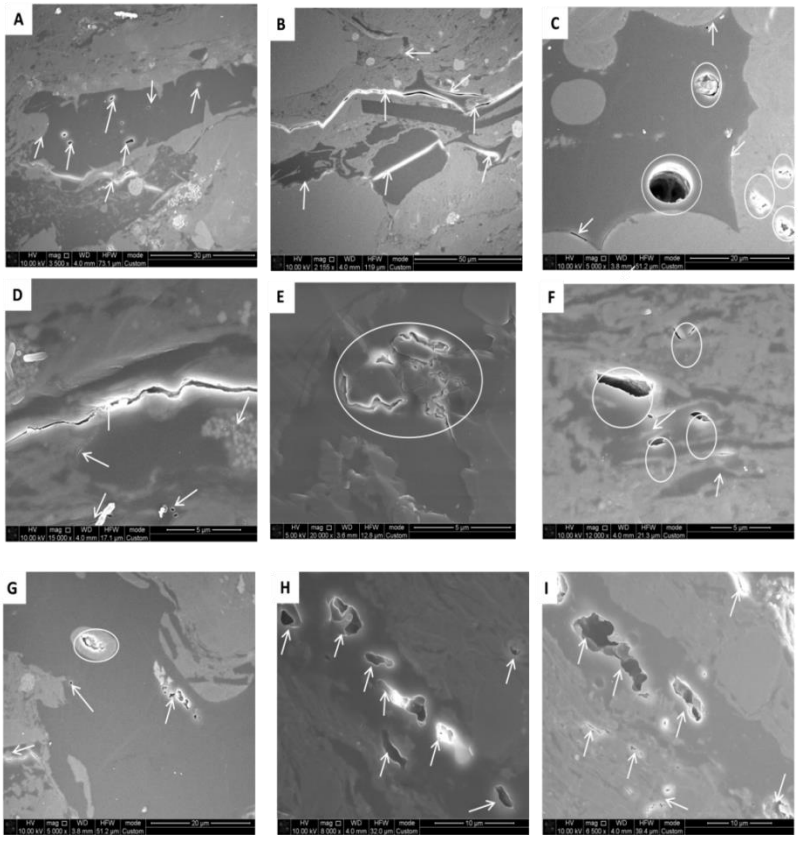

Figure 6-8: FIB-SEM images of selected sites of interest illustrate the different prominent features of organic porosity (in white arrows and circles) in the selected Kimmeridge Clay samples. (A) Organic-rich mudstone dominated sample showing fracture pores and bubble-like and isolated organic matter pores of varied sizes within homogenous organic matter from Well 16/17-14 (4194.7 m) with TOC of 7.32 wt.% and Ro of 0.70 % (B) Organic microstructure showing fractures within organic matter and on the edge of a fragment of woody material displaying arcuate edges showing former cell walls from Well 16/17-14 (4194.7 m) with TOC of 7.32 wt.% and Ro of 0.70 % (C)

Organic porosity within the organic matter with subtle fracture pores along the edges, and intra-organic pores within the grains from Well 16/17-14 (4211.7 m) with TOC of 2.32 wt.% and Ro of 0.74 % (D) Fracture porosity within the organic matter showing elongated cracks , this fracture may be due to the excess volume created during oil generation from Well 16/17-14 (4194.7 m) with TOC of 7.32 wt.% and Ro of 0.70 % (E) Organic pores in dispersed organic matter with complex internal structures from Well 16/18- 2 (4126.2 m) with TOC of 6.38 wt.% and Ro of 0.65 % (F) Cluster of organic pores within and along the edge of the organic matter from Well 16/17-14 (4194.7 m) with TOC of 7.32 wt.% and Ro of 0.70 %. (G) Sandstone dominated sample with organic pores within homogeneous organic matter from Well 16/18- 2 (4127.4 m) with TOC of 1.72 wt. % and Ro of 0.65 % (H) Elongated and irregular-shaped organic pores aligned in the direction of elongation from Well 16/17-14 (4193.6 m) with TOC of 1.1 wt. % and Ro of 0.52 % (I) Cluster of organic pores interconnected and forming larger pores with complex internal structure from Well 16/17-14 (4193.6 m) with TOC of 1.1 wt.% and Ro of 0.52 %.

Organic pores are limited in one of the sandstone-dominated samples (SSK47814); this sample contains 1.1 wt.% TOC and maturity range of 0.52 % R_o (Table 6-1). Overall, the observed organic pores are largely similar in shape and abundance from sample to sample regardless of TOC and maturity (Figure 6-.8). Sizes of the organic pores range from < 0.1 μm to about 0.5 μm across and are similar in all samples regardless of the level of maturity. They are irregular ellipsoidal shapes from rounded-oval, triangular, isolated and elongated, imbibed in the organic matter (Figure 6-8). Some organic pores have shapes similar to cellulosic "woody" material (terrestrial organic porosity) as seen in Figure 8B. The edges of the organic pores are moderate to well-defined with fractures also occurring in alignment to the organic pores in sharp boundaries (Figure 6-8B to Figure 6-8D) while some appears to be in shrinkage cracks (Figure 6-8B & Figure 6-8D). Sharp boundaries and fracture or rectilinear alignment were also observed within the organic matter, where some are seen with more complex patterns that may be related to underlying structure of the host material (Loucks et al., 2010). Fracture porosity within the organic matter may be due to the excess volume that may also have been created during oil generation (Loucks et al., 2009; Curtis et al., 2012). Pores in organic matter do not compact due to their nanometer scale sizes (Modica and Lapierre, 2012), which means organic porosity is mainly controlled by mass balances during transformation of kerogen (Romero-Sarmiento et al., 2013).

There also appears to be a complete lack of porosity in some of the homogenous organic matter observed (e.g. some part of Figure 6-8G). Organic porosity has the potential to form a connected pore network (Loucks et al., 2009; Curtis et al., 2012a; Loucks et al., 2012; Milliken et al., 2013; Löhr et al., 2015); and is widely recognised to have contributed to total porosity in some of the successful North American shale reservoirs used as analogues for this study such as: the Haynesville Formation (Milner et al., 2010; Curtis et al., 2010), the Eagle Ford Formation (Loucks et al., 2010; Curtis et al., 2010), the Barnett Shale (Loucks et al., 2009; Milner et al., 2010; Sondergeld et al., 2010; Curtis et al., 2010) and the Marcellus Formation (Milner et al., 2010; Curtis et al., 2010; Milliken et al., 2013). Organic pores have contributed to the connected pore network in some shale-gas systems, such as the Mississippian Barnett Shale (Loucks et al., 2009; Ambrose et al., 2010; Curtis et al., 2010).

6.6.2: Interparticle porosity in the Kimmeridge Clay Formation

Secondary porosity in shale is developed from the preservation of silicate minerals and illite platelets and the volume reduction of organic matter following hydrocarbon generation (Loucks et al., 2010; Fisherman et al., 2012). In fine- grained mudstones, primary pores commonly occur initially between soft and ductile particles, the interparticle pore network may be destroyed or rigid grains may resist compaction following extensive compaction during burial (Dawson and Almon, 2002; Desbois et al., 2009; Schieber, 2010; Desbois et al., 2009 Loucks et al., 2010). Due to the burial history (depth and maturity dependent) of these Upper Jurassic Kimmeridge samples (3,564.1- 4211.7 m), interparticle pores differ across the samples. Interparticle pores between mineral grains were observed in samples from all wells (Figure 6-9). They are generally the most abundant pore type in the sandstone-rich and the sand-mudstone interface samples (Figure 6-9A to Figure 6-9E). These interparticle pores typically appear elongated and triangular in shape between detrital grains and-pyrite framboids and the surrounding illite, kaolinite and organic matter (Figure 6-9). Interparticle pores are also found along the edges of organic matter and mineral grain boundaries (Figure 6-9E), which may be related to matrix separating from the particles during compaction (Loucks et al., 2012).

The clay minerals in interparticle porosity show considerable variation in size with randomly oriented micro-fractures locally evident and are usually tightly packed (Figure 6-6 & Figure 6-7). In the clay-rich intervals, interparticle porosity commonly occurs; as interspersed between illite plates (lath-like or fibrous illite flakes), and clay aggregates with pores ranging in size from 0.1 to 0.5 μm across and up to 2 μm in length in the sandstone-mudstone interface samples, and in the mudstone-dominated samples range in size from ~0.1 to 0.5 μm across and up to 10 μm in length (Figure 6. 9F). Some appear to have formed by bending deformation of clay particles, and with some parallel or subparallel to bedding. In some of the samples, shrinkage cracks were observed (Figure 6-9E, Figure 6-9G & Figure 6-9H); these may have been formed as shrinkage features due to desiccation (Loucks, 2009). These interparticle pores are generally related to the primary pore network and are significant in the storage and

production of hydrocarbons (Loucks et al., 2010; Fisherman et al., 2012). The preservation of interparticle pores in these samples provides a potential mechanism for oil storage capacity in the Kimmeridge Clay Formation (Loucks et al., 2010; Fisherman et al., 2012).

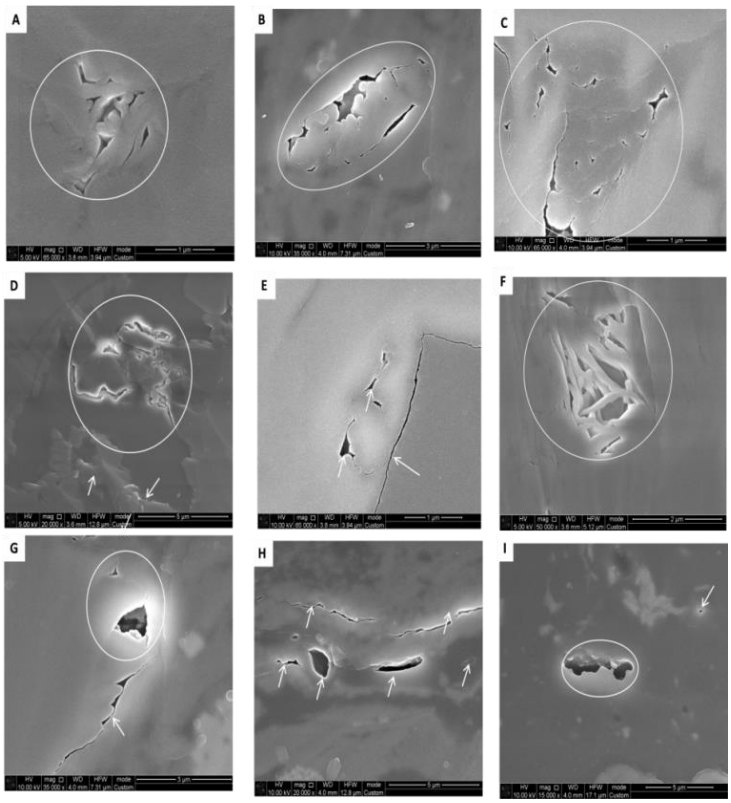

Figure 6-9: FIB-SEM images of selected sites of interest to illustrate the different features of interparticle porosity observed in all samples (in white arrows and circles). (A) Organic-rich mudstone sample (SSK47870) showing isolated pores within the mineral grains from Well 16/17- 19 (3564.1 m) with TOC of 5.25 wt.% and Ro of 0.58 %. (B) Mudstone dominated sample (SSK47815) showing elongated and irregular shaped pores aligned in the direction of elongation within a mineral matrix from Well 16/17-14 (4194.7 m) with TOC of 7.32 wt.% and Ro of 0.70 %. (C) Mudstone dominated sample (SSK47815) with cluster irregular shaped pores within and at the edge of organic matter from Well 16/17-14 (4194.7 m) with TOC of 7.32 wt.% and Ro of 0.70 %. (D) Mudstone/sandstone sample (SSK47858) showing irregular and angular shaped pores within the organic matter from Well 16/18- 2 (4126.2 m) with TOC of 6.38 wt.% and Ro of 0.65 %.(E) Mudstone/sandstone sample (SSK47813) with interparticle fractured pores developed at the edge of the organic matter and some intraparticle pores within the mineral grain from well 16/17-14 (4211.7 m) with TOC of 2.32 wt. % and Ro of 0.74 %.(F) Mudstone/sandstone sample (SSK47858) showing pores within illite platelets from Well 16/18- 2 (4126.2 m) with TOC of 6.38 wt.% and Ro of 0.65 %. The cracks may have been formed by the shrinking of clay minerals during diagenesis. (G) Mudstone dominated sample (SSK47815) with oval-shaped and fractured pores from Well 16/17-14 (4194.7 m) with TOC of 7.32 wt.% and Ro of 0.70 %. (H) Fractured, round to elongated shaped pores from Well 16/17-14 (4194.7 m) with TOC of 7.32 wt.% and Ro of 0.70 % (I) Elongated shaped mineral-associated isolated pores within organic matter in sandstone-dominated sample (SSK47814) from Well 16/17-14 (4193.6 m) with TOC of 1.1 wt.% and Ro of 0.52 %.

6.6.3: Intraparticle porosity in the Kimmeridge Clay Formation

Intraparticle pores occurred within mineral grains, within clay and mica-mineral grains and in the organic matter in all samples (Figure 6-3), and it is seen in all samples of the Kimmeridge Formation and in all wells. Primary intraparticle pores observed appear to be clustered within aggregates of mineral grains and within individual crystallites of authigenic framboidal pyrite and disseminated pyrite crystals (Figure 6-10). It ranges in sizes from <1 to ~5 μm (Figure 6-10), and is generally larger than the organic pores (Figure 6-8). Secondary intraparticle pores found within grains are commonly pores resulting from complete or partial dissolution of K-feldspar, calcite or calcareous fossils (Loucks et al., 2010; Fishman et al., 2012). Chemical dissolution of detrital K-feldspar at high maturity also favours the formation of intraparticle pores in the Kimmeridge Clay Formation (Fishman et al., 2012). Fracture and micro-fracture–related pores (Figure 6-10G) are seen within mineral grains as intra-pore; these natural fractures are significant for induced hydraulic fracturing of shale reservoirs (Gale et al., 2007; Loucke et al., 2009).

6.7: Implications for hydrocarbon migration and storage in the Kimmeridge Clay Formation

Organic, interparticle and intraparticle pores have been identified in all the selected sandstone and mudstone samples with the exception of sandstone sample (SSK47814) which has limited organic porosity. Organic porosity plays an important role in primary migration and hydrocarbon storage in the Kimmeridge Clay Formation. Adsorption affinity is an important factor in hydrocarbon storage as organic-rich shales tend to hold onto hydrocarbon better than either organic lean rocks (Jarvie, 2014) or rocks with predominantly quartz and carbonate minerals (Schettler and Parmely, 1991). At an early stage of maturation, the oil generated from kerogen in the Kimmeridge Clay source rock will start to saturate any available porosity. With increasing maturation, the mudstone porosity will be filled and, subject to adequate permeability, localised expulsion will start to fill the open pore spaces of sandstones in close proximity. Migration of generated oil from the mudstone into the interbedded

sandstone involves a short vertical distance from the source to storage in the interbeds (Turner et al., 1987; Reitsema, 1983; Roberts, 1991).

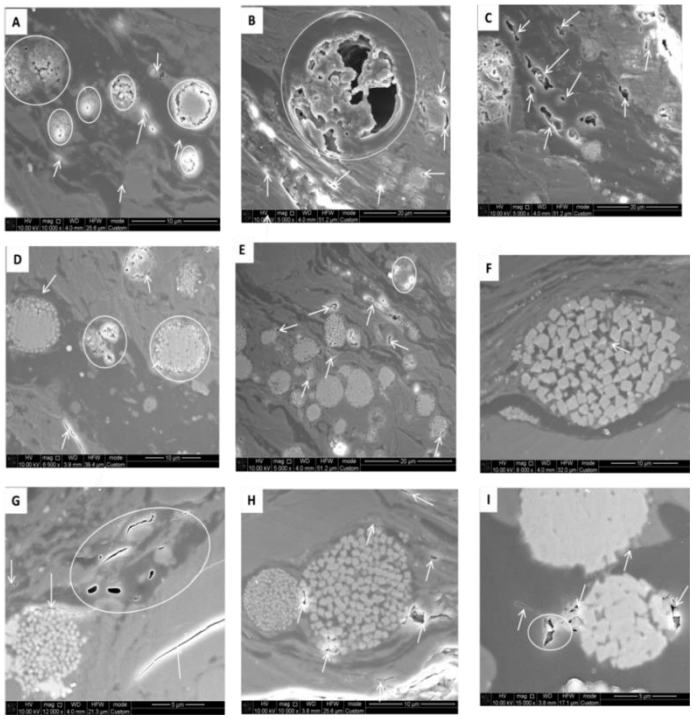

Figure 6-10: FIB-SEM images of selected sites of interest to illustrate the different prominent features of intraparticle pores within pyrite framboids, organic matter and mineral grains seen in sandstone -dominated sample SSK47813 (A-E) (in white arrows and circles). (A) sandstone-dominated sample (SSK47813) intraparticle pores in pyrite and grains from Well l 16/17-14 (4193.6 m) with TOC of 1.1 wt. % and Ro of 0.52 %. (B) sandstone-dominated sample (SSK47813) with intraparticle and organic pores within complex distorted organic matter with a distinct dissolution rim from Well 16/17-14 (4193.6 m) with TOC of 1.1 wt.% and Ro of 0.52 %. (C) sandstone-dominated samples with intraparticle pores within organic matter and pyrite from Well 16/17-14 (4193.6 m) with TOC of 1.1 wt. % and Ro of 0.52 %, the pores within the organic matter have a wide-size distribution interval. (D) sandstone-dominated sample (SSK47813) with both interparticle and intraparticle pores from Well 16/17-14 (4193.6 m) with TOC of 1.1 wt.% and Ro of 0.52 %. (E) sandstone-dominated sample (SSK47813) showing abundant of pyrite with interparticle pores and intraparticle pores within the organic matter from Well 16/17-14 (4193.6 m) with TOC of 1.1 wt.% and Ro of 0.52 %. (F) organic-rich mudstone dominated sample (SSK47815) with organic matter within inter-crystalline pores, the intraparticle pores in the framboids conforms to the outline of the organic matter along the bottom from well 16/17-14 (4194.7 m) with TOC of 7.32 wt.% and 0.70 %Ro. (G) Organic-rich mudstone dominated samples showing discrete sponge-like intraparticle pores within organic matter and pores at the edge of framboids and some fracture pores from Well 16/17-14 (4194.7 m) with TOC of 7.32 wt.% and 0.70% Ro. (H) sandstone dominated sample (SSK47860) showing well-developed organic matter pores within pyrite framboids and interparticle pores at the edge of rigid pyrite minerals from Well 16/18- 2 (4127.4m) with TOC of 1.72 wt.% and Ro of 0.65 % (I) Organic-rich mudstone/sandstone interface sample (SSK47813) with intraparticle pores within the organic matter and pyrite and some interparticle pores between pyrite and organic matter from Well 16/17-14 (4211.7 m) with TOC of 2.32 wt.% and 0 .742 %Ro.

The mudstones will contain the retained oil within sub-nano-micro pores in the kerogen prior to, during and after expulsion, and the sandstone will absorb the expelled free oil (S_1). Using Rock-Eval S_1 values (Table 6-1) sandstone-dominated samples have S_1 (free oil) values (1.32-2.77mg/g), suggesting that that free oil (S_1) has migrated into the pores of sandy layers.

Observations from the SEM-FIB analysis have shown the organic porosity to be well developed within the Kimmeridge Clay; a well-connected organic pore network is an important contribution to porosity, permeability and storage capacity for this hybrid shale reservoir. A number of studies have shown that organic pores in a continuous organic framework can form an effective pore system and can enhance the hydrocarbon flow pathway in a shale reservoir (Loucks et al., 2009; Ambrose et al., 2010; Curtis et al., 2010). Interparticle and intraparticle pores are created during hydrocarbon maturation with burial as overburden stress and diagenesis increases (Jarvie et al., 2007; Loucks et al., 2009; Ambrose et al. 2010; Curtis et al., 2010). Diagenetic alteration, precipitation, preservation and realignment of the silicate and clay minerals occurred from compaction during deep burial in the South Viking Graben area resulting in the formation of interparticle and intraparticle porosity seen (Loucks, 2009; Fishman et al., 2012) in the Kimmeridge Clay Formation.

Interparticle and intraparticle pores developed between and within soft and ductile to hard and rigid (e.g. quartz, calcite, feldspars, authigenic pyrite, and skeletal material) mineral grains and crystals. During further burial, the soft and ductile grains can be distorted due to compaction and cementation; the developed interparticle pores may be reduced or destroyed, however the rigid grains are able to resist compaction (Pytte and Reynolds, 1988; Loucks et al., 2010, 2012; Milliken and Reed, 2010). Given burial history (depth and maturity dependent) and diagenetic processes of these Upper Jurassic Kimmeridge samples (3,564.1 - 4211.7 m), interparticle and intraparticle porosity is significant present in these samples. Interparticle pores can also develop where more ductile grains bend around a rigid grain or be preserved where a cluster of rigid grains form a sheltering effect, preventing compaction of the ductile grains (Pytte and Reynolds, 1988; Desbois et al., 2009; Schieber, 2010; Loucks et al., 2010).

The interparticle pores observed in these samples appear to be concentrated around elongated to round angular rigid mineral grains, pyrite crystals and clay platelets. Intraparticle pores developed within particles, pyrite framboids, clay sheets, quartz, feldspar and mica grains) are commonly observed in the Kimmeridge Clay samples. Some of the intraparticle pores appear to be controlled by the shapes and sizes of its original host grain such as those formed by partial or complete dissolution of grains and crystals.

Each pore type (organic, interparticle and intraparticle) is widely distributed in all the Kimmeridge Clay samples; interparticle pores are generally better connected to one another, while intraparticle pores are commonly connected to the overall pore system (Loucks et al., 2012). Combination of these pores can have a significant effect on the overall total porosity of hydrocarbon storage, and may contribute to the connectivity of permeability for hydrocarbon flow pathway in the Kimmeridge hybrid shale reservoir (Pittman, 1979, 2001; Lucia, 1999; Loucks et al., 2012). Further analysis of multiple 2-D images of more representative Kimmeridge Clay samples from several wells and different depth intervals are needed to better characterise each rock type to quantitatively understand the pore networks. 3-D Micro computed tomography (MicroCT) analyses performed on these samples to confirm that the pores are connected and forms an effective pore network was discarded due to 'noise' in the acquired data.

6.8: Conclusions

Study of samples from the Upper Jurassic Kimmeridge Clay Formation was used to investigate the nature and types of pores within the organic-rich source rock. Three gross lithologies; mudstone dominated, sandstone dominated and the interface between sandstone and mudstone are recognized from visual examination and estimated from full core samples, with the estimates substantiated by thin sections observation under an optical microscope. Observations from thin-sections suggest that–the mudstone-dominated lithologies are in general black-dark grey, silty, and partly laminated with gradational boundaries between the mudstones and the

interbedded light-grey sandstones. The interbedded sandstones are fine-medium grainedand silty with high organic carbon content in the mixed sandstone/mudstones.

Interpretation of the X-ray diffraction (XRD) results suggests these samples are dominated by quartz, clay, organic matter and pyrite. Kaolinite and illite/smectite are the dominant clay minerals identified in all samples. Further mineralogical observations were made using energy-dispersive X-ray analysis (EDS), a very good mapping tool used to identify mineral phases and their relative proportion in sediment. Abundance and preservation of silicate minerals is observed in the sand-rich samples suggesting little diagenetic alteration. Lithological and compositional heterogeneity of the mudstone-sandstone interbeds is caused in part by variation in organic richness (TOC) and kerogen type as evidenced by the core samples selected for this study.

In terms of organic-richness, the samples containing a high proportion of mudstone (> 70 %) have a TOC content range of 5.25- 7.23 wt. %, whereas samples with a high proportion of sandstone have a TOC content range of 1.1-1.72 wt.%. As expected, these values suggest that the mudstones contain higher amounts of organic matter in contrast to the predominantly sandstone samples. The maturation levels of the investigated Kimmeridge Clay Formation samples estimated from Rock-Eval T_{max} range from 0.52-0.65 $\%R_o$ for the sandstone dominated samples, to 0.58-0.70 $\%R_o$ for the mudstone dominated samples and 0.65-0.74 $\%R_o$ for the sandstone-mudstone interface samples. The measured TOC and maturity values are in agreement with the TOC/Rock-Eval data and previous vitrinite reflectance measurement reported in the literature (Fuller, 1980; Goff, 1983: Cornford, 1998; Isaksen et al., 2002).

Due to the fine grained nature of the mudstone and the interface between the mudstone stone and sandstone in the Kimmeridge Clay samples; FIB-SEM high resolution imagining was used to investigate the nature of porosity and pore type in these samples. Understanding the porosity in mudstone is a key component in identification of sweet-spot area in the evaluation of shale reservoir for unconventional resources as discussed in Chapter 1. Observations from this study reveal three types of porosity (organic porosity, interparticle porosity and

intraparticle porosity) throughout the samples across all wells. Organic pores appear to be the dominant pores within the organic matter in the mudstone-rich samples with higher TOC (SSK47815 and SSK47870). Which occurs as a result of hydrocarbon generation in the organic-rich mudstone (Jarvie et al., 2007; Loucks et al., 2009; Bernard et al., 2012), and it contributes to more storage of free oil (S_1) in the Kimmeridge Clay Formation (Raji et al., 2015). Inorganic pores observed in all samples and wells include interparticle and intraparticle pores, which developed at various times in the secondary post-depositional history of the Kimmeridge Clay Formation. Interparticle pores are the most common porosity observed in all the samples at all levels of maturity followed by intraparticle pores within clay minerals, grains and organic pores in organic matter. The type of porosity observed in this study is consistent with the results from Fishman et al., 2012 on the Kimmeridge Clay Formation. Depending on the overall pore throat sizes; combination of these porosities in the Kimmeridge Clay Formation may significantly contribute to the effective porosity, the connectivity of permeability flow path for the hydrocarbon in the Kimmeridge hybrid shale reservoir.

6.9: References

Ambrose, R. J., Hartman, R. C. Diaz-Campos, M. Akkutlu, I. Y. and Sondergeld, C. H. 2010. New pore-scale considerations for shale gas in place calculations: Society of Petroleum Engineers Unconventional Gas Conference, Pittsburgh, Pennsylvania, February 23–25, 2010, SPE Paper 131772, 17 p.

Aplin, A.C., Macquaker, J.H.S., 2011. Mudstone diversity—origin and implications for source, seal, and reservoir properties in petroleum systems. American Association of Petroleum Geologists Bulletin 95, pp.2031–2059.

Aplin, A.C. and Moore, J.K.S. 2016. Observations of pore systems of natural siliciclastic mudstones. Pp. 33– 44 in: Filling the Gaps – from Microscopic Pore Structures to Transport Properties in Shales (T. Scha¨fer, R. Dohrmann, and H.C. Greenwell, editors). CMS Workshop Lectures Series, 21, The Clay Minerals Society, Chantilly, Virginia, USA

Barnard, P. C., and Cooper, B. S. 1981. Oils and source rocks of the North Sea area. In:Illing, L. V. and Hobson, G. D. ed., Petroleum geology of the Continental Shelf of northwest Europe: Heyden, London, Institute of Petroleum, 169–175.

Bernard, P. C., Collins, A.G. & Cooper, B.S., 1981. Identification and distribution of kerogen facies in a source rock horizon—examples from the North Sea basin, in Brooks, J., eds., Organic maturation studies and fossil fuel exploration: London, Academic Press, 271–282.

Bernard, S., Horsfield, B., Schulz, H.M., Wirth, R., Schreiber, A., Sherwood, N., 2012. Geochemical evolution of organic-rich shales with increasing maturity—a STXM and TEM study of the Posidonia Shale (Lower Toarcian, northern Germany). Marine and Petroleum Geology 31, pp.70–89.

Bertier, P., Schweinar, K., Stanjek, H., Ghanizadeh, A., Clarkson, C.R., Busch, A., Kampman, N., Prinz, D., Amann-Hildenbrand, A., Krooss, B.M., Pipich, V., and Di, Z. 2016. On the use and abuse of N2 physisorption for the characterization of the pore structure of shales. Pp. 151–161 in: Filling the Gaps – from Microscopic Pore

Structures to Transport Properties in Shales (T. Scha¨fer, R. Dohrmann, and H.C. Greenwell, editors). CMS Workshop Lectures Series, 21, The Clay Minerals Society, Chantilly, Virginia, USA

Cooper, B. S., and Barnard,P.C. 1984. Source rocks and oils of the central and northern North Sea, In: Demaison. G and Murris, R. J., ed., Petroleum geochemistry and basin evaluation: American Association of Petroleum Geologists Memoir , 35, 303–314.

Cornford, C., Morrow, J.A., Turrington, A., Miles, J.A., Brooks, J., 1983). Some geological controls on oil composition in the UK. North Sea, in: Brooks, J. ed., Petroleum Geochemistry and Exploration of Europe. Geological Society Special Publication, Blackwell Scientific Publications, Oxford, 12, 175-194.

Cornford, C. 1984. Source rocks and hydrocarbons of the North Sea. In: Glennie, K. W., ed., Introduction to the Petroleum Geology of the North Sea. Blackwell Scientific Publications, Oxford, pp.171-209.

Cornford, C. 1998. Source rocks and hydrocarbons of the North Sea, in Glennie, K.W., ed., Petroleum geology of the North Sea (4th eds): London, Blackwell Science Ltd., 376–462.

Cornford, C. & Brooks, J. 1989. Tectonic controls on oil and gas occurrences in the North Sea area. In: Extensional tectonics and stratigraphy of the North Atlantic margins, Tankard, A.J. & Balkwill, H.R. (eds). American Association of Petroleum Geologists/Canadian, Geological Foundation, 46- 641.

Cornford, C., Birdsong, B. and Groves, G. 2014. Offshore Unconventional Oil from the Kimmeridge Clay Formation of the North Sea: A Technical and Economic Case. Unconventional Resources Technology Conference Proceedings, August 25-27, 2014.

Curtis, M. E., Ambrose, R. J. Sondergeld, C. H., and Rai, C. S. 2010. Structural characterization of gas shales on the micro- and nano-scales: Canadian Unconventional Resources and International Petroleum Conference, Calgary, Alberta, Canada, October 19–21, 2010, SPE Paper 137693, 15 p

Curtis, M.E., Sondergeld, C.H., Ambrose, R.J., Rai, C.S., 2012. Microstructural investigation of gas shales in two and three dimensions using nanometer-scale resolution imaging. American Association of Petroleum Geologists 96, pp.665–677.

Dawson, W., and W. R. Almon, 2002. Top seal potential of Tertiary deep-water shales, Gulf of Mexico: Gulf Coast Association of Geological Societies Transactions, v. 52, pp. 167–176

Desbois, G., Urai, J.L. and Kukla, P.A. 2009. Morphology of the pore space in claystones—evidence from BIB/FIB ion beam sectioning and cryo-SEM observations. eEarth Discussion 4, pp.1–9.

Desbois, G., Hemes, S., Laurich, B., Houben, M., Klaver, J., Ho¨hne, N., Urai, J.L., Viggiani, G., and Be´suelle, G. 2016. Investigation of microstructures in naturally and experimentally deformed reference clay-rocks by using innovative methods in scanning electron microscopy. Pp. 1–14 in: Filling the Gaps – from Microscopic Pore Structures to Transport Properties in Shales (T. Scha¨fer, R. Dohrmann, and H.C. Greenwell, editors). CMS Workshop Lectures Series, 21, The Clay Minerals Society, Chantilly, Virginia, USA

Davies, D. K., Bryant, W. R. Vessell, R. K. and Burkett, P. J. 1991. Porosities, permeabilities and microfabrics of Devonian shales, in R. H. Bennett, W. R. Bryant, and M. H. Hulbert, eds., Microstructure of fine-grained sediments: From mud to shale: New York, Springer-Verlag, p. 109– 119

Fishman, N. S., Hackley, P. C., Lowers, H. A., Hill, R. J., Egenhoff, S. O., Eberl, D. D., and Blum, A. E., 2012. The nature of porosity in organic-rich mudstones of the Upper Jurassic Kimmeridge Clay Formation, North Sea, offshore United Kingdom: International Journal of Coal Geology, v. 103, p. 32–50, doi:10.1016/j.coal.2012.07.012

Fuller, J. G. C. M. 1980. Progress report on fossil fuels—exploration and exploitation. In Proceedings of Yorkshire Geology Society, (eds) Jones J. M., Scott P. W. 33:pp.581–593

Gale, J. F. W., R. M. Reed, and J. Holder, 2007. Natural fractures in the Barnett Shale and their importance for hydraulic fracture treatments: AAPG Bulletin, v. 91, pp. 603–622, doi:10.1306/11010606061.

Gasparik, M., Ghanizadeh, A., Bertier, P., Gensterblum, Y., Bouw, S., Krooss, B.M., 2012. High-Pressure Methane Sorption Isotherms of Black Shales from The Netherlands, Energy & Fuels, 26 (8), pp. 4995-5004. DOI: 10.1021/ef300405g

Gautier, D. L., 2005. Kimmeridgean Shales Total Petroleum System of the North Sea Graben Province: U.S. Geological Survey Bulletin 2204-C, 24. (Available online http://pubs.usgs.gov/bul/2204/c (accessed June 15, 2014).

Goff, J. C. 1983. Hydrocarbon generation and migration from Jurassic source rocks in the East Shetland Basin and Viking Graben of the northern North Sea: Journal of the Geological Society, 140, p. 445–474.

Goldstein, J., Newbury, D. E., Joy, D. C. and Lyman, C.E 2002. Scanning Electron Microscopy and X-ray Microanalysis by (3rd ed), Springer

Heath, J.E., Dewers, T.A., McPherson, B.J.O.L., Petrusak, R., Chidsey, T.C., Rinehart, A.J. and Mozley, P.S., 2011. Pore networks in continental and marine mudstones—characteristics and controls on sealing behavior. Geosphere 7, 429–454

Hillier S, Matyas J, Matter A. and Vasseur, G. 1995. Illite/smectite diagenesis and its variable correlation with vitrinite reflectance in the Pannonian Basin.Clays and Clay Minerals, 43(2), 174-83.

Jarvie, D. M., Brenda L. C., Floyd "Bo" H. and John T. Breyer, 2001. Oil and Shale Gas from the Barnett Shale, Ft. Worth Basin, Texas, AAPG National Convention, June 3-6, 2001, Denver, CO, American Association of Petroleum Geologists Bulletin 85, 13 (Supplement), A100.

Jarvie, D.M., Hill, R.J., Ruble, T.E. and Pollastro, R.M. 2007. Unconventional shale gas systems: the Mississippian Barnett Shale of north-central Texas as one model for

thermogenic shale gas assessment. American Association of Petroleum Geologists Bulletin, 91, pp. 475-499

Jarvie, D.M., 2012. Shale resource systems for oil and gas: part 1 shale-gas resource systems. In: Breyer, J.A. ed., Shale Reservoirs Giant Resources for the 21st Century, American Association of Petroleum Geologists Memoir, 97, pp.69-87

Jarvie, D. M. 2014. Components and processes affecting producibility and commerciality of shale resource systems, ALAGO 2012 Special Publication, GeologicaActa, 12, 4, pp.307-325.

Isaksen, G.H., Patience, R., van Graas, G. and Jenssen, A.I. 2002.Hydrocarbon system analysis in a rift basin with mixed marine and non-marine source rocks; the South Viking Graben, North Sea. American Association of Petroleum Geologists Bulletin, 86 (4), pp. 557–591.

Kemp, S.J., Bouch, J. and Murphy, H.M. 2001. Mineralogical characterisation of the Nordland Shale, UK Quadrant 16, northern North Sea.British Geological Survey Commissioned Report, CR/01/136, 52.

Kwon, O., Herber, B.E. &Kronenberg, A. K. 2004. Permeability of illite-bearing shale: 2. Influence of fluid chemistry on flow ad functionally connected pores, Journal of Geophysical Research, B10206, doi:10,.1029/2004B003055.

Lanzirotti, A., Newville, M., Manoukian, L., and Lange, K. 2016. High-speed, coupled micro-beam XRD/ XRF/XAFS mapping at GSECARS: APS beamline 13-ID-E. Pp. 53–64 in: Filling the Gaps – from Microscopic Pore Structures to Transport Properties in Shales (T. Scha¨fer, R. Dohrmann, and H.C. Greenwell, ed.,. CMS Workshop Lectures Series, 21, The Clay Minerals Society, Chantilly, Virginia, USA.

Löhr, S.C., Baruch, E.T., Hall P.A. and Kennedy, M.J. 2015. Is organic pore development in gas shales influenced by the primary porosity and structure of thermally immature organic matter? Journal of Organic Geochemistry, v 87, pp. 119-132.

Lothe, A.E. and Zweigel, P. 1999. Saline Aquifer CO2 Storage (SACS). Informal annual report 1999 of SINTEF Petroleum Research's results in work area 1 'Reservoir Geology'. SINTEF Petroleum Research report 23.4300.00/03/99, 54.

Loucks, R.G., Reed, R.M., Ruppel, S.C., Jarvie, D.M., 2009.Morphology, Genesis, and Distribution of Nanometer-Scale Pores in Siliceous Mudstones of the Mississippian Barnett Shale. Journal of Sedimentary Research 79, pp.848-861.

Loucks, R.G., Reed, R.M., Ruppel, S.C. and Hammes, U., 2010. Preliminary classification of matrix pores in mudrocks. Gulf Coast Association of Geological Societies Transactions 60, pp. 435–441.

Loucks, R.G., Reed, R.M., Ruppel, S.C., Hammes, U., 2012. Spectrum of pore types and networks in mudrocks and a descriptive classification for matrix-related mudrock pores. American Association of Petroleum Geologist Bulletin 96, pp.1071–1098.

Lu, J., Milliken, K.L., Reed, R.M., Hovorka, S., 2011. Diagenesis and sealing capacity of the middle Tuscaloosa Mudstone at the Cranfield carbon dioxide injection site,Mississippi, U.S.A. Environmental Geosciences 18, pp.35–53.

Lucia, F. J., 1999. Carbonate reservoir characterization: New York, Springer-Verlag, 226 p.

Ma, L., Taylor, K., Lee, P., Dobson, K. J., Dowey, P. J. and Courtois, L. Apr 2016. Novel 3D centimetre- to nano-scale quantification of an organic-rich mudstone: the Carboniferous Bowland Shale, Northern England. Journal of Marine and Petroleum Geology. 72, pp. 193-205.

Ma, L., Fauchille, A-L., Dowey, P., Figueroa Pilz, F., Courtois, L., Taylor, K. and Lee, P. 2017. Correlative Multi-scale Imaging of Shales: A Review and Future Perspectives. Geological Society Special Publication, volume 454

Ma, L., Taylor, K., Dowey, P., Courtois, L., Gholinia, A. & Lee, P. 2017. Multi-scale 3D characterisation of porosity and organic matter in shales with variable TOC content

and thermal maturity: Examples from the Lublin and Baltic Basins, Poland and Lithuania. Abstract accepted in International Journal of Coal Geology

Marschall, P., Keller, L., Giger, S.B., and Becker, J. 2016. Microstructural insights into the petrophysical characteristics of indurated clays. pp. 191–198 in: Filling the Gaps – from Microscopic Pore Structures to Transport Properties in Shales (T. Scha¨fer, R. Dohrmann, and H.C. Greenwell, editors). CMS Workshop Lectures Series, 21, The Clay Minerals Society, Chantilly, Virginia, USA.

Milliken, K. L., and R. M. Reed, 2010. Multiple causes of diagenetic fabric anisotropy in weakly consolidated mud, Nankai accretionary prism, IOPD Expedition 316: Journal of Structural Geology, v. 32, pp. 1887–1898, doi:10 .1016/j.jsg.2010.03.008.

Milner, M., R. McLin, and J. Petriello, 2010. Imaging texture and porosity in mudstones and shales: Comparison of secondary and ion milled backscatter SEM methods: Canadian Unconventional Resources and International Petroleum Conference, Calgary, Alberta, Canada, October 19–21, 2010, Canadian Society for Unconventional Gas/ Society of Petroleum Engineers Paper 138975, 10 p

Modica, C.J and Lapierre, S.G. 2012. Estimation of kerogen porosity in source rocks as a function of thermal transformation: Example from the Mowry Shale in the Powder River Basin of Wyoming. Association of Petroleum Geologists Bulletin, 96, pp.87-108.

Montgomery, S.L., Jarvie, D.M., Bowker, K.A., Pollastro, R.M., 2005. Mississippian Barnett Shale, Fort Worth basin, north-central texas: Gas-shale play with multi-trillion cubic foot potential, AAPG Bulletin, 89 (2), pp. 155-175. DOI: 10.1306/09170404042

Kaufhold, S., Grathoff, G., Halisch, M., Plo¨tze, M., Kus, J., Ufer, K., Dohrmann, R., Ladage, S., and OstertagHenning, Ch. 2016. Comparison of methods for the determination of the pore system of potential German gas shale. pp. 163–189 in: Filling the Gaps – from Microscopic Pore Structures to Transport Properties in Shales (T. Scha¨fer, R. Dohrmann, and H.C. Greenwell,

Klaver, J., Hemes, S., Houben, M., Desbois, G., Radi, Z., and Urai, J.L. 2015. The connectivity of pore space in mudstones: insights from high-pressure Wood's metal

injection, BIB-SEM imaging, and mercury intrusion porosimetry. Geofluids, 15, 577–591.editors). CMS Workshop Lectures Series, 21, The Clay Minerals Society, Chantilly, Virginia, USA

Kwon, O., Herber, B.E. and Kronenberg, A. K. 2004. Permeability of illite-bearing shale: 2. Influence of fluid chemistry on flow ad functionally connected pores, Journal of Geophysical Research, B10206, doi:10,.1029/2004B003055

Raji, M., Grocke, D.R, Greenwell, H.C., Gluyas, J.G., Cornford, C., 2015.The effect of interbedding on shale reservoir properties. Marine and Petroleum Geology 67, pp.154-169.

Reitsema, R. H. 1983. Geochemistry of North and South Brae areas, North Sea. In: Brooks, J. (ed) Petroleum Geochemistry and Exploration of Europe, Geological Society, London, Special Publication, 12, 203-212.

Rexer, T.F.T., Benham, M.J., Aplin, A.C., Thomas, K.M., 2013. Methane Adsorption on Shale under Simulated Geological Temperature and Pressure Conditions, Energy & Fuels, 27 (6), pp. 3099-3109. DOI: 10.1021/ef400381v

Roberts, M. J. 1991. The South Brae Field, Block 16/7a, U.K. North Sea. In: Abbotts, I. L. ed., United Kingdom Oil and Gas Fields 25 Years Commemorative Volume. Geological Society, London, Memoir, 14, pp.55-62

Robinet, J.C., Sardini, P., Siitari-Kauppi, M., Pret, D., and Yven, B. 2015. Upscaling the porosity of the Callovo-Oxfordian mudstone from the pore scale to the formation scale; insights from the 3H-PMMA autoradiography technique and SEM BSE imaging. Sedimentary Geology, 321, pp.1–10

Partington, M.A., Mitchener, B.C., Milton, N.J., Fraser, A.J., 1993. Genetic sequence stratigraphy for the North Sea Late Jurassic and early Cretaceous: distribution and prediction of Kimmeridgian-Late Ryazanian reservoirs in the North Sea and adjacent areas, in: Parker, J.R. (Ed.), Petroleum Geology of Northwest Europe: Proceedings of the 4th Conference on Petroleum Geology of NW. Europe, at the Barbican Centre, London. Geological Society, London, pp.347-370

Passey, Q.R., Bohacs, K.M., Esch, W.L., Klimentidis, R., Sinha, S., 2010. From oil-prone rock to gas-producing shale reservoir—geological and petrophysical characterization of unconventional shale-gas reservoirs. Society of Petroleum Engineers Paper 131350. 29 pp.

Pearson, M.J., Watkins D., Pittion J-L., Caston, D. and Small, J.S. 1983. Aspects of burial diagenesis, organic maturation and palaeothermal history of an area in the South Viking Graben, North Sea, 161- 173 in: Petroleum Geochemistry and the Exploration of Europe, Brooks, J., ed., Blackwell, Oxford.

Peters, K.E., Walters, C.C. and Moldowan, J.M., 2005. The Biomarker Guide, 2nd edition, Cambridge University Press, Cambridge, UK.

Pitman, J. K., L. C. Price, and J. A. LeFever, 2001. Diagenesis and fracture development in the Bakken Formation, Williston Basin: Implications for reservoir quality in the middle member: U.S. Geological Survey Professional Paper 1653, 19 p.

Pittman, E. D., 1979. Porosity, diagenesis and productive capability of sandstone reservoirs, in P. A. Scholle and P. R. Schluger, eds., Aspects of diagenesis: SEPM Special Publication 26, pp. 159–173

Pytte, A. M., and Reynolds, R. C., 1988. The thermal transformation of smectite to illite, in N. D. Naeser and T. H. McCulloh, eds., Thermal histories of sedimentary basins: New York, Springer-Verlag, pp. 133–140.

Romero-Sarmiento, M.-F., Ducros, M., Carpentier, B., Lorant, F., Cacas, M.-C., Pegaz-Fiorent, S., Wolf, S., Rohais, S., Moretti, I. 2013. Quantitative evaluation of TOC, organic porosity and gas retention distribution in a gas shale play using petroleum system modeling: Application to the Mississippian Barnett Shale. Marine and Petroleum Geology, 45, pp.315-330.

Schaefer, R.G., Schenk, H.J. and Harms, R. 1990. Determination of gross kinetic parameters for petroleum formation from Jurassic source rocks of different maturity levels by means of laboratory experiments. Advances in Organic Geochemistry, 3, 16, I-3, pp.115-120.

Schettler Jr., P.D. and Parmely, C.R. 1991. Contributions to total storage capacity in Devonian shales, Society of Petroleum Engineers, 23422, 9.

Schieber, J., 2010. Common themes in the formation and preservation of porosity in shales and mudstones—illustrated with examples across the Phanerozoic. Society of Petroleum Engineers Paper 132370. 12 pp.

Schlakker,A., Csizmeg, J., Pogácsás, G. &Horti, A., 2012. Burial, Thermal and Maturation History in the Northern Viking Graben (North Sea).American Association of Petroleum Geologists Search and Discovery Article #50545.Poster presentation at American Association of Petroleum Geologists International Convention and Exhibition, Milan, Italy, October 23-26, 2011.

Schurig, C., Schrank, T., Mu¨ller, C.W., Ho¨schen, C., Lugmeier, J., Pohl, L., and Ko¨gel-Knabner, I. 2016. Spatially resolved quantification by nanosims of organic matter sorbed to (clay) minerals. in: Filling the Gaps – from Microscopic Pore Structures to Transport Properties in Shales (T. Scha¨fer, R. Dohrmann, and H.C. Greenwell, editors). CMS Workshop Lectures Series, 21, The Clay Minerals Society, Chantilly, Virginia, USA. pp. 45–51.

Sondergeld, C. H., R. J. Ambrose, C. S. Rai, and J. Moncrieff, 2010. Microstructural studies of gas shales: Society of Petroleum Engineers Unconventional Gas Conference, Pittsburgh, Pennsylvania, February 23–25, 2010, SPE Paper 131771, 17.

Turner, C. C., Cohen, J. M., Connel J. R. and Cooper, D. M. 1987. A depositional model for the South Brae oilfield. In: Brooks, J. & Glennie, K. W. ed., Petroleum geology of North West Europe,London, Graham and Trotman, 853-864.

Welch, N., Crawshaw, J., and Boek, E. 2016. Multi-scale imaging and transport properties in shales from experiments and molecular dynamics simulations. Pp. 87–103 in: Filling the Gaps – from Microscopic Pore Structures to Transport Properties in Shales (T. Scha¨fer, R. Dohrmann, and H.C. Greenwell, ed., CMS Workshop Lectures Series, 21, The Clay Minerals Society, Chantilly, Virginia, USA.

Yang, Y.L. and Aplin, A.C. 2007. Permeability and petrophysical properties of 30 natural mudstones. Journal of Geophysical Research-Solid Earth, 112(B3).

Chapter 7: The Effect of Demineralization on Isolated Kimmeridge Clay Kerogens, North Sea and Isolated Kerogens of Lower Lias Limestone-Shale Sequences

This chapter is based on a paper in preparation for submission to Journal of Unconventional Resource Technology: Raji, M., Gröcke, D. R., Greenwell, C. H. and Cornford, C.

In this chapter, the interaction between the kerogens and the inorganic mineral matrix during pyrolysis is investigated to understand how mineral matter may affect the quality and quantity of organic matter, the kerogen type, thermal maturation and the generative potential of the Kimmeridge Clay Formation. A study of the changes in the physical and chemical properties of kerogen in source rocks enables a better understanding of the role of kerogen in hydrocarbon generative potential.

7.1: Abstract

Rock-Eval pyrolysis and organic petrographic analysis of mature whole-rock samples and isolated kerogen from the Upper Jurassic Kimmeridge Clay Formation, North Sea, were used to better understand the effect of demineralisation on the quality of organic matter, kerogen type, maceral composition, thermal maturation and the generative potential. The effects were evaluated based on whole-rock and isolated kerogen results. Comparisons were made between UK onshore field samples from Liassic outcrops in Dorset, Somerset and Glamorgan (South Wales) and international standards (Kimmeridge Clay from Kimmeridge Bay (Dorset). These source rocks are characterised by varying amounts and quality of organic matter, kerogen types with various degrees of thermal maturation. Comparisons were made between the offshore and onshore whole rock samples and the effects of the mineral matrix on isolated kerogen during maturation were investigated from laboratory pyrolysis data of the same set of samples. Interpretation from geochemical data was corroborated by microscopic examination.

The average total organic carbon (TOC) content of the North Sea samples is > 2 wt.% in the whole rock, and > 50 wt.% in the isolated kerogen samples; the kerogen is

primarily a mix of Type I and Type II based on Rock-Eval pyrolysis. Petrographic analyses of the isolated kerogens show a combination of marine liptinites (bituminite and alginite) and terrestrial organic matter (vitrinite and inertinite). The distribution of kerogen types is similar in both the isolated kerogen and the whole rock samples suggesting that mineral dissolution has had no effect on the relative abundance of macerals.

In the outcrop samples, on average, higher TOC values are recorded for the laminated and blocky mudstone and bioturbated marl whereas lowest TOC values of 0.77 wt.% with high carbonate content is recorded for the limestone, and an average 55 wt.% for the isolated kerogen samples. A plot of Hydrogen Index (HI) versus T_{max} indicates that both the whole rock and the isolated kerogen is mainly Type I containing well-preserved alginite and Type II containing bacterially degraded algal kerogen. The mineral matrix has a significant effect on the relative quantity and quality of the organic-richness, but no effect on the kerogen types. According to the carbon isotope analyses of the kerogens, the δ^{13}Corg values range from -29.61 ‰ to -25.84 ‰, with a mean value of -28.94 ‰ and show a predominant marine origin for the organic matter with a minor contribution from terrestrial material.

Recorded T_{max} and HI values for both isolated kerogens and whole-rock in the North Sea range between 423-454 ˚C (averaging 438 ˚C), and 235-255 mgHC/g TOC. For the outcrop samples, $T_{max\ values}$ range between 414-435 ˚C (averaging 427˚C), and HI values range between 332-768 mgHC/g TOC. The recorded values in both sets of samples suggest there is no significant effect from the HCI/HF treatment used during the process of kerogen isolation from mineral matrix. The T_{max} and vitrinite reflectance measurements place the two sample sets within the early to late oil maturity window, and indicates that generated oil is still retained within both the organic-rich shale and in the isolated kerogen matrix. For the outcrop samples, TOC and Rock-Eval pyrolysis data show that the sediments are good potential source rocks, but they are immature with a slight progressive increase in maturity from south (Dorset) to north (Glamorgan).

7.2: Introduction

Varying degrees of physical and chemical metabolic decomposition and transformation of dead organisms result in the formation of sedimentary organic matter (OM) that is preserved in sediments (Durand, 1980). Kerogen is the insoluble part of this sedimentary OM, and hydrocarbon (oil and gas) is generated from the kerogen (Durand and Nicaise, 1980). Source rocks that are characterized by hydrogen-rich kerogen produce oil (and possibly gas upon further maturation); whereas those with hydrogen-poor kerogen yield only gas (Horsfield and Douglas, 1980). The transformation process involved in the conversion of kerogen to hydrocarbon is accelerated by increased depth of burial, temperature, pressure, and duration of heating. The type of hydrocarbon, oil or gas, that a source rock generates, depends largely on the type of kerogen, the chemical nature of the original organic matter, and the degree of maturation.

Previously, the evaluation of the hydrocarbon source potential of kerogen has been carried out using both geochemical and organic petrographic techniques in a large number of basin-scale studies, e.g., Rimmer et al., (2004); Johannes et al. (2006); Yalcin and Altunsoy (2006); East et al., (2012); Bernard and Horsfield, (2014); Fishman et al., (2015); Furmann et al., (2015); Hackley et al., (2016); Hackley and Cardott, (2016). Several other analytical techniques for investigating kerogen type (e.g., optical characterisation, pyrolysis, geochemical and elemental composition), and degree of maturation (e.g., spore coloration and vitrinite reflectance) have been developed over the years. The initial interpretation of Rock-Eval II pyrolysis, as established in the 1980s by Espitalié and Marquis (1985), has been updated by subsequent studies e.g., Jarvie, (2001); Sykes and Snowdow, (2002); Sykes and Johansen, (2003); Dahl et al., (2004); Akinlua et al., (2005); Petersen, (2006); Kim et al., (2007); Marchand et al., (2008); Poot et al., (2009); Riboulleau et al., (2011); Boussafir et al., (2012); Carrie et al., (2012); Pillot et al., (2013); Saenger et al., (2013); Stanley et al., (2014); King, (2015); Romero-Sarmiento et al., (2016). These studies used the application of Rock-Eval pyrolysis for effective evaluation of source rocks for a better understanding of kerogen types, level of thermal maturation and hydrocarbon generation capacity of the source rocks being investigated. The use of Rock-Eval pyrolysis in the

determination of kerogen kinetics for basin modelling has been described extensively in the literature (e.g., Jarvie, 1991; Burnham, 1994; Pelet, 1994; Johannes et al., 2006, 2007; Khasaei and Eftekhari, 2007). The technique has also been widely compared with the hydrous pyrolysis method (Langford and Blanc-Valleron, 1990; Behar et al., 1997; Behar et al., 2001; Lewan and Ruble, 2001; Behar et al., 2010).

More recent work on Rock-Eval 6 pyrolysis has focused on characterising OM in soils and recent sediments (Disnar et al., 2003; Sanei et al., 2005; Sebag et al., 2006; Copard, et.al., 2006; Johannes and Veski, 2007; Carrie et al., 2012; Delarue et al., 2013; Hare et al., 2014). Stepwise pyrolysis has been proposed as a superior method for characterising mixed OM in soils (Hetényi and Tóth, 2005). In studies of recent sediment, the effect of mineral matrix by kerogen isolation using HCl/HF pre-treatment has been reported (Dembicki, 1992; Tambach et al., 2009); where absorption of organic matter by the mineral matrix results in a significant upward shift in T_{max} due to a release of exothermic energy by pyrolysis of OM. These influences were attributed to the release of OM retained by the mineral matrix; the associated mineral stabilizes the OM relative to bulk kerogen and modifies its pyrolysis in rock or soil samples (Tambach et al., 2009).

Rock-Eval data report T_{max} values (the temperature of the S_2 peak maximum yield) as a maturity parameter and comparisons have been made between T_{max} and vitrinite reflectance (Bostick and Daws, 1994; Gentzis et al., 1993) and other maturity parameters (Boudou, 1984; Riediger, 1993; Snowdon, 1995, Banerjee et al., 1998; Potter, 1998; Cornford and Kelly, 2002; Kalkreuth et al., 2002; Petersen et al, 2013; Rippen et al., 2013; Pernia et al., 2015). These comparisons shows good correlation between T_{max} and vitrinite reflectance (%Ro); OM may have higher T_{max} values at a certain level of thermal maturity, and thus be used as a good maturation parameter in Type II and III kerogens.

The main objective of this study is to better understand the effect of kerogen isolation by HCI/HF treatment on the mineral matrix in mature organic-rich shale using total organic carbon (TOC), Rock-Eval pyrolysis and carbon isotope data, together with organic petrography. The results obtained by the comparison of the whole rock and

isolated kerogen were used to assess demineralisation effects on organic-richness, kerogen type (source rock quality and hydrocarbon potential), and maturation of Kimmeridge Clay Formation samples from the UK North Sea and Liassic outcrops in Dorset, Somerset and Glamorgan. The integration of TOC/Rock-Eval/isotope data from both whole rock and isolated kerogen samples with petrographic data enables a successful characterisation of these source rocks by relating OM amounts and types with the level of thermal maturation and the effect of demineralisation.

7.3: Geologic Setting

7.3.1: The Upper Jurassic Kimmeridge Clay Formation, South Viking Graben, North Sea.

The shales in the Upper Jurassic to Lower Cretaceous Kimmeridge Clay Formation have been studied extensively as a major source rock for conventional North Sea oil and gas (Bernard et al., 1981; Bernard and Cooper, 1981; Goff, 1983; Cooper and Barnard, 1984; Cornford, 1984, Cooper and Bernard, 1995; 1998; Kalkreuth et al., 2002), with further potential as an unconventional hydrocarbon reservoir (Cornford et al., 2014; Raji et al., 2015). The South Viking Graben is located within the United Kingdom (UK) and Norwegian sectors of the northern North Sea and is bounded by the Shetland Platform to the west and the Utsira High to the east (Figure 7-1).

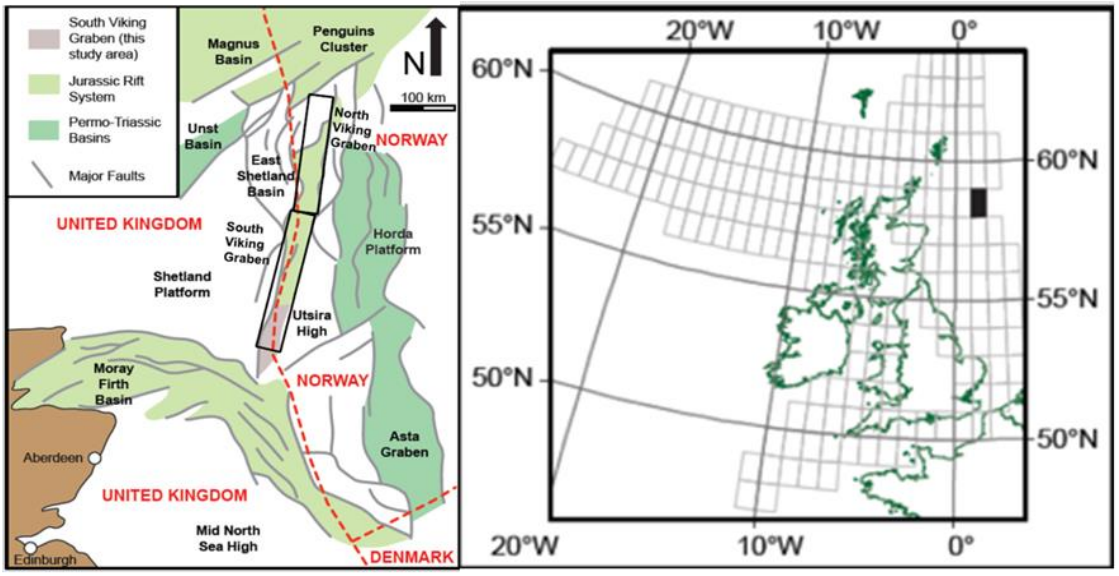

Figure 7-1: Structural elements of the North Sea showing the framework of the Viking Graben (modified from Dominguez, 2007) with inset of UK Quadrant 16 showing the location of wells studied (modified from DECC, 2013).

In the South Viking Graben area, dark olive-grey, black to dark brown, calcareous to non-calcareous, carbonaceous mudstones range in age from Volgian to Ryazanian (Cornford, 1984; Cornford and Brookes, 1989; Cooper et al., 1995). These shales accumulated in a restricted marine embayment of the Boreal Seaway in the north during a period of major extensional faulting leading to the formation of the three main North Sea grabens (Glennie, 1986; Cornford and Brookes, 1989; Cooper et al., 1995; Erratt et al., 2010). Sediment accumulation followed the widespread subsidence that occurred during the late Jurassic to early Cretaceous rifting episodes. With the closing of the Boreal–Tethyan connection, high sedimentation rates, elevated organic matter productivity and increased water depths all promoted stratified anoxic bottom waters (Cornford, 1998). With greatly improved organic matter preservation, this resulted in the formation of the thick, organic-rich shales to form the Kimmeridge Clay (Cornford and Brookes, 1989; Tyson, 2004). Rapid subsidence and burial favoured the maturation of the accumulated source rocks with oil generation beginning in the Cretaceous and peak generation during the Tertiary (Cornford and Brookes, 1989).

7.3.2: The Lower Jurassic (Liassic) of South-West Britain.

In this study, adjacent limestone and shales were collected from several outcrops and cliffs in south-west England and south Wales (Figure 7-2). The Lower Lias (Jurassic) of South-west Britain encompasses the marine limestone-shale sequence, deposited some 200Ma-180Ma, which crops out extensively from Northern England (Yorkshire) to south-west England (Somerset) and some parts of southern South Wales (Figure 7.2). The sequence is characterised by a broad range of basinal facies representing a diverse environment (Cornford and Douglas 1980; Hesselbo and Jenkyns, 1995; Callomon and Cope, 1995; Simms et al., 2004) collectively referred to as the Lias Group (Cox et al., 1999). Several authors such as Huc, 1976; Tissot et al., 1971; Hagemann, 1975; Littler et al., 2010 have investigated organic geochemistry of the Lias Group.

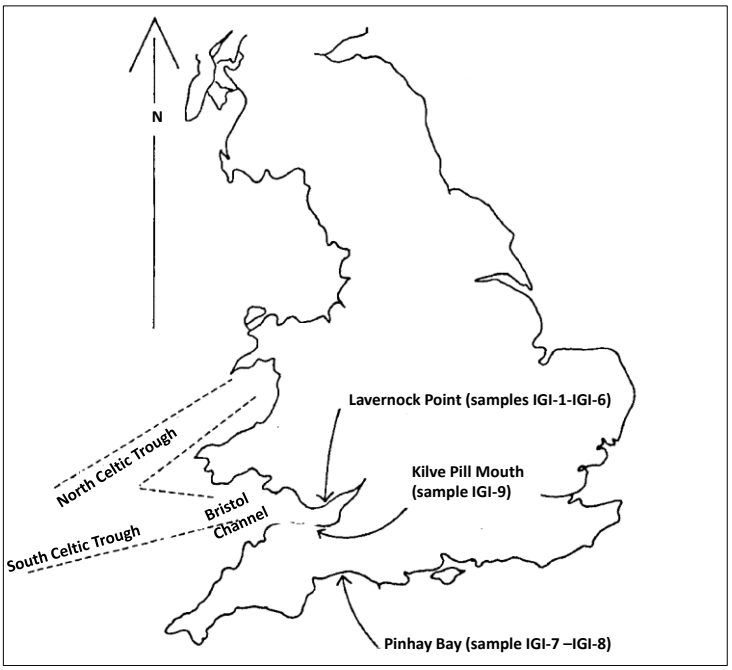

Figure 7-2: Map of England and Wales showing sample localities, and the trend of the Lower Jurassic (Liassic) outcrop.

These studies have shown the sediments to be immature at outcrops (Hagemann, 1975), though, higher maturities have been reported in the down-faulted graben structures (Goff, 1983). The Lias Group was deposited in a series of wide and shallow epeiric (intracontinental) basins and interconnected shelf areas, creating local variations in sedimentary facies (Cornford and Douglas 1980; Simms et al., 2004).

Sedimentation was controlled by a series of interlocking basins and swells. Basins are areas of negative relief formed by relatively rapid subsidence in which thicker shale sections are dominant (Hallam, 1960; 1968; Cornford and Douglas, 1980; Cornford, 1986; Simms et al., 2004). Swells are tectonically broader areas ofpositive relief formed by comparatively slow subsidence on which a reduced section, often with abundant carbonates is deposited. Basins are generally characterized by argillaceous sediments, and swells by calcareous or arenaceous sedimentation, condensed sequences or non-deposition (Sellwood et al., 2000).

These basal Liassic facies are characterised by a background of slowly depositing argillaceous sediments, interspersed with periods of more rapid limestone deposition giving a characteristic 'limestone-shale' sequence of discrete beds on a decimetre scale with local development of carbonate nodules (Duff et al., 1992; Sellwood et al., 2000). Sedimentation of the basinal Lias has been extensively studied and reviewed by Hallam (1960, 1964, 1984), and placed in a regional context (Sellwood et al., 2000; Hallam, 1975; Hallam and Sellwood, 1976; Hesselbo and Jenkyns. 1998). Climate and sea level have been described as the two major environmental factors that influence the Lower Jurassic facies (Jenkyn et al., 2002; Simms et al., 2004; Hesselbo et al., 2004).

The climate-driven model suggests climatic fluctuations in the depositional environment, evidenced by series of micritic and occasionally bioclastic limestone grading via bioturbated marl to black blocky or finely laminated mudstone (Samples No: IGI- 5, 7, 8 and 9). The bioclastic limestones were deposited in a more oxygenated environment with higher energy, finely laminated shale were deposited in a more anoxic environment, whereas the bioturbated marls (Samples IGI-4 and IGI-6) reflect a transitional environment (Cornford and Douglas 1980). In such a situation both terrestrial and marine influence would be expected with relatively rapid lateral changes in facies. The widespread facies variation within the Lias Group is also influenced by eustatic sea-level changes in the Lower Jurassic (Simms et al., 2004).

7.4: Sampling and Methods

7.4.1: Sampling

For the North Sea, a total of 27 samples were collected from cores retrieved from 10 wells drilled within UK Quadrant 16 of the South Viking Graben of the North Sea (Figure 7-1; Tables 7-1 and 7-2). These core samples were made available by the British Geological Survey at their core storage facility in Nottingham. The samples are predominantly comprised of black-olive-grey, organic-rich, marine clastic mud rocks, with some interbedded thin silt and sand layers. Samples were selected to cover a range of depths and hence maturities, and a range of mudstone types potentially equating to different amounts and types of organic matter. An average of 120 g of each sample was split and used for kerogen isolation, TOC, Rock-Eval, carbon isotope analysis and organic petrography.

Eight samples were collected from outcrops and cliff exposures (Figure 7-2; Table 7-3 and 7-4). The Lavernock Point samples (IGI-2, IGI-3, IGI-5 and IGI-6) were taken from the cliff face 200 m west of Lavernock Point in Glamorgan (Figures 7-2 and 7-3a), and represented limestone with faint banding and blocky and laminated mudstone. The Pinhay Bay samples (IGI-7, IGI-08) were collected as examples of the blocky and laminated mudstone facies from the limestone-shale-limestone cycles to the west of Lyme Regis, Dorset (Figures 7-2 and 7-3b). The Kilve Pill Mouth sample was taken from a cliff below Quantock's Head in West Somerset (Figures 7-2 and 7-3c). An average of 200 g of each sample was split and used for TOC, Rock-Eval, kerogen isolation, organic petrographic and carbon isotope analysis.

Table 7-1: TOC and Rock-Eval pyrolysis data for 27 whole-rock core samples of the Kimmeridge Clay Formation from South Viking Graben, North Sea.

Well	Sample name	Top-depth (m)	TOC (wt. %)	S_1 (mgHC/g)	S_2 (mgHC/g)	S_3 (mgHC/g)	S_1/TOC (Norm. oil content)	T_{max} (°C)	HI (mg/gTOC)	OI (mg/gTOC)	PI ($(S_1/S_2+S_2))/2$)	Calculated %R_o (from T_{max})
16/12b- 6	4,683	MR1	4.72	1.77	7.38	0.31	38	442	156	7	0.19	0.8
16/12b- 6	4,681	MR2	2.88	1.59	2.71	0.2	55	442	94	7	0.37	0.8
16/12b- 6	4,706	MR3	5.03	2.52	6.35	0.3	50	440	126	6	0.28	0.76
16/12b- 6	4,688	MR4	3.68	1.66	3.5	0.3	45	443	95	8	0.32	0.81
16/12b- 6	4,693	MR5	4.43	1.74	5.13	0.28	39	438	116	6	0.25	0.72
16/08c- 13	4,894	MR6	6.49	2.54	6.43	0.64	39	451	99	10	0.28	0.96
16/08c- 13	4,906	MR7	5.82	2.38	5.11	0.27	41	451	88	5	0.32	0.96
16/08c- 13	4,907	MR8	3.85	1.16	3.25	0.28	30	454	84	7	0.26	1.01
16/08b- 3	4,007	MR9	7.13	7.49	26.5	0.4	105	423	372	6	0.22	0.45
16/08b- 3	4,006	MR10	8.89	5.8	52.98	0.3	65	435	596	3	0.1	0.67
16/12a- 18Z	4,085	MR11	5.89	6.5	26.68	0.34	110	439	453	6	0.2	0.74
16/12a- 18Z	4,100	MR12	5.95	3.75	18.43	0.29	63	435	310	5	0.17	0.67
16/17-5	3,680	MR13	2.7	1.22	4.45	0.33	45	427	165	12	0.22	0.53
16/17- 5	3,681	MR14	2.77	2.1	7.75	0.31	76	426	280	11	0.21	0.51
16/17-18	3,745	MR15	5.78	10.76	25.54	0.33	186	437	442	6	0.3	0.71
16/17- 18	3,745	MR16	3.33	5.14	7.67	0.33	154	426	230	10	0.4	0.51
16/17- 18	3,738	MR17	3.08	6.93	9.84	0.17	225	437	319	6	0.41	0.71
16/17- 18	3,744	MR18	4.46	5.1	8.66	0.32	114	428	194	7	0.37	0.54
16/17-19	3,597	MR19	8.17	6.31	35.2	0.21	77	433	431	3	0.15	0.63
16/17- 19	3,596	MR20	6.22	4.79	21.73	0.25	77	429	349	4	0.18	0.56
16/17- 19	3,605	MR21	7.48	5.46	27.82	0.38	73	431	372	5	0.16	0.6

Table 7-1 (cont'd): TOC and Rock-Eval pyrolysis data for 27 whole-rock core samples of the Kimmeridge Clay Formation from South Viking Graben, North Sea.

Well	Sample name	Top-depth (m)	TOC (wt. %)	S_1 (mgHC/g)	S_2 (mgHC/g)	S_3 (mgHC/g)	S_1/TOC (Norm. oil content)	T_{max} (°C)	HI (mg/gTOC)	OI (mg/gTOC)	PI ($(S_1/S_2+S_2))/2$)	Calculated %R_o (from T_{max})
16/03b- 8Z	4,283	MR22	4.58	1.78	6.43	0.35	39	445	140	8	0.22	0.85
16/03b- 8Z	4,285	MR23	4.58	1.63	6.6	0.35	36	438	144	8	0.2	0.72
16/07b- 23	4,092	MR24	4.33	2.62	16.26	0.22	61	432	376	5	0.14	0.62
16/07b- 23	4,093	MR25	3.43	1.1	6.67	0.22	32	433	194	6	0.14	0.63
16/08a- 11	4,037	MR26	5.15	3.59	18.53	1.41	70	443	360	27	0.16	0.81
16/08a- 11	4,236	MR27	5.11	3.2	15.85	0.36	63	434	310	7	0.17	0.65

Table 7-2: TOC and Rock-Eval pyrolysis data for 27 isolated kerogens from core samples of the Kimmeridge Clay Formation from South Viking Graben, North Sea.

Well	Sample name	Top-depth (m)	TOC (wt. %)	S_1 (mgHC/g)	S_2 (mgHC/g)	S_3 (mgHC/g)	S_1/TOC (Norm. oil content)	T_{max} (°C)	HI (mg/gTOC)	OI (mg/gTOC)	PI ($(S_1/S_2+S_2))/2$)	Calculated %R_o (from T_{max})
16/12b- 6	4,683	MR1	72.20	18.70	113.22	2.90	26	443	157	4	0.14	0.81
16/12b- 6	4,681	MR2	71.00	37.90	103.25	3.72	53	446	145	5	0.27	0.87
16/12b- 6	4,706	MR3	67.00	36.36	73.18	3.40	54	449	109	5	0.33	0.92
16/12b- 6	4,688	MR4	74.30	32.05	85.38	3.33	43	445	115	4	0.27	0.85
16/12b- 6	4,693	MR5	72.10	33.00	114.60	3.20	46	441	159	4	0.22	0.78
16/08c- 13	4,894	MR6	71.40	32.89	78.15	2.63	46	454	109	4	0.30	1.01
16/08c- 13	4,906	MR7	70.00	24.83	78.06	2.25	35	454	112	3	0.24	1.01
16/08c- 13	4,907	MR8	66.80	28.94	76.05	3.42	43	454	114	5	0.28	1.01

Table 7-2 cont'd): TOC and Rock-Eval pyrolysis data for 27 isolated kerogens from core samples of the Kimmeridge Clay Formation from South Viking Graben, North Sea.

Well	Sample name	Top-depth (m)	TOC (wt. %)	S_1 (mgHC/g)	S_2 (mgHC/g)	S_3 (mgHC/g)	S_1/TOC (Norm. oil content)	T_{max} (°C)	HI (mg/gTOC)	OI (mg/gTOC)	PI ($(S_1/S_2+S_2))/2$)	Calculated %R_o (from T_{max})
16/08b- 3	4,007	MR9	60.20	43.05	242.77	4.16	72	433	403	7	0.15	0.63
16/08b- 3	4,006	MR10	57.60	46.28	229.71	4.28	80	434	399	7	0.17	0.65
16/12a-18Z	4,085	MR11	57.40	52.14	197.61	3.57	91	439	344	6	0.21	0.74
16/12a-18Z	4,100	MR12	60.90	34.11	113.23	4.41	56	437	186	7	0.23	0.71
16/17-5	3,680	MR13	55.30	39.45	174.05	3.78	71	435	315	7	0.18	0.67
16/17- 5	3,681	MR14	52.60	38.75	223.12	4.06	74	429	424	8	0.15	0.56
16/17-18	3,745	MR15	54.90	70.54	168.37	4.86	128	434	307	9	0.30	0.65
16/17- 18	3,745	MR16	56.80	70.88	157.64	3.52	125	432	278	6	0.31	0.62
16/17- 18	3,738	MR17	53.30	105.09	155.29	3.33	197	423	291	6	0.40	0.45
16/17- 18	3,744	MR18	61.60	75.31	166.25	4.68	122	433	270	8	0.31	0.63
16/17-19	3,597	MR19	61.00	33.41	171.95	3.65	55	431	282	6	0.16	0.60
16/17- 19	3,596	MR20	57.00	30.00	165.94	5.67	53	431	291	10	0.15	0.60
16/17- 19	3,605	MR21	60.10	37.35	177.35	4.11	62	432	295	7	0.17	0.62
16/03b- 8Z	4,283	MR22	68.80	23.78	70.54	5.13	35	445	103	7	0.25	0.85
16/03b- 8Z	4,285	MR23	63.50	22.88	86.88	3.55	36	440	137	6	0.21	0.76
16/07b- 23	4,092	MR24	56.40	27.16	136.03	2.64	48	435	241	5	0.17	0.67
16/07b- 23	4,093	MR25	65.40	32.10	143.94	4.47	49	434	220	7	0.18	0.65
16/08a- 11	4,037	MR26	61.20	34.16	165.41	4.58	56	431	270	7	0.17	0.60
16/08a- 11	4,236	MR27	51.90	19.06	135.81	3.48	37	437	262	7	0.12	0.71

Table 7-3: TOC and Rock-Eval pyrolysis results for eight Lower Jurassic (Liassic) whole-rock samples.

Sample name	Sample location	Lithology	Carbonate percentage	TOC (wt. %)	S_1 (mgHC/g)	S_2 (mgHC/g)	S_3 (mgHC/g)	T_{max} (°C)	HI (mg/gTOC)	OI (mg/gTOC)	PI ($(S_1/S_2+S_2))/2$)	$S_{1/TOC}$ Norm. oil content	Calculated %R_o (from T_{max})
IGI-02 (LP-1)	Lavernock Point, Glamorgan	Laminated Limestone	89.18	0.77	0.16	2.56	0.24	435	332	31	0.06	21	0.67
IGI-03 (LP-2)	Lavernock Point, Glamorgan	Blocky Mudstone	16.78	2.96	0.31	9.9	0.76	432	334	26	0.03	10	0.62
IGI-04 (LP-3)	Lavernock Point, Glamorgan	Bioturbated Marl	54.49	2.87	0.59	17.9	0.77	429	624	27	0.03	21	0.56
IGI-05 (LP-4)	Lavernock Point, Glamorgan	Laminated Mudstone	35.55	3.29	0.74	23.25	0.6	429	707	18	0.03	22	0.56
IGI-06 (LP-5)	Lavernock Point, Glamorgan	Laminated Mudstone	62.73	2.46	0.46	13.47	0.62	431	548	25	0.03	19	0.6
IGI-07 (PB-1)	Pinhay Bay, west of Lyme Regis	Laminated Mudstone	15.41	7.73	0.87	37.79	2.22	418	489	29	0.02	11	0.36
IGI-08 (PB-2)	Pinhay Bay, west of Lyme Regis	Blocky Mudstone	16.52	8.09	1.05	49.41	2.3	419	611	28	0.02	13	0.38
IGI-09 (Kilve)	Kilve Pill Mouth, West Somerset	Laminated Marl	47.65	4.35	0.94	33.14	0.95	428	762	22	0.03	22	0.54

Table 7-4: **and Rock-Eval pyrolysis results for eight Lower Jurassic (Liassic) isolated Kerogen samples.**

Sample name	**Sample location**	**Lithology**	**TOC (wt. %)**	**S_1 (mgHC/g)**	**S_2 (mgHC/g)**	**S_3 (mgHC/g)**	**T_{max} (°C)**	**HI (mg/gTOC)**	**OI (mg/gTOC)**	**PI ($(S_1/S_2+S_2))/2$)**	**S_1/TOC (Norm. oil content)**	**Calculated %R_o (from T_{max})**
IGI-02 (LP-1)	Lavernock Point, Glamorgan	Laminated Limestone	46.4	7.27	308.48	4.54	425	665	10	0.02	16	0.49
IGI-03 (LP-2)	Lavernock Point, Glamorgan	Blocky Mudstone	61.4	2.9	224.83	6.45	426	366	11	0.01	5	0.51
IGI-04 (LP-3)	Lavernock Point, Glamorgan	Blocky Mudstone	56	11.89	321.08	7.83	426	573	14	0.04	21	0.51
IGI-05 (LP-4)	Lavernock Point, Glamorgan	Laminated Mudstone	53.6	12.35	411.47	5.29	427	768	10	0.03	23	0.53
IGI-06 (LP-5)	Lavernock Point, Glamorgan	Laminated Mudstone	58.3	11.42	382.57	5.71	425	656	10	0.03	20	0.49
IGI-07 (PB-1)	Pinhay Bay, west of Lyme Regis	Laminated Mudstone	51.6	7.5	235.27	12.5	414	456	24	0.03	15	0.29
IGI-08 (PB-2)	Pinhay Bay, west of Lyme Regis	Blocky Mudstone	52.7	7.07	248.04	9.51	416	471	18	0.03	13	0.33
IGI-09 (Kilve)	Kilve Pill Mouth, West Somerset	Laminated Mudstone	56	16.25	369.37	7.81	422	660	14	0.04	29	0.44

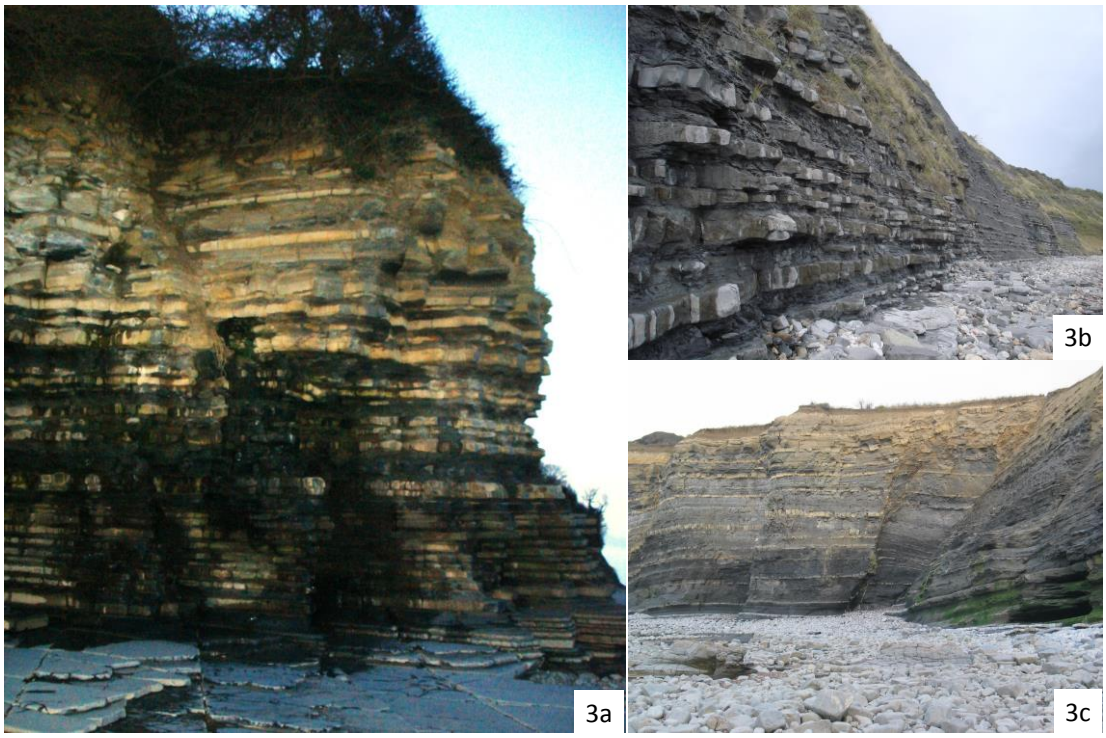

Figure 7-3: Outcrop samples of (A) Lower Lias limestone/shale cycle in Lavernock Point, Glamorgan, (B) blue Lias limestone/shale cycles in Pinhay Bay, Lyme Regis, Dorset, and (C) laminated black shales (upper), and the blocky mid-grey mudstone (lower) in Kilve Pill Month, West Somerset (Images from IGI Ltd).

7.4.2: Methods

The methodologies used for kerogen isolation, total organic carbon/Rock-Eval Pyrolysis, stable isotope and organic petrography analyses have been described in detail in Chapter 2, Section 2.5.3-Section 2.7.1.

7.5: Results and Discussion

7.5.1: Effect on Total Organic Carbon (TOC) and Rock-Eval Pyrolysis on the North Sea.

TOC content and Rock-Eval pyrolysis data were used to determine the effects of demineralisation on source rock quality, kerogen type, generative potential and organic maturation, as established by Tissot and Welte (1984) and Peters (1986). Results from the TOC and pyrolysis of whole rock and isolated kerogen are given in Table 7-1 & 7-2.

For the North Sea , the TOC values for the whole-rock samples (TOC_{rock}) range from 2.7–8.9 wt %, compared to 51.9–74.3 wt % for isolated kerogen ($TOC_{kerogen}$) (Table 7-1 and 7-2). The TOC results suggest that there are significant differences between the whole rock and the isolated kerogen in terms of their organic matter quality. The total amount of organic matter is way higher in the kerogen after the minerals have been removed, this shows the effect of the mineral matrix on organic matter quality. However, the range of $TOC_{kerogen}$ suggests that not all minerals were removed during the demineralization process. Petrographic observations indicate that minerals such as quartz and clay (silicates), and carbonates had been removed, but pyrite remained. This is to be expected since the demineralization process did not include nitric acid (HNO_3) oxidation (often used to remove pyrite), as this procedure can alter the OM, particularly AOM (Tambach et al., 2009).

The Rock-Eval S_1 value is the peak area for the thermally vapourised free hydrocarbon (mg S_1 per g of rock released up to 300 °C during pyrolysis), whereas S_2 values represent the amount of hydrocarbon resulting from the cracking of non-volatile OM in mg per g of rock released over the range of 300–650 °C (Peter, 1986). Heating is undertaken at a rate of 25 °C per min (Peter, 1986). The S_1 yield from isolated kerogen, plus non-reactive minerals (i.e., pyrite) left after the HCl/HF maceration ranges from 19–105 mg HC/g kerogen isolate (average 40 mg HC/g kerogen isolate), whilst the whole rock S_1 values derived from the free oil in the kerogen plus minerals (carbonate, silicates, pyrite) range from 1–10 mg HC/g rock (average: 3.7 mg HC/g rock). Given the difference in the range of S_1 values, It is clear that the HCI/HF treatment shows significant effects on the measured S_1values. These effects are attributed to the release of OM that was retained by the mineral matrix; although it could be argued that the free oil S_1 is trapped in the porosity of the kerogen. This means any S1 adsorbed onto the mineral matrix is liberated during acid maceration, and attaches to the kerogen upon sample drying (Tambach et al., 2009).

Based on the initial free oil yields (Rock-Eval S_1) there is a tendency for the higher TOC samples to retain more of the S_1 yield. Separation of the effects of poor recovery of TOC from the contamination of the isolated kerogen fraction with pyrite is shown

in Figure 7-4. This plot shows the correlation of S_1 yields from the whole-rock pyrolysis with the S_1 yields from the pyrolysis of the isolated kerogens multiplied by the TOC_{rock} value. With 100% kerogen recovery, the S_{1rock}, and the $S_{1kerogen}$ values should be related as follows:

$$S_{1rock} = S_{1kerogen} \times (TOC_{whole} / 100)$$

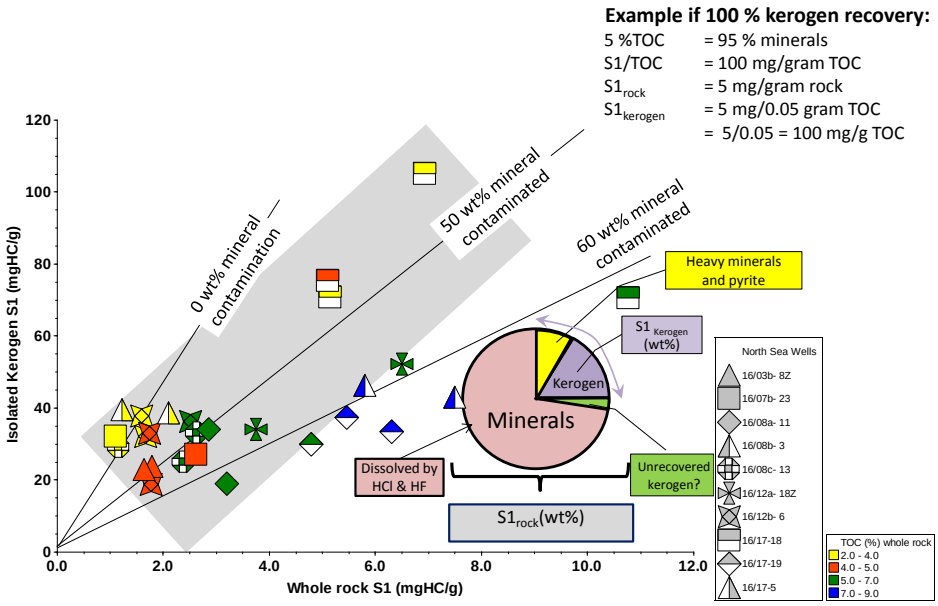

Figure 7-4: Correlation of Rock-Eval S_1 pyrolysate yield for whole-rock samples (mgHC/g) and the S_1 yield for isolated kerogens corrected for TOC enrichment with 100 % kerogen recovery. Note: $S_{1rock} = S_{1kerogen} \times (\%TOC_{rock}/100)$. Note: $S_{1rock} = S_1$ of whole rock and $S_{1kerogen} = S_1$ of isolated kerogen, coloured legend for TOC in whole-rock and symbols for well location.

Lines of similar levels of kerogen recovery or lack of non-reactive (mainly pyrite) are shown and labelled in black (Figure 7-4). Once corrected for TOC enrichment with 100% kerogen recovery (Figure 7-5), an improved correlation is observed, and the scatter is attributed to the degree of kerogen contamination by pyrite. This suggests that low TOC_{rock} samples show better S_1 recovery than high TOC_{rock} samples, this arguably resulting from there being more pyrite (anoxic sulphate reduction) in the high TOC_{rock} samples where anoxia favours organic matter preservation; this would also contribute to a different maceral composition in the more anoxic facies.

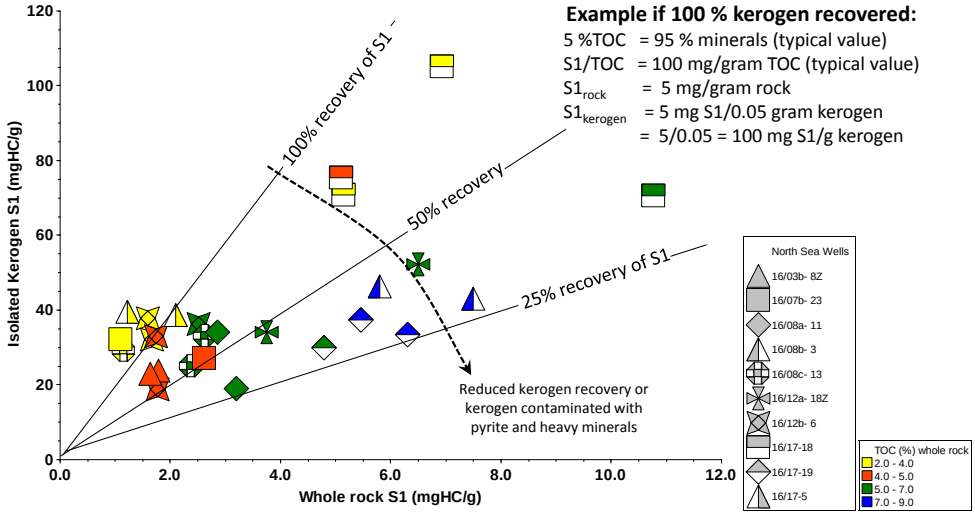

Figure 7-5: A comparison of Rock-Eval S_1 for whole rock samples and isolated kerogens (±pyrite ±heavy minerals) from the same samples implying kerogen recovery.

A similar trend is shown for the equivalent S_2 data (Figure 7-6). Both the S_1 and S_2 TOC-corrected plots (Figures 7-4 and 7-6) suggest that the isolated kerogen fractions are typically contaminated by about 50 % by weight of pyrite . This means that the S_{1rock} yield is carried forward into the $S_{1kerogen}$ fraction but that the total weight of the isolated kerogen fraction is about 5 0% kerogen and 50 % un-reactive minerals (Figure 7-7). The same conclusion can be drawn for the S_{2rock} and $S_{2kerogen}$ yields (Figure 7-6) related as follows: $S_{2rock} = S_{2Kerogen} \times (\%TOC_{rock}/100)$.

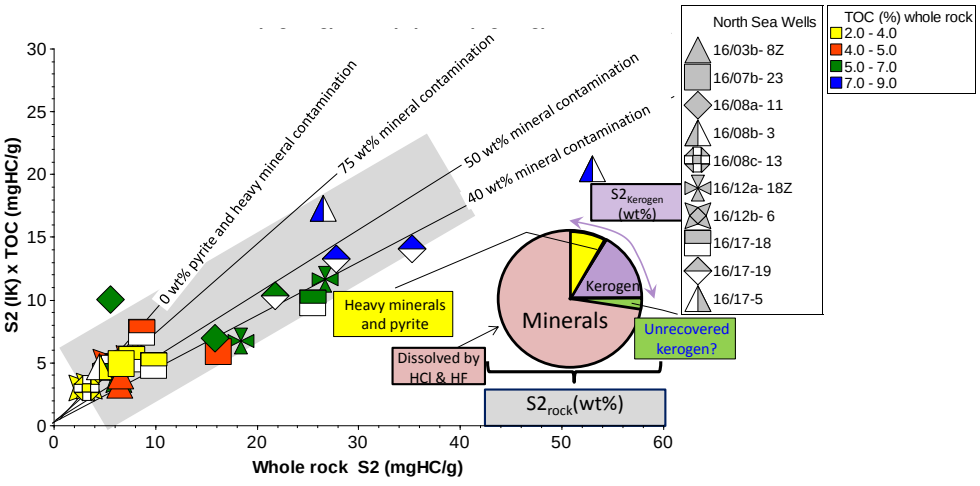

Figure 7-6: Correlation of Rock-Eval S_2 yield (mgHC/g) for whole-rock samples and the S_2 yield for isolated kerogens corrected for TOC enrichment with 100 % kerogen recovery. Note: $S_{2rock} = S_{2Kerogen} \times (\%TOC_{rock}/100)$. $S_{2rock} = S_2$ of whole rock and $S_{2IK} = S_2$ of isolated kerogen, coloured legend for TOC in whole-rock and symbols for well location.

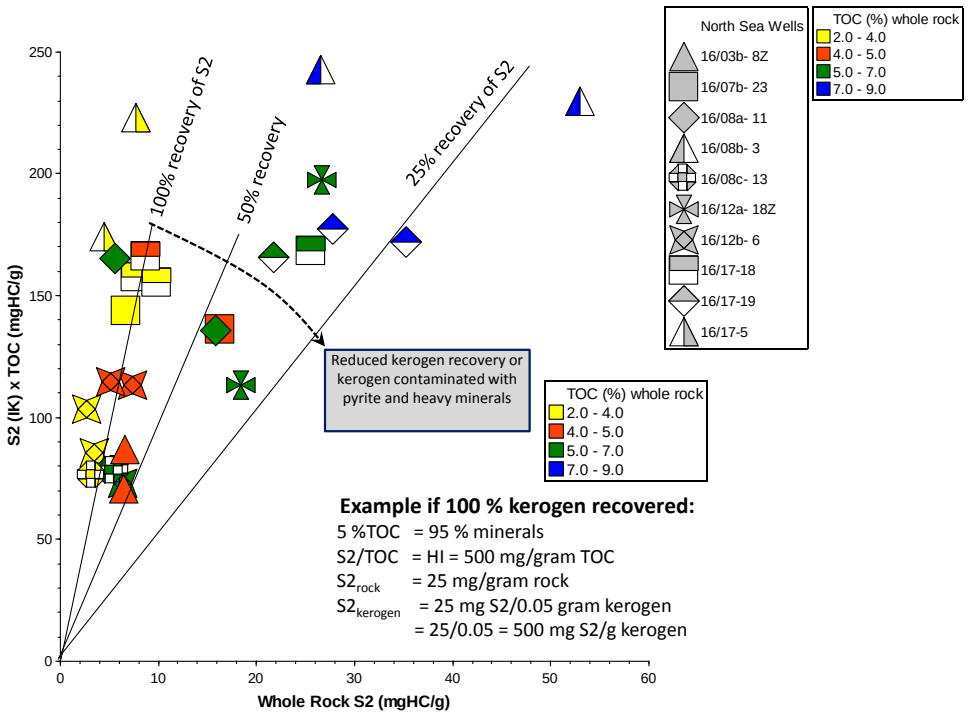

Figure 7.7: A comparison of Rock-Eval S_2 yield (mgHC/g) for whole rock samples and isolated kerogens + pyrite + heavy minerals from the same samples implying kerogen recovery. Note: $S2_{rock} = S2_{Kerogen}$ x (%TOC_{rock}/100). $S2_{rock} = S_2$ of whole rock and $S_2IK = S_2$ of isolated kerogen, coloured legend for TOC in whole-rock and symbols for well location.

The ratio of free hydrocarbons to total organic carbon (S_1/TOC), the normalised oil content (Jarvie, 2012), can be used as an Oil Saturation Index (OSI) to differentiate between immature and mature source rocks (Jarvie and Baker, 1984). Once in the oil window, the S_1 value is only the retained oil, where the expelled oil has left the source rock. In this study, the isolated kerogen OSI ranges from 26–197 mg HC/g TOC (Table 7-1) and the whole-rock values from 30–225 mg HC/g TOC (Table 7-2). The higher S_1/TOC ratios exceeding 100 mg HC/g TOC all appear in samples from well 16/17-18 in both the isolated kerogen and whole-rock samples (Tables 7-1 and 7-2). Saturation threshold for producible liquids direct from fracking mature source rocks is around 100 mgHC/g TOC (Jarvie, 2012). Taking this threshold, indicates high oil saturation in Well 16/17-18 and individual samples from Wells 16/12a-18z and 16/08b-3.

Comparison of the OSI based on the S_1 "free oil" per unit carbon shows remarkably good correlation but with lower values for the isolated kerogen relative to the whole-rock kerogen pyrolysates (Figure 7-8). The oil saturation indices show a strong correlation and are spread with little scatter along a line related to the depth of burial.

Low depth of burial (< 400 m.kb) show OSI values > 70 mg S_1/g TOC, with the deeper samples mainly in the range of 30-70 mg S_1/g TOC, this suggesting expulsion in the deeper samples (Figure 7-8).

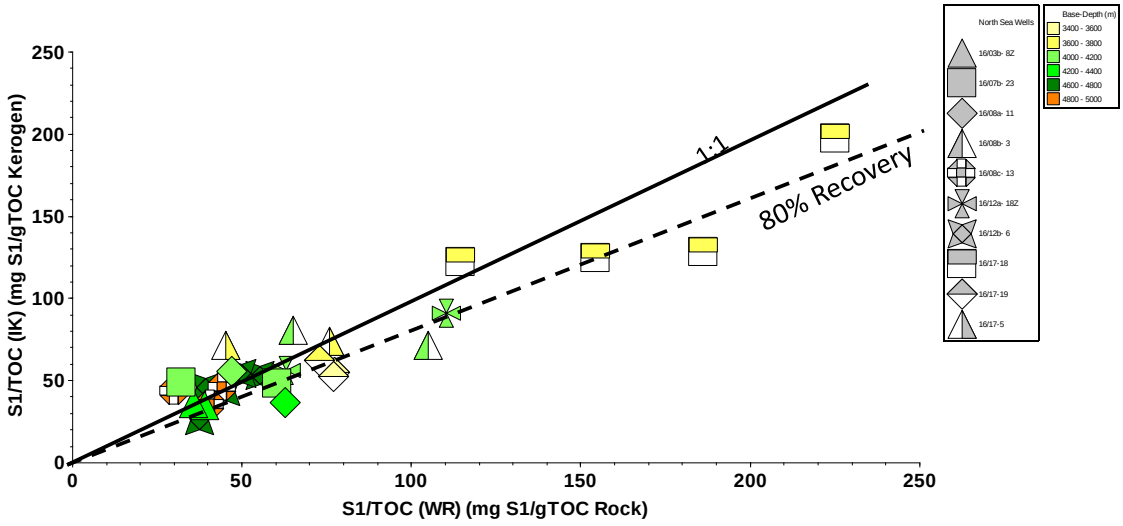

Figure 7-8: A comparison of Rock-Eval Oil Saturation Index (mg S_1/g TOC) for whole rock and isolated kerogens from the same samples.

Since the removal of the mineral matrix has minimal effect on the OSI values, the strong correlation in Figure 7-8 confirms that the free hydrocarbon S_1 yields are mainly adsorbed on kerogen surfaces or trapped within kerogen pores. Any S_1 adsorbed within the mineral matrix will be liberated and attached to the kerogen pores during sample processing. However, a decrease in S_2 values does not correspond with an increase in S_1 values, therefore suggesting it is an open pore system (Cornford et al., 2014; Raji et al., 2015). This supports the findings by others (Jarvie, 2000; 2012; Abrams, 2014; Cornford et al., 2014; Raji et al., 2015).

7.5.2: Effect on Total Organic Carbon Content on the Outcrop Samples

In the whole-rock samples, the mudstones have higher TOC values than the limestone. TOC values for the whole-rock samples range from 0.8-8.1 wt.% with 15.4-89.2 wt.% carbonate contents (Table 7-3). The high calcium carbonate values (89.2 wt.%) recorded in the laminated limestone (IGI-2) are in good agreement with previous results from the same localities (Cornford and Douglas, 1984). The laminated mudstone sampled at two different locations gave TOC contents of 3.29 wt.% (IGI-5) and 2.46 wt. % (IGI-6) for the Lavernock samples and 7.73 wt. % (IGI-7) for the Pinhay

Bay sample (Table 7-3). The homogenous blocky mudstone has a higher TOC content (8.09 wt. %) than the adjacent laminated mudstones. The TOC value of 4.35 wt. % recorded for the laminated marl (IGI-9) is slightly higher than the 2.87 wt. % value for the bioturbated marl (IGI-4). This suggests that laminated sediments accumulated in quiet still water without bioturbation and correlates with their high total carbon content. This also suggests that it is the survival and preservation of the organic matter rather than its rate of supply that controls the ultimate organic content of the sediments. The TOC data reported in Table 7-3 are in units of weight % of rock, but the carbonate content values (column 3) allow the TOC to be calculated on a carbonate-free basis (Figure 7-9B and 7-9C). Correction of the TOC values shows a much smaller spread of values (3.6-9.7 wt.%TOC (CF)) with the marl and limestone values exceeding the TOC (CF) values of the mudstones (Figure 7-9). With the carbonate-free data, TOC (CF) values are still higher in Pinhay Bay in the south than at Lavernock Point in the north, with Kilve giving intermediate values.

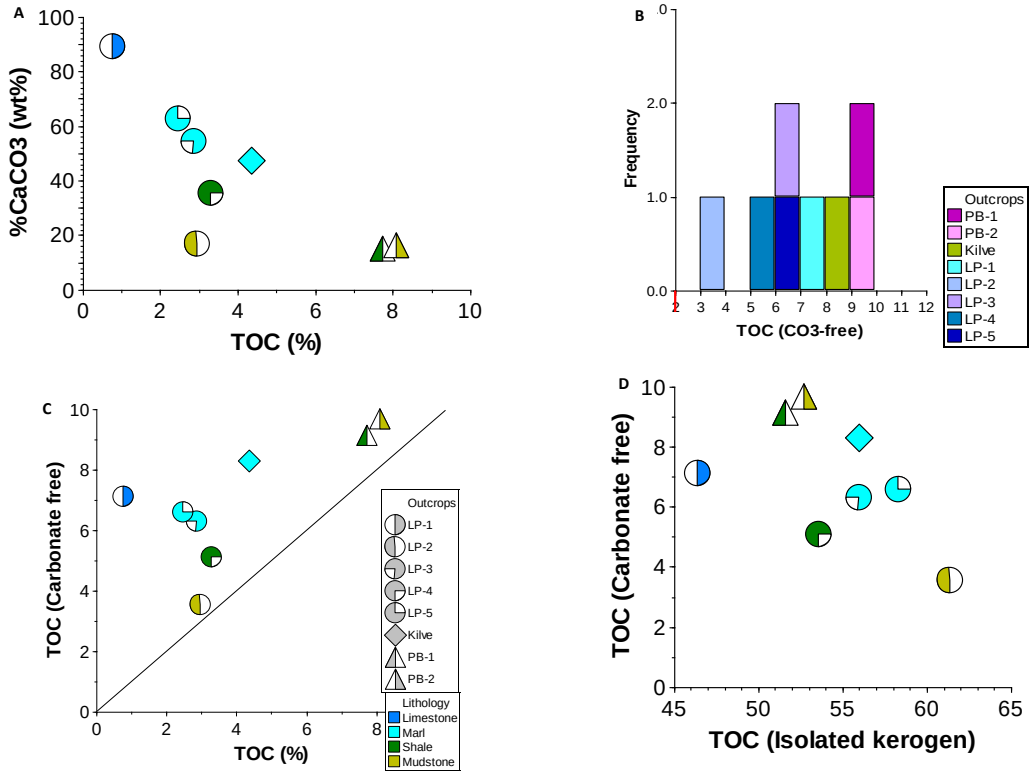

Figure 7-9: Total Organic Carbon (TOC) relationships: (A) whole-rock TOC ($TOC_{(rock)}$) vs. carbonate content and (B) histogram of TOC(CF), (C) TOC_{rock} vs.TOC recalculated on a carbonate-free basis (TOC(CF)) and (D) TOC (CF) vs. TOC of the isolated kerogens ($TOC_{(Kerogen)}$).

As expected, there is evidence of a significant effect from the HF/HCl acid treatment for kerogen isolation, as the TOC content without the minerals is significantly higher than in the whole-rock samples. The isolated kerogen TOC values ($TOC_{(Kerogen)}$) range from 46.40-61.40 wt. % with an average of 54.50 wt. % TOC (Table 7-4). A maturity gradient exists from south (Pinhay Bay) to north (Lavernock Point), the isolated kerogen TOC (IK) is lowest in the south (51.6-52.7 wt.%) and highest in the north (53.6-61.0 wt. %). Lower TOC samples from Lavernock Point (GI-2-IGI-6) have much higher maturities with higher post-depositional sedimentation rates that are indicative of anoxia. If these high sedimentation rates were operative during Liassic deposition, the implied dilution of the kerogen by mineral input could explain the lower preserved TOC values. Using this argument, the Pinhay Bay samples at the Lyme Regis location represent a 'swell' during both syn- and post-sedimentary times, whereas the sample from Lavernock Point location represent more basinal conditions based on the implied sedimentation rates.

I-D basin modelling in the Bristol Channel (Cornford, 1986) based on oil industry drilling (Kammerling et al., 1979) and the sub-Chalk regional unconformity in the Dorset Basin (Stoneley, 1982; Stoneley and Selley, 1991; Underhill and Stoneley, 1998) places maximum burial as a mid-Cretaceous event, some 90 Ma after the basal Lias was deposited. Using Cornford's (1986) burial values for the three locations (1,400 m, 2,400 m and 3,200 m from south to north), the implied gross post-depositional sedimentation rates are 16 m/Ma for Lyme Regis, 27 m/Ma for Kilve, and 36 m/Ma for Lavernock Point. This suggests the gross sedimentation rate is about 2.3 times higher in the basin in the north compared to the swell in the south during the Jurassic and Lower Cretaceous. Assuming similar bioproductivity and preservation for the laminated mudstone depositional environments at all three locations (Table 7-3) with equal amounts of pyrite, then the TOC values of 7.73 wt.% TOC, 4.35 %TOC and 3.29 wt.% TOC from south to north imply a 7.73/3.29 = 2.4 fold increase in sediment dilution for the laminated shales in particular from south to north. These two relative sedimentation rate estimates are in remarkable agreement given the above assumptions and the presence of presumably more rapidly deposited interbedded carbonates. However, based on biostratigraphic subdivisions of the Pinhay Bay, Kilve

Pill Mouth, and Lavernock outcrops, Palmer (1972) suggest the highest sedimentation rates are in Kilve Pill Mouth area.

The correlation of T_{max} with the TOC values shows a positive trend (Figure 7-10b), a trend which continues into more mature samples of isolated kerogens from the Kimmeridge Clay Formation of the South Viking Graben. With the minerals removed (except pyrite), the black trend line is essentially identical to the relatively isolated kerogen (van Krevelen, 1993). The extent to which the measured $TOC_{(Kerogen)}$ falls below that predicted from the trend line (using the sample T_{max} and the gradient (i.e. the residual from the trend line on the $TOC_{(Kerogen)}$ axis) can be taken as an indicator of the presence of pyrite+/- other heavy minerals in the sample (Figure 7-10b).

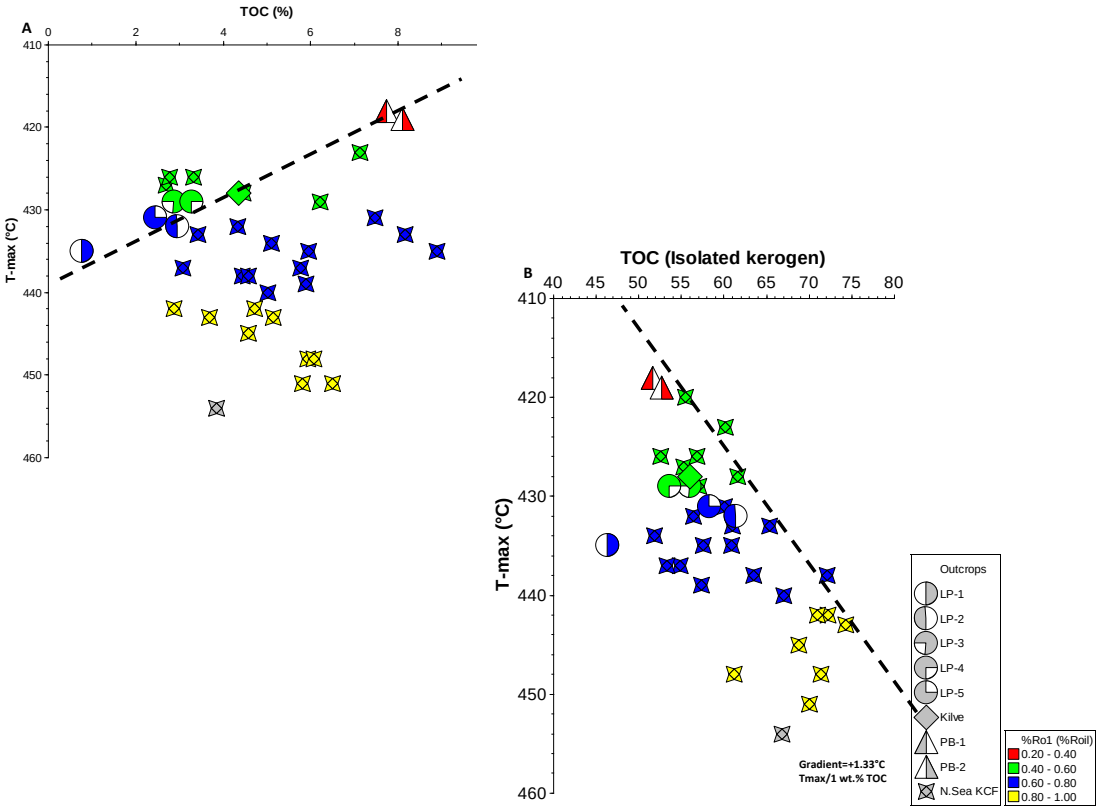

Figure 7-10: Correlations of whole-rock T_{max} values with whole-rock TOC (A) and isolated kerogen TOC (B) illustrating control of sediment dilution (see text). The correlation of T_{max} with the TOC values shows a positive trend, which is continued by more mature samples of isolated kerogens from the Kimmeridge Clay Formation.

7.5.3: Effect on Kerogen Types and Organic Maturation of the North Sea Samples

In this study, Rock-Eval T_{max} and HI values were used as an indicator of both the type of organic matter and maturity (Espitalié et al., 1977). These two parameters can be used to identify relative kerogen type present, the level of thermal maturation and hydrocarbon generative potential (Rimmer, 1993). T_{max} is the temperature at which the S_2 peak reaches its maximum yield in the laboratory and is dependent on the maturity level previously reached in the sub-surface (Espitalié et al., 1977). Recorded T_{max} for both isolated kerogen and whole rock are between 423–454 ˚C (average, ~ 438 ˚C), showing relatively uniform values.

In terms of maturity, the T_{max} values plotted against burial depth place most of the samples within the oil window for both the whole rock and the isolated kerogen (Figure 7-11). On a sample by sample basis, HI values are slightly higher in the whole-rock samples, with values between 84–596 mgHC/g TOC and an average of 255 mg HC/g TOC (Table 7-1) than the HI values for isolated kerogen which range from 103–424 mgHC/g TOC with an average of 235 mgHC/g TOC (Table 7-2). After the HCI/HF treatment, destruction of the mineral matrix has no significant effect on the HI values.

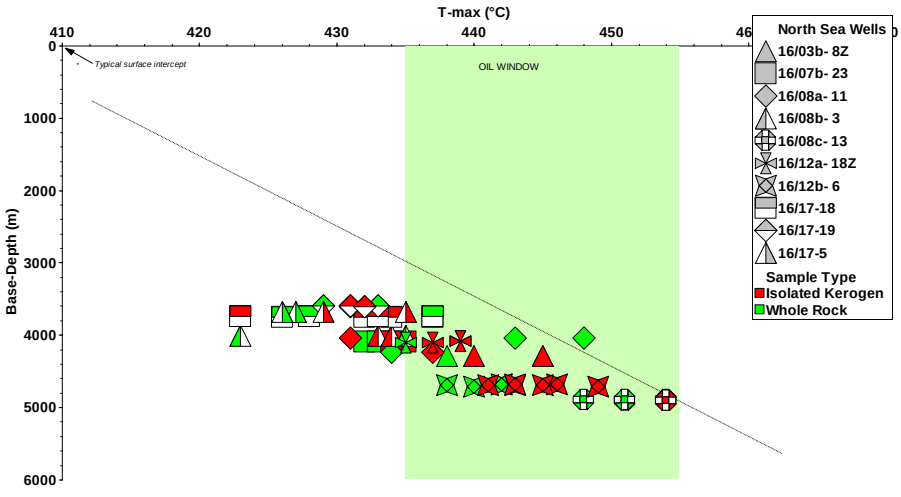

Figure 7-11: T_{max} vs. depth plot showing no difference between whole rock and isolated kerogens, with the majority of samples plotting in the main oil maturity window.The dashed line is established as the regional trend from overlying Tertiary and Cretaceous samples and underlying Middle and Lower Jurassic samples. Note: the kinetically defined maturity pathways are after equations by Banerjee et al (2004) in automatically added in p: IGI-3 software

The kerogen type and level of maturity are derived from the relationship between HI and T_{max} ; which determines the samples as Type II marine (oil and gas-prone), and mixed Type II/III kerogens with a strong maturity (T_{max}) overprint (Figure 7-12). The terrigenous input to the sediment transported from the East Shetland Platform and deposited into the deep anoxic South Viking Graben is indicated by the Type III kerogen contribution to the samples (Figure 7-12). The mixed marine and terrigenous kerogen samples have lower HI and OI values due to partial degradation and the loss of hydrogen from terrestrial organic matter during sediment transport into the graben. The distribution of kerogen type is similar in both the isolated kerogen and whole rock indicating no effect from mineral removal on the determination of kerogen type from HI.

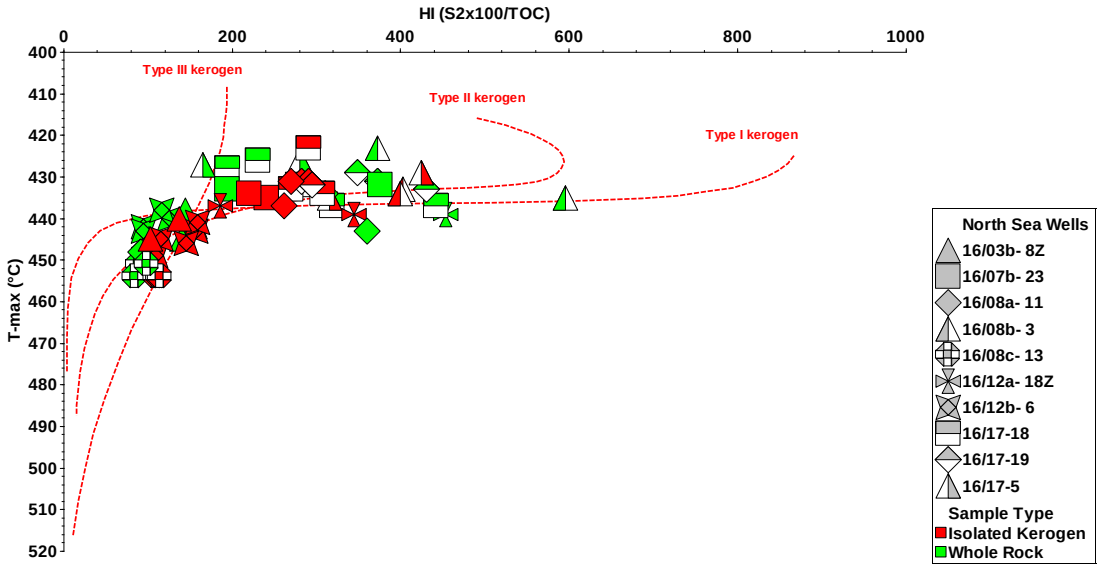

Figure 7-12: A cross-plot of T_{max} and HI showing the kerogen types based on trends from maturity parameters. Note: the kinetically defined maturity pathways are after equations by Banerjee et al (2004) in automatically added in p: IGI-3 software

Production Index (PI) can also be used to estimate the conversion of kerogen (transformation ratio) into free hydrocarbon (Espitalié et al., 1985) and this is expected to increase with maturity until expulsion takes over. The average PI for the isolated kerogen is 0.22 (range: 0.12–0.40; Table 7-2). Similarly, the average PI value for the whole rock is about 0.24 (range: 0.10–0.41; Table 7-1). The standard threshold of potential production of oil occurs at 0.1 to 0.4 (Espitalié, 1982), a range which has been

refined for the North Sea as starting at PI > 0.05 (Cornford, 1998). The low T_{max} samples confirm this low value for immature samples (Figure 7-13).

Based on these values all the samples have initiated oil generation, with the main trend falling within the region of the chart that defines well-drained and poorly-drained source rocks. Given the poor drainage of some of these shales (Figure 7-13), it is expected that a significant amount of oil is still being retained. The mineral matrix has no effect in the transformation of kerogen into free hydrocarbon in the isolated kerogen samples. In terms of unconventional exploitation, the recorded values indicate the potential for un-expelled hydrocarbon in both the whole rock and isolated kerogen samples.

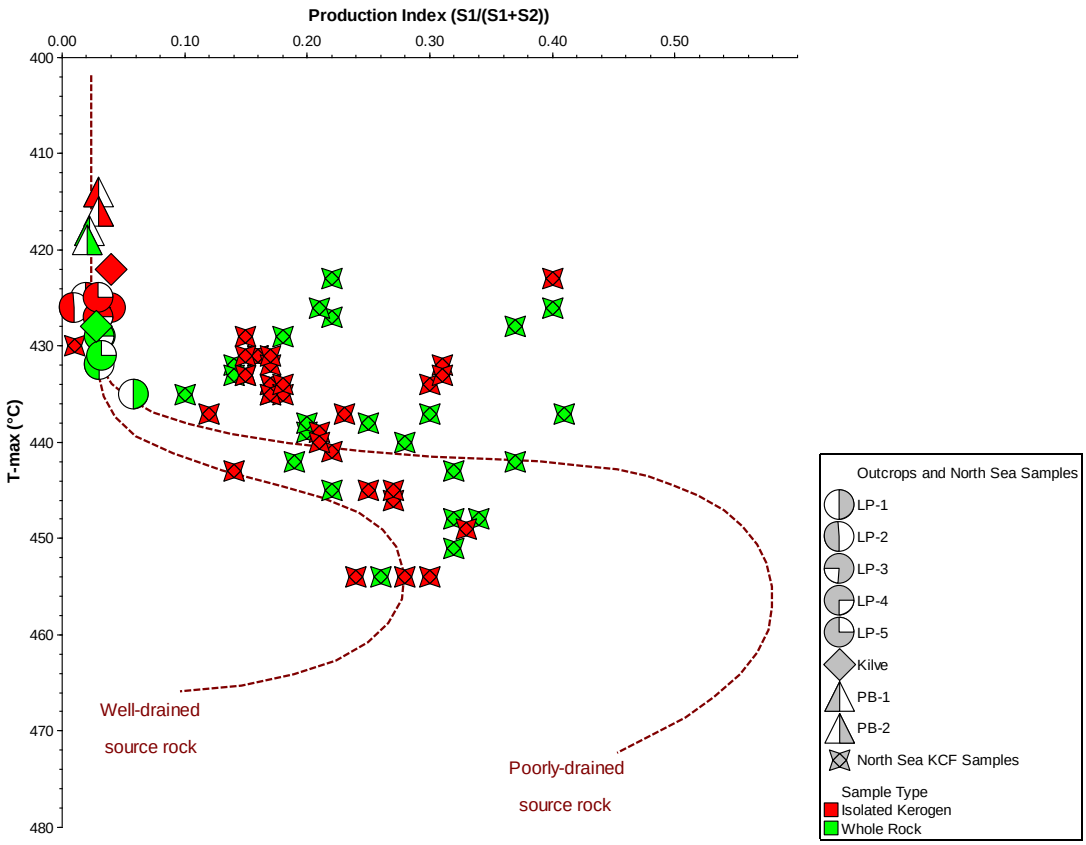

Figure 7-13: Rock-Eval Production Index (PI=S_1/ (S_1+S_2)) versus T_{max} for whole rock and isolated kerogens for the North Sea and outcrop samples. Note: standard surface intercept line automatically added in p: IGI-3 software).

T_{max} values can be converted to vitrinite reflectance using the equation: R_o = (0.018 x T_{max}) – 7.16 (Jarvie, 2007) and can also be used as a maturity parameter (Figure 7-14). There is no effect of demineralisation on the calculated vitrinite reflectance data of

either the isolated kerogen or the whole rock. The samples all appear to fall within the early to mid- oil window with reflectance values ranging from 0.45–1.01 % R_o (with an average between 0.73 % and 0.70 % R_o). Most values fall above 0.50 % R_o, confirming the results from HI (Figure 7-12) and PI (Figure 7-13). In summary, both sample sets have high oil potential with TOC values above 2 wt % and an average maturity of 0.7 % R_o (Figure 7-13; Table 7-1-7-2).

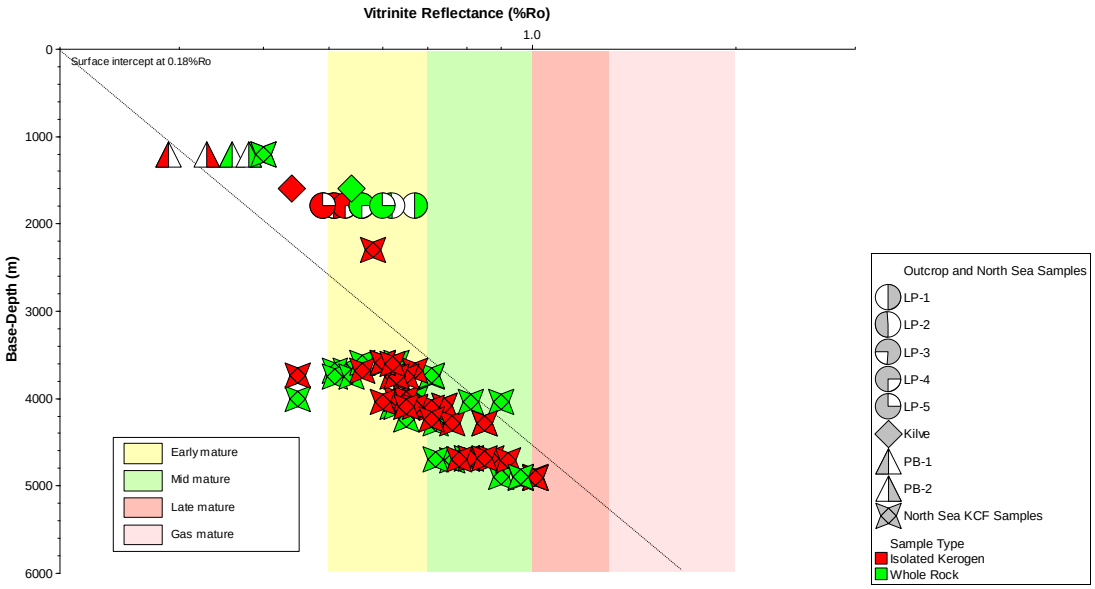

Figure 7-14: Equivalent vitrinite reflectance (converted from T_{max} °C) for whole rock and isolated kerogens for the North Sea and outcrop samples. The dashed line is established as the regional trend from overlying Tertiary and Cretaceous samples and underlying Middle and Lower Jurassic samples which include coals. Note: the low maturity UK outcrop sample depths are estimated from other regional data.

7.5.4: Effect on Kerogen Type and Thermal Maturation of the Outcrop Samples

A plot for a relationship between HI *versus* OI indicates that both the isolated kerogen and whole rock samples are mainly Type I and Type II kerogens, the Pinhay Bay laminated mudstone (LP-1) and the Lavernock laminated limestone samples plot as Type III kerogen (Figure 7-15). There is generally no effect of demineralisation on the kerogen types of the outcrop samples.

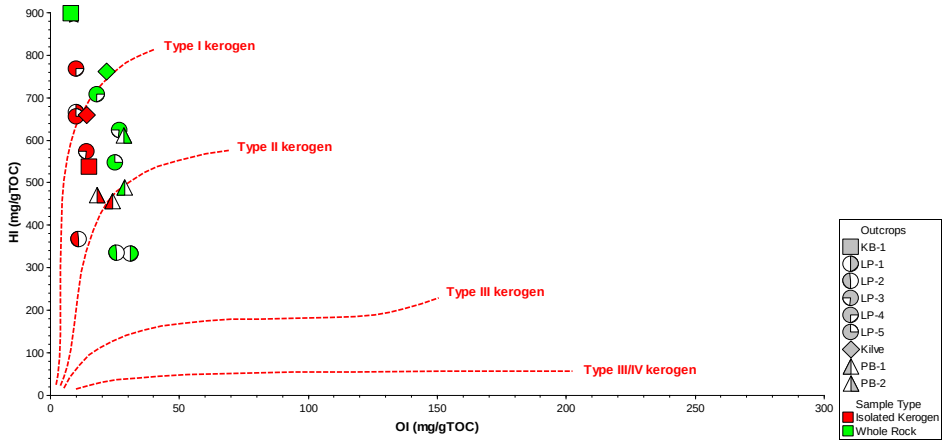

Figure 7-15: Kerogen type and maturity from Rock-Eval pyrolysis: pseudo-van Krevelen Oxygen Index (OI) and Hydrogen Index (HI) plot. Note: the kinetically defined maturity pathways are after equations by Banerjee et al (2004) in p: IGI-3 software and does not allow lines to be removed).

The T_{max} parameter is considered a very reliable indicator of thermal maturity (Espitalié, 1986). For these outcrop samples, the T_{max} values range from 414 ˚C (immature) to 427 ˚C (early-mature) for the isolated kerogen and 419 °C (immature) to 435 °C (early-mature) for the whole rock samples (Table 7-3 and 7-4). The HCI/HF treatment has a minor effect on the isolated kerogen, but nothing exceptional. These T_{max} values were converted to vitrinite reflectance (R_o), using Jarvie's equation: $R_o = (T_{max} \times 0.018) - 7.16$ (Jarvie, 2007; Peters et al., 2005). The converted T_{max} values are based on R_o values ranging from 0.29 to 0.67 % R_o; with an average of 0.49 % R_o (Tables 7.3 and 7.4); this suggests that the majority of the samples are immature-early-mature (Figure 7-14).

On a sample by sample basis (Table 7-3 and 7-4), there is a slight maturity decrease from the Lavernock Point, samples (0.49-0.53 % R_o (whole rock), 0.56-0.67% R_o (isolated kerogen) to the Kilve Pill Mouth (0.44 % Ro (whole rock), 0.54 (isolated kerogen) sample with the Pinhay Bay in Lyme Regis recorded as immature (0.29-0.33 % R_o (whole rock), 0.36-0.38 %R_o (isolated kerogen). Slightly higher Ro values were noted in the isolated kerogens; however no changes in the known maturity or hydrocarbon potential were indicated. The maturity is similar to the 0.36 %R_o for Dorset, 0.46 %R_o for North Somerset and 0.51 %R_o for Glamorgan recorded by Cornford (1986) and Cornford and Douglas (1980). In terms of oil generation, most of the samples appear to be immature the exception of Lavernock Point samples which

appear to have entered the early oil maturity window. There is no significant effect of demineralisation on the maturity of these samples.

In terms of the thermal maturity of each sample site, there is a clear maturity trend from south (immature at Pinhay Bay) via Kilve to early oil mature at Lavernock in the north. The maturity estimates for both whole rock (Table 7-3) and isolated kerogens (Table 7-4) are internally consistent in terms of the maturity trend; no effect of demineralisation is indicated. The lowest maturity samples have suffered the least post-depositional burial; this is reasonable as the low syn-depositional sedimentation rate controls the subsequent maximum thermal event (Cornford and Douglas 1980). The increased maturity in the Lavernock samples may be due to the eastern extension of the South Celtic Sea Trough in the Bristol Channel area. This fault bounded structure could give higher maturity levels either due to greater burial depths in the down-faulted region, or due to higher geothermal gradients associated with fault-bounded trough structures in the North Sea and Rhine graben (Donovan and Kellaway, 1984; Cornford and Douglas, 1980).

The amount and type of organic matter is discussed in terms of a simple model where the kerogen derives from land plants is represented by vitrinite and inertinite, and alginite in the photic zone is represented by liptinite (Figure 7-16). This primary kerogen input is then reworked by bacteria in the first few meters of seabed sediments, thus reducing some algal liptinite (alginite) to amorphous liptinite under anoxic conditions or progressively destroying it under oxic conditions at the Liassic sea floor. This schematic model of the Liassic shelf seaway (Figure 7-16) shows both terrigenous higher plant debris and planktonic algal biomass were potentially available for sedimentation only accumulated under anaerobic conditions where bacterial activity continued. In the normal aerobic water, the algal/bacterial matter is dominantly destroyed and the terrigenous material altered (oxidised). The amount of terrigenous material being oxidised could have reduced the oxygen content of the water and hence facilitated the development of truly anoxic conditions (Cornford and Douglas, 1980).

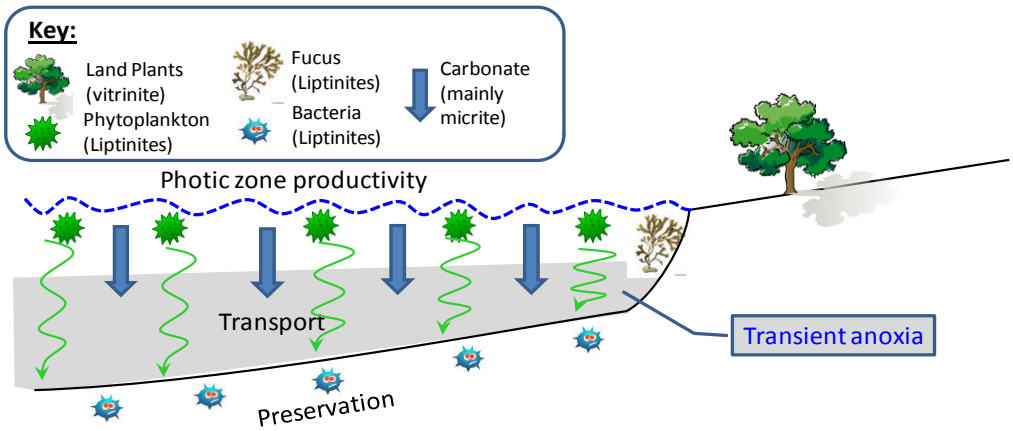

Figure 7-16: Schematic of depositional conditions leading to the amounts and types of kerogen in a shallow Liassic seaway of the southern UK.

Rock-Eval Production Index (PI) values (0.01-0.06) calculated as the ratio of S_1/ (S_1+S_2) track the transformation of kerogen into free hydrocarbon (Table 7-3 and 7-4). The PI ratio changes by both by the reduction in S_2 and the increase in S_1 with increasing maturation. There is no significant change in the PI values of either the isolated kerogen or the whole rock suggesting there is no demineralisation effect on these samples. The relationship between PI and T_{max} suggests that these samples are poorly-drained source rocks with limited levels of maturity achieved, implying that the samples have retained rather than drained any oil generated (Figure 7-13). Given the poor drainage of these samples, it is expected that additional burial with further maturity with would be needed to expel any significant amount of oil from these source rocks.

7.5.5: Effect on carbon isotope composition of the kerogens

Carbon isotope ratios are used to classify the origin of organic matter in terms of marine (aquatic) or continental (land) plant origins (Meyers,1994; Galimov, 2006), with stratigraphically restricted deviations based on global climate variation (Jarvis et al., 2011) and on changes in sea level (Gröcke et.al., 2006). Carbon isotope values may be used together with post-depositional changes of the original organic input to place limits on the source of the organic matter in sediments (Meyers and Eadie, 1993; Calvert, 2004). The carbon isotope of kerogen can also be used to identify the kerogen type which is dependent on the thermal maturation of the organic matter (Lewan, 1986; Maynard, 1981). In both the North Sea and the outcrop samples, the $\delta^{13}C_{org}$

carbon for the kerogen samples ranges from -29.61 ‰ to -25.84 ‰, with a mean value of -28.94 ‰ (Table 7-5) which is typical of marine organic matter (Meyer et al., 1984a; Meyer and Benson, 1988; Gunter and Mensing, 2004) or n-alkanes derived from land plant leaf waxes (Meyers, 1994; Galimov, 2006). These δ^{13}Corg values represent the isotopic value of bulk organic-matter in the sediment, and any change in this value reflects a change in the relative contribution of one type of organic-matter over another (Littler et al., 2010). The mean value of -28.94 ‰ reported for the North Sea Kimmeridge Clay kerogens suggest that the mixing and preservation of isotopically light end members controls the gross kerogen properties and reflects bacterially degraded algea (Galimov, 2006).

The relationship between the kerogen carbon isotopes and the Hydrogen Index (HI) is used as an indicator of kerogen type at comparable maturities and shows that low HI samples (gas prone and presumably vitrinite rich) have isotopically heavier carbon, whereas the higher HI samples are isotopically lighter (Figure 7-17). In this plot, the lower HI values have δ^{13}Corg values of around -25 to -26 ‰ and are associated with terrestrial OM, while the highest HI values (up to 400) correspond to the most depleted δ^{13}Corg values of around to -26 to -30 ‰) ,and are indicative of marine OM (Meyers and Bernasconi, 2005 ; Junium and Arthur, 2007).

A depth-trend of δ^{13}Corg values for the North Sea samples shows a good relationship and is consistent with the source of kerogen being derived from marine organic matter with a contribution from terrestrial organic material (Figure 7-18). The slight decrease in δ^{13}Corg values with depth may have resulted from the selective preservation of isotopically heavy land plant material from the Shetland Platform. This material was presumably carried by the rivers transporting the fan sands into the South Viking Graben where it was deposited with the organic-rich Kimmeridge Clay Formation. This slight depletion of δ^{13}Corg can also be attributed to diagenetic effects and microbial degradation of δ^{13}C-enriched carboxyl during maturation carbon (Hatcher et al., 1983; Peters et al., 2005). There is a positive correlation between the TOC value for the kerogens and the occurrence of an isotopically lighter signature of marine and an isotopically heavier signature of terrestrial origin. The result indicates

demineralisation has no effects on the factors used to identify the origin and the kerogen type of the organic matter in either set of samples.

Table 7-5: TOC, $\delta^{13}C_{org}$ results and vitrinite reflectance measurements for North Sea and Outcrop Kerogen Samples.

Sample name	Well and location name	Depth (m)	$\delta^{13}C_{org}$	TOC (isotope)	Measured R_o (isolated kerogen)
MR1	16/12b- 6	4,683	-25.77	74.16	0.7
MR2	16/12b- 6	4,681	-26.25	73.34	0.66
MR3	16/12b- 6	4,706			0.71
MR4	16/12b- 6	4,688	-25.83	75.95	0.8
MR5	16/12b- 6	4,693	-26.21	71.65	0.88
MR6	16/08c- 13	4,894	-25.92	74.26	0.68
MR7	16/08c- 13	4,906	-26.47	72.24	0.67
MR8	16/08c- 13	4,907	-26.02	69.98	0.66
MR9	16/08b- 3	4,007			0.8
MR10	16/08b- 3	4,006	-29.78	59.85	0.84
MR11	16/12a- 18Z	4,085	-29.89	58.62	0.56
MR12	16/12a- 18Z	4,100	-28.03	63.3	0.61
MR13	16/17-5	3,680	-28.47	60.65	0.94
MR14	16/17- 5	3,681	-29.62	51.25	0.97
MR15	16/17-18	3,745	-29.73	52.94	0.75
MR16	16/17- 18	3,745	-29.4	55.44	0.68
MR17	16/17- 18	3,738	-29	59.87	0.62
MR18	16/17- 18	3,744	-29.21	60.74	0.82
MR19	16/17-19	3,597	-28.86	62.75	0.6
MR20	16/17- 19	3,596	-28.8	57.54	0.85
MR21	16/17- 19	3,605	-29.2	60.84	0.7
MR22	16/03b- 8Z	4,283	-25.62	70.52	0.84
MR23	16/03b- 8Z	4,285	-25.21	65.63	0.63
MR24	16/07b- 23	4,092	-26.14	55.92	0.67
MR25	16/07b- 23	4,093	-26.65	66.6	0.67
MR26	16/08a- 11	4,037	-27.8	61.38	0.88
MR27	16/08a- 11	4,236	-28.62	50.05	0.7
IGI-02 (LP-1)	Lavernock Point, Glamorgan		-29.42	50.22	0.49
IGI-03 (LP-2)	Lavernock Point, Glamorgan		-25.84	64.1	0.5
IGI-04 (LP-3)	Lavernock Point, Glamorgan		-29.44	57.49	0.52
IGI-05 (LP-4)	Lavernock Point, Glamorgan		-28.25	54.51	0.52
IGI-06 (LP-5)	Lavernock Point, Glamorgan		-29.43	60.38	0.51
IGI-07 (PB-1)	Pinhay Bay, west of Lyme Regis		-29.97	53.88	0.3
IGI-08 (PB-2)	Pinhay Bay, west of Lyme Regis		-29.56	53.89	0.33
IGI-09 (Kilve)	Kilve Pill Mouth, West Somerset		-29.61	56.59	0.43

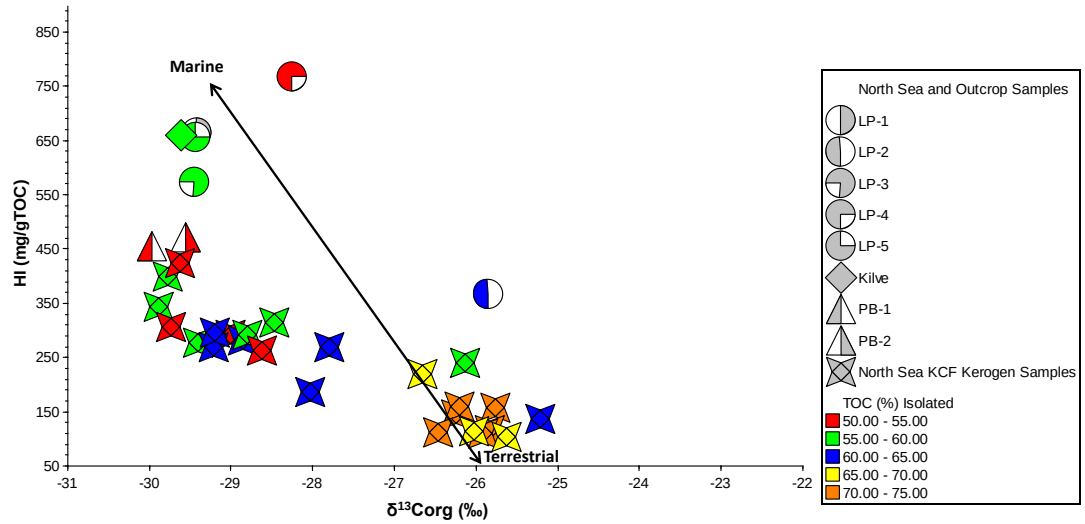

Figure 7-17: HI (kerogen and maturity dependent) versus carbon isotope ratios plot of isolated kerogen from North Sea and Outcrop samples.

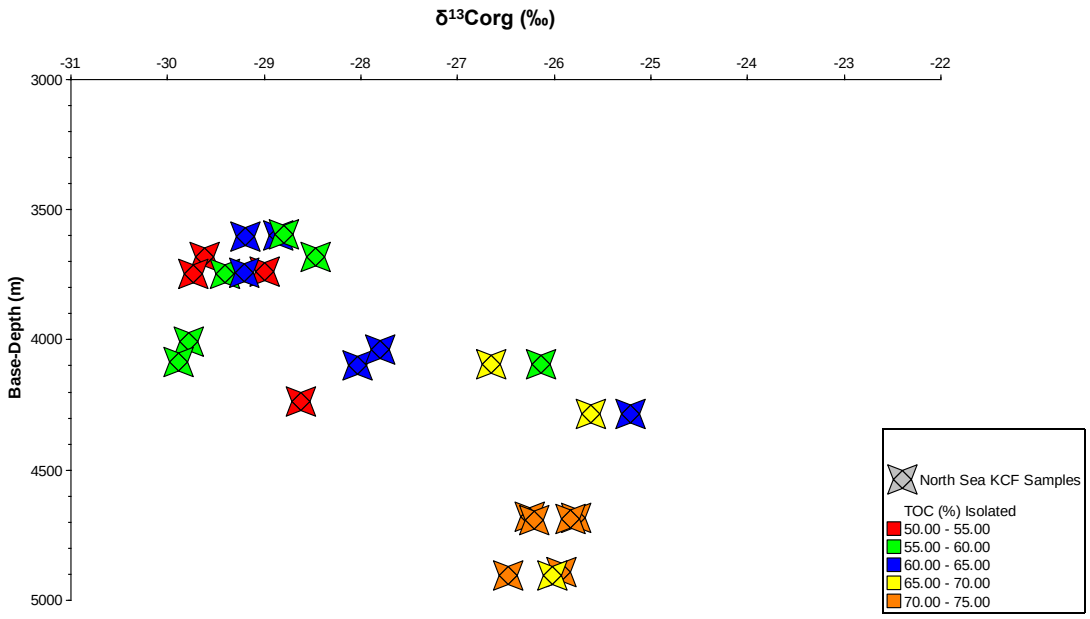

Figure 7-18: The relationship between δ^{13}Corg (‰) and base-depth (m) for the North Sea samples.

7.6: Organic petrography of the North Sea Samples

In terms of mineralogy, the whole-rock samples contain quartz, clay, mica, and a significant amount of pyrite. Pyrite occurs as particles and framboids throughout the whole rock and in isolated kerogen matrices. In both set of samples, vitrinite occurs as elongate, angular or rounded, bodies that are grey under reflected light, with or without recognisable telinite and collotelinite cell structure (Figure 7-19A-C), or as a

vitrinitic groundmass (collodetrinite) (Figure 7-19D). Degraded vitrinite has a lower reflectance, appearing darker grey, and mostly occurs as rounded or sub-angular pieces, often with blind fractures around particle edges, that have likely been reworked or altered during transport. Vitrinite represents terrestrial OM, specifically derived from woody tissues (Taylor et al., 1998), and in this study is in general agreement with the Type I and Type II kerogen data from Rock-Eval.

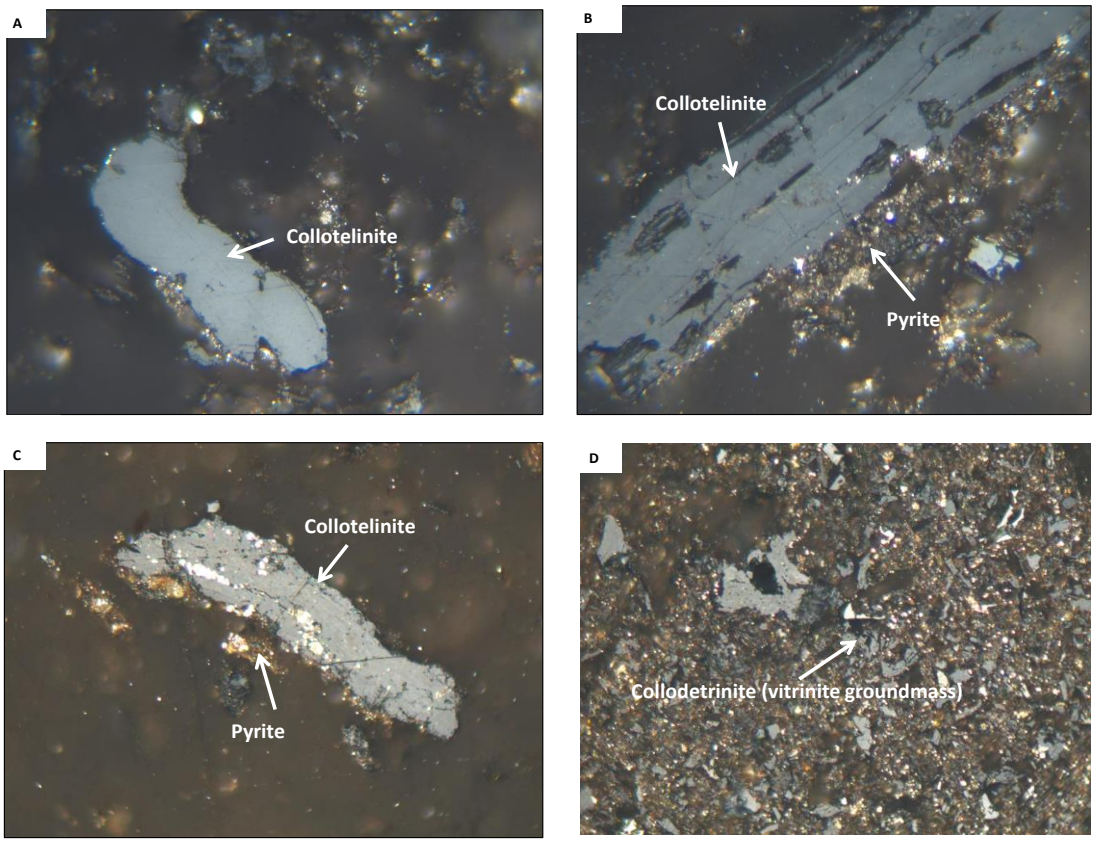

Figure 7-19: Photomicrographs of vitrinite macerals in white fluorescence light.

The liptinitic macerals include well preserved thin- and thick-walled alginite bodies that are a dull, dark brown colour under white-light illumination with a fairly intense greenish-yellow fluorescence under blue-light illumination (telalginite and lamalginite) indicating a marine origin for the kerogen as shown by the carbon isotope data. Telalginite occurs as elliptical or disc-shaped bodies, thicker than ~ 5 μm with bright yellow fluorescence (Figure 7-20A). Lamalginite occurs as very thin-walled (< 5 μm) lamellae with little recognisable structure, and it appears dark brown

under white light and has a greenish-yellow low fluorescence under blue light (Figure 7-20B). Bituminite occurs as dark-gray to brown masses or fine threads and wisps, and shows low levels of fluorescence under blue-light illumination; this AOM is derived from the breakdown of algae and degraded bacterial (Figure 7-20C). Solid bitumen appears along mineral grains and laminae (Figure 7-20D), indicating that mature kerogens generated hydrocarbon that migrated through the rocks and solidified in situ.

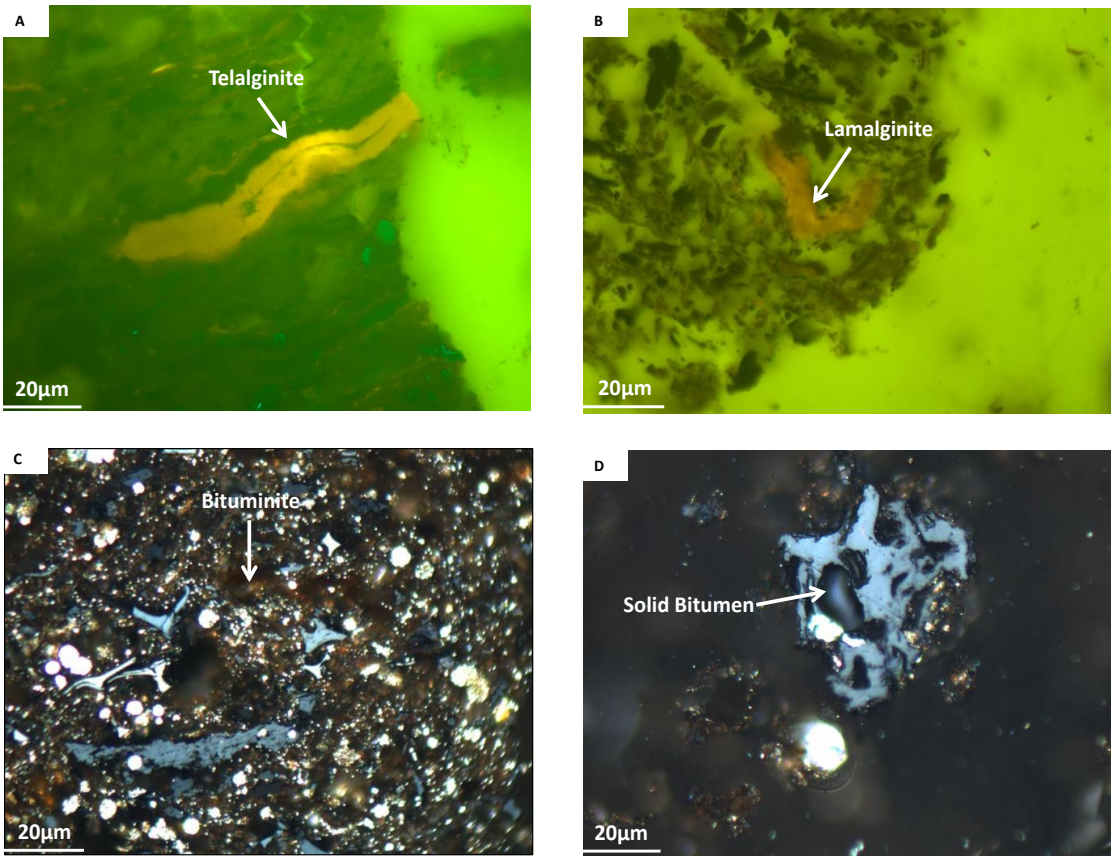

Figure 7-20: Photomicrographs of Liptinite macerals in blue and white florescence light.

The most common inertinite macerals are non-fluorescent fusinite (Figure 7-21A, B & D), semifusinite (Figure 7-21C), and inertodetrinite. They occur as light grey to white bodies of varying shape and size, with partially to well-preserved cell structures showing high to intermediate reflectance. The inertinite macerals represent partially pyrolysed terrestrial OM (Taylor et al., 1998). Vitrinite reflectance measurements of preserved vitrinite macerals on polished isolated kerogen samples under white-light

illumination generated a range of values between 0.5–0.9 $\%R_o$, supporting the results obtained from T_{max} .

Distinctive AOM was better observed under transmitted light and is represented by orange-yellowish homogenous flakes with sharp edges (Figure 7-22). Vitrinite appears as brownish heterogeneous flakes and inertinite macerals appear black (Figure 7-22). The kerogen type and maceral assemblages of these samples indicate Type II marine kerogen with minor input from terrestrial Type III kerogen.

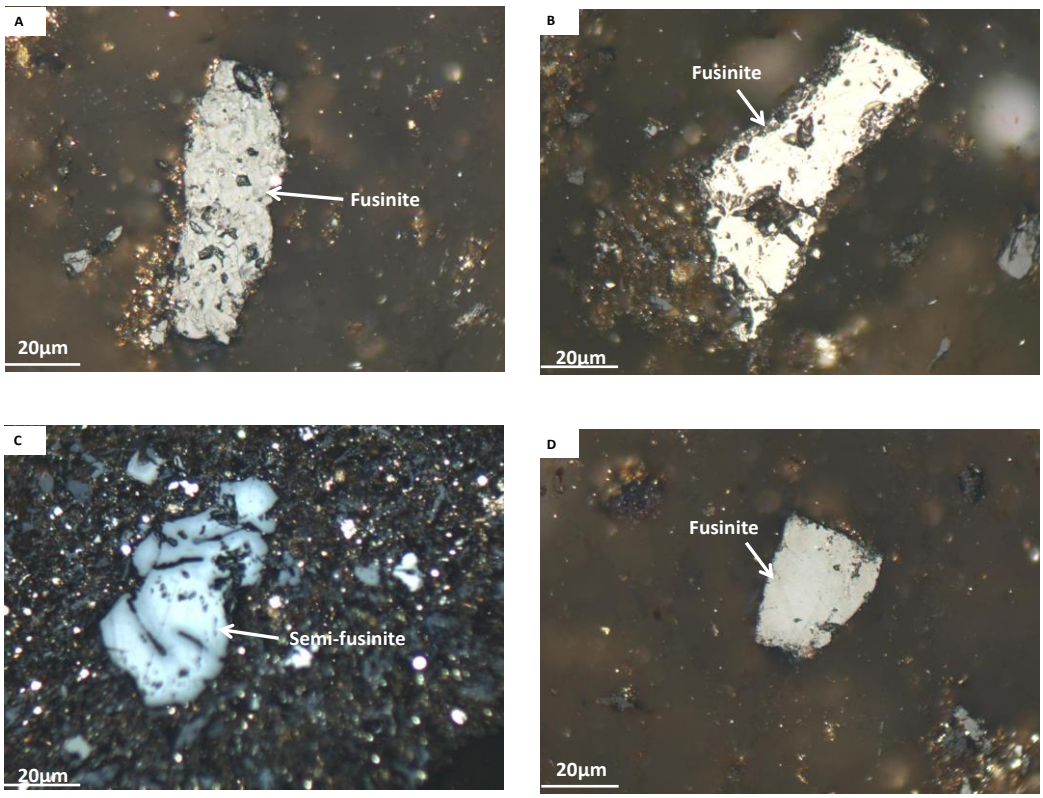

Figure 7-21: Photomicrographs of inertinite macerals in white fluorescence light.

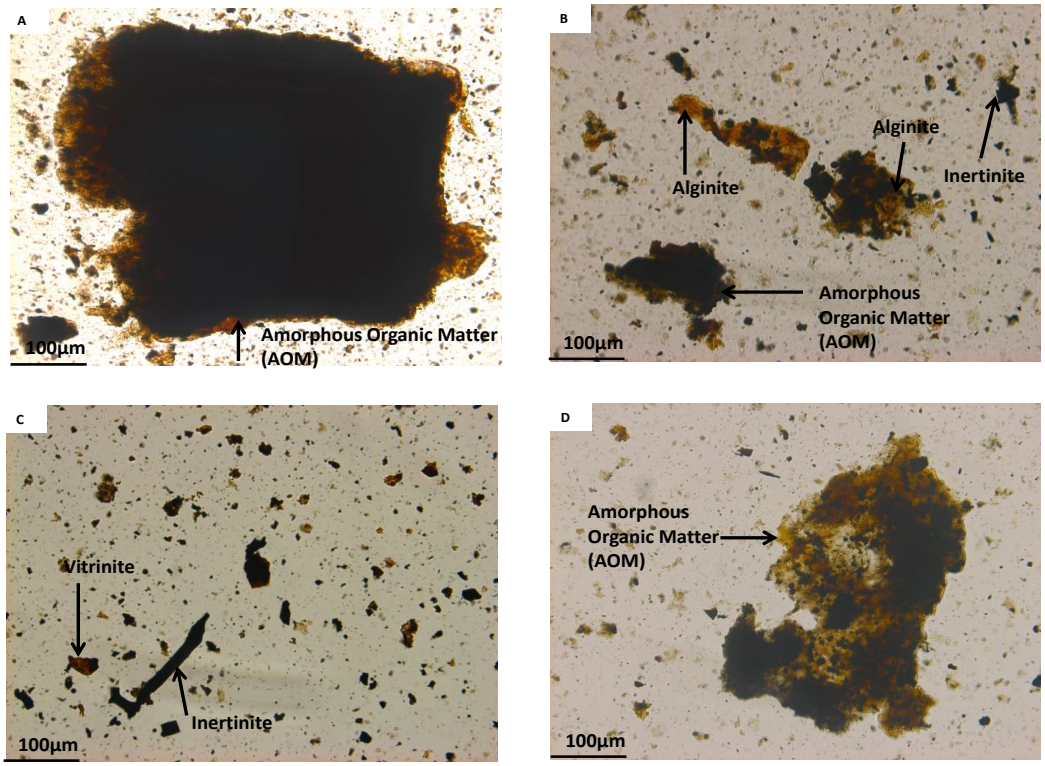

Figure 7-22: Photomicrographs of kerogen samples taken under transmitted light.

7.7: Organic petrography of the Outcrop Samples.

Petrographic observations on the whole-rock samples indicate an abundance of quartz, calcite, clay, and high pyrite minerals. Framboidal pyrite is common in both whole-rock and isolated kerogen samples. Geochemical changes during the transformation of kerogens are well reflected in the changing optical properties of microscopic organic matter, these changes are most noticeable in the reflectance of vitrinite particles. High concentrations of fluorescent lamalginite and telalginite macerals derived from algal type bodies, (Figure 7-23A) amorphous organic matter (AOM) and solid bitumen were observed in these samples. This observation is supported by a high relative abundance of hydrogen as recorded by Rock-Eval HI values (Table 7-3 and 7-4) for these samples, and also reflects better preservation. Some higher terrigenous plant remains such as vitrinite (mostly degraded), fusinite and semifusinite macerals were also observed (Figure 7-23B & Figure 7-23C).

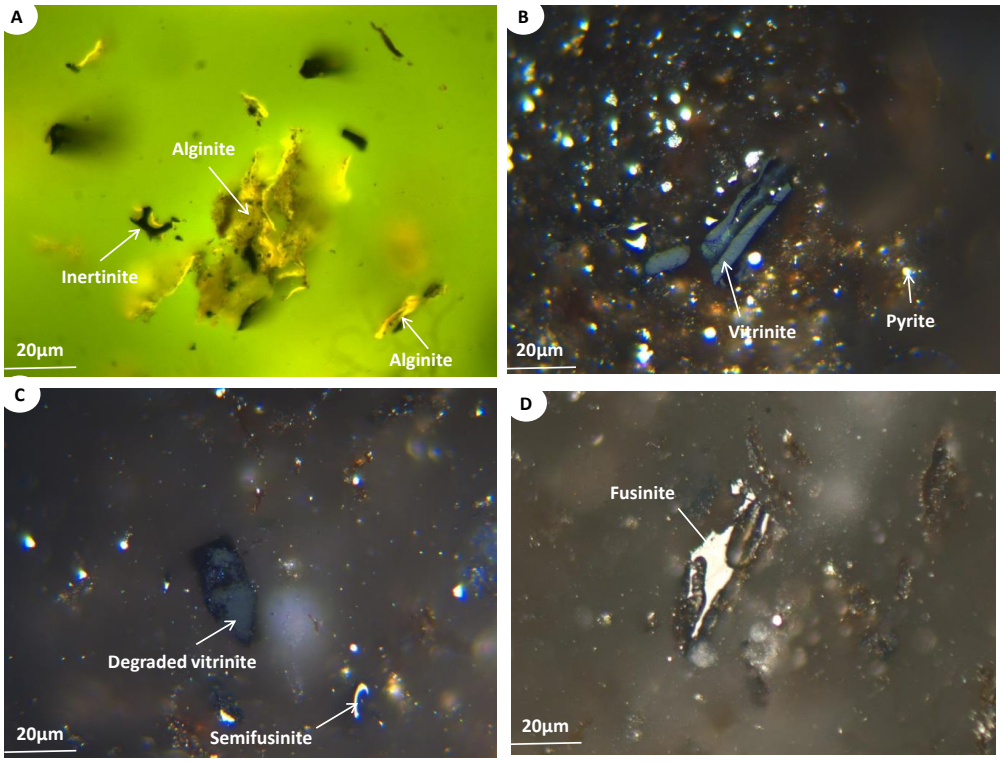

Figure 7-23: (A) Liptinite maceral in isolated kerogen sample under blue light illumination, (B) Vitrinite, alginite macerals and pyrite under white-light illumination, (C) an example of degraded vitrinite and semi-fusinite macerals in whole rock under white-light illumination (D) Fusinite maceral in isolated kerogen under white-light illumination.

Degraded vitrinite may have resulted from the oxidation of lignocellulose terrigenous plant debris during transport and deposition. Available dissolved oxygen in the basin is used up during this oxidation, producing an oxygen-deficient water body and an anoxic environment (Byers, 1977; Cornford and Douglas, 1980). Under anoxic conditions, the mixture of bacteria and algae will be altered and degraded in the water column, and in the upper layers of the sediment, where reworking by benthonic organisms will disrupt the lamination of sediments (Cornford and Douglas, 1980). Sedimentation into this environment favours the accumulation of the readily degraded algal debris and subsequent high pyrite content in the sediment. In a relatively shallow sea with stratified water such as this, lowering of dissolved oxygen (0.1-1 ml) levels will consequently result in the formation of local anoxic environments. Under this condition, laminated mudstones and limestone sedimentation occurs followed by survival and preservation of algae bodies (Cornford and Douglas, 1980).

Smear slides of isolated kerogens under transmitted light showed more clearly the shape and sizes of these amorphous liptinite, vitrinite and inertinite (Figure 7-23). Distinctive amorphous organic matter (AOM) was better observed under the transmitted light, represented by orange-yellowish. Vitrinite appears as brownish heterogeneous flakes and inertinite macerals occur as black-dark brown (Figure 7-23).

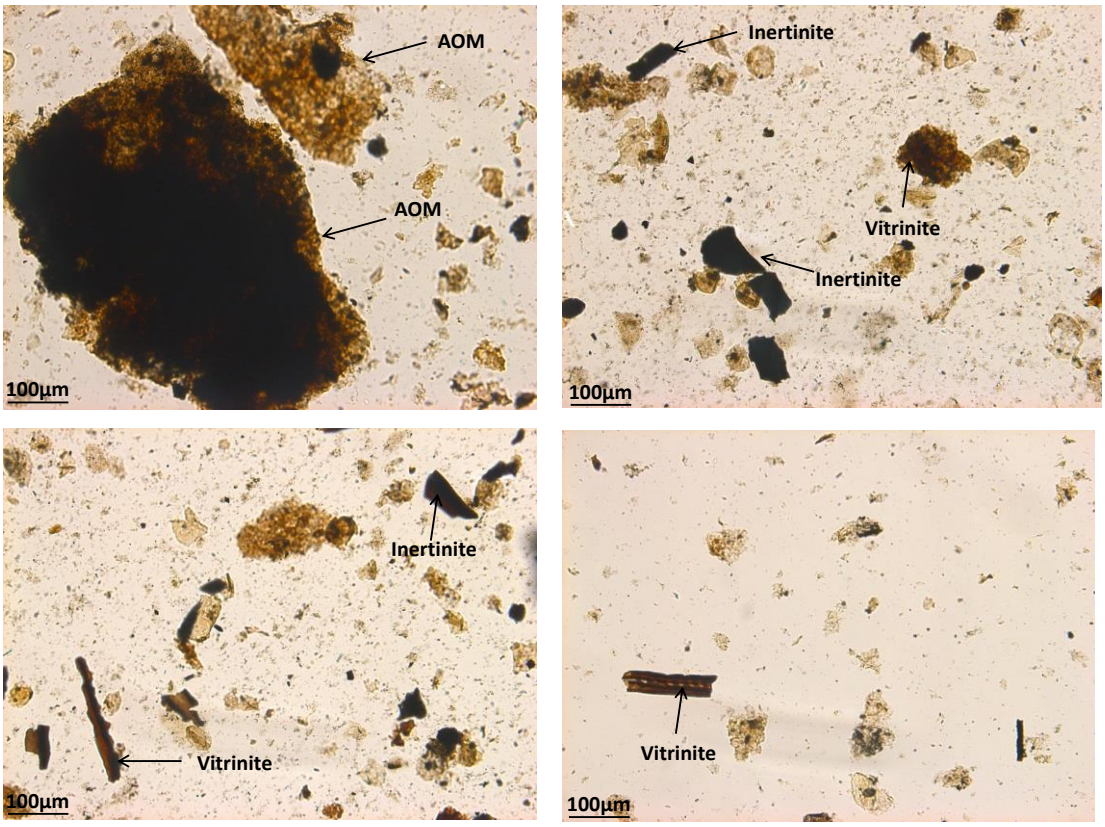

Figure 7-24: Showing transmitted light photomicrographs of amorphous organic matter (AOM), liptinite, vitrinite and inertinite isolated kerogen.

7.8: Vitrinite Reflectance Measurement on Outcrop Samples

Vitrinite reflectance measurements were carried out on the polished isolated kerogen samples. Obtaining these measurements was problematic because most of the grey polished particles are mainly fusinite, semi-fusinite, or degraded and reworked vitrinite showing erroneous value as high as 2.4 %R_o. A range of values (0.39-0.53 %R_o) was exhibited by well-preserved vitrinite particles where measurements were possible (Table 7-5). Degraded and reworked vitrinite is also abundant in the limestone sample (IGI-2), giving high reflectance values. These high reflectance values

from oxidized vitrinite ultimately derived from Lias land plants (William and Douglas, 1983; Cornford and Douglas 1980).

In terms of maturity, using the measured vitrinite reflectance as a parameter, these values suggest that all the samples are relatively immature (0.35 $\%R_o$) in the Pinhay Bay (IGI-7 and IGI-8) and Kilve Pill Mouth (IGI-9) samples to early mature (0.52 $\%R_o$) in the Lavernock Point samples (IGI-2 through IGI-6). This suggests a maturity increase from south (Dorset) to north (Glamorgan).These values are in broad agreement with Rock-Eval maturity, T_{max} and HI data.

7.9: Conclusions

The effect of the mineral matrix on the laboratory pyrolysis of the Upper Jurassic Kimmeridge from the North Sea and Liassic kerogen from the coastal outcrop in Dorset, Somerset and South Glamorgan has been investigated. Kerogen was isolated from the mineral matrix by acid solution of the minerals using hydrochloric (HCl) and hydrofluoric (HF) acids. TOC/Rock-Eval Pyrolysis, carbon isotope and organic petrography analyses were carried out on the isolated kerogen and whole rock samples. Comparison between the whole rock and isolated kerogen was used to understand the effect of mineral matrices on organic matter and laboratory pyrolysis of the same set of samples.

For the North Sea samples, the TOC of the isolated kerogens was taken as a measure of the effectiveness of the isolation procedure. These values fall in the range of 50 wt.%TOC to 80 wt.%TOC, indicating substantial mineral matter remains within the sample post isolation. Subsequent analysis shows this mineral matter is predominantly pyrite, often physically attached to the kerogen. The average total organic carbon content of these shales is over 2 wt.% in the whole rock, and kerogen is primarily Type I and II, with minor amounts Type III based on both pyrolysis and organic petrography. The demineralisation process has a significant effect on the quality of the OM, but no effect on their kerogen types.

S_1 yield from isolated kerogen plus non-reactive minerals left after the HCl/HF maceration (pyrite) ranges from 19-105 mgHC/g kerogen isolate (average 40 mgHC/g

kerogen isolate), whereas the whole-rock S_1 values derived from the free oil in the kerogen plus minerals (carbonate, silicates, pyrite) range from 1-10 mgHC/g rock (average: 3.7 mgHC/g rock). It is assumed that no S_1 matter is lost or destroyed by HCl/HF treatment. The S_1 yield from these samples is largely associated with (adsorbed on) the kerogen pores and any S_1 adsorbed on the mineral matrix is liberated during acid maceration, and attached to the kerogen upon sample drying.

Over a multi-well depth trend there is no systematic variation of the T_{max} values for whole rock and isolated kerogen samples. On a sample by sample basis, T_{max} values for most isolated kerogens are higher than and apparently more mature than the whole rock equivalent values. Generally, little or no effect of HF treatment during kerogen isolation was observed on the HI values; however, high HI samples have higher TOC and S_2 values for whole rock and lower TOC but higher S_2 values for isolated kerogen. Pyrolysis T_{max} and vitrinite reflectance measurements place the samples within the oil window, and generated oil is still retained within the whole rock and in the isolated kerogen matrix; the mineral matrix does not affect the maturity of the samples. In terms of generative potential, there is the potential to generate a significant amount of un-expelled hydrocarbon in both the whole-rock and isolated kerogen samples, these findings are relevant for unconventional exploitation of shale reservoirs with mixed kerogen assemblages.

In the Liassic outcrop samples, both whole-rock samples and isolated kerogen are shown to be generally immature, with a progressive increase of maturity from south (Dorset) to north (Glamorgan). This is interpreted in terms of high organic carbon content and thermal maturity from T_{max} and vitrinite reflectance. The increase in maturity trend from south (Pinhay Bay) to north (Lavernock Point) is in agreement with structural study of Jurassic sediment in this area.

On average, higher TOC values are recorded for the laminated and blocky mudstone, the average TOC values for the whole rock is 4 wt.% and 55 wt.% for the isolated kerogen samples. A plot of HI versus T_{max} and petrographic data indicates both the whole rock and isolated kerogen is Type I kerogen containing well-preserved alginite and Type II containing bacterially degraded algal kerogen. In the North Sea and the

outcrop samples, the δ13Corg carbon for the kerogen samples range from -29.61 ‰ to -25.84 ‰, with a mean value of -28.94 ‰ which is typical of marine organic matter or n-alkanes derived from land plant leaf waxes. These values suggest that mixing and preservation of an isotopically light end member controls the gross kerogen properties.

Petrographic observation of the whole-rock samples indicates abundant quartz, calcite, clay, and pyrite minerals. High concentrations of fluorescent lamalginite, telalginite, amorphous organic matter (AOM), solid bitumen and higher terrigenous plant remains such as vitrinite (mostly degraded), fusinite, and semifusinite macerals were observed. Vitrinite reflectance measurements suggest that the samples range from relatively immature (0.35 % Ro) in the Pinhay Bay and Kilve Pill Mouth area to early mature (0.52 %Ro) at Lavernock Point. In terms of the thermal maturity of each sample site, there is again clear maturity trend from south (immature at Pinhay Bay) to early oil mature at Lavernock. The maturity estimates for both whole rock and isolated kerogens are internally consistent in terms of the maturity trend. The mineral matrix has no effect on the kerogen type or maturity of the samples.

7.10: Acknowledgements

This study is partly funded by the European Association of Organic Geochemistry (EAOG) research grant awarded to MR. MR acknowledges receipt of a Durham University Doctoral Scholarship (DDS). The authors would like to thank Two Fields Consulting (TFC) and Trapoil for supporting this research. We are grateful to the British Geological (BGS) Survey for providing the core samples for this study. Special thanks to Brian Jarvie of GeoMark Research, Ltd. for TOC/Rock-Eval pyrolysis analyses, and Integrated Geochemical Limited (IGILtd) for the use of their p: IGI-3 software for the geochemical interpretation.

7.11: References

Abrams, M.A. 2014. Petroleum System Charge Analysis for Liquid-Rich Unconventional Plays. Unconventional Resources Technology Conference Proceedings, August 25-27, 2014.

Akinlua, A., Ajayi, T.R., Jarvie, D.M., Adeleke, B.B., 2005. A re-appraisal of the application of Rock-Eval pyrolysis to source rock studies in the Niger Delta. Journal of Petroleum Geology 28,pp. 39-48.

Ballice, L. 2005. Effect of demineralization on yield and composition of the volatile products evolved from temperature-programmed pyrolysis of Beypazari (Turkey)Oil Shale, Fuel Processing Technology 86 pp.673-690.

Banerjee, A., Sinha, A.K., Jain, A.K., Thomas, N.J., Misra, K.N., Chandra, K., 1998. A mathematical representation of Rock-Eval hydrogen index vs. T_{max} profiles. Organic Geochemistry 28, pp. 43-55.

Behar, F., Vandenbroucke, M., Tang, Y., Marquis, F., Espitalié, J., 1997. Thermal Cracking of Kerogen in Open and Closed Systems: Determination of Kinetic Parameters and Stoichiometric Coefficients for Oil and Gas Generation. Organic Geochemistry 26, pp. 321-339.

Behar, F.H., Beaumont, V., Penteado, H.L.d.B., 2001. Rock-Eval 6 technology: performances and developments. Revue de l'Institut Francais du PetroleOil and Gas Science and Technology, 56, pp. 111-134.

Behar F., Roy S., Jarvie D. 2010. Artificial maturation of a Type I kerogen in closed system: Mass balance and kinetic modelling, Organic Geochemistry 41, pp.1235-1247

Barnard, P. C., and Cooper, B. S. 1981. Oils and source rocks of the North Sea area, in L. V. Illing and G. D. Hobson, (eds) Petroleum geology of the Continental Shelf of northwest Europe: Heyden, London, Institute of Petroleum, pp.169–175.

Bernard, S and Horsfield, B. 2014. Thermal maturation of gas shale systems. Annual Review of Earth Planetary Sciences 42, pp. 635-651

Bernard, P.C., Collins, A.G., Cooper, B.S., 1981. Identification and distribution of kerogen facies in a source rock horizon examples from the North Sea basin. In: Brooks, J. ed., Organic Maturation Studies and Fossil Fuel Exploration. Academic Press, London, pp. 271-282.

Bostick, N.H., Daws, T.A., 1994. Relationships between data from Rock-Eval pyrolysis and proximate, ultimate, petrographic and physical analysis of 142 diverse US.coal samples. Organic Geochemistry 21, pp. 35-49.

Boudou, J.-P., 1984. Relations between Rock-Eval T_{max} and other parameters in a sedimentologically homogeneous coal series. Fuel 63, pp. 430-431.

Boussafir,M., Sifeddine, A., Jacob, J., Foudi, M., Cordeiro, R.C., Albuquerque, A.L.S., Abrao, J.J. and Turcq, B., 2012. Petrographical and geochemical study of modern lacustrine sedimentary organic matter (Lagoa do Caco, Maranao, Brazil): Relationship between early diagenesis, organic sedimentation and lacustrine filling. Organic Geochemistry 47, pp.88-98.

Burnham, A.K., 1994. Comments on 'The effects of mineral matrix on the determination of kinetic parameters using modified Rock-Eval pyrolysis' by Dembicki, H., and the resulting comment by Pelet, R. Organic Geochemistry 21, pp. 985-987.

Byers, C.W., 1977. Biofacies Patterns in Euxinic Basins: A General Model. The Society of Economic Paleontologists and Mineralogists (SEPM) Special Publication, 5, pp.5-17.

Callomon, J H and Cope, J C W. 1995. The Jurassic geology of Dorset. 51-103 in Taylor, P D (Editor), Field Geology of the British Jurassic. The Geological Society.

Calvert, S.E., 2004. Beware intercepts: interpreting compositional ratios in multicomponent sediments and sedimentary rocks. Organic Geochemistry 35, 981-987.

Carrie, J., Sanei, H., Stern, G., 2012. Standardisation of Rock-Eval pyrolysis for the analysis of recent sediments and soils. Organic Geochemistry 46, pp. 38-53.

Copard, Y., Di-Giovanni, C., Martaud, T., Albéric, P., Olivier, J.-E., 2006.Using Rock-Eval 6 pyrolysis for tracking fossil organic carbon in modern environments: implications for the roles of erosion and weathering. Earth Surface Processes and Landforms 31, pp. 135-153.

Cooper, B.S., Barnard, P.C., 1984. Source rocks and oils of the central and northern North Sea. In: Demaison, G., Murris, R.J. (Eds.), Petroleum Geochemistry and Basin Evaluation, American Association of Petroleum Geologists Memoir 35, pp. 303-314.

Cooper, B.S., Bernard, P.C. and Telnaes, N., 1995. The Kimmeridge Clay formation of the North Sea. In: Katz, B.J. (Ed.), Petroleum Source Rocks. Springer-Verlag, Berlin, pp. 89-110.

Cornford, C and Douglas, A.G. 1980. Maturity, Depositional Environment and Hydrocarbon Source Potential of Lower Lias Limestone/Shale Sequences of South-West Britain. Unpublished manuscript.

Cornford, C. 1986. The Bristol Channel Graben: organic geochemical limits on subsidence and speculation on the origin of inversion. Proceedings of the Ussher Society, 6, pp.360-367.

Cornford, C., 1984. Source rocks and hydrocarbons of the North Sea. In: Glennie, K.W. (Ed.), Introduction to the Petroleum Geology of the North Sea. Blackwell Scientific Publications

Cornford, C., Brooks, J., 1989. Tectonic controls on oil and gas occurrences in the North Sea area. In: Tankard, A.J., Balkwill, H.R. (Eds.), Extensional Tectonics and Stratigraphy of the North Atlantic Margins. American Association of Petroleum Geologists/Canadian, Geological Foundation, 46e641.Oxford, pp. 171-209.

Cornford, C., 1998. Source rocks and hydrocarbons of the North Sea. In: Glennie, K.W. (Ed.), Petroleum Geology of the North Sea (4th eds). Blackwell Science Ltd., London, pp. 376-462.

Cornford, C., Kelly, R., 2002. The petroleum systems of the North Slope, Alaska - a volumetric paradox, Abstract submitted for consideration in the 'Arctic Petroleum Systems' session (Chair W. D. Masterson) at the AAPG/SPE meeting, Anchorage, Alaska, pp. 1.

Cornford, C., Birdsong, B. and Groves-Gidney, M., 2014. Offshore Unconventional Oil from the Kimmeridge Clay Formation of the North Sea: A Technical and Economic Case. Unconventional Resources Technology Conference Proceedings, August 25-27, 2014.

Cox, B.M., Sumbler, M.G., and Ivimey-Cook, H.C., 1999. A Formational Framework for the Lower Jurassic of England and Wales (onshore area), British Geological Survey Research Report RR/99/01, pp.1–28.

Dahl, B., Bojesen-Koefoed, J., Holm, A., Justwan, H., Rasmussen, E., Thomsen, E., 2004. A new approach to interpreting Rock-Eval S_2 and TOC data for kerogen quality assessment. Organic Geochemistry 35, pp. 1461-1477.

Department of Energy and Climate Change (DECC), 2013. United Kingdom Continental Shelf (UKCS) Geological Basins. Available online: https://www.gov.uk/oil-and-gas-offshore-maps-and-gis-shapefile$S_2$0140331_UKCS_Geological_Basin (accessed 12.March.2014.).

Delarue, F., Disnar, J.-R., Copard, Y., Gogo, S., Jacob, J., Laggoun-Défarge, F., 2013. Can Rock-Eval pyrolysis assess the biogeochemical composition of organic matter during peatification? Organic Geochemistry 61, pp. 66-72.

Dembicki, H., Jr., 1992. The effects of the mineral matrix on the determination of kinetic parameters using modified Rock-Eval pyrolysis. Organic Geochemistry 18, pp. 531-539.

Disnar, J.R., Guillet, B., Keravis, D., Di-Giovanni, C., Sebag, D., 2003.Soil organic matter (SOM) characterization by Rock-Eval pyrolysis: scope and limitations. Organic Geochemistry 34, pp. 327-343.

Dominguez R. 2007. Structural evolution of the Penguins Cluster, UK northern North Sea. In: Jolley S.J., Barr D., Walsh J.J., Knipe R.J. (eds) Structurally Complex Reservoirs. Geological Society, London, Special Publications, 292,pp. 25–48.

Donovan, D T, and Kellaway, G A 1984. Geology of the Bristol district: Lower Jurassic rocks. Memoir of the British Geological Survey, Bristol Special Sheet (England and Wales).

Duff, P. McL. D. and Smith, A.J. 1992. Geology of England and Wales. Geological Society, London. Pp.651

Durand, B. 1980. Definition kerogen in Kerogen: insoluble organic matter from sedimentary rocks. Technip, Paris, pp. 22-33,

Durand, B. and Nicaise, G., 1980. Procedures for kerogen isolation in Kerogen: insoluble organic matter from sedimentary rocks. Technip, Paris, pp. 35-52.

East, J.A., Swezey, C.S., Repetski, J.E. and Hayba, D.O. 2012. Thermal maturity map of Devonian shale in the Illinois, Michigan, and Appalachian basins of North America. US Geological Survey. Scientific Investigation. Map, 3214 [Online] Available: http://pubs.usgs.gov/sim/3214/ [Accessed 18 March, 2017].

Erratt, D., Thomas, G.M., Hartley, N.R., Musum, R., Nicholson, P.H. and Spisto, Y., 2010. North Sea hydrocarbon systems: some aspects of our evolving insights into a classic hydrocarbon province. In: Vining, B., Pickering, S.C. (Eds.), Petroleum Geology: from Mature Basins to New Frontiers Proceedings of the 7th Petroleum Geology Conference. Geological Society of London, London, England,pp. 37-56.

Espitalié, J., Deroo, G., Marquis, F., 1985. Rock-Eval Pyrolysis and Its Applications (Part One). Oil & Gas Science and Technology - Rev. IFP 40, pp. 563-579.

Espitalié, J., Laporte, L.J., Madec, M., Marquis, F., Leplat, P., Paulet, J., Boutefeu, A., (1977).Methode rapide de caractérisation des roches mères, de leur potentialpetrolier et de leur degré d'evolution. Rev. Inst. Franc. Pétrole 32, pp. 32-42.

Espitalié, J., Deroo, G., Marquis, F., 1985. Rock-Eval Pyrolysis and Its Applications (Part Two). Oil & Gas Science and Technology - Rev. IFP 40, pp. 755-784.

Fishman, N.S., Egenhoff S.O., Boehlke, A.R. and Lowers, H.A. 2015. Petrology and diagenetic history of the upper shale member of the Late Devonian–Early Mississippian Bakken Formation, Williston Basin, North Dakota D. Larsen, S.O. Egenhoff, N.S. Fishman (Eds.), Paying Attention to Mudrocks: Priceless!, Vol. 515, Geological Society of America Special Paper, Denver, CO , pp. 125-151

Furmann, A. Mastalerz, M., Brassell, S.C Pedersen, P.K., Zajac, N.A and Schimmelmann, A. 2015. Organic matter geochemistry and petrography of Late Cretaceous (Cenomanian-Turonian) organic-rich shales from the Belle Fourche and Second White Specks formations, west-central Alberta, Canada. Organic Geochemistry, 85, pp. 102-120.

Galimov, E.M., 2006. Isotope organic geochemistry. Journal of Organic Geochemistry. 37 (10), 1200

Gautier, D.L., 2005. Kimmeridgean Shales Total Petroleum System of the North Sea Graben Province: U.S. Geological Survey Bulletin 2204-C, 24. Available online http://pubs.usgs.gov/bul/2204/c [accessed 15. July.2014].

Gentzis, T., Goodarzi, F., Snowdon, L.R., 1993. Variation of maturity indicators (optical and Rock-Eval) with respect to organic matter type and matrix lithology: an example from Melville Island, Canadian Arctic Archepelago. Marine and Petroleum Geology 10, pp. 507-514.

Glennie, K.W., 1986. Development of northwest Europe's southern Permian gas basin. In: Brooks, J., Goff, J.C., van Hoorn, B. (Eds.), Habitat of Palaeozoic Gas in NW Europe, Geological Society, London, Special Publication 23, pp. 3-22.

Goff, J.C., 1983. Hydrocarbon generation and migration from Jurassic source rocks in the East Shetland Basin and Viking Graben of the northern North Sea. Journal of the Geology Society 140, pp. 445-474.

Gunter, F and Mensing, T.M., 2004. Isotopes: Principles and Applications, 3rd Edition pp.928

Hackley, P.C., Fishman, N., Wu, T., Baugher, G., 2016. Organic Petrology and Geochemistry of Mudrocks from the Lacustrine Lucaogou Formation, Santanghu Basin, Northwest China: Application to Lake Basin Evolution. International Journal of Coal Geology, 168, pp.20-34.

Hackley, P.C. and Cardott, B.J. 2016. Application of organic petrography in North American shale petroleum systems: A review. International Journal of Coal Geology 163, pp. 8–51.

Hagemann, H.W., 1975. Petrographische and palynologische Untersuchung der organischen Substanz (Kerogen) in denliassischen Sedimenten Luxemburgs. In: Tissot, B. andBienner, F. ed., Advances in Organic Geochemistry, 1973.Technip, Paris, 29-37.

Hallam, A. 1960. A sedimentary and faunal study of the Blue Lias of Dorset and Glamorgan. Philosophical Transactions of the Royal Society, London, B243, 698, pp.1-44.

Hallam, A. 1968. The Lias. In The Geology of the East Midlands (eds P.C. Sylvester-Bradley and T.D. Ford), Leicester University Press, pp. 188–210.

Hallam, A. 1975. Jurassic Environments. Cambridge University Press, Cambridge.

Hallam, A. and Sellwood, B. W. 1976. Middle Mesozoic Sedimentation in Relation to Tectonic in the British Area. Journal of Geology No. 84, pp. 301-21.

Hallam, A. 1984. Pre-Quaternary Sea-level Changes Annual Review of Earth Planetary Science. No.12, pp. 205-43.

Hare, A.A., Kuzyk, Z.Z.A., Macdonald, R.W., Sanei, H., Barber, D., Stern, G.A.and Wang, F., 2014. Characterization of sedimentary organic matter in recent marine sediments from Hudson Bay, Canada, by Rock-Eval pyrolysis. Organic Geochemistry 68, pp. 52-60.

Hatcher, P.G., Spiker, E.C., Szeverenyi, N.M., Maciel, G.E., (1983). Selective preservation and origin of petroleum-forming aquatic kerogen. Nature 305, 498–501.

Hetényi, M., Nyilas, T., Tóth, T.M., 2005. Stepwise Rock-Eval pyrolysis as a tool for typing heterogeneous organic matter in soils. Journal of Analytical and Applied Pyrolysis 74, pp.45-54.

Hesselbo, S P and Jenkyns, H C A, 1995. A comparison of the Hettangian to Bajocian successions of Dorset and Yorkshire. 105-150 in Taylor, P D (Editor). Field geology of the British Jurassic London Geological Society.

Hesselbo, S.P. and Jenkyns, H.C. 1998. British Lower Jurassic sequence stratigraphy In: De Graciansky, P.C., Hardenbol, J., Jacquin, T., Farley, M.B. and Vail, P.R. (eds.) Mesozoic-Cenozoic Sequence Stratigraphy of European Basins. Special Publication of the Society for Sedimentary Geology (SEPM), 60, pp. 561-581.

Hesselbo, S.P., Robinson, S.A. and Surlyk F. 2004. Sea-level change and facies development across potential Triassic–Jurassic boundary horizons, SW Britain. Journal of the Geological Society, London, 161, pp.365-379.

Horsfield, B. and Douglas, A. G., 1980. The influence of minerals on the pyrolysis of kerogens. GeochimicaetCosmochimicaActa 44, pp. 1119-1131.

Hutton, A. C., 1987. Petrographic classification of oil shales. International Journal of Coal Geology 8(3), pp.203-231.

ICCP, 1995. International Committee for Coal and Organic Petrology (ICCP), 1995. Vitrinite Classification; ICCP System 1994. ICCP, Aachen.

Jarvie, D., Baker, D., 1984. Application of the Rock-Eval III Oil Show Analyzer to the study of gaseous hydrocarbons in an Oklahoma gas well, 187th American Chemical Society National Meeting, Geochemistry Division.American Chemical Society, St. Louis, Missouri.pp.1-22.

Jarvie, D.M., 1991. Factors affecting Rock-Eval derived kinetic parameters. Chemical Geology 93, pp. 79-99.

Jarvie, D. M., 2000. Assessment and prediction of hydrocarbon generation of the Barnett Shale (abstract), in L. Brogdon, ed., Barnett Shale Symposium, Fort Worth, Texas: Oil Information Library of Fort Worth, Texas, p. 7.

Jarvie, D. M., and Lundell, L. L., 2001. Amount, type, and kinetics of thermal transformation of organic matter in the Miocene Monterey Formation,in C. M. Isaacs and J. Rullkotter, eds., The Monterey Formation: From rocks to molecules: New York, Columbia University Press, chapter 15, p. 268 – 295.

Jarvie, D.M., Hill, R.J., Ruble, T.E., Pollastro, R.M., 2007. Unconventional shale gas systems: the Mississippian Barnett Shale of north-central Texas as one model for thermogenic shale gas assessment. American Association of Petroleum Geologists Bulletin91, pp. 475-499.

Jarvie, D.M., 2012. Shale Resource Systems for Oil and Gas: Part 2 - Shale-oil Resource Systems. American Association of Petroleum Geologist Memoir 97, pp. 89-119.

Jenkyns, H.C., Jones, C.E., Gröcke, D.R., Hesselbo, S.P. and Parkinson, D.N. 2002. Chemostratigraphy of the Jurassic System: applications, limitations, and implications for palaeoceanography. Journal of the Geological Society, London, 159, pp.351-378.

Johannes, I., Kruusement, K., Veski, R., 2007. Evaluation of oil potential and pyrolysis kinetics of renewable fuel and shale samples by Rock-Eval analyzer. Journal of Analytical and Applied Pyrolysis 79, pp. 183-190.

Johannes, I., Kruusement, K., Palu, V., Veski, R. and Bojesen-Koefoed, J.A., 2006. Evaluation of oil potential of Estonian shales and biomass samples using Rock-Eval analyzer. Oil Shale 23, pp. 110-118.

Johannes, I., Kruusement, K., Veski, R. and Bojesen-Koefoed, J., 2006. Characterisation of pyrolysis kinetics by Rock-Eval basic data. Oil Shale 23, pp. 249-257.

Johannes, I., Kruusement, K. and Veski, R., 2007. Evaluation of oil potential and pyrolysis kinetics of renewable fuel and shale samples by Rock-Eval analyzer. Journal of Analytical and Applied Pyrolysis 79, pp. 183-190.

Junium, C.K. & Arthur, M.A. 2007. Nitrogen cycling during the Cretaceous, Cenomanian-Turonian Oceanic Anoxic Event II, Geochemistry, Geophysics, Geosystems, 8, 3, doi:10.1029/2006GC001328.

Langford, F.F. and Blanc-Valleron, M.M., 1990. Interpreting Rock-Eval pyrolysis data using graphs of pyrolizable hydrocarbons vs. total organic carbon. American Association of Petroleum Geologists Bulletin 74, pp. 799-804.

Lewan, M.D., 1986. Stable carbon isotopes of amorphous kerogens from Phanerozoic sedimentary-rocks, Geochimica et Cosmochimica Acta, 50 (8), pp. 1583-1591. DOI: 10.1016/0016-7037(86)90121-3

Lewan, M.D., Ruble, T.E., 2001. Comparison of petroleum formation kinetics by hydrous pyrolysis and rock-eval pyrolysis, 20th International Meeting on Organic Geochemistry, Nancy, France, pp. 202-203.

Littler, K., Hesselbo, S.P and Jenkyns, H.C. 2010. A carbon-isotope perturbation at the Pliensbachian–Toarcian boundary: evidence from the Lias Group, NE England. Geology Magazine 147 (2), pp. 181–192.

Kalkreuth, W., Ade, M.V.B., Henz, G., Ganz, H., Kommeren, K., 2002. Source rock maturity in the Central and Viking Graben structures, North Sea - evaluation of optical and geochemical (Rock-Eval, infrared spectroscopy) maturity parameters. Revista Latino-Americana de GeoquimicaOrganica 6, pp. 5-22.

Khasaei, N.M., Eftekhari, N.A., 2007. Determination of source rocks kinetic parameters by using Rock-Eval pyrolysis system. Amirkabir 18, pp. 19-26.

Kamerling, P., 1979. Geology and hydrocarbon habitat of the Bristol Channel Basin. Journal of Petroleum Geologists,vol .2, pp.75-93.

Kim,J.H., Park, M.H., Tsunogai, U., Cheong, T.J., Ryu, B.J., Lee, Y.J., Han, H.C., Oh, J.H. and Chang, H.W., 2007. Geochemical characterization of the organic matter, pore waterconstituents and shallow methane gas in the eastern part of the Ulleung Basin, East Sea (Japan Sea). Island Arc 16, pp.93-104.

King, R. R., 2015. Modified Method and Interpretation of Source Rock Pyrolysis for an Unconventional World. AAPG Search and Discovery Article #41704. Available on http://www.searchanddiscovery.com/documents/2015/41704king/ndx_king.pdf (Accessed on 19th June, 2017.

Marchand, C., Lallier-Vergès, E., Disnar, J.R., Kéravis, D., 2008. Organic carbon sources and

transformations in mangrove sediments: A Rock-Eval pyrolysis approach. Organic

Geochemistry 39, pp.408-421.

Maynard, J.B., 1981. Carbon isotopes as indicators of dispersal patterns in DevonianMississippian shales of the Appalachian Basin, Geology, 9, pp. 262-265.

Meyers, P.A., Benson, L.V., 1988. Sedimentary biomarker and isotopic indicators of the paleoclimatic history of the Walker Lake basin, western Nevada. Organic Geochemistry. 13, 807-813.

Meyers, P.A., Eadie, B.J., 1993. Sources, degradation and recycling of organic matter associated with sinking particles in Lake Michigan. Org. Geochem. 20, 47-56.

Meyers, P.A., Leenheer, M.J., Eadie, B.J. and Maule, S.J., 1984. Organic geochemistry of suspended and settling particulate matter in Lake Michigan. Geochim. Cosmochim.Acta 48, 443-452.

Meyers, P.A and Bernasconi S.M. 2005. Carbon and nitrogen isotope excursions in mid-Pleistocene sapropels from the Tyrrhenian Basin: evidence for climate-induced increases in microbial primary production. Marine Geology, 220, pp. 41–58

NIGOGA: The Norwegian Guide to Organic Geochemical Analyses. [Online] Available: http://www.npd. no/engelsk/nigoga/default.htm (accessed 10.05.14.). [Accessed 10 Jun. 2014].

Palmer, C.P., 1972. The Lower Lias (Lower Jurassic) between Watchet and Lilstock in North Somerset (United Kingdom). Newsletter on Stratigraphy,vol.2, pp.1-30.

Pelet, R., 1994. Comments on the paper 'The effects of mineral matrix on the determination of kinetic modified Rock-Eval pyrolysis' by Dembicki, H. Organic Geochemistry 21, pp. 979-981.

Pernia, D., Bissada, K.K.A. and Curiale J. 2015. Kerogen based characterization of major gas shales: effects of kerogen fractionation. Organic Geochemistry, 78, pp. 52-61.

Peters, K.E., 1986. Guidelines for evaluating petroleum source rock using programmed pyrolysis. American Association of Petroleum Geologists Bulletin 70, pp. 318-329.

Peters, K.E; Walters, C.C. and Moldowan, J.M., 2005. The Biomarker Guide Volume 2: Biomarkers and Isotopes in Petroleum Exploration and Earth History, 2nd Ed. Cambridge, pp.475-1155.

Petersen, H.I., 2006.The petroleum generation potential and effective oil window of humic coals related to coal composition and age: International Journal of Coal Geology, v. 67, pp. 221–248.

Petersen, H.I., Schovsbo N.H. and Nielsen A.T. 2013. Reflectance measurements of zooclasts and solid bitumen in Lower Paleozoic shales, southern Scandinavia: correlation to vitrinite reflectance. Internal Journal of Coal Geology, 114, pp. 1-18

Pillot, D., Deville, E. and Prinzhofer, A., 2013. Identification and quantification of carbonate species using Rock-Eval pyrolysis. Oil and Gas Science and Technology 69, pp.341-349.

Poot, A., Quik, J.T.K., Veld, H.and Koelmans, A.A., 2009. Quantification methods of black carbon: Comparison of Rock-Eval analysis with traditional methods. Journal of Chromatography A 1216, pp.613-622

Potter, J., (1998). Organic petrology, maturity, hydrocarbon potential and thermal history of the Upper Devonian and Carboniferous in the Liard Basin, Northern Canada.Newcastle University, Ph.D. Thesis.pp.508

Raji, M., Grocke, D.R, Greenwell, H.C., Gluyas, J.G., Cornford, C., 2015.The effect of interbedding on shale reservoir properties. Marine and Petroleum Geology 67, pp.154-169.

Riboulleau, A., Tribovillard, N., Baudin, F., Bout-Roumazeilles, V.and Lyons, T., 2011. Unexpectedly low organic matter content in Cariaco Basin sediments during the

Younger Dryas: Origin and implications. Comptes Rendus Geosciences 343, pp.351-359.

Riediger, C.L., 1993. Solid bitumen reflectance and Rock-Eval T_{max} as maturation indices: an example from the "Nordegg Member", Western Canada Sedimentary Basin. International Journal of Coal Geology 22, pp. 295-315.

Rimmer, S. M., Cantrell, D. J. and Gooding, P. J., 1993. Rock-eval pyrolysis and vitrinite reflectance trends in the Cleveland Shale Member of the Ohio Shale, eastern Kentucky. Organic Geochemistry 20, pp. 735-745.

Rimmer, S.M., Thompson, J.A. Goodnight, S.A. and Robl, T.L. 2004. Multiple controls on the preservation of organic matter in Devonian-Mississippian marine black shales: geochemical and petrographic evidence. Palaeogeography Palaeoclimatology Palaeoecology, 215, pp. 125-154

Rippen, D., Littke, R., Bruns, B. and Mahlstedt N. 2013. Organic geochemistry and petrography of Lower Cretaceous Wealden black shales of the Lower Saxony Basin: the transition from lacustrine oil shales to gas shales. Organic Geochemistry 63, pp. 18-36.

Romero-Sarmiento, M.F, Pillot,D., Letort, G. Lamoureux-Var, V., Beaumont, V.,Huc,A.Y and Garcia, B 2016. New Rock-Eval Method for Characterization of Unconventional Shale Resource Systems. Oil & Gas Science and Technology – Rev. IFP Energies nouvelles, 71, 37, pp.1-8

Saenger,A., Cecillon, L., Sebag, D., Brun, J.J., 2013. Soil organic carbon quantity, chemistry and thermal stability in a mountainous landscape: A Rock-Eval pyrolysis survey. Organic Geochemistry 54, pp.101-114.

Sanei, H., Stasiuk, L.D., Goodarzi, F., 2005. Petrological changes occurring in organic matter from Recent lacustrine sediments during thermal alteration by Rock-Eval pyrolysis. Organic Geochemistry 36, pp. 1190-1203.

Sebag, D., Disnar, J.R., Guillet, B., Di Giovanni, C., Verrecchia, E.P. and Durand, A., 2006. Monitoring organic matter dynamics in soil profiles by Rock-Eval pyrolysis': bulk characterization and quantification of degradation. European Journal of Soil Science ,55, pp. 344-355.

Sellwood, M., Davis, G., Brunsden, D., and Moore, R. 2000. Ground models for the coastal landslides at Lyme Regis, Dorset, UK. In: Landslides in Research, Theory & Practice. Thomas Telford, London, 3, pp1361-1366.

Snowdon, L.R., 1995. Rock-Eval T_{max} suppression: documentation and amelioration. American Association of Petroleum Geologists Bulletin79, pp. 1337-1348.

Simms, M.J., Chidlaw, N., Morton, N. and Page, K.N., 2004. British Lower Jurassic Stratigraphy, Geological Conservation Review Series, No. 30, Joint Nature Conservation Committee, Peterborough, pp.458.

Stanley, R.G., Lillis, P.G., Pawlewicz, M.J., and Haeussler, P.J., 2014 Rock-Eval pyrolysis

and vitrinite reflectance results from the Sheep Creek 1 well, Susitna basin, south-central Alaska: U.S. Geological Survey Open-File Report 2013-1307, 12 p.

Stoneley, R., 1982. The structural development of the Wessex Basin. Journal of the Geological Society 139, pp.543-554.

Stoneley, R. and Selley, R C. 1991. A Field Guide to the Petroleum Geology of the Wessex Basin (3rd edition). R. C. Selley & Co., Dorking.

Sykes, R. and Snowdon, L.R., 2002. Guidelines for assessing the petroleum potential of coaly source rocks using Rock-Eval pyrolysis. Organic Geochemistry 33, pp. 1441-1456.

Sykes, R., Snowdon, L.R. and Johansen, P.E., 2003. Rock-Eval-based maturation pathways for humic coals: how well do they represent the natural evolution of oil and gas? 21stInternational Meeting on Organic Geochemistry (21st IMOG).Abstracts.EAOG., Krakow, Poland, pp. 31-32.

Tambach, T.J., Veld, H. and Griffioen, J., 2009. Influence of HCl/HF treatment on organic matter in aquifer sediments: A Rock-Eval pyrolysis study. Applied Geochemistry 24, pp. 2144-2151.

Taylor, G.H., Teichmüller, M., Davis, A., Diessel, C.F.K., Littke, R. and Robert, P., (1998.Organic Petrology. GebrüderBorntraeger, Berlin, 704 pp.

Tissot B.P., Califet-Debyser Y., Deroo G. and Oudin J.L. 1971. Origin and evolution of hydrocarbons in Early Toarcian shales, 55, pp. 2177-2193.

Tissot, B. P. and Welte, D. H. 1984. Petroleum formation and occurrence, 2nd edition. Springer,New York, pp. 55-73.

Tyson, R. 2004. Variation in marine total organic carbon through the type Kimmeridge Clay Formation (Late Jurassic), Dorset, UK. Journal of the Geological Society, 161(4), pp.667-673.

Underhill J.R. and Stoneley, R., 1998. Introduction to the development, evolution and petroleum geology of the Wessex Basin,in: Underhill, J.R. ed., Development, Evolution and Petroleum Geology of the Wessex Basin. Geological Society Special Publication No. 133. Geological Society, London, pp. 1-18. vanKrevelen, D.W., (1993). Coal. Elsevier, Amsterdam.

Williams, P. F. V. and Douglas, A. G., 1983. Advances in Organic Geochemistry 1981 Bjoroy, M., ed., Wiley, pp. 568-75

Yalçın Erik, N., Özçelik, O. and Altunsoy, M. 2006. Interpreting Rock–Eval pyrolysis data using graphs of S_2 vs. TOC: Middle Triassic–Lower Jurassic units, eastern part of SE Turkey. Journal of Petroleum Science and Engineering, 53(1-2), pp.34-46.

Chapter 8: Thesis Summary, Research Limitations and Recommendations for Future Work

This chapter summarises the key results of the application of geochemical, petrographic and geomechanical techniques in the assessment of the Kimmeridge Clay Formation as a potential unconventional resource. The main findings relating to the identification of the sweet-spot parameters discussed in Chapter 1 are bought together, research limitations including work on the separation of maceral endmembers using Density Gradient Centrifugation that was undertaken but did not feature in this thesis are discussed and recommendations for future work are proposed.

8.1: Research Summary

8.1.1: Introduction

The Kimmeridge Clay Formation is one of the most prolific world-class source rocks for conventional oil and gas in the North Sea region. Recent re-evaluation of a large database of conventional source rock analyses and recent pyrolysis data show that the Kimmeridge Clay Formation of the UK contains large volumes of residual (i.e. un-expelled) oil where buried below about 3.2 km. Petroleum expulsion efficiency is about 2-12 %, suggesting significant amounts of un-expelled oil and gas remain within the source rock and in the migration paths of the basin.

The research in this thesis was undertaken to evaluate the potential of offshore unconventional resources in the South Viking Graben area of the North Sea. Some of the advantages of exploring for unconventional resources offshore UK include: larger basin centres than onshore; the continuous subsidence in the North Sea allows drilling directly into an actively generating world class oil-prone source rock; the availability of existing under-utilised drilling platforms and pipelines in the North Sea; drilling deviated wells from onshore; existing seismic surveys and well data to define extent and thicknesses; large database of geology, geochemistry and mineralogy from conventional drilling to define the structural and tectonic history, organic-richness, kerogen types, thermal maturation, burial history, mineralogical

composition and geochemical properties; limited environmental constraints compared to onshore; unlimited water supply to use in hydraulic fracturing; and a lack of significant political issues.

The principal aim of this research is to evaluate the future prospects of offshore unconventional liquid hydrocarbon and identify "sweet-spot" areas for optimum extraction of the remaining residual oil in the South Viking Graben area of the North Sea. A sweet-spot has been defined as an area with certain reservoir properties and attributes where well penetration will be most economical for optimum recovery. Predicting the sweet-spot areas where well penetration will be most economical is critical for the assessment and evaluation of unconventional reservoirs. Integration of certain reservoir parameters such as lithology, mineralogy, area extent, depth, thicknesses, total organic carbon (TOC), maturity, porosity, permeability and adsorption capacity of source rocks is important for the identification and mapping of sweet-spot areas. Optimum combinations of these properties have been successfully used to predict and identify sweet spot areas, although the controlling processes seem to vary from basin to basin (Jarvie et al, 2007).

The principal focus of this research is the application of geochemical, mineralogical, petrographical and porosity related techniques in the assessment and evaluation of Upper Jurassic Kimmeridge Clay Formation as a potential unconventional hydrocarbon resource. The results of this research can be applied to the assessment of other well-known prolific source rocks that have produced conventional oil and gas for potential unconventional exploration. Throughout this research, the key sweet-spot reservoir parameters for successful shale oil and gas exploration adopted are largely based on analogue information from unconventional shale play in the United States. The importance of these reservoir parameters-has been discussed in Chapter 1. The main results from each analytical techniques used for the assessment of these reservoir parameter are summarised in this chapter and recommendations for future work are suggested.

In this research, the sweet-spot parameters for the Kimmeridge Clay Formation were assessed using a combination of database and analytical techniques such as

geochemistry; (TOC, Rock-Eval Pyrolysis, δ13C and kerogen isolation for organic matter quality, kerogen type, maturity, hydrocarbon potential and source origin); mineralogical (thin-section and XRD analyses for mineral composition); petrography (microscopic analysis of macerals under reflected and transmitted light); and porosity (for the nature and type of porosity in this hybrid reservoir).

8.1.2: Unconventional Hydrocarbon Potential of the Kimmeridge Clay Formation

Chapter 1: (overview of Kimmeridge Clay as an unconventional resource)

Unconventional oil and gas is found in fine-grained reservoirs with relatively low permeability (micro-nano Darcies) and porosity. Given the low permeability and porosity of these reservoirs, in order for the gas to be produced commercially enhanced drilling techniques, including fracture stimulation, are required. The potential of the Kimmeridge Clay Formation source rock as an unconventional resource was determined using sweet-spot adopted from unconventional resource evaluation in the United States.

Chapter 2: Database, sample selections and analytical methods

For application of these sweet-spots criteria to the assessment of Kimmeridge Clay reservoir properties, it was possible to first of all make a synthesis of all database information presently held in commercial and public databases, as well as literature reviews and particularly the area of interest in the licence blocks held by Trap oil Ltd in Quadrant 16, and 17 in the South Viking Graben area. Using the available data sets, core samples were selected based on well location, lithologies, organic matter content and on the different level of thermal maturation. The selected core samples were examined for a variety of reservoir properties using a wide range of geology, geochemistry, petrographic, petrology, and porosity analytical methods. Results of these analyses described in Chapter 2 were discussed in Chapters 3, 4, 5, 6 and 7 and the set aim and objectives in Chapter 1 for this PhD research were achieved.

Chapter 3: Thickness, depth and organofacies distribution

The depth, area extent and thickness of the Kimmeridge Clay Formation have been investigated in Chapter 3. The present-depth may be related to the maturity of the source rocks, where maturity covers a depth interval of 2500 m- 4200 m. The thickness of the KCF/Draupne Formation varies considerably in both the UK and Norway, with a thickness of up to 600 m in the north-western part towards the graben centre and from about 0-200 m in south eastern part with an average thickness of 85 m. The maximum recorded thickness of 807 m is observed in Well 15/3-1 S (the Gudrun discovery). Further noticeable examples of thickness include 453 m thick in Well 15/3-7, 541 m thick in Well 15/3-8 and 347 m in Well 15/3-9 all located in the Norwegian acreage in the deepest part of the graben. Where the KCF-Draupne has the highest maturity it can have a thickness of over 1100 m in the South Viking Graben area, this is considerably higher than the average thickness (> 50 ft.) required for unconventional shale resources.

The kerogen types as reflected by Rock-Eval HI, T_{max} values shows both vertical and lateral variation, it predominantly consist of classic Type II mostly derived from marine bacterially degraded algae with terrigeneous input. Type II kerogen have the best characteristics for unconventional exploration compared to Type I and Type III; because they are oil prone and highly generative, though similar to Type I, but retain a high proportion of oil and gas in the source rock. Type II kerogens found in the majority of the samples is similar to the kerogens of North American Shale play (e.g. Haynesville, Bakken, Eagle Ford, Barnett and Marcellus), and has the optimum potential to produce significant hydrocarbons in the North Sea.

Carbon and Nitrogen (C/N) ratios and δ^{13}Corg values were used to classify the origin and source of the organic matter in the source rocks. The δ13C values range from -29.73 ‰ to -26. 88 ‰, these values are characteristic of marine organic matter with input from terrestrial fragments. The average TOC values recorded for the Viking Group is up to 5 wt.%, with a maximum TOC of 11 wt.% indicating a good to very good organic-richness. TOC content of the source rocks have been extensively discussed in Chapters 3 -7. The quantity of organic matter as indicated by the TOC

values of the Kimmeridge Clay Formation is relatively high for an unconventional resource, which is equivalent to the Barnett Shale (0.9-12 wt.% TOC), Marcellus Shale (2-13 wt.% TOC) and Bakken Shale (3.5-40 wt.% TOC) of North American.

Chapter 4: The effect of Sand Interbedding on Shale Reservoir Properties)

From this study, three gross facies are recognized; Kimmeridge Clay "hot shale" (both Upper and Lower), an intermediate facies of interbedded sands and mudstones termed the tiger stripe facies, and massive sand and conglomerates of the Brae Formation. Within the 'hot shale' organic-lean sandstone and siltstone intervals are intimately interbedded; this sediment association forms the target for this present study. Once oil is generated in the Kimmeridge Clay, the expelled oil ultimately migrates to accumulate in sandstone reservoirs. The source rock shales, however, still contain the portion of the oil that was not expelled. As a consequence such shales and juxtaposed non-source lithofacies can form the targets for the exploration for 'unconventional oil'. The term "hybrid system" is used to describe this type of organic-rich mudstone with juxtaposed (interbedded, underlying and/or overlying) organic-lean non-source lithofacies. This organic-lean non-source lithofacies has less affinity for oil so it produces more readily leading to higher recovery of the original oil in place (OOIP). In contrast, the organic-rich mudstone tends to retain more oil due to its sorptive affinity and lower permeability.

The lithological and compositional heterogeneity of the mudstone-sandstone interbeds is caused in part by variation in organic richness (TOC) and kerogen type as evidenced by the core samples in the study area. Migration of free oil (S_1) from the mudstone into the interbedded sandstone involves a short lateral distance through the sandstone pores from the source to storage in the interbeds resulting in high productivities. Thus the conclusion is that free oil (S_1) has migrated into the sandy layers, this implies that the sandier samples have retained rather than drained oil, and hence that they may enhance the potentially producible oil content in the study area. The abundance of sandy layers would be expected to define drainage. However, the relationship between PI and T_{max} suggest these bulk samples to be poorly-drained source rocks at the maturity levels encountered.

At an early stage of maturation, the oil generated from kerogen in the mudstones will start to saturate any available porosity. With increasing maturation, the mudstone porosity will be filled and, subject to adequate permeability, localised expulsion will start to fill the open pore spaces of sandstones in close proximity. The mudstones will contain the retained oil prior to, during and after expulsion. The Oil Saturation Index (OSI = S_1/TOC) shows higher values for sandstone-rich samples relative to the mudstones, and higher values for lower TOC samples at the encountered early-mature level of maturation. These data suggest that the optimal unconventional samples have ~50 % sand and TOC values in the range of 1-2%. The key points of this hybrid system are the thickness, storage capacity and the possibility to capture a portion of the expelled as well as retained oil.

In terms of mineralogy, X-ray diffraction (XRD) results suggest these samples are dominated by quartz, clay, organic matter and pyrite. Kaolinite and illite/smectite are the dominant clay minerals identified in all samples. The abundance and preservation of silicate minerals in the sand-rich lithofacies suggest little diagenetic alteration, with the primary quartz content likely to exert control on the brittleness of the interbedded sandstone and mudstone. Finding an area in this hybrid system with > 50 % quartz content can be used to infer brittleness, a key factor in creating vertical fracture pattern that are large enough to connect the maximum amount of rock volume during hydraulic fracturing stimulation.

Chapter 5: S_1 (free hydrocarbon), Porosity and Productivity in the Kimmeridge Clay Formation

The S_1 peak (kg free liquid per tonne of rock) data was used to determine the volume of oil that can be potentially produced by hydraulic fracking of these organic rich Kimmeridge mudstones at peak oil maturity. Using the mass balance argument that indicates that the decrease in S_2 is an indication of 'oil generation', and then S_1 indicate 'oil retention' rather than production. This means an increase in S_1 is indicative of an increase in available storage of 'free oil S_1' whereas a decrease indicates loss of storage of 'free oil S_1' or a decrease in adsorptive surface area. Relationships between TOC and S_1 derived from cross-plots where the majority of > 2 %TOC samples (89.5 %)

show a strong positive correlation. The comparisons of S_1 volumes (1.8 vol. %) against mudstone porosities (1.62 vol. %), suggest that the open porosity is fully saturated with oil at peak maturity. The distributions of porosity and S_1 yields are similar, which means S_1 storage and hence porosity appear to be within the kerogen (intra-kerogen porosity) rather than between the grains (inter-granular mineral porosity).

Chapter 6: Porosity Types

Identification of microscale and nanoscale characterisation of the mudstone fabric, distribution, porosity and permeability is important for hydrocarbon storage and flow within. Mineral and textural analyses combined with pore-scale imaging at the core scale have identified organic porosity within the kerogen and interparticle and intraparticle porosity in the kerogen and mineral matrixes. Organic porosity is well developed in mudstone-rich samples, and it was observed that there is a good correlation between the samples with high TOC content and organic porosity, suggesting a greater potential for hydrocarbon storage may exist in higher TOC mudstone-rich intervals depending on pore connectivity. Interparticle and intraparticle porosity is abundant in the sandstone-rich, sandstone-mudstone interfaces and mudstone-rich intervals of the Kimmeridge Clay Formation. Depending on the overall pore throat sizes, the combination of these porosities in the Kimmeridge Clay Formation may significantly contribute to the effective porosity and the connectivity of the permeability flow path for hydrocarbons in the Kimmeridge hybrid shale reservoir.

Chapter 7: Effect of Demineralisation on Kimmeridge Kerogens

The effect of demineralisation on isolated Kimmeridge Clay kerogens on the quality of organic matter, kerogen type, maceral composition, thermal maturation and the generative potential was investigated. This analysis was undertaken to study the changes in the physical and chemical properties of macerals at each step to enable a better understanding of the role of kerogen in the Kimmeridge Clay. The TOC values in the whole rock samples is between 2.7-8.9 wt. % TOC, while the TOC values in the isolated kerogens (52-74 wt. %) are much higher. The range of TOC values in isolated

kerogen suggests that not all mineral matrixes were removed during the demineralization process and petrographic observations indicate that minerals such as quartz and clay (silicates), and carbonates had been removed, but that pyrite remained. The distribution of kerogen types is similar in both the isolated kerogen and whole rock indicating no effect of mineral removal on the determination of the kerogen types from HI values. In terms of maturity, the T_{max} values plotted against burial depth placed most of the samples within the oil window, and indicate no effect of demineralisation on oil window maturity.

8.2: Research Limitations

In order to fully gain more understanding on the hydrocarbon potential of thinly inter-bedded source rocks the individual components of the organic matter (kerogen macerals) needs to be separated and analysed using conventional petroleum techniques (i.e., TOC, Rock Eval, etc.). This logical next step in the research would help to understand the role of kerogen and what makes up the kerogen in the Kimmeridge Clay "hot shale". Taking apart the kerogen and looking at component macerals in particular will provide information with respect to the retention and/or expulsion of liquid hydrocarbons at sand/shale interfaces of thinly interbedded source rocks. For this analysis, 27 kerogen samples of the Kimmeridge Clay Formation were isolated from the mineral matrix by acid digestion of the inorganic phases (methodology is described in Chapter 7, Section 7.4.2). These core samples were selected based on lithology, depth, TOC, kerogen type and level of maturity from the BGS core store in Nottingham. Density Gradient Centrifugation (DGC) analysis was performed on the isolated kerogen at Southern Illinois University in Carbondale, USA. The DGC techniques involves suspension of 1 g of pure kerogens with cesium chloride density gradient ranging from 1 to 1.5 g cm-3 in a 30 cm3 plastic centrifuge tube. The gradient was centrifuged in a Beckman J2-21M centrifuge using a zonal rotor at 17 500 rpm (g at rmax = 30 500) for 1 hour. The gradient was fractionated and densities of the fractions were measured using a Mettler density meter. The kerogen fractions were recovered by filtration for further analysis. TOC, Rock-Eval pyrolysis and petrological analyses were performed on the selected fractions.

Irregular and anomalous density readings were recorded for all the fractionated macerals. Petrographic observations indicate that pyrite remained in kerogens. This is to be expected since the demineralization process did not include nitric acid (HNO3) oxidation (often used to remove pyrite), as this procedure can alter the organic matter, particularly Amorphous Organic Matter (Tambach et al., 2009). A separate experiment using Liquid Nitrogen, Nitric acid (HNO3) and Chromium (II) Chloride (CrCl2) treatment was performed on the kerogen before the fractionation. However, when further petrographic examination with reflected white light and fluorescence microscopy was performed on the density fractionated macerals, evidence of pyrite was still observed (Figure 8-1 to Figure 8-3).

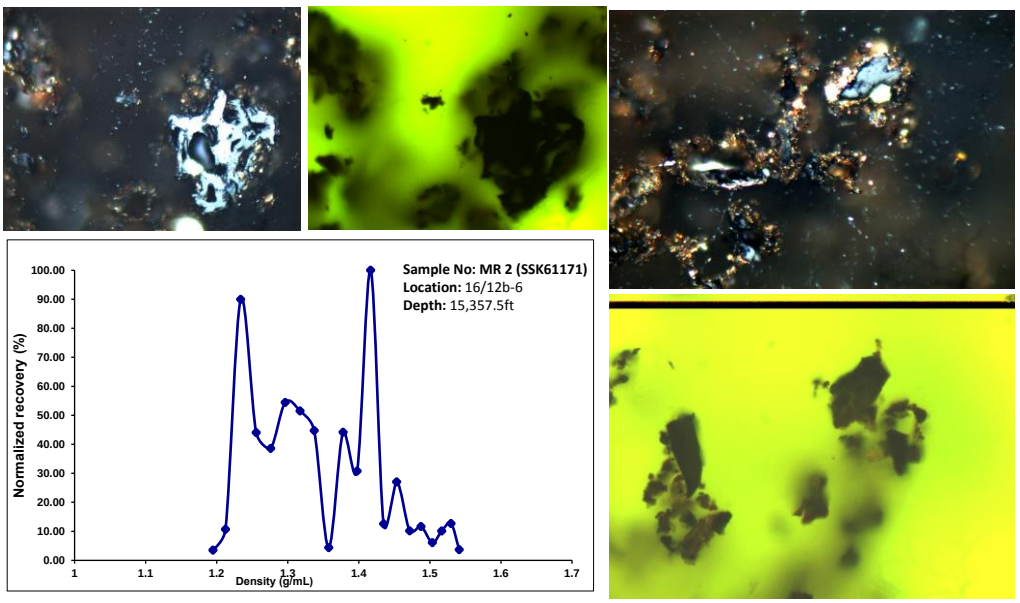

Figure 8-1: Density gradient profile range of 1.2-1.55 g/mL for distinct density peaks showing anomalous density reading and pyrite in the separated fractions from petrographic observation.

Even the samples with normal density gradient profile and peaks appeared to still contain pyrite in the fractionated macerals (Figure 8-4). It is concluded that these samples are not essentially pure kerogens but further experimentation to remove pyrite would destroy the organic matter because the pyrite is organically bound. The efforts to completely remove pyrite minerals from the maceral fractions were unsuccessful in this study; more time is needed to come up with perfect techniques for pyrite removal without altering the organic matter.

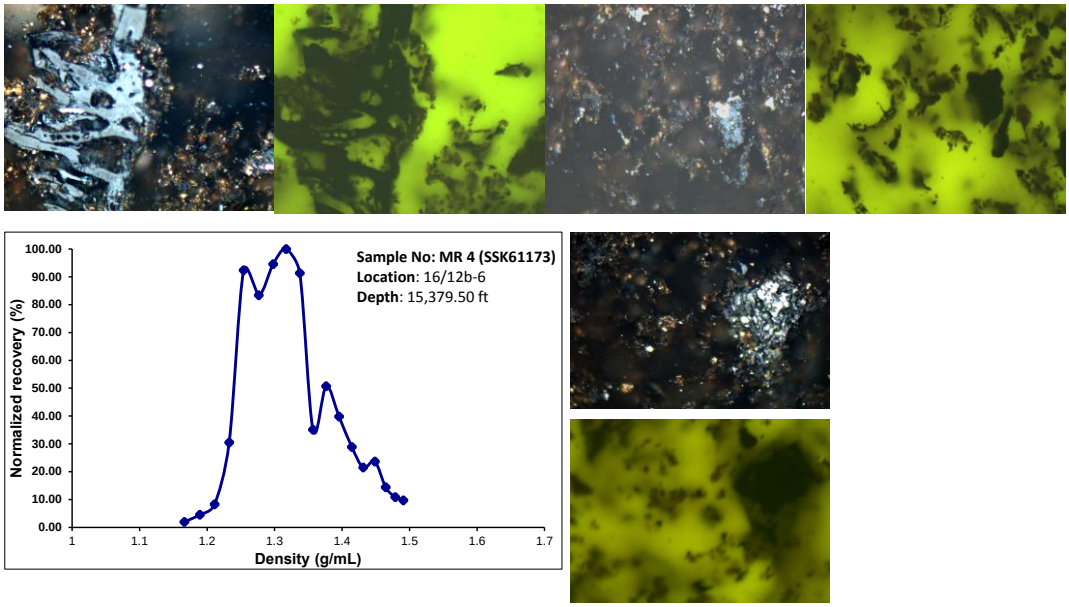

Figure 8-2: Density gradient profile range of 1.18-1.50 g/mL for distinct density peaks showing anomalous density reading and pyrite in the separated fractions from petrographic observation.

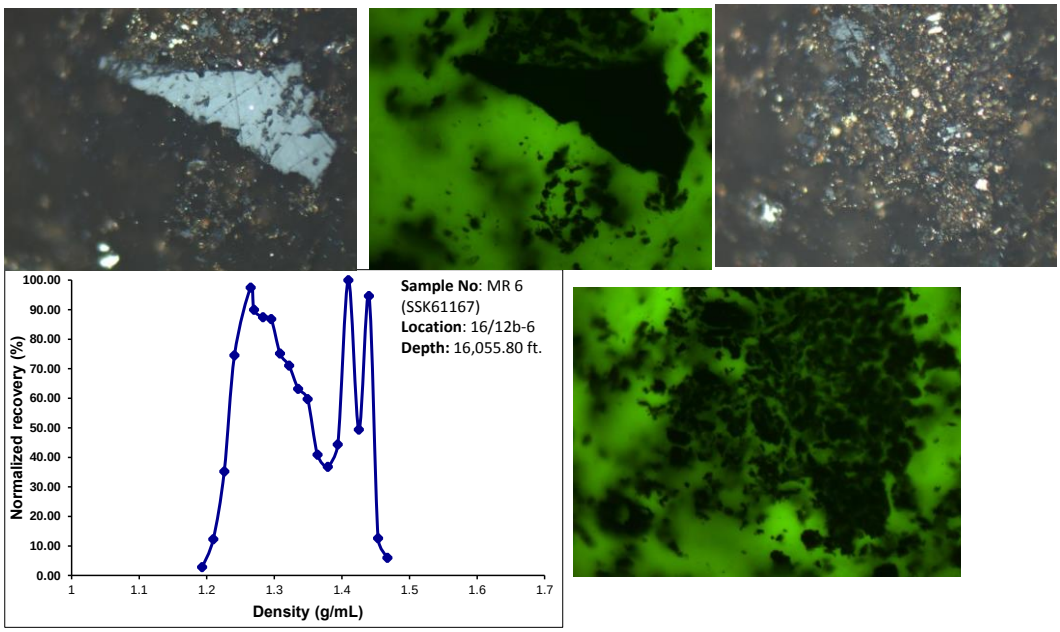

Figure 8-3: Density gradient profile range of 1.2-1.48 g/mL for distinct density peaks showing anomalous density reading and pyrite in the separated fractions from petrographic observation.

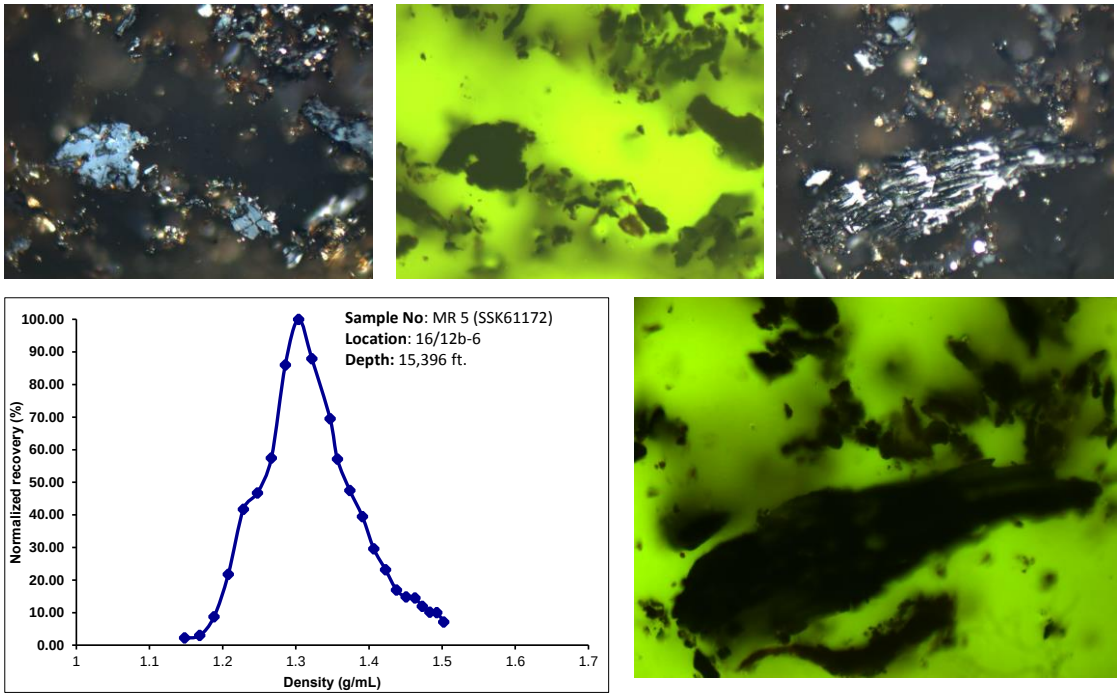

Figure 8-4: Density gradient profile range of 1.14-1.5g/mL for distinct density peaks showing a normal density reading; however pyrite in the separated fractions can still be seen from the petrographic observation.

8.3: Recommendations for Future Work

The results from this research have contributed to our knowledge and understanding of oil expulsion pathways in hybrid unconventional petroleum systems and quantifying oil (Rock-Eval S_1 yields) in interbedded shale/silt/sand sequences in the Kimmeridge Clay Formation of the South Viking Graben of the North Sea. Throughout this research, many challenging questions for further research arose, only some of these questions were answered due to the time constraint allowed for this project. The following questions remain unanswered as their investigation was beyond the time limit and scope of this PhD thesis.

8.3.1: Isolated kerogen and maceral separation using density gradient centrifugation (DGC)

Isolated kerogen and maceral separation experiments were performed but difficulties were encountered in the separation of the heavy minerals (e.g. pyrite) from the macerals and this affected the final density readings during the maceral separation with DGC (described in Section 8.2 of this chapter). A study of the changes in the physical and chemical properties of macerals at each step would enable a better

understanding of the role of kerogen in the Kimmeridge Clay and provide further characterisation of where the highest S_1 (free oil) is in the three maceral groups (liptinite, vitrinite and inertinite). The chemical method of maceral separation is more effective than the physical method, but this method may alter the kerogen properties (Robl and Taulbee, 1995; Tambach et al., 2009). Finding the best method of kerogen isolation that completely removes pyrite is the key to understanding the fundamentals of maceral chemistry. This will provide more detailed information with respect to the retention and/or expulsion of liquid hydrocarbons at sand/shale interfaces of thinly interbedded source rocks. Optical microscopy (transmitted white light and UV-fluorescence), SEM-BIB, total organic carbon (TOC), carbon isotope ratios, Rock-Eval and Pyrolysis GC of S_1 (adsorbed gas and liquids) should also be performed on the separated maceral fractions.

8.3.2: Total Porosity and Fluid Typing

The porosity of the mudstone, sandstone and the interface between sand-mudstone were investigated using focused ion beam-scanning electron microscope (FIB-SEM) methods. However, this method cannot be used to quantify total porosity. Future analysis of multiple 2-D images of more representatives Kimmeridge Clay samples from several wells with lithological variation and different depth intervals are needed to better characterise each rock type to quantitatively understand the pore networks. Future research on porosity should focus on comparing 2-D and 3-D microscale information of core samples, and experimentation of SEM stimulation with hydraulic fracturing, fluid injections and pyrolytic artificial maturation. Furthermore, quantifying the amount of porosity using fluid injection methods such as; N2 physisorption (Bertier et al., 2016); gas adsorption (Kaufhold et al., 2016); nitrogen adsorption/desorption measurements (Marschall et al., 2016), mercury intrusion, or small-angle neutron scattering (Mastalerz et al., 2013; Bahadur et al., 2015) in the sand layer and mudstone layer will also be useful in determining the effective total porosity in this hybrid reservoir. Nuclear magnetic resonance (NMR) measurement can be used for fluid typing in shale reservoirs to differentiate between water, oil and gas filled porosity; structured and free water; free oil and kerogen-adsorbed oil.

8.3.3: Mechanical Analysis of the source rocks.

Quantitative evaluation of mechanical properties of the Kimmeridge Clay Formation such as density, Young's Modulus, Poisson's Ratio and micro-hardness of the sandy layers, mudstone layers and interbeds between sand-mudstone layers should be undertaken to minimise drilling risk and optimise well stimulation and productivity in shale reservoirs. This information will enable a better frack model design and enhance our understanding of frackability of thin layers (micro-indentation).

8.3.4: Nature of fluids

An understanding of the nature and effects of fluids in fine grained (and interbedded) mudstones is a major key in predicting reservoir productivity. Important parameters to investigate in the assessment of the nature of fluids include: the composition and phase of oil and gas (initial and after drawdown); static and dynamic fluid pressures and their effect on oil delivery; water saturation (Sw) (log vs lab) and the effects of fluid pressure on horizontal drilling.